Mouse chemical mutagenesis to identify new immune mechanisms against cytomegalovirus and herpes simplex virus 1

Gabriel André Leiva-Torres

Department of Human Genetics,
McGill University, Montreal, Quebec, Canada
August 2017

A thesis submitted to McGill University in partial fulfillment of the requirements of the degree of Doctor of Philosophy.

Abstract

Herpes simplex virus 1 (HSV-1) and cytomegalovirus (CMV) are ubiquitous and very prevalent pathogens. Infections with these agents result in a variety of clinical syndromes, ranging from asymptomatic to severe infection, with high mortality rates and significant long-term morbidity, particularly in vulnerable in immunocompromised or immature populations. The use of inbred mouse strains that accurately replicate disease and exhibit natural genetic variation in susceptibility has been particularly useful to understand fundamental mechanisms of virus disease pathogenesis. Further, random chemical mutagenesis with N-Ethyl-N-Nitrosourea (ENU) is a powerful tool to identify new mutations on genes and pathways critical to immunity. We have developed an ENU mutagenesis platform followed by a high-throughput infection pipeline allowing us to screen a high number of mice for susceptibility to either CMV or to HSV-1 infection. We generated and tested more than 264 pedigrees, for a total of 4200 animals for gained susceptibility to infection. Doing so, we found 6 families exhibiting susceptibility to HSV-1 and 1 to CMV. We selected one pedigree susceptible to HSV-1 for further analysis. We found a non-synonymous mutation in the linker domain (LD) of STAT5A (W484G). CD8+ T cells and NK cell responses were affected in STAT5A^{W484G} mice, as their numbers were reduced following infection with HSV-1, as were the antigen experienced CD44+ CD8+ T cells. After stimulation with IL-2, which is mediated in part by STAT5A, NK cells did not increase the expression of IL-2Rβ as much as wild type mice, while the expression of IL-2Rα on CD4 and CD8 T cells was abrogated. These results show that STAT5A is important to the T cell and NK cell immune responses to HSV-1 and CMV infection and a single point mutation in its LD is sufficient to compromise STAT5A function. We also analysed a pedigree susceptible to CMV and identified a critical mutation on the uncharacterized GTPase GNL1. NK cells, which play a non-redundant role in CMV resistance, were drastically reduced in mutant animals, causing viral susceptibility. NK cells also exhibited an increase in caspase 3 activity accompanied with a dysfunctional cell cycle progression after IL2 and IL15 stimulation, two cytokines critical for NK cell

biology. The inactivation of p53 rescues the NK deficiency and cell death. We showed that GNL1 is crucial for NK cells homeostasis and that GNL1 inactivation leads to NK deficiency and MCMV susceptibility. Taken together, our results allow for a better understanding of the mechanism governing the immune response to herpesviruses and lymphocyte biology, facilitating the elaboration of antiviral and immune treatment.

Résumé

Le virus de l'Herpès Simplex de type 1 (VHS-1) et le Cytomégalovirus (CMV) sont des pathogènes très prévalents. Les symptômes cliniques sont variés, allant d'une infection asymptomatique à de sévères infections pouvant causer la mort ou des effets morbides a long-terme. Les populations immunosupprimées ou au système immunitaire immature sont particulièrement à risque. Afin de comprendre les mécanismes fondamentaux de la pathogenèse, l'utilisation de souche de souris consanguines fut particulièrement utile. Ces différentes souris répliquent les hauts points de l'infection et possède une variation génétique naturelle dans la résistance au virus. De plus, l'introduction aléatoire de mutation chez la souris par l'agent chimique N-Ethyl-N-Nitrosourée (ENU) est un outil puissant afin de découvrir de nouvelles cascades de signalisation et gènes mutés critiques à l'immunité. Dans le cadre de cette thèse, nous avons développé une plateforme de mutagenèse couplée à un pipeline d'infection à haut volume permettant de tester de grandes quantités de souris pour la susceptibilité à CMV et VHS-1. Nous avons généré et infecté plus de 264 pédigrées, pour un total de 4200 animaux. Ce faisant, nous avons trouvé 6 familles susceptibles à VHS-1 et 1 à CMV. Nous avons sélectionné un pédigrée susceptible à VHS-1 pour de plus amples analyses et avons identifié une mutation non synonyme dans le domaine de liaison (DL) de STAT5A (W484G). Les cellules T CD8 et NK étaient affectés par la mutation. Leurs nombres étaient réduits suivant l'infection, tout comme ceux des cellules T CD44+ CD8+ ayant déjà vu l'antigène. Après stimulation avec IL-2, donc le signal est en partie médié par STAT5A, les cellules NK n'ont pas augmenté l'expression du récepteur IL-2Rβ, tandis que l'expression de IL-2Rα était abrogée chez les cellules T CD4 et CD8. Ces résultats démontrent que STAT5A est important pour la réponse immunitaire à VHS-1 et CMV des cellules T et NK, et qu'une mutation ponctuelle dans le DL de STAT5A est suffisant pour compromettre sa fonction. Nous avons aussi sélection un pédigrée susceptible a CMV et identifié une mutation critique dans la GTPase non caractérisée GNL1. Les cellules NK, qui jouent un rôle essentiel et non redondant dans la résistance à CMV, étaient drastiquement réduites,

causant la susceptibilité au virus. Le niveau d'activité de caspase 3 était élevé chez les NK, en plus d'avoir un cycle cellulaire dysfonctionnel après stimulation avec IL-2 et IL-15, deux cytokines critiques à la biologie de ces cellules. L'inactivation de p53 restaure un nombre normal de NK et diminue la mort cellulaire. Nous avons démontré que GNL1 est crucial à l'homéostasie des cellules NK et l'inactivation de GNL 1 cause une déficience en cellules NK et la susceptibilité à CMV. Dans l'ensemble, nos résultats permettent une meilleure compréhension des mécanismes régissant la réponse immune aux virus herpétiques et la biologie des lymphocytes, facilitant l'élaboration de traitements antiviraux et immunitaires.

Table of contents

Acknowledgements

This thesis is the result of many years of reading, discussing and experimenting. I could not have achieved this without the invaluable help of mentors and colleagues. First, I would like to thank Dr. Silvia Vidal for giving me the occasion to work and study in her laboratory. I'm extremely grateful for her guidance, support and enthusiasm. Thank you for this invaluable opportunity.

I would also like to thank the members of my supervisory committee, Dr. Danielle Malo and Dr. Anastasia Nijnik, for their help and guidance during my studies. I am also grateful to Dr. Jorg Fritz, who gave me his support as an occasional supervisory committee member.

A special thanks have to be given to Benoit Charbonneau for his help during many experiments. I would also like to thank Dr. Nassima Fodil, Dr. Michal Pyzik and Peter Moussa for their help and advice. Mathieu Mancini and Dr. Gregory Caignard also assisted me during my studies and I am grateful to them. I would like to express my appreciation to Natasha Barone for her contribution to the study of the Glynn pedigree and proofreading this thesis. Particular recognition must be given to all the animal technicians that attended to the thousands of mice necessary for this thesis. In alphabetical order: Patricia D'Arcy, Vanessa Guay, Chantal Lacroix, Geneviève Perreault, Leigh Piercey-Brunet, Nadia Prud'homme, Cynthia Villeda-Herrera.

I would like to thank all the members, past and present, of the Dr. Vidal laboratory. Your help, discussions and "joie de vivre" were always appreciated. I am also grateful to all my colleagues from my studying room. When you pass so much time away from home, it is nice to know you are doing it with great people.

Finally, this thesis would not have been possible without the invaluable support of my friends and family. Thank you to my parents for encouraging me during this long project. I would like to give a special thanks to my wife, Noémie Bérubé-Carrière, and my daughter, Éléonore Leiva-Carrière, for their love and support. Thank you for making me smile even when the data did not.

List of Figures

Chapter 1 – General introduction and literature review

Chapter 2 – Strategies to establish an ENU mutagenesis pipeline to identify novel herpesviruses susceptibility genes

Chapter 3 – Altered immune responses to infections with herpesviruses are associated with an N-ethyl-N-nitrosourea-induced mutation in the linker domain of STAT5A

Chapter 4 – An ENU induced mutation in the GNL1 GTPase causes a p53-dependent NK cells deficiency

List of Tables

List of Abbreviations

ADCC	Antibody-dependent cell-mediated cytotoxicity
B10	C57BL/10
B6	C57BL/6
BMDC	Bone marrow derived dendritic cell
BMDM	Bone marrow derived macrophage
BrdU	Bromodeoxyuridine
CILP	Common innate lymphoid progenitor
CIML	Cytokine-induced memory-like
CLP	Common lymphoid progenitor
CMP	Common myeloid progenitor
CMV	Cytomegalovirus
CNS	Central nervous system
cNK	Conventional natural killer
DC	Dendritic cells
DN	Double negative
DP	Double positive
EILP	Early innate lymphoid progenitors
ENU	N-ethyl-N-nitrosourea
G0	Generation 0
G1	Generation 1
G2	Generation 2
G3	Generation 3
GNL1	Guanine Nucleotide Binding Protein-Like 1
GWAS	Genome-wide association studies
HCMV	Human cytomegalovirus
HSE	Herpes simplex encephalitis
HSV	Herpes virus simplex
HSC	Hematopoietic stem cell
i.p.	Intraperitoneal
i.v.	Intravenous
IFN	Interferon
IL	Interleukin
ILC	Innate lymphoid cell
iNK	Immature NK
IRF3	IFN regulatory factor 3
IRF7	IFN regulatory factor 7
ITAM	Immunoreceptor tyrosine-based activation motif
ITIM	Immunoreceptor tyrosine-based inhibitory motif
KIR	Killer Ig-like receptor
KO	Knock-out
LAK	Lymphokine activated killer
lncRNA	Long non-coding RNA
LOD	Logarithm of the odds
MCMV	Murine cytomegalovirus
MEF	Murine embryonic fibroblast
MHC	Major histocompatibility complex
MIEP	Major immediate early promoter
mNK	Mature NK
MPP	Multipotent progenitor
mTOR	mammalian target of rapamycin

NK	Natural killer
NKC	NK-cell complex
NKD	NK cell deficiency
NKP	NK progenitor
Oca2	Oculocutaneous albinism II
ORF	Open reading frame
p.i.	Post-infection
PBS	Phosphate-buffered saline
pDC	Plasmacytoid dendritic cells
PDK1	Phosphoinositide-dependent kinase-1
PFU	Plaque forming unit
PMA	Phorbol 12-myristate 13-acetate
ppNK	pre-pro NK
PRR	Pattern recognition receptor
QTL	Quantitative trait locus
RCS	Recombinant congenic strains
RIG-I	Retinoic acid-inducible gene I
S6K	S6 Kinase
SD	Standard deviation
SH2	Src homology 2
SI	Spleen index
SMURF2	SMAD Specific E3 Ubiquitin Protein Ligase 2
SNP	Single nucleotide polymorphism
SNV	Single nucleotide variation
SP	Single positive
STAT	Signal transducers and activators of transcription
TLR	Toll-like receptor
VZV	Varicella-zoster virus

Preface and author contributions

This thesis consists of five chapters: a literature review, three original manuscripts and a general discussion. One manuscript (chapter 4) has been submitted, while the two other manuscripts are currently in preparation. A statement has been included bridging the materials presented in each chapter. I, Gabriel André Leiva-Torres, under the supervision of Dr. Silvia M. Vidal, have designed, performed, analyzed the experiments and written the manuscript described below unless indicated otherwise. The co-authors listed below contributed as follows:

Strategies to establish an ENU mutagenesis pipeline to identify novel herpesviruses susceptibility genes. *Leiva-Torres GA, Charbonneau B, Leney-Greene M, Mancini M, Caignard G, Vidal SM***.** Manuscript in preparation

The generation of the G0 mice and the subsequent breeding was performed by Patricia D'Arcy and Nadia Prud'homme. The infection and monitoring of the animals were done with the assistance of Benoit Charbonneau and Grégory Caignard. Micheal Leney-Greene and Mathieu Mancini assisted in the characterization of the Tre pedigree. I was responsible for the experimental design, performance and analysis of the data, as well as the writing of the manuscript.

An N-Ethyl-N-Nitrosourea Induced mutation in the GNL1 GTPase causes NK cells deficiency by impairing cell homeostasis, IL2 and IL15 response. *Leiva-Torres GA, Charbonneau B, Caron M, Sladek R and Vidal SM.* Manuscript in preparation

Benoit Charbonneau's technical assistance was crucial for the infection experiment. Maxime Caron and Dr Rob Sladek analyzed the exome sequencing data. The animal colonies were maintained by Patricia D'Arcy and Geneviève Perreault. I was responsible for the elaboration of the rationale, experimental design, performance and analysis of the data, as well as the writing of the manuscript.

Altered immune responses to infections with herpesviruses are associated with an N-ethyl-N-nitrosourea-induced mutation in the linker domain of STAT5A. *Leiva-Torres GA, Charbonneau B, Eveleigh R, Bourque G, Vidal SM*. Manuscript in preparation

Benoit Charbonneau's technical assistance was crucial for the infection experiments. Robert Eveleigh and Guillaume Bourque analyzed the exome sequencing data. The animal colonies were maintained by Patricia D'Arcy and Geneviève Perreault. I was responsible for the elaboration of the rationale, experimental design, performance and analysis of the data, as well as the writing of the manuscript.

Under the supervision of Dr Silvia Vidal, I have also co-written one review and one book chapter. These reviews are either published or under revision.

Regulation of natural killer cells memory. *Leiva-Torres GA, Barone N, Lee SH, Vidal SM.* F1000 Prime reports, in revision.

This review provides new insight on the mechanism regulating NK cells homeostasis and the generation of memory-like NK cells.

Discovery of Variants Underlying Host Susceptibility to Virus Infection Using Whole-Exome Sequencing. *Leiva-Torres GA, Nebesio N, Vidal SM*. Methods Mol Biol. 2017. 1656:209-227.

This review describes the general aspects of a workflow of whole-exome sequencing to identify the genetic determinant of host susceptibility to viral infection.

In addition, my work was instrumental to the publication of the following papers:

Rel-dependent crosstalk between hematopoietic and resident compartments overcomes viral replication and neuroinflammation in a new ENU model of herpes

simplex encephalitis. *Mathieu Mancini, Grégory Caignard, Benoit Charbonneau, Anne Dumaine, Nila Wu, Gabriel A. Leiva-Torres, Maxime Caron, Steve Gerondakis, Angela Pearson, Salman T. Qureshi, Robert Sladek, Silvia M. Vidal***.** PLOS Pathogen, submitted

During a HSV-1 screen of ENU mutated mice that we performed in our laboratory, we identified a pedigree carrying a mutation on Rel. Mathieu Mancini and Grégory Caignard have pursued the study of that mutation. I provided assistance during the screening of the pedigree, as well as providing expertise for the study of the HSV-1 susceptibility.

USP15 regulates type I interferon response and is required for pathogenesis of neuroinflammation. *Torre S, Polyak MJ, Langlais D, Fodil N, Kennedy JM, Radovanovic I, Berghout J, Leiva-Torres GA, Krawczyk CM, Ilangumaran S, Mossman K, Liang C, Knobeloch KP, Healy LM, Antel J, Arbour N, Prat A, Majewski J, Lathrop M, Vidal SM, Gros P.* Nat Immunol. 2017 Jan;18(1):54-63.

During an ENU screen for cerebral malaria, Sabrina Torres, under the supervision of Philippe Gros, found a deviant pedigree carrying a mutation on the *Usp15* gene. I contributed to the study of USP15 and its role in neuroinflammation and its expression in human CNS resident cells using qPCR.

Mapping of a quantitative trait locus controlling susceptibility to Coxsackievirus B3-induced viral hepatitis. *Wiltshire SA, Marton J, Leiva-Torres GA, Vidal SM*. Genes Immun. 2015 Jun;16(4):261-7.

During his doctoral studies in Dr Silvia Vidal's laboratory, Sean Wilthshire mapped a susceptibility locus on chromosome 13, linked to Coxsackievirus B3 susceptibility. I contributed to this paper by identifying and validating various polymorphic markers used in this project.

Genome-wide mouse mutagenesis reveals CD45-mediated T cell function as critical in protective immunity to HSV-1. *Caignard G, Leiva-Torres GA, Leney-Greene M, Charbonneau B, Dumaine A, Fodil-Cornu N, Pyzik M, Cingolani P, Schwartzentruber*

J, Dupaul-Chicoine J, Guo H, Saleh M, Veillette A, Lathrop M, Blanchette M, Majewski J, Pearson A, Vidal SM. PLoS Pathog. 2013 Sep;9(9):e1003637.

During the ENU screen for susceptibility to HSV-1 that we previously performed in our laboratory, Grégory Caignard identified a mutation of ptprc (CD45) causing viral susceptibility. I contributed to various experiments involving HSV-1 and flow cytometry. I also provided expertise for the usage of HSV-1.

An N-ethyl-N-nitrosourea (ENU)-induced dominant negative mutation in the JAK3 kinase protects against cerebral malaria. *Bongfen SE, Rodrigue-Gervais IG, Berghout J, Torre S, Cingolani P, Wiltshire SA, Leiva-Torres GA, Letourneau L, Sladek R, Blanchette M, Lathrop M, Behr MA, Gruenheid S, Vidal SM, Saleh M, Gros P*. PLoS One. 2012;7(2):e31012.

In another ENU screen, Sylayuv Bongfen, under the supervision of Dr Philippe Gros, identified a mutation on JAK3 causing cerebral malaria. In collaboration with Sean Wilthshire, I contributed to this study by designing and validating the genotyping panel necessary for the identification of the mutation.

I, Gabriel André Leiva-Torres, have read, understood and abided by all norms and regulations of academic integrity of McGill University.

Chapter 1 – General introduction and literature review

Throughout known time, viruses and humans have been in a fight for their survival. For some viruses, co-evolution with their host has helped them to increase their efficiency, while minimizing the negative impact on the host, allowing them to propagate. However, these pathogens can be opportunistic, causing severe disease if the host immune system is compromised or immature. Herpesviruses are among those types of pathogen. These highly prevalent viruses have adapted to their host, whether human or animal, allowing them to replicate and survive without causing severe damage. Yet, infections result in a variety of clinical syndromes, ranging from asymptomatic infection to a severe infection with high mortality risk and significant long-term morbidity. This is particularly true in vulnerable populations, including infants or individuals with a compromised immune system (graft recipients, HIV-infected patients, cancer patients and the elderly) (*1*, *2*). In this thesis, we focused on two of these viruses: herpes simplex virus 1 (HSV-1) and cytomegalovirus (CMV). More specifically, we investigated the immune response to infection and a host gene that is important for resistance to the virus.

The first chapter of the thesis consists of a literature review separated in three sections. The first section discusses the biology of HSV-1 and CMV, their pathology and the immune response to these viruses. The second section focuses on the biology, regulation and functions of natural killer (NK) cells. These lymphocytes are central to resistance to CMV and are also the main subject of chapter 4 of this thesis. Lastly, the third section of this literature review examines different genetic approaches to the study of host resistance, with an emphasis on forward genetics and ENU mutagenesis.

Herpesviridae

Early descriptions of herpesvirus infection date to thousands of years ago. Sumerian tablets (~3000 BC) and Ebers papyrus (~1500 BC) contain descriptions of genital lesions resembling those of HSV (*3*, *4*). Later, in ancient Greece, the physician Hippocrates described what were possibly HSV lesions and named them herpes, from the Greek word *Herpein* (to creep, to crawl). It was only during the 1930s that the first link between recurrent lesions and the individuals carrying neutralizing antibodies was made (*4*). Herpes simplex viruses were the first human herpesvirus to be discovered and they are the most studied.

The first description of the cytomegalovirus came much later than the first identification of HSV-1. The asymptomatic nature of the virus in healthy patients might have contributed to the delay in the recognition of this viral disease. Enlarged cells from the kidney section of stillborns were first described only in the 1880s (*5*). Later, during the 1930s, the same cellular inclusions were also described in the salivary glands of children deceased from various causes. During the 1950s, Margaret Smith isolated the murine CMV (MCMV) found in salivary glands, thus giving her name to the strain (*6*).

Herpesviruses are not limited to HSV-1 and CMV. The Herpesviridae family is composed of various viruses that are able to infect a large spectrum of species, from catfish to humans (*7*). This family is constituted of enveloped viruses with a large encapsidated DNA genome and the ability to establish lifelong latent infection in the host cell following the initial acute infection. These viruses are classified in three sub-families, according to their genomic similarity, biological properties and cellular tropism (*8*, *9*). The *Alphaherpesvirinae* are neurotropic viruses that are also able to infect epithelial cells. They have a short replication cycle (around 12h) and establish latency in neurons (*10*). In humans, this sub-family is composed of the herpes simplex virus 1, herpes simplex virus 2 (HSV-2) and the varicella-zoster virus. Although HSV-1 and HSV-2 are closely related, the former is associated with non-genital disease (mainly labial lesion), while the

latter is associated with genital lesions. The *Betaherpesvirinae* are able to infect a variety of cell types, including immune cells. These viruses have a larger genome and are characterized by a long replication cycle (up to 24h) (*11*). The human CMV (HCMV) along with the human herpes virus 6 and 7 compose this subfamily in humans. The last subfamily is the *Gammaherpesvirinae*. These lymphotropic viruses also possess oncogenic properties (*9*). The Epstein Barr virus and the Kaposi sarcoma virus are the two human viruses that form this family.

HSV-1 and CMV virion structure

As mentioned above, HSV-1 and CMV are two large enveloped DNA viruses. Their genome is comprised of a single double-stranded DNA molecule, with both strands encoding for approximately 192 open reading frames (ORF) on a ~230kb molecule for CMV and ~90 ORF on ~152kb for HSV-1 (*11-13*). In both viruses, the genome is contained in an icosahedral capsid with a T=16. The capsid is surrounded by a matrix of protein forming the tegument. These proteins play an important role during the early steps of viral replication. The tegument/capsid complex is enclosed by a lipid envelope containing viral glycoproteins.

The HSV-1 and CMV genomes share a common structure that has a peculiar arrangement. Indeed, both genomes are composed of two main regions, called unique long and unique short regions. Each contains single copies of different genes (*14*, *15*) and is flanked by two small inverted repeated regions. This means that there will be two copies of the viral gene when a gene is encoded in the repeated regions, while only one copy of the viral gene will be found in unique regions. Since the unique regions are flanked by repeated inverted sequences, these viruses have the ability to rearrange their genome. This can result in a virus having unique long and unique short regions pointed in different directions. Moreover, if a cell is infected with two different viruses, new genome particles can be composed of the unique long section from virus A and the unique short section from virus B.

The HSV-1 and CMV replication cycles

Although they are from two different sub-families, HSV-1 and CMV share a similar replication cycle (reviewed in (*10*, *11*)). Briefly, following the interaction between the viral glycoprotein and their cellular receptor, the viral and cellular membrane fuse, allowing for the release of the viral capsid and tegument protein into the cytoplasm. These proteins allow the virus to regulate the cellular host's immune and stress response, but they are also important for the initial transcription of viral genes. The capsid migrates to the nucleus, releasing the viral DNA in the nucleoplasm. At this point, the viral genome circularizes. Viral gene expression occurs in three sequential steps. First, immediate early genes are transcribed by the cellular RNA polymerase II. These genes mainly encode for viral transcription factors. Second, following the production of immediate-early protein, delayed early genes are transcribed, allowing for the replication of the viral genome. The viral genome is replicated as a concatemer, forming a long strand of viral DNA, which can then be cleaved to encapsulate a single genome copy. Third, the late genes are transcribed. These genes encode for capsid and structural protein as well as tegument protein.

The capsid formation occurs in the nucleus of the infected cells, where one copy of the viral genome is inserted in the newly produced capsid. The fully formed capsid then exits the nucleus via enveloping and de-enveloping events within the double nuclear membrane. The naked capsid and the tegument protein are then re-enveloped with cytoplasmic vesicles containing the viral glycoprotein. The viral envelope originates from the endoplasmic reticulum and the Golgi. The virus exits the cell via budding or cellular lysis. Although the replication cycle of HSV-1 and CMV are similar, their length differs; around 12 hours for HSV-1, while the CMV cycle can take up to 24 hours.

HSV-1 pathogenesis and immunology

Herpes simplex infections are very common. Indeed, about 80% to 100% of the population is seropositive for HSV-1 (*16*, *17*). HSV-1 infection, when it is not asymptomatic, usually causes mild symptoms. Typically, infection of the oro-labial epithelium will result in pustules that later rupture and form an ulcer and a crust (*18*). HSV-1 is usually associated with oro-labial infection, while HSV-2 is the main cause of genital infection. However, this dichotomy is changing, as HSV-1 represents nearly half of the cases of genital HSV-1 in the United States (*19*). Although HSV-1 cold-sores contain infectious viral particles, asymptomatic virus shedding can also occur. Indeed, about 65% of HSV reactivations are asymptomatic (*20*).

Herpetic keratitis is a complication of viral reactivation. During the initial orolabial infection, the virus infects the sensory neurons, innervating that region, and is then transported to the trigeminal ganglia, where the virus replicates and establishes latency, facilitating the propagation of the virus to the cornea (*21*). The damage caused on the cornea by the virus and the subsequent immune inflammation can cause loss of visual acuity and even blindness (*22*).

HSV-1 can cause severe symptoms in immunocompromised or immature individuals. The infection can lead to fulminant herpetic lesions as well as injury of internal organs, such as the inner mouth, trachea and oesophagus, as well the cornea (causing keratitis) and even the retina (*18*). The most severe outcome is herpes simplex encephalitis (HSE), a complication during which the virus uses retroaxonal transportation in neurons to infect the central nervous system (CNS), causing necrosis and brain tissue destruction (*23*). If untreated, HSE provokes life-long damage and leads to death. People of all ages can suffer from HSE. About 90% of HSE cases are due to HSV-1 (the other 10% are linked to HSV-2) and 33% of HSV-1 encephalitis cases affect children and young patients between 6 months and 20 years old (*24*, *25*). The majority of cases in neonates are caused by HSV-2 infection during delivery (*26*, *27*). Individuals over the age of 50

represent 2/3 cases of HSE, highlighting the importance of aging in susceptibility to herpetic encephalitis (*24*).

Typically, HSV-1 infection can be treated using the medication, acyclovir, which is an analogue to guanine. After being converted by the viral thymidine kinase, it inhibits the viral polymerase from replicating the virus genome (*28-30*). However, this type of drug has limited potency and efficacy, and has also been prone to the development of resistant infection in immunocompromised patients. To this day, there is no HSV-1 vaccine. As a result, there is an urgent need for the development of alternative therapeutic strategies.

HSV-1 latency

HSV-1 has the ability to establish latent infection in sensory nerves. Following an initial infection of the epithelial cells, where it produces the typical cold-sore, the virus propagates to the sensory neurons in that region (*31*). For oro-labial infection, the viral capsid is then transported via retro-axonal transport to the neuron nucleus, in the trigeminal ganglia (*32*, *33*). At this point a second acute infection occurs in the trigeminal ganglia. In highly susceptible individuals, the virus can propagate to the central nervous system via anterograde axonal transport, causing severe complications such as herpes simplex encephalitis (HSE).

Following acute nervous system infection, a shutdown of viral activity occurs. Although the exact causes are unclear, immune pressure by CD8 T cells on the infected cells could contribute to the establishment and maintenance of viral latency (*34*, *35*). During latency, the viral genome stays in the nucleus as a circular episome and only the latency associated transcripts (also known as LATs) are produced (*36*). After a stress, hormonal change, fever, UV exposure or immune change, the virus can reactivate. The new viral capsid is transported to the epithelium to produce another acute infection (*37*, *38*). This latency-reactivation cycle can persist throughout the infected individual's lifetime.

The immune response to HSV-1 infection

HSV-1 is a well-studied natural human virus that involves an immune response from various actors. To better understand the mechanism of the anti-HSV-1 response, the mouse model of infection has been used. Although HSV-1 is not a natural murine pathogen, the mouse model can replicate the hallmarks of the human disease. The use of this model has made it possible to elucidate the critical role of type 1 IFNs in the immune response to HSV-1. During the mid-70s, a study by Gresser et al. showed that inhibition of the IFN response by anti-interferon antibodies increases LD50 as well as shortening the latency period of HSV-1 (*39*). Later work using laboratory inbred mouse strains has found that IFN production was much higher in resistant C57BL/6 (B6) mice than in susceptible BALB/c animals (*40*). A study of IFN-α/β knock-out (KO) mice has confirmed the importance of type 1 IFN, as these mice were highly susceptible to ocular infection by HSV-1 (*41*). Indeed, IFN-α/β, in collaboration with IFN-γ, is crucial to the resistance to the early stages of HSV-1 infection, even in absence of lymphocytes (T, B or NK cells).

Molecular recognition of HSV-1

The early production of type 1 IFN is the consequence of the detection of viral components by pattern recognition receptors (PRRs). Viral DNA and RNA can be recognized by a variety of PRRs, leading to the activation IKKε and TBK1, which in turn activate IRF3. Along with the activation of NF-κB, these cascades ultimately lead to the expression of type 1 IFN. The paracrine and autocrine effect of IFN will then stimulate the expression of interferon-stimulated genes NF-κB and the STATs to induce a strong innate and adaptive response to HSV-1 (*42*, *43*).

During HSV-1 infection, various PRRs are engaged and implicated in the production of IFN. Wand et al. showed that the DNA-dependent activator of IFN regulatory factor (also known as DAI or DLM-1/ZBP1) can recognize HSV-1 infection and induce IFN-β production (*44*). Cytosolic RNA sensors contribute to the type 1 IFN production. Both retinoic acid-inducible gene I (RIG-I) and melanoma differentiation-associated gene-5, which traditionally sense the HSV-1 dsRNA during infection, also participate in the

sensing of viral DNA and contribute to the secretion of IFN (*45-48*). Activation of RIG-I mediates STING upregulation, which in turn is essential for the IFN-α/β response and anti-HSV-1 immunity (*49*).

HSV infection can also be recognized in synergy by RIG-I and TLR9 to induce the production of type 1 IFN (*50*). TLR9 can sense the CpG motif of the HSV genome to induce an appropriate antiviral response (*51*, *52*). TLR3 can also be engaged by the viral double-stranded RNA, inducing a type 1 IFN response. Mutations in TLR3 can cause severe complications, such as viral encephalitis (*53-55*). The end goal of the production of cytokines, such as IFNs, by the infected cells is to block viral replication, but also to activate the various cellular actors of the immune compartment.

NK cells

NK cells are the prominent cellular effectors of the innate immunity system against HSV-1 infection. NK cells express activating and inhibitory receptors that are important for the regulation of their function (*56*). The balance between these two signals dictates whether target cells will be killed or not. In healthy cells, binding of class I MHC to the inhibitory receptor causes the inhibition of the cytotoxic and secretory NK functions. During infection, viruses downregulate MHC-I expression to escape their recognition by T cells and, as a side effect, lower the inhibitory signals in NK cells, thus enabling their activation.

HSV-1 expresses the viral protein ICP47, which blocks MHC-I expression by inhibiting TAP1 antigen transporters. This allows the virus to escape CD8 T cells, but makes it a target of NK cells' cytotoxic activity (*57*, *58*). Although NK cells play an important role in HSV immunity, their necessity for viral resistance is debatable. In mice, depletion of NK cells, using either anti-NK1.1 or asalio-GM1, increases susceptibility to ocular, intra-venous (i.v.) and cutaneous HSV-1 infection (*59-62*). However, no effect was observed using an intra-peritoneal (i.p.) or a footpad infection (*63-66*). Although their importance might be variable, the activation of NK cells contributes to the anti-HSV-1 response.

Dendritic cells

IFN α/β production by dendritic cells is also a defense mechanism against HSV-1. More specifically, human plasmacytoid dendritic cells (pDC) recognize HSV-1 in order to produce type 1 IFN *ex-vivo* (*67*). This recognition seems to be mediated by TLR9, although inactivation of either pDC or TLR9 in mice does not increase susceptibility to the virus (*68*, *69*). The function of pDC might be subtler and differ in mice and humans, as a decrease in pDC numbers is associated with an increase in HSV-1 dermatitis in human patients (*70*). However, their role in the activation of other immune cells, such as CD8 T cells, is important for the build up of a robust antiviral response.

B and T cells

Activation of the adaptive compartment is crucial to the resistance to HSV-1. Both B and T cells play an important role in controlling infection. Indeed, a transfer of serum containing neutralizing immunoglobulin increases survival of immunosuppressed mice (*71*). Moreover, B cell deficiency in mice is associated with an increase in keratitis and encephalitis in the ocular model of infection (*72*), thus highlighting the importance of the humoral immunity in HSV-1 resistance.

Cellular immunity is particularly important for the anti-HSV immune response. Lymphopenic mice are highly susceptible to HSV-1 infection and viral encephalitis (*66*). CD8 T cells are central to HSV-1 adaptive immunity. Following cutaneous infection, a rapid increase in the number and activation of CD8 T cells that are specific to viral glycoprotein and activation is observed in the draining lymph node (*73*). This quick response is due to the presence of antigen presenting cells such as DCs. Once the CD8 T cells are activated and recognize infected cells, they can produce perforin and granzyme to induce apoptosis in the infected cells, limiting the virus spread (reviewed by (*43*)). Helper CD4 T cells are also important for the anti-HSV-1 response, as their IFN-γ production contributes to CD8 T cell recruitment and to protection from encephalitis (*66*). Infiltration of cytotoxic T cells in the trigeminal ganglia is essential to control viral replication and prevent viral reactivation (*35*). Interestingly, the interaction of CD8 T cells

with infected neurons do not cause apoptosis, as that could be detrimental to the host. Instead, granzyme A and B seem to act in a non-cytotoxic fashion to limit viral spread (*74*, *75*). For instance, granzyme B directly cleaves to the immediate-early viral protein ICP4, a molecule essential for the expression of viral genes. Thus, the T cells compartment is central to resistance to HSV-1 during acute and latent infection in both epithelial and neuronal tissues.

Immune response during herpes simplex encephalitis

HSE is not only one of the most severe complications of herpes simplex infection, but also the most common viral encephalitis in the developed world (*76*). HSE was first discovered in the early 1940s when evidence of HSV infection in the brains of neonates with encephalitis was found by Smith et al. (*77*). We had to wait until the 1980s and the commercialisation of acyclovir to finally be able to treat the disease, which was otherwise lethal to adult and infant patients alike (*4*, *78*, *79*). The mechanism of the disease has only begun to be deciphered over the last 20 years.

Immune response in HSE patients

Although HSV-1 infection is quite ubiquitous, only a small fraction of the population is affected by HSE. It was hypothesized that genetics factors could play a major role in the development of the disease. The first description of a recessive mutation causing lethal HSE was on the *Stat1* gene (*80*). Infants carrying the mutation had an impaired response to IFN-α/β and IFN-γ couldn't activate the STAT1-containing transcription factor. Later, studies by the Casanova group identified the NF-κB essential modulator (NEMO) as a genetic etiology of HSE (*81*). Further genetic studies of rare cases of herpes encephalitis in children have elucidated the role of UNC-93B, TLR3 and IFN-α/β/λ in resistance to the virus. Indeed, loss-of-function mutation in *UNC93B1, TLR3, TRIF, TRAF3* or *TBK1* has resulted in severe encephalitis. Transformed fibroblast cells from these patients weren't able to properly respond to HSV-1 or TLR3 ligands such as poly I:C, and showed a deficiency in the production of IL-6, IFN-α, β and λ (*54*, *55*, *82-84*).

The TLR3-IFN pathway is crucial to the resistance to HSV-1 in the CNS. A crucial proof of this was obtained using induced pluripotent stem cells derived from dermal fibroblasts of TLR3 and UNC93B1 deficient patients, which were differentiated into neurons and oligodendrocytes (*85*). Cells from the patients were much more susceptible to HSV-1 infection than wild-type individuals, highlighting the importance of the TLR pathway in CNS cells (*85*, *86*). These cells show a deficiency in their intrinsic antiviral response, dependent on the TLR3 pathway and type 1 IFN, which can account for the brain specific damage observed during HSE infection. Recently, Andersen et al. have found that a functional deficit in the *IFN regulatory factor 3* (*IRF3*) caused by an autosomal dominant mutation on that gene leads to HSE in adolescent patients (*87*). PBMCs from that patient had an impaired IFN-β induction after poly(dA:dT) or HSV-1 stimulation due to a lack of phosphorylation and dimerization of IRF3, highlighting the central role of IFN in the control of HSV-1 in the CNS. These studies on children affected with HSE are important, as they allow for an understanding the role that innate immunity plays in the resistance to herpes encephalitis. However, they do not explain the whole extent of the disease. Indeed, these studies focus on children affected with HSE, which only account for a third of all the cases of HSV-1 encephalitis (*24*). This raises an important question: what are the mechanisms, either from innate or adaptive immunity, leading to HSE in the other two-third of patients suffering from HSV-1 encephalitis? To answer this, the usage of the mouse model of infection can be extremely useful.

Mouse model of HSE

Although the study of sporadic cases of HSE has allowed a better understanding of the disease, the usage of laboratory mice has shown to be a powerful model for the investigation of their immune mechanisms. Very early, it was found that resistance to HSV-1 varied from one inbred strain to another, as A/J and BALB/c succumb to the virus, while C57BL/6 resisted (*88*). This discovery gave rise to a multitude of mouse models of infection for HSV-1. Indeed, depending on the route of infection, different aspects of the pathogenesis, including acute and latent infections, can be studied.

Intra-peritoneal inoculation involves the spread of the virus to visceral organs as well as the infection of the CNS (*66*, *89*, *90*). This route also involves the immune system from both regions. The cutaneous model of infection allows for the evaluation of the immune response in the periphery and imitates the classical cold sore commonly observed in the general population (*90*, *91*). Although the evaluation of the HSE is less obvious in this model, footpad infection with HSV-2 has been extremely useful in understanding the mechanism of neuronal replication and latency of that virus in the dorsal root ganglia (*92*). The ocular route of infection is quite versatile as it allows for the study of different aspects of natural infection in humans, including keratitis, latency in trigeminal ganglia and HSE (*93*, *94*). Using this model, Lundberg et al. performed an association study and found a susceptibility locus on chromosome 6 that determines HSV-1 resistance and influences latency (*89*). The intra-cranial model of infection directly involves the viral replication in the CNS, by bypassing any viral replication in the periphery (*95*). The intra-nasal model of infection also has the advantage of directly involving the infection of neurons and the propagation of the virus to the CNS, while being less invasive and demanding than the intra-cranial model (*96*).

The mouse model of HSV-1 infection is used to validate human HSE genes and understand the mechanism of action. Using knock-out mice, both STAT1 and UNC93B1 were confirmed as essential to HSE resistance (*97*, *98*). Moreover, these studies highlight the importance of type 1 IFN in the control of HSE, as seen in human patients. Interestingly, although the UNC93B1 deficient mice were able to control virus replication in the brain, these mice still exhibited HSE.

Susceptibility to viral encephalitis is not limited to the TLR3 pathway. Indeed, KO mice for *Myd88*, an adaptor molecule for TLR7 and 9, are susceptible to HSE (*96*). Recognition of cytosolic viral DNA is crucial to the resistance to encephalitis. Reinert et al. have shown that HSV-1 sensing by cyclic GMP–AMP synthase (known as cGAS) followed by the activation of STING in the microglia is necessary for resistance to HSE (*99*). As such,

mice deficient in either of those molecules have an impaired IFNα/β production in microglial cells and succumb to HSV-1 infection.

More recently, using an i.p. model of infection, we have shown that the loss-of-function mutation in the *ptprc* gene (encoding for CD45) causes HSE (*66*). These mice showed defective T and B cell development. Resistance to HSE was restored when CD4 and CD8 T cells were adoptively transferred to the mice. Encephalitis was shown to result from of a lack of control of the virus in the periphery. However, the benefit of T cells is site dependent. For instance, T cell infiltration in the brain of infected mice is associated with an increased mortality rate. In an intra-nasal (i.n.) model of infection, mice deficient in the chemokine receptor CXCR3 showed a reduction in T cell recruitment, microglia activation and decreased weight loss (*100*). The neuro-inflammation caused by the T cells infiltration is detrimental to the infected animal, causing HSE. However, using the corneal model of infection, dysregulation of CXCL10 was detrimental to the animal, as the HSV-1 specific CD8 T cells could not be recruited to the trigeminal ganglia to control viral replication and spread (*101*). Thus, it is crucial to maintain a balance between an efficient anti-HSV-1 immune response limiting the risk of HSE, while controlling the extent of the inflammation to reduce damage to brain tissue.

Overall, these studies demonstrate that crucial cell-specific and time-dependent immune mechanisms need to be tightly regulated not only to curb viral replication but also to avoid overwhelming inflammatory responses, which can be productively studied in mouse models.

CMV pathogenesis and immunology

CMV is an extremely prevalent virus, with an IgG of seroconversion ranging from 60 to 100%, depending on socioeconomic and geographical status (*102*). The virus is easily transmitted via fluid exchange, like saliva, blood or breast milk, as well as transplacental transmission. HCMV infection usually causes mild to no symptoms in healthy individuals,

both during acute infection and reactivation following latency. As the name of the virus suggests, it tends to form a large owl eye inclusion in infected cells, which were initially found in biopsies of stillborn babies, infected newborns and in organ transplantation patients with complications (*102-104*).

The large cellular tropism of CMV allows the virus to produce a diversity of symptoms in individuals with an immature or compromised immune system. Solid organ transplantation recipients under immunosuppressive treatment can suffer from severe HCMV viremia causing end-organ disease including hepatitis, pneumonitis, retinitis and gastrointestinal ulceration (*102*, *105*). Although prophylactic treatment with ganciclovir reduces the risk of complications, these late onset diseases can occur after treatment is withdrawn. In AIDS patients, CMV is an opportunistic pathogen mainly causing retinitis, although other organs can also be affected by the virus. HCMV is also associated with an increased mortality, even in patients undergoing antiretroviral therapies (*106*). Congenital HCMV infection, either from primary or latent maternal infection, can also cause severe damage to the foetus. This can be exacerbated by the mother sometime not recognizing the CMV related symptoms (fever and malaise) (*107*). HCMV infections are the most common cause of congenital viral infection leading to hearing loss and brain damage causing cerebral palsy or mental retardation (*108*).

HCMV is also a risk factor for the elderly population. Indeed, cytomegalovirus infection is associated with an increased inflammation rate, changes in numbers and frequencies of different types of immune cells and increased mortality rate (*109*). Latent infection also contributes the immunosenescence of both the adaptive and innate compartments, which limits their capacity to respond to pathogens and vaccines, increasing susceptibility to novel infections. Latent HCMV induces a reduction in the naïve and immature T and NK cells (*110*, *111*). The latent infection accelerates epigenetic aging: Patients who are seropositive for CMV have the kind of increased DNA methylation change that is associated with aging in the immune cells, which causes a premature dysregulation of

the immune compartment (*112*). Overall, although CMV infection might initially be benign, the latent and opportunistic nature of the virus makes it a concern for public health.

The main treatment for CMV infection is ganciclovir. As with acyclovir, ganciclovir inhibits the viral DNA polymerase after phosphorylation via the viral kinase UL97, thus blocking viral replication (*113*). However, ganciclovir cannot be used for a long-term treatment, since bone marrow toxicity has been observed (*114*). Foscarnet is another viral DNA polymerase inhibitor that directly targets the enzyme without need for pre-activation or conversion. Foscarnet has to be administered intravenously, limiting the ease of use of the treatment (*115*, *116*). This drug is mainly used for the treatment of keratitis in AIDS patients. Long-term use of ganciclovir and foscarnet is known to produce viral resistance. No vaccine is available against HCMV, reinforcing the need to develop novel and innovative treatments against the virus.

CMV latency

As explained previously, CMV is able to infect a large variety of cell types, including hematopoietic, epithelial and stem cells. Consequently, latency is not limited to one cell type (*117*, *118*). Studies with both HCMV and murine CMV (MCMV) have shown the capacity of the virus to establish latency in hematopoietic progenitors, myeloid cells, macrophages and epithelial cells (*119*, *120*). In humans, the myeloid lineage seems to be the major carrier of the latent viral genome. More recently, neuronal progenitors have been proposed as a potential latency site for HCMV, which would not be surprising in view of the neuronal pathogenesis observed during congenital infection (*121-123*).

As is the case with HSV-1, CMV latency is characterized by a shutdown of most of the viral activity. The major immediate early promoter (MIEP), which is essential for the expression of the immediate-early lytic gene, is highly repressed during latency via histone methylation, thus blocking viral replication (*124*). Consequently, one major reactivation trigger is chromatin modification, which occurs during the differentiation of monocytes, macrophages and DCs (*117*, *118*). More recently, IL6 stimulation of the ERK

pathway in DCs and the CREB transcription factor have been shown to induce MIEP activation and HCMV reactivation (*125-127*). This induction leads to the production of new viral particles, further dissemination of the virus and activation of a subsequent anti-CMV immune response.

Immune response to CMV infection

Contrarily to HSV-1, which can infect both human and mouse hosts, HCMV is restricted to humans, limiting its analysis to an *in-vitro* and *ex-vivo* context. To skirt this limitation, usage of the murine CMV, a natural mouse pathogen, have been particularly successful both at replicating the hallmark of the human disease and at deciphering the mechanism of resistance to the virus *in-vivo*.

As with HCMV, the murine virus has the ability to infect many types of tissues, including epithelial cells, fibroblasts, monocytes and macrophages (*128*). MCMV can also establish latency in myeloid cells and reactivate following immuno-suppresive or cortisone treatment (*129*, *130*). Both viruses share many features, including their genetic organisation, viral replication and pathogenesis. These similarities make MCMV a practical and powerful tool for the study of the antiviral immune response to cytomegalovirus in a controlled laboratory model.

T cells

As discussed previously, T cells are important for the control of CMV infection. More specifically, CMV infection induces a strong CD8 T cell response, leading to the production of a large pool of cytotoxic T cells (review by (*131*)). Helper CD4 T cells also contribute to the activation of CD8 T cells via the secretion of IL-2 , especially during the latent phase of the infection (*132*, *133*). Following clearance of the virus, this population will contract and form memory T cells. Sylwester et al. have demonstrated that in a HCMV seropositive patient, around 10% of memory CD4 and CD8 T cells are devoted to this virus, showing the high imprint of the CMV on the adaptive immune system (*134*). The CMV specific CD8 T cells numbers tends to increase with age, which results in the

accumulation over time of the CMV-specific memory T cells (*135*, *136*). The capacity of the virus to enter latency and reactivate can explain this. This capacity ultimately leads to a premature "aging" of the T cells compartment (as discussed previously) (*112*).

B cells

CMV infection is also known to induce a humoral response against a variety of antigens. In humans, HCMV infection induces the production of immuglobulin targeting surface glycoproteins B and H, tegument protein pp65/3 and pp150, and the non-structural viral protein EI1 (*137*, *138*). The production of neutralizing antibodies seems to be especially important for restraining the propagation of the virus and the development of systemic or aggravated disease. In a guinea pig model of infection, the presence of neutralizing antibodies increases survival during congenital infection in pregnant mothers (*139*). Thus the production of CMV specific antibodies reduces the severity of the infection.

Innate responses: PRRs, dendritic cells and NK cells

During the early stage of infection, MCMV infects a variety of cells, such as epithelial cells, hepatocytes and hematopoietic cells. Infection of dendritic cells lead to the recognition of viral particles causing the secretion of type 1 IFN (*140*, *141*). Activation of TLR3 and TLR9 by the viral components causes the activation of TRIF and MyD88 respectively, leading to the secretion of IFN-α/β (*142*, *143*). CMV infection also triggers TLR2, which is better known for the recognition of bacterial peptidoglycan (*144*). Indeed, HCMV glycoprotein B and H can bind to TLR2, promoting the secretion of pro-inflammatory cytokines (*145*). Following the recognition of the virus, pDCs and conventional DCs will produce IFN-α/β, which is important for the activation of NK cells (*142*, *146-148*). Moreover, pDCs secrete IL-12, IL-15 and IL-18, which contribute to NK cell proliferation and IFN-γ secretion. Interestingly, although DCs are important for NK activation during MCMV infection, their ablation has limited impact on the capacity of NKs to respond to the virus and does not cause an increase in overall susceptibility (*149*, *150*). This suggests that the activation of NK cells relies on various redundant signals. However

NK cells provide a key barrier to early infection. This will be further discussed below (see section "*Recognition of CMV infection by NK cells in mice*").

NK cells

NK cells are essential and are non-redundant in the resistance to CMV infection. In both human and mouse, NK deficiency, either in absolute number or functional deficiency, causes severe susceptibility to CMV infection (review by (*151*) and (*141*)). During acute infection, NK cells' capacity to produce IFN-γ is crucial to the activation of the immune system and the antiviral response. Moreover, following activation and recognition of the infected cell via the NK receptors, natural killer cells can directly kill the infected target by secreting perforin and granzymes. Viral proteins, or immunoevasins encoded by *m04*, *m06* and *m152* will block the expression of certain MHC-Is, allowing evasion from the T cells of the adaptive immune system(*141*, *152*, *153*). MCMV immunoevasins also interact with NK cell receptors. Recognition of CMV-infected cells by NK cells is discussed in more detail in the next section. Nonetheless, recognition of the virus by the NK cells and the subsequent production of IFN-γ is important for the activation of the T cells response. NK cells are essential actors in the anti-CMV response, bridging innate and adaptive immunity.

Recognition of CMV infection by NK cells in mice.

As discussed previously, NK cells are essential for the resistance to CMV infection. Recognition of infected cells by NK cells, NK activation and cytokine production controls the propagation of the virus and contributes to the extent and quality of the immune response. NK cells directly contact the infected cells via surface receptors to trigger cell death. NK cells express a great diversity of activating and inhibitory receptors that are able to interact with MHC I molecules and viral proteins.

Usage of the mouse model of infection has allowed us to decipher the complexity of the anti-MCMV response to NK cells. The cells express various receptors that recognize

ligands on target cells and modulate their activation, either to increase or to dampen it (reviewed in (*56*)). Inhibitory receptors signal via immunoreceptor tyrosine-based inhibitory motifs (ITIM) located in the cytoplasmic tail of the receptor. This leads to the recruitment of phosphatase containing Src homology 2 domains (SHP1 and 2) to interfere with the activating signal (*154*). This is important, as NK cells must not kill normal cells that express a normal level of MHC-I. In contrast, with the engagement of an activating receptor, a signal is transmitted via the immunoreceptor tyrosine-based activating motifs (ITAM). This time, kinase containing Src homology 2 domains (Syk and ZAP70) are recruited to trigger different signals leading to degranulation and the production of cytokines and chemokines (*154*).

The NKs express many receptors, some of which will be discussed in more detail in the section "*Regulation of NK activation*". Briefly, the CD94-NKG2 family of heterodimer receptors recognize non-classical MHC-I on cells and can activate (NKG2C and E) or inhibit (NKG2A) NK cells (*56*, *155*, *156*). NKG2D can recognize a multitude of ligands leading to the activation of the cell (*157*, *158*). KLRG1 is an inhibitory receptor able to recognize cadherins on cells. In mice, Ly49 receptors are also an important family that is capable of recognizing MHC-1 molecules on cell surfaces, leading to the inhibition of the cells (reviewed in (*56*)). Ly49H is a particularly important receptor since it is able to directly recognize the viral protein m157 (*159*). The Ly49 family will be discussed in more detail in the next section (*Genetics of MCMV recognition by NK cells*).

In mice the Ly49 NK receptors are encoded by C-type lectin-like *Ly49* genes. In humans, the killer Ig-like receptor (KIR) family is responsible for recognition (*160*). Although the molecular nature of these receptors differs between humans and mice, their overall function remains the same. As such, it is the genetic background that dictates the allele of the receptors and the H2 molecule expressed in a given individual, which is a major determinant of the viral recognition of NK cells. The mechanism of viral recognition by NK cells has been greatly improved by the study of various inbred mouse strains that show differential resistance to MCMV infection.

Genetics of MCMV recognition by NK cells

The natural resistance of inbred mouse strains to the MCMV has been a valuable tool to decipher the mechanism that underlies NK cells antiviral response. For example, C57BL/6 mice are naturally resistant to MCMV infection, while BALB/c mice are susceptible. Using classical genetics methods with these two strains, Scalzo et al. were able to map the resistance to MCMV to the new *Cmv1* locus on chromosome 6 located in the NK-cell complex (NKC) region (*161*). This resistance was independent of the mouse major histocompatibility complex (H-2). Subsequent studies with C57BL/6 and DBA/2 mice determined that the activating receptor Ly49H was driving the resistance to MCMV (*162*, *163*). Like other activating receptors, Ly49H signalling is transduced via DAP12, an ITAM. Following infection, Ly49H-DAP12 signalling is necessary to build an adequate resistance to MCMV (*164*, *165*), as engagement of this complex leads to an increased proliferation of NK cells and the production of IFNγ is necessary to build a proper antiviral response.

Although most Ly49 receptors are known to interact with class I molecules, Ly49H does not interact with self-MHC-I, but rather directly recognizes the viral MHC-class 1-like glycoprotein m157 (*159*). When expressed on the surface of infected cells, m157 binds to Ly49H, activating the NK cell (*166*). As such, cells infected with *m157*-gene deficient viruses are not recognized by Ly49H+ NK cells, resulting in a higher viral load (*167*). Recognition of m157 by Ly49H+ NK cells leads to a strong activating response able to counter an inhibitory signal. Indeed, NK cells can kill cells expressing m157, even if the target cells express a normal level of MHC-I, which would normally protect against NK killing (*168*). Interestingly, m157 also binds to the inhibitory receptor Ly49I from 129/J mice (*159*, *168*). Although the virus expresses an MHC-class 1 like protein capable of triggering a strong antiviral response in C57BL/6J mice, the engagement of an inhibitory receptor in 129/J mice allows the virus to escape NK killing. This could explain why the virus kept the expression of m157.

Other wild-type variants of m157 can bind even more inhibitory receptors. The m157 from the G1F wild type strain of MCMV can be recognized by the inhibitor receptor Ly49C from the C57BL/6, NZB and BALB/c strain (*169*). Although $m157^{G1F}$ predominantly interacts with the inhibitory receptor Ly49C over Ly49H, no increase in susceptibility was observed in C57BL/6 NK cells expressing both receptors. Furthermore, the recognition of m157 by Ly49C is regulated in cis by the MHC-I. Indeed, β2m KO mice that do not express the MHC class 1 are susceptible to the virus, allowing for the inhibitory signal from Ly49C to be triggered by $m157^{G1F}$ (*170*). Using BALB substrains that are congenic for different H-2, Pyzik et al. were able to determine that the strength of the signal between the MHC-I and Ly49C vary from one haplotype to another, thus modulating the interaction between m157 and Ly49C (*171*). These studies demonstrate the importance of NK cells in the control of herpesviruses infections. Thus, understanding the mechanism regulating their functions and biology will help to better define HSV-1 and CMV pathogenesis.

Natural killer cell biology

NK cells are defined by the surface markers $CD3^-$ $CD56^+$ in humans and $CD3^-$ $NK1.1^+$ or $CD3^-$ $NKp46^+$ in mice (review in (*172*)). Murine NK cells also express the integrin α_2 CD49b, which can be recognized by the DX5 monoclonal antibody (*173*). The asialoganglio-N-tetraosylceramide (asialo-GM1) is also an NK antigen that is expressed in most species.

As discussed above, NK cells play an important role in the control of CMV infection. However, they were originally known for the capacity to kill tumor cells without the need of prior sensitization (*174-176*). Indeed, NK cells receive both activating and inhibitory signals from target cells. This prepares them to kill a cell unless they receive an inhibitory signal, which puts them in a tolerance state. The MHC-I molecule is one the main molecules that sends that tolerance signal to the NK cells. During infection or in tumor cells, down regulation of the MHC-I leads to a reduction of the inhibitory signal in NK cells,

the subsequent activation of the NK cells and the killing of the target cells. This process is known as the missing self hypothesis (*177*).

NK role in tumor control

NK cells play a central role in the clearance of tumors. Unlike T and B lymphocytes, recognition of tumor cells by NK cells depends on signals delivered by activating and inhibitory receptors (*176*, *178*) and/or stimulation by cytokines such as IL-2, IL-15, IL-18 and IL-21(*179-181*). In humans, there are two major categories of NK cells which are divided according to the potency of their cytokine or cytotoxic response (*182-185*). 1) $CD3^{-}CD56^{bright}$ NK cells are high producers of IFN-γ, which is central to tumor elimination, as IFN-γ allows Th1 differentiation for the direct killing of tumor cells. 2) $CD3^{-}CD56^{dim}$ NK cells efficiently release cytotoxic molecules, directly killing cancer tumors that express low levels of MHC-I (*182*). Manipulating NK cells functions could allow the development of novel anti-cancer therapy. Over 177 clinical trials targeting NK cells were reported over the last four years in North America and Europe (according to www.clinicaltrials.gov).

NK cell development

NK cell development is a well-regulated process whereby they acquire the capacity to rapidly kill a deviant cell, while maintaining tolerance for healthy cells. The development of these lymphocytes occurs in the bone marrow and involves a series of steps of differentiation (Fig. 1.1).

Overview of hematopoiesis

Like other lymphocytes and hematopoietic cells, NK cells originate from hematopoietic stem cells (HSC). These cells can be further subdivided into three subtypes (*186-190*). The earliest progenitors are the long-term HSCs, which are long-lived self-renewal cells capable of long-term reconstitution within the hematopoietic compartment in irradiated mice. Long-term HSCs are pluripotent, as they can give rise to all cells from the

hematopoietic compartment. These cells will then give rise to the short-term HSCs. These cells are also self-renewing and pluripotent. However, their capacity for self-renewal and reconstitution is limited to 8-12 weeks after transplantation in an irradiated individual, hence the name short-term HSC (*190*, *191*).

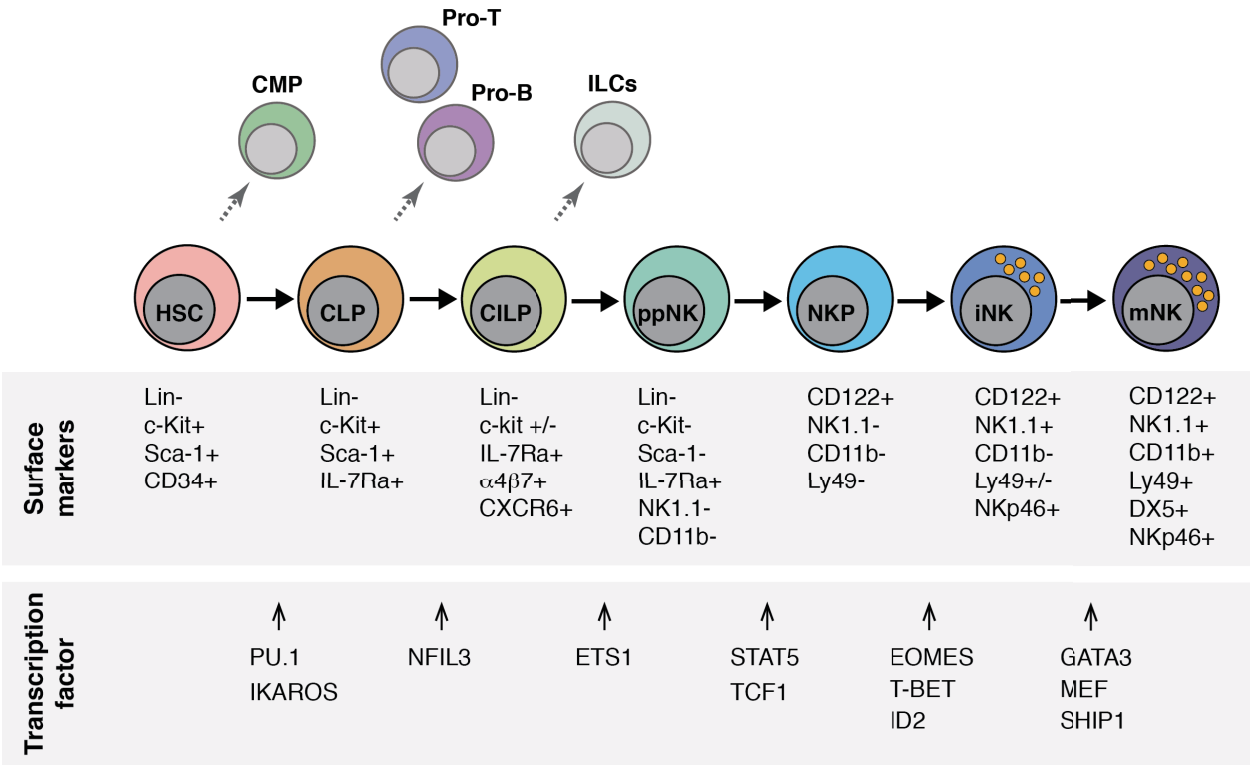

Figure 1.1 – Development of conventional NK cells

The different stages of the NK development are illustrated. The surface marker used to identify them by flow cytometry are listed below. Lineage negative (Lin-) are defined as CD11b-, Gr-1-, B220-, CD3- and Ter119-. The transcription factors involve in the transition between each step are also identified. The dash line represents the bifurcation to another lineage during differentiation process. References: (*173*, *187-192*).

As HSCs continue their differentiation, they produce multipotent progenitors (MPP), losing the capacity for self-renewal, but remaining capable of producing all hematopoietic cell types. From here, MPPs differentiate into two lineage-specific progenitors: the common myeloid progenitor (CMP) and the common lymphoid progenitor (CLP) (*191*). CMPs have the capacity to produce all myeloid cells, including erythrocytes, megakaryocytes, granulocytes and monocytes. Dendritic cells can originate from both CMPs and CLPs. CLPs can produce all lymphocytes (*192*). These cells will give rise to B, T and NK progenitors. Both B and NK progenitors will remain in the bone marrow throughout their development, while T progenitors migrate to the thymus for further specialisation.

Development in the NK cell lineage

From the CLP, NK cell development follow various highly regulated differentiation steps. Although the exact walkthrough of the earliest steps of the NK lineage development is still up to debate, it seems that CLPs differentiate into early innate lymphoid progenitors (EILP), which are able to produce all innate lymphoid cells (ILC1, 2, 3 and NK). EILP use the T-cell factor 1 (TCF1) transcription factor and express the α4β7 integrin as well as CD127 (IL-7Rα) (*193*). The next step would be the common innate lymphoid progenitor (CILP). This progenitor is also restricted to the innate lymphoid cells and cannot produce T nor B cells. CILP is dependent on the expression of the transcription factor *E4pb4* (also known as NFIL3), as KO mice lack that population (*194*, *195*). However, whether the CILP originates from EILP or directly from CLP is still unclear (*195*).

CILP then produces the earliest NK progenitor: the pre-pro NK (ppNK) (*196*, *197*). At this stage, ppNK still do not express CD122 (IL-2Rβ, a subunit of the IL-15 receptor), which is essential for further NK development. However, they express high levels of IL-7Rα. Expression of the transcription factor inhibitor of DNA binding 2 (ID2), which is essential to the development of NK cells and other innate cells, also starts at this stage (*198-201*).

Following this, ppNK develop into NK progenitors (NKP). At this point they start expressing CD122, but lose expression of CD127. The NKP will then develop into immature NK cells (iNK). At this stage, expression of NK1.1 and the transcription factor T-bet and Eomes start, which are necessary for the production of mature NK cells (*202*). From here, iNK become mature NK (mNK) cells and can exit the bone marrow. The transition from iNK to mNK is dependent on the expression of the SH2-containing inositol phosphatase-1 (SHIP1), which regulates PI3K function (a key player in the mTOR pathway)(*203*). At this step, mNK cells express the integrin CD11b as well as high levels of Eomes and T-bet.

NK cell maturation

Mature NK cells are not a uniform population. They can be separated into 4 stages of maturation, according to the expression of CD27 and CD11b (*204*). These stages are defined as followed, from less to most mature: double negative (DN, $CD27^{-}CD11b^{-}$), CD27 single positive (CD27 SP, $CD27^{+}CD11b^{-}$), double positive (DP, $CD27^{+}CD11b^{+}$) and CD11b single positive (CD11b SP, $CD27^{-}CD11b^{+}$). The function of these cells varies, as less mature NK cells have a higher proliferative capacity, while more mature NK cells are more cytotoxic as well as having a higher presence in peripheral sites (*204-206*). Moreover, expression of different Ly49 NK receptors is higher in the mature NKs, as they are ready to respond and attack deviant cells. Indeed, gene expression profiles have shown that DN and CD27 SP NK cells have a higher expression level of cell cycle genes, such as the cyclins, while CD11b SP preferentially express genes involved in secretory pathways and cytotoxicity (*204*). Thus, NK maturation is necessary a fully functional NK cells compartment.

NK cell education

The main mechanism by which NK cells regulate their activation is an interaction with MHC-I molecules. Their ability to recognize the MHC-I molecules has to be validated in order to assure the efficiency of the inhibitory signal and avoid any risk of autoimmunity. During their development, NK cells are “educated” to recognize MHC-I molecules. This

concept is called classical education. It was highlighted by studies of MHC-I or inhibitory receptor deficient mice in which NKs were not autoreactive, but rather hyporesponsive (*207-209*). The developing NK cells have to be able to interact with MHC-I, using the Ly49 molecules for example, in order to be fully mature and become "licensed". This inhibitory signal is required for NK cells to acquire their full effector function. If the NK cells fail this interaction, the result will be a hyporesponsive "unlicensed" NK with a killing ability lower than normal cells (*210*). Education of NK cells can also be achieved via the interaction of the NK inhibitory receptors and non-classical MHC-I molecules (*210*). This process, called non-classical education, can be either MHC-I dependent or independent. For instance, interactions between the non-classical H-2Q1^{a} (HLA-E in humans) and the NKG2A/CD94 inhibitor receptors can induce the education of NK cells (*211*, *212*). The same result can be observed with the MHC-I independent binding of CD48 to the inhibitory receptor 2B4 (*213*). The end result of these interactions is the development of tolerant NK cells capable of cytotoxic and secretory activity.

NK cell diversification

Historically, natural killer cells were considered as a somewhat homogeneous lymphocyte population. However, multiple recent studies have highlighted the diversification of NK cells (as reviewed by Tesi et al., (*214*)). Indeed, diverse type of NK cells can be found in various organs, playing different roles and functions. For instance, conventional NK (cNK) cells are mainly found in the spleen and blood. These cells originate in the bone marrow, where they follow the classical development, maturation and education processes. By contrast, tissue-resident NK cells, such as liver or thymic NK cells, follow a different development path (*215*). Liver NK cells originate from hematopoietic stem cells (HSC) that stayed in the fetal liver during embryonic development (embryonic day 16-17 in mice), at which point most HSC migrate and colonize the bone marrow (*216*). As for thymic NK cells, they also follow a different development path, since they originate from the pro-T progenitors that migrated from the bone marrow to the thymus (*172*, *215*). Although different NK cells share a common function, the tissue resident cells exhibit some unique properties. Liver NK cells express TRAIL, enabling them to directly kill target cells, but do

not express DX5, nor the Ly49 receptors that cNK cells express (*205*, *217*, *218*). Thymic NK cells also express CD127, which blurs the lines between NK cells and the other innate lymphoid cells (*215*, *219*).

NK cells as Innate Immune Cells

In recent years, the classification of NK cells in the context of innate immunity has changed. NK cells are now being considered as a part of the Innate lymphoid cells, a group of lymphoid cells lacking Rag-dependent rearrangement cells that are important for the immune response, especially in the periphery (*220*, *221*). These cells include the NK cells, the ILC1, ILC2 and ILC3. Like NK cells, ILCs quickly produce cytokines following activation, but are mainly found in mucosal tissue and in the periphery (*201*, *220*). ILC1 are IFNγ producers and are dependent on the transcription factor T-bet for their development. Unlike NK cells, ILC1 do not require the transcription factor EOMES nor do they depend on IL-15. ILC2 requires IL-7 and the transcription factor GATA3 for their development. They produce IL-5 and IL-13 following activation. ILC3 are IL-17 and IL-22 producers and are dependent on RORγt during development.

Although the function of ILCs and NK cells might differ, they share the same lymphoid progenitor and require the expression of the γc receptor for their development (also named CD132, a subunit of the IL-2 family of receptors) (*198*, *222*). NK and ILC1 form the group 1 ILCs (*223*). They share a common early development, dependence on T-bet and the capacity to produce IFNγ. This can sometimes make them difficult to distinguish, especially during inflammation in peripheral organs.

NK cells regulation by IL-2 and IL-15

Cytokines, such as IL-2 and IL-15, play a central role in modulating NK cell biology (*224*). Both cytokines bind the IL-2Rβ and γc receptor subunits. Soluble IL-2 binds IL-2Rα, IL-2Rβ and γc complex on the NK cell surface. Traditionally, IL-15 is trans-presented by IL-

15Rα expressed on the surface of activating cells, such as dendritic cells and monocytes. The IL-15/IL-15Rα complex then binds the γc/IL-2Rβ receptor on the surface of the NK cells (*225*, *226*).

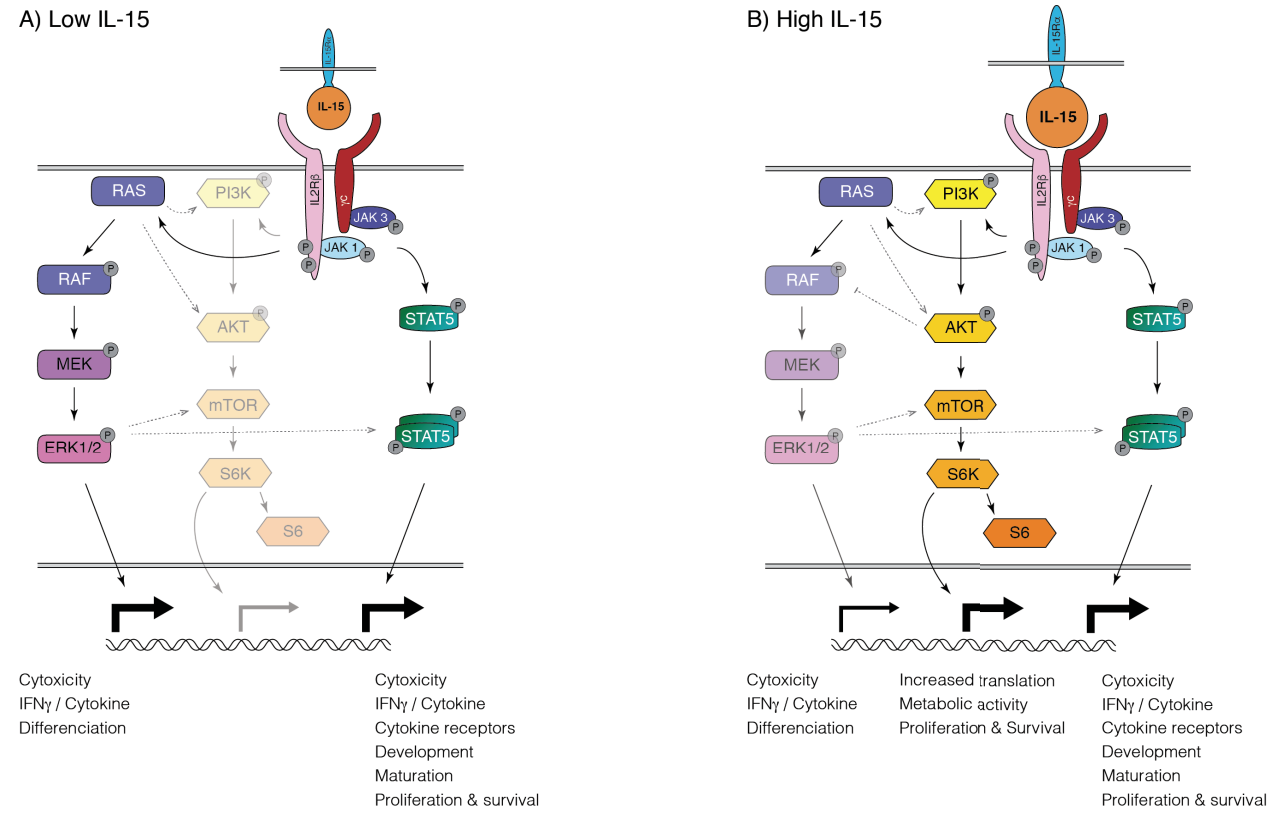

Figure 1.2 – IL-15 pathway in NK cells

Low and high dose of IL-15 have different effects on the NK cells function. A) At a low IL-15 dose, the MAPK pathway and the JAK/STAT5 pathway are activated, while phosphorylation of the mTOR pathway is low. Engagement of these pathways also result is cross-activation (dashed arrows). B) At high IL-15 dose, the mTOR pathway is activated, leading to an increase in translation and metabolic activity. Cross-inhibition between AKT and RAF occurs at high doses (dashed blunted line). The size of the angled arrow illustrates the level of the gene transcription and its effect on NK function for each pathway at the different conditions. References: (*230-235*)

Signalling downstream of the IL-2 and IL-15 receptors triggers three main pathways crucial for NK cell biology. Following cytokine-receptor interaction, phosphorylation of the receptor tails engages: i) MAPK, ii) PI3K-mTOR and iii) the JAK1/3-STAT5 pathways (*224*, *227*, *228*) (Fig. 1.2). The activation and phosphorylation of the Ras-Raf-MEK1-ERK-1/2 lead to the expression of various genes, which in turn leads to increasing proliferation, IFN-γ production and activation of NK cells (*179*, *229*). The phosphorylation of JAK1 and JAK3 leads to the phosphorylation of two STAT5 molecules; STAT5A and STAT5B, which dimerize to form the STAT5 complex and translocate to the nucleus to induce gene transcription (*230-233*). Finally, the activation of the serine-threonine kinase complex mTORC1 pathway promotes various anabolic processes, including protein and lipid synthesis, while inhibiting catabolic processes such as autophagy (*234-236*).

Although IL-2 and IL-15 share similar receptors and signalling pathways, their function is not entirely conserved. The temporal expression of IL-2 and IL-15 during NK cell development, maturation and activation explains the different functions performed by each cytokine (*224*, *237-239*). Although not exclusive, the predominant role of IL-15 is in NK homeostasis and development, while IL-2 is more involved during inflammatory and immune response (*224*). Moreover, the dosage of IL-15 determines the pathway engaged; low doses of IL-15 trigger phosphorylation of STAT5, thereby resulting in an increase in viability, whereas a high concentration of IL-15 triggers the mTOR metabolic pathways (*240*).

The affinity of the IL-15/ IL-15Rα complex for the IL2Rβ and γc chain is greater and stronger than the receptor affinity for soluble IL-2. Although both IL-2 and IL-15 induce the expression of similar genes, cytokine concentration and receptor availability influence gene expression (*241*). As such, temporal expression of the IL-2Rβ, γc and the IL-2Rα following stimulation of the NKs dictates the function of IL-15 and IL-2. Initially, high expression of IL-15Rα, IL-2Rβ and γc on the cell surface is coupled with low expression levels of IL-2Rα, making IL-15 a stronger and more efficient inducer of NK activation, proliferation and survival than IL-2 (*237*, *242*, *243*). Interestingly, following NK cell

activation by the IL-15/IL-15Rα complex, the receptor IL-15Rα is cleaved by the presenting cells (e.g. DC). The complex IL-15/IL-15Rα is internalized by the NK cells, leading to a reduction in STAT5 phosphorylation (*244*). The NK cells can later recycle the IL-15/IL-15Rα complex by sending it back to its surface to be presented in *cis* and stimulate its own survival and proliferation.

Control of NK cell homeostasis

Stimulation of NK cells by cytokines, such as IL-2 and IL-15, engage in a variety of cascades involved in NK cell biology and homeostasis. For instance, activation of STAT5 is central to the survival and development of NK cells. Mice deficient in STAT5 show significantly reduced NK numbers (*231*, *245*, *246*). Later studies have shown that IL-15-induced phosphorylation of STAT5 increases the expression of the anti-apoptotic MCL-1 and blocks the expression of pro-apoptotic BIM and NOXA (*247*, *248*). The IL-15/STAT5 signalling pathway is also regulated by ID2, a transcription factor involved in NK development and maturation (*200*). *Id2*$^{-/-}$ NK cells have impaired NK development and increased apoptosis leading to an NK deficiency, caused by an upregulation of the E-protein SOCS3, which causes a reduction of STAT5 phosphorylation and NK survival (*199*). SOCS3 mediates the ID2/STAT5 pathway, which in turn regulates NK development, homeostasis and survival. STAT5 has also been shown to regulate NK cell maturation. In STAT5 deficient mice, NK cells number are decreased and the remaining NK cells exhibit an accumulation of immature $CD27^{-}CD11b^{-}$ and $CD27^{+}CD11b^{-}$ populations (*249*).

Cytokine stimulation of NK cells also triggers the mTOR pathway, which is central to NK development and homeostasis. NK cell specific deletion of mTOR affects normal NK cell development, leading to a severe loss of NK cells in peripheral organs (*240*). Presumably, this loss is a result of the requirement for mTORC1, which is involved in robust proliferation during the immature NK cell stage. Meanwhile, residual NKs present a

substantial block in differentiation. Similarly, the deletion of PDK1, an upstream mTOR kinase, causes severe defects in NK cell development (*250*). Interestingly, a recent report showed that tuberous sclerosis 1 (Tsc1)-dependent regulation of mTOR is critical for the regulation of proliferation in immature NK cells undergoing extensive proliferation to generate a pool of peripheral NK cells (*251*). Without this regulation, immature NK cells seem to die with elevated mTOR activity, leading to a decrease in NK cell frequency during development by activation-induced apoptosis. Thus, Tsc1-dependent negative regulation of mTOR provides a checkpoint during NK cell development.

mTOR pathway regulation of ribosome biogenesis and function

The activation of the mTOR pathway and the mTORC1 complex directly controls ribosome function. mTORC1 activates the ribosomal protein S6 Kinase (S6K), which in turn phosphorylates ribosomal protein S6, a component of the 40S ribosome (*252-254*). Consequently, activation of S6K increases ribosome biogenesis, leading to an increase in protein synthesis. The phosphorylation of S6 and the increase in ribosomal activity stimulate both cell growth and size, thus reinforcing the importance of the mTOR pathway in cell homeostasis (*255*).

Following activation of mTOR and S6K, the Eukaryotic initiation factor 4E-binding protein (4EBP) is phosphorylated (*252*, *256*). 4EBP initiates the cap-dependent translation by the eukaryotic initiation factor 4E (eIF4E), thus increasing RNA translation and ribosomal activity (*257*). Thus, mTOR is an important regulator of protein synthesis, both via a direct control of ribosome biogenesis and the modulation of RNA translation.

Regulation of mTOR by Transforming Growth Factor-β

Transforming growth factor–β (TGF-β) is one of the best-known immunosuppressive cytokines that maintains immune homeostasis and prevents autoimmunity (*258*). Recently, Viel et al., demonstrated that the anti-proliferative and anti-inflammatory aspect of TGF-β on NK cells is mediated by the inhibition of the mTOR pathway (*259*). In this study, NK cell specific TGF-βR2 deficient mice exhibited enhanced mTOR activity and

cytotoxic activity in response to IL-15. This was further confirmed by the shared gene expression signature involved in metabolism, proliferation, and effector functions of NK cells treated with TGF-β or rapamycin along with IL-15 stimulation. Although the exact molecular mechanism remains unclear, this study suggests the involvement of the SMAD pathway in the inhibition by TGF-β of the NK differentiation.

Interestingly, neither development nor homeostasis were affected in NK-TGF-βR2$^{-/-}$ mice (*259*). This is inconsistent with a previous study showing an increase in NK numbers and maturation in the spleen and bone marrow of transgenic mice expressing a dominant negative form of TGF-βR2 under the control of the CD11c promoter (*260*). SMAD phosphorylation indicated that NK cells from both strains were unresponsive to TGF. The discrepancy in NK cell phenotypes might be due to the different timing of the abrogation of TGF-β signalling, e.g., the CD11c promoter turns on earlier than does the NCR1 promoter. Nonetheless, suppression of TGF-β signaling in NK cells using the respective models enhanced either antiviral or anti-tumor immunity (*259*, *260*).

The mechanism of NK cell activation

Whether it is via recognition of infected or tumoral cells, or following cytokine stimulation, NK cell activation involves various pathways leading to the production of cytokines and the triggering of the killing activity. Engagement of MAPK is particularly important for the cytotoxic function of NK cells. Activation of the NK activating receptor NKG2D leads to the phosphorylation of ERK2 and JNK1, causing the reorganization of microtubules and the polarization of granules to the cytotoxic synapse (*261*, *262*). Moreover, co-activation of NK cells with IL-12 and the activating receptors 2B4 or NKG2D increase phosphorylation of the Vav-1 and ERK pathways, leading to an enhanced killing activity (*263*).

mTORC1 activation is indispensable for the induction of NK cell effector functions. During poly(I:C) induced inflammation *in vivo*, NK cells upregulate the mTORC1 activity, increase

in cell size and increase their glucose uptake, all of which are characteristic of glycolytic reprogramming (*240*, *264*). Notably, treatment of NK cells with the mTOR inhibitor rapamycin disturbs their effector functions during poly(I:C) induced inflammation *in vivo*. This treatment resulted in reduced expression of IFN-γ and granzyme B (*240*, *264-266*). This supports the idea that mTORC1-mediated metabolic reprogramming is linked to NK cell effector function. Furthermore, rapamycin treatment in MCMV-infected mice also affects NK cell effector function and proliferation, leading to an elevated viral burden (*240*, *266*).

Regulation of NK activation

We previously extensively discussed the role of different activating and inhibitory receptors in the regulation of the anti-MCMV functions in NK cells. Ly49 receptors in mice and KIRs in humans play a central role in the inhibition and activation of NK cells during infection via the recognition of MHC-I molecules or viral protein. However, NK cells express various receptors responsible for their activation in other contexts.

NKG2D is a C-type lectin glycoprotein expressed in the surface of human and mouse NK cells which are part of the NKC. Its expression is not limited to NK cells, as CD8 T cells, TCRγδ T cells, macrophage and NKT cells can also express the receptor (*267*). NKG2D recognizes various ligands that resemble MHC-I, which are upregulated during transformation or infection (*268*). These ligands are present in a large variety of tumors and infected cells. Multitudes of ligands bind to NKG2D at different affinities, which in turn can modulate the level of activation of the NK cells (*157*, *158*). NKG2A is another C-type lectin receptor that forms a heterodimer with CD94. After binding the non-classical HLA-E molecule in human or H-2Q1^{a} in mice, NKG2A/CD94 triggers the inhibition of NK function (*155*, *156*).

The killer cell lectin-like receptor subfamily G member 1 (KLRG1) is a C-type lectin receptor that is coupled with an ITIM in its intracellular domain (*269*). KLGR1 binds the E, N and R-cadherin, leading to the inhibition of the IFN-γ production and cytotoxic activity

by NK cells (*270*, *271*). Its expression is increased during MCMV infection, which suggests that KLRG1 has a role in the cessation of NK function after activation.

2B4 (also known as CD244) is part of the immunoglobulin superfamily and is expressed on various cell types, including NK cells (*272*). Its ligand is CD48, which is expressed on hematopoietic cells. 2B4 has a dual activating and inhibitory function. The exact nature of the dual function remains unclear. Indeed, engagement of 2B4 with antibodies or CD48 activates NK cells (*273*). However, in patients with immunodeficiency X-linked lymphoproliferative disease with a mutated signaling adaptor protein (also known as SAP, downstream of 2B4), stimulation of 2B4 causes inhibition of NK cells (*274*, *275*).

NK cells are also capable of antibody-dependent cell-mediated cytotoxicity (ADCC) via the expression of the Fc receptor CD16 (FcγRIIIa) (*276*). Binding of CD16 causes not only killing of the target cells, but also increases production of IFN-γ and expression of IL-2Rα (CD25) (*277*). This efficient cytotoxic ability of NK cells shows potential for the development of novel therapeutic antibodies.

NK cell memory

Recently, the dogma that immunological memory is only elicited by adaptive immunity has been challenged by several studies demonstrating that enhanced response upon re-exposure to the same antigen can be generated by cells of the innate immunity such as NK cells (*278*, *279*). During the last few years, several findings regarding memory or memory-like NK cells prompted the study of epigenetic modifications related to the long-lasting effect and rapid induction of effector functions by NK cells (*280*, *281*). To this day, three stimuli are known to generate memory-like NK cells: hapten, viral pathogens (such as cytomegalovirus) and cytokine cocktails (Fig 1.3).

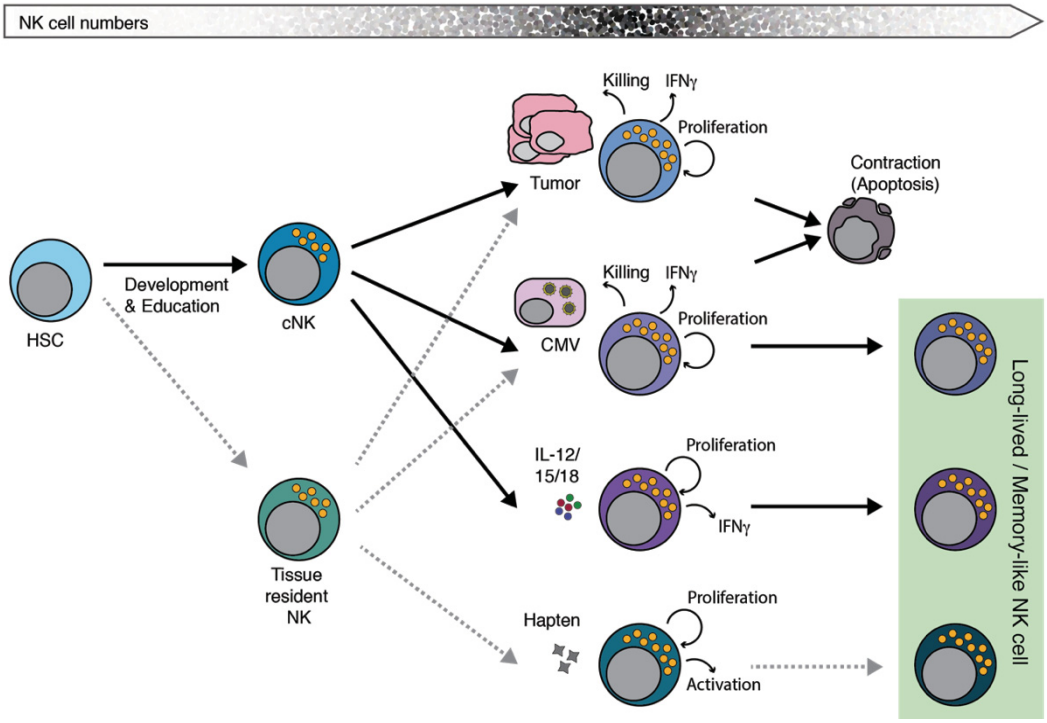

Figure 1.3 – Development, activation and memory of NK cells

Hematopoietic stem cell give rise to conventional NK cells and tissue resident NK cells. After stimulation and/or recognition of a threat, NK cells activate, proliferate, produce cytokine and/or kill the target cells. This also lead to an increase of the NK compartment. Following the clearance of the tumor or the infected cells, the NK cell compartment contract via apoptosis, to return to its size prior to the stimulation. CMV, cytokine cocktail and hapten can also generate memory-like (long-lived) NK cells, which can then be easily reactivate.

Hapten-induced memory NK cells.

An original work on memory NK cells employed contact hypersensitivity in which hapten sensitization induced long-lived hepatic NK cells with antigen-specific memory responses in mice lacking both B and T cells (*282*). A later study showed that memory NK cells

mediate contact hypersensitivity caused by hapten monobenzone (*283*). The generation of the memory NK cells requires the activation of NLRP3 and the inflammasome in tissue resident macrophages.

CMV-induced memory NK cells.

Clear evidence was obtained in the model of murine cytomegalovirus (MCMV) infection in which Ly49H+ NK cells expanded in response to the m157 MCMV glycoprotein expressed on infected cells, and formed a memory pool of NK cells following a contraction phase (*284*). After the primary infection, the Ly49H+ NK cells persist for months and display enhanced IFN-γ production and degranulation upon secondary MCMV infection. More recently, virus-specific NK cell memory responses have also been observed in infected or vaccinated immunocompetent rhesus macaques (*285*). Analogous to MCMV infection, long-lasting NK cells are also observed upon human CMV (HCMV) infection. These long-lived cells are called memory-like NK cells or adaptive NK cells due to their ambiguous antigen specificity.

A long-lasting NK cell subset was initially characterized by the expression of NKG2C and CD57 in individuals serologically positive for HCMV (*286*). The expansion of the NKG2C+ NK cell subset was observed in response to acute infection or reactivation of latent HCMV (*286-290*). More recently, the HCMV induced memory-like NK cells were further defined by the lack of expression of the FcεRIγ chain, one of the adaptor proteins that associates with CD16, and the additional loss of SYK kinase expression, a molecule downstream of CD16 signalling (*291*). Although there is a complete shutdown of FcεRIγ, SYK expression remains elusive. The NK cell subset shows enhanced ADCC against target cells coated with autologous serum from HCVM-infected individuals (*292-295*). Thus, NK cells can broaden the recognition of target cells using ADCC as the diversity and specificity of ADCC is determined by the antigen recognized by the antibody.

Cytokine-induced memory-like NK cells.

Lastly, memory-like NK cells were generated by *in-vitro* exposure of either human or mouse NK cells to inflammatory cytokines IL-15/IL-12/IL-18 (*296*). These cytokine-induced memory-like (CIML) NK cells acquired the ability to elicit enhanced IFN-γ production when stimulated with the same cytokine cocktail up to 4 months later (*297*, *298*). The subsequent CIML NK cell response is mediated by the IL-2Rα-STAT5 pathway. Following the pre-activation with IL-12, IL-15 and IL-18, CIML NK cells quickly respond to a minimal concentration of IL-2, in a CD25/STAT5 dependent manner (*298*, *299*). The increased STAT5 phosphorylation is followed by high proliferation and IFN-γ production by the CIML NK cells. This type of memory-like NK cell has shown a high potential for immunotherapy: Adoptive transfer of cytokine-induced memory NK cells into tumor-bearing mice induced greatly enhanced anti-tumor response (*300*) and is currently being tested in a Phase I clinical trial for the treatment of AML patients (NCT01898793).

The enhanced capacity to produce IFN-γ by the cytokine-induced memory NK cells is maintained after homeostatic expansion in lymphopenic Rag- and common γ-chain-deficient recipient mice (*301*), suggesting that the memory property is stably heritable. A study showing epigenetic imprinting of the IFN-γ locus in the CIML NK cells demonstrated stable hypomethylation of the *IFN-γ* conserved non-coding sequences-1 (CNS-1) region, in contrast to a completely methylated CNS-1 region in naïve NK cells (*302*). This CNS-1 displays binding sites for T-bet, STAT4, NF-kB, and NFAT and is also found hypomethylated in Th1 cells possessing the ability to stably express IFN-γ (*303*). This indicates that CIML NK cells acquire enhanced effector functions through epigenetic remodeling similar to that found to occur in Th1 cells.

Genetic approach to the immune response

As discussed in previously, genetic approaches have been extremely useful in deciphering the different mechanisms used by the immune system and NK cells to control

viral infections. Indeed, *in-vitro* cell cultures and the mouse model involving gene inactivation allow for the study of the importance of NK cells during infection.

Human studies

Studying the genetic cause of an infectious disease in humans can be quite difficult. HSV-1 and HCMV are very prevalent viruses that either cause mild symptoms or are asymptomatic. The most aggravated cases are usually observed in patients with rare and severe immunodeficiency (*78*, *151*). The study of those patients has allowed for a better understanding of HSE and genes that are important for lymphocyte and NK development. As the type of sample acquired (mainly blood) is limited in human patients, confirmation of a candidate gene has to be done in *in-vitro* cell culture or knock-out mice. Recently, the development of CRISPR/Cas9 technology, which accelerates the generation of genetic models, has facilitated this process (*304*).

The sequencing and annotation of the human genome has allowed the emergence of novel genetic methods, such Genome-wide association studies (GWAS), which do not rely on prior hypotheses related to the genes of interest. Such a method allowed for the association of the IFNL3 variant in the clearance hepatitis C virus following ribavirin and IFN-α treatment (*305*-*307*). However, the extremely high prevalence of HSV-1 and HCMV makes the success of GWAS studies harder to achieve, due to high numbers of confounding variables.

More recently, the increased availability and reduced cost of next-generation sequencing has made it possible to use it to pinpoint mutations that cause viral susceptibility. Loss-of-function mutations in IFN regulatory factor 7 (IRF7) were successfully identified via this approach in a child suffering from life-threatening influenza that compromised IFN-α/β response (*308*). This method is currently actively applied in clinical patients affected with severe herpesviruses infection.

Studies of human patients afflicted with severe diseases have been extremely useful to understand different immune mechanisms that are important for host resistance to viral infection. However, this approach is limited by the natural occurrence of severe mutations in the population, which tends to be extremely low. For instance, there is only 1 case of HSE per ~500,000 individuals per year worldwide (*23*). The type of tissue available and the amount and variety of experiments available is also restrictive when working with human patients. Thus, the usage of the mouse model complements and extends the research of genetic factors that are important for the immune response to viral infection.

The mouse model

Usage of the mouse model has furthered understanding of the importance of various genes in the immune response to pathogens. This model permits for the evaluation of the pathogenesis in various organs at different time points, which is not possible in human studies. Moreover, many genetic and immunological tools are available for the study of host resistance in mice. Thus the mouse model is a powerful tool for the study of the immune response. Indeed, the mouse model tracks infection via various routes, which can target specific aspects of disease from a variety of pathogens. Numerous laboratory inbred strains are available that display either resistance or susceptibility to different pathogens.

The ability to directly question the role of a gene in a controlled environment was instrumental to the advancement of our knowledge of the immune system. The candidate gene approach, or reverse genetic approach, in which a gene of interest is altered, is a powerful method of directly investigating the role of a specific gene (*309*). By targeting specific genes and inactivating them, it is possible to assess the importance of a given gene in various infectious contexts and its role in the development of immune cells. This can be achieved by introducing a specific DNA sequence into oocytes. It can also be accomplished by targeting a gene in the embryonic stem cells to create a knock-out

(ablation of expression) or to produce a knock-in (alteration of the expression) (*310*). Recently, the development of CRISPR-Cas9 technology, which can insert mutations at the zygote level, has facilitated the production of mutated mice, resulting in the generation of animals carrying mutations on both alleles within weeks (*311*).

The reverse genetic approach is a powerful method of dissecting and building a better understanding of different pathways and genes that are important for host resistance. This method was instrumental in the discovery and understanding of many pathways involved in HSV-1 and MCMV immune responses. The reverse genetic approach, however, is limited by prior knowledge of the gene and the topography of its genetic region (*312*). However, this is an ideal method to complement and confirm linkage analysis or forward genetic studies.

Forward genetics

Forward genetics is a powerful method to discover novel genes important for a given disease. Instead of testing the role of a specific gene in a disease or infection (candidate gene approach or reverse genetic), forward genetics takes advantage of natural or chemically induced phenotypic variation and genetic analysis using crosses of mice to discover new genes or new alleles at the source of the phenotype of interest (*313*, *314*). This approach does not require a prior hypothesis, as any gene can potentially be causing the phenotype.

The use of inbred mouse strains has been particularly useful to understand the genetics of MCMV resistance. The natural variation of the resistance of different inbred strains can be used to map and identify important loci containing potential candidate genes that can then by targeted for inactivation (*315*). Indeed, the variation in viral susceptibility of the C57BL/6, DBA/2, BALB/c and MA/MY mouse strains, among others, have been exploited in various linkage analyses for MCMV resistance (*162*, *163*, *316*, *317*). The usage of F2 crossed between two strains exhibiting polymorphic markers and quantitative trait loci

(QTL) mapping have been instrumental to the discovery of various genes involved in the NK response to MCMV, including the NKC locus, which was discussed above.

Recombinant congenic strains (RCS) can also be used for host resistance analysis. The RCS consist in a panel of sub-strains originating from two parental mouse strains, such as A/J and C57BL6, that were intercrossed and backcrossed to produce mice carrying different fragments of the parental genome (around 12.5% of one strain and 87.5% of the other) (*318*). In our group, we successfully used RCS mice to map resistance loci for coxsackievirus B3 and influenza (*319*, *320*).

Mutagenesis of the mouse genome

As the usage of inbred mice strains is limited by their diversity, chemical mutagenesis offers a powerful alternative to generate mutated animals carrying genetic lesions in any type of gene. It allows for the discovery of novel genes and pathways involved in host resistance. The alkylating agent N-Ethyl-N-Nitrosourea, or ENU, is considered one of the most potent mutagens of the mouse germline (*321*). Indeed, ENU has the ability to induce more mutations per locus (~$150x10^5$) than X-rays ($13x10^5$ to $50x10^5$) or chlorambucil (~$127x10^5$) (*322-324*). Both X-rays and chlorambucil produce complex lesions in the genomic DNA, such as deletions or inversions, while ENU has the advantage of introducing single point mutations. It preferentially mutates spermatogonial stem cells, thus facilitating the propagation of the mutation. When coupled with a rigorous breeding scheme and infection protocol that facilitates the isolation of a phenovariant mutation, the usage of this mutagen can result in the generation of a monogenic model of infection.

The random nature of ENU mutagenesis results in the introduction of a mutation in any region of a gene (*325*). A gene could be mutated in two different ENU studies in ways that impact different sections and which could reveal the multifunctional nature of the protein. Although mutations are most frequently AT to TA transversions, ENU mutations are randomly distributed across the genome at a frequency that depends on the ENU

dosage and the mouse genetic background (*326*). It has been estimated that male C57BL/6 mice (G0) receiving an intra-peritoneal injection of ENU (90 mg/kg) over three weeks and mated to wild-type female mice produce G1 animals carrying on average one/two DNA variants per Mb and 90 exonic ENU-induced mutations. Second-generation (G2) progeny of these mice inherit about 45 ENU-induced exonic mutations, which are all heterozygous. For a recessive screen, two of the G2 mice are back-crossed to their G1 father, resulting in third-generation (G3) progeny bearing on average five homozygous protein-coding mutations (*327*). Then, large cohorts of G3 mice are tested to identify the phenotypically distinct mice most likely to bear a large-effect mutation, which can be first localized by genetic mapping and sequencing.

Working with a pathogen can however present challenges, as the infection can result in a complex disease involving more than one gene. Thus the identification of the ENU mutation causing the viral susceptibility can be challenging. The usage of new technologies, such as next-generation sequencing for exome sequencing, will help to identify the ENU mutations that cause phenodeviance (*328*).

The three main advantages of this approach for novel genes discovery are: 1- point mutations induced by ENU are random and can therefore alter any gene; 2- the spectrum of possible phenotypes is broader and more profound than what would normally be tolerated by natural selection; 3- ENU mutations can alter individual protein domains and splicing products such that multiple functions of genes can be separately revealed. Thus, an ENU mutagenesis platform coupled with an efficient phenotyping system allows for the discovery of genes that are important for host resistance.

The possibilities that ENU mutagenesis offers have resulted in a worldwide effort to discover genes and pathways crucial to cancer, development, neurology, metabolism, immunity and host resistance (*329*). Many groups have used this approach, resulting in the generation of hundreds of phenovariant mouse pedigrees. For example, at the time of writing, the Mutagenetics database, reporting ENU efforts at the UT Southwestern

Medical Center and the Australian Phenomics Network, had found over 260 genes mutated by ENU that cause a phenotype (*330*, *331*). In our more recent ENU attempt, our research group identified more than 8 genes involved in host resistance to cerebral Malaria (*332*-*335*), Salmonella (*336*, *337*) and HSV-1 (*66*, *338*). In this thesis, I will also present two more ENU pedigrees susceptible to HSV-1 and MCMV infection.

Thesis rationale, hypothesis and objectives

Rationale

CMV and HSV-1 are extremely prevalent viruses that can establish life-long latent infection (*16*, *17*). Infections result in a variety of clinical syndromes, ranging from asymptomatic infection to severe, if not lethal, infection in individuals with an immature or compromised immune system. In these individuals, CMV infection can cause fever, mononucleosis and even neurological lesions as significant as blindness and mental retardation (*108*). HSV-1 infection in infants can result in fulminant eruptions and lethal herpes simplex encephalitis (*2*). As such, HSV1 is the leading cause of viral encephalitis in the developed world.

Treatment options for the management of organ specific or disseminated disease are limited to compounds that target the viral polymerase, have long-term toxicity and inevitably lead to the emergence of drug resistance (*29*, *339*). These shortcomings together with the increasing prevalence of genital HSV1 (*340*) and a corresponding rise in neonatal infection, an aging population and technological advances in health care create an urgent need for the development of alternative therapeutic strategies. A possible approach to filling this gap is the investigation of host genes that are critical to the outcome of host-pathogen interactions. Indeed, a large body of clinical, epidemiological and experimental data has demonstrated the role of inheritable host factors in governing susceptibility to infectious diseases (reviews in (*341*)). Further, chemical mutagenesis of the mouse germline with N-Ethyl-N-Nitrosourea has been proved to be a powerful tool to screen and identify new mutations critical to immunity to infection. ENU allows for the discovery of novel genes or pathways involved in host resistance; the discovery of novel functions on known genes; and the dissection of functional domains of genes involved in viral infection.

Hypothesis

The severity and outcome of CMV and HSV1 infections are dependent upon host response to infection. I hypothesize that random chemical mutagenesis in mice followed by high-through phenotyping for susceptibility to viral challenge represents a systematic approach to investigate genes that are critical to the outcome of infection. Identification and functional characterization of such genes should provide new insights into the molecular mechanisms underlying viral pathogenesis and therefore facilitate the design of innovative and effective interventions for improved outcomes.

Objectives

Aim 1

The first objective of this thesis is to initiate an ENU mutagenesis platform to perform recessive screens to identify deviant mouse pedigrees susceptible to HSV-1 and MCMV. We aim to develop a high-throughput infection platform for HSV-1 and CMV allowing the phenotyping of high numbers of animals. To do so, a mouse model of infection for MCMV and HSV-1 infection has to be developed and tested. Deviant families with a progeny showing a susceptibility of 20 to 25% would then be selected for further analysis.

Aim 2

The second objective is to identify and characterize the ENU mutation causing HSV-1 susceptibility in a deviant pedigree, using next-generation sequencing and genetic mapping. We selected the Keagan pedigree, a family susceptible to HSV-1 infection identified during the completion of Aim 1. Following the identification of the mutation, we aim to decipher the role of the mutated gene in the immune response to HSV-1 and its function in the immune system.

Aim 3

The third objective is to identify the mutated gene causing MCMV susceptibility in the ENU pedigree Glynn (identified in Aim 1), using genetic mapping and exome sequencing. Once identified, we aim to characterize the gene, its function in MCMV susceptibility and the immune system. We also aim to understand the importance of the mutation in NK cell biology, as these cells are essential to host resistance to MCMV.

Bridging statement from Chapter 1 to Chapter 2

Host genetics play an important role in resistance to HSV-1 and CMV. Since analysis of the human patient affected with severe herpesviruses infection relies on rare cases and involve severe immunodeficiency, the mouse model of infection is a powerful alternative to understand the mechanism involved in the antiviral response. Indeed, usage of inbred strains showing various levels of susceptibility has allowed to decipher the genetic structure of host resistance to complex diseases. To discover novel genes and pathways involved in susceptibility to HSV-1 and MCMV, we have used ENU-induced mutagenesis. Coupled with robust a breeding scheme and phenotyping platform, this method allows generation of monogenic model of infection carrying mutations critical to the antiviral response. During my Ph.D., we have produced over 261 G1 ENU animals and tested more than 4200 G3 progenies for resistance to HSV-1 and MCMV. Chapter 2 describes the development of the ENU platform, including the generation of the high-throughput infection models and the identification of 7 deviant pedigrees.

Chapter 2 – Strategies to establish an ENU mutagenesis pipeline to identify novel herpesviruses susceptibility genes.

Gabriel André Leiva-Torres[1,2], Benoit Charbonneau[1,2], Michael Leney-Greene[1], Mathieu Mancini[1,2], Grégory Caignard[1,3], Angela Pearson[4] and Silvia M Vidal[1,2]

Affiliations: [1]Department of Human Genetics, Centre for the Study of Host Resistance, McGill University, Montréal, Quebec, Canada. [2]McGill University Research Centre on Complex Traits, McGill University, Montréal, Quebec, Canada. [3]Université Paris-Est, École Nationale Vétérinaire d'Alfort, UMR1161 Virologie, Maisons-Alfort, France. [4] INRS-Institut Armand Frappier, Laval, Quebec, Canada.

Parts of this manuscript are in preparation for submission to the journal G3 (Genes, Genomes, Genetics)

Work from the mutagenesis screen and applications of the SNP mapping panel published in:

Genes Immun. 16, 261–267 (2015)

PLoS Pathog. 9, e1003637 (2013)

PLoS ONE. 7, e31012 (2012)

Abstract

Herpes viruses infect a majority of the population but only a portion of exposed individuals manifest severe clinical disease. Host genetics is an important determinant of the onset, severity and outcome of pathogen challenge. The use of inbred mouse strains has been particularly useful for understanding fundamental mechanisms of infectious disease pathogenesis, including the impact of host genetics. Here, we have developed an ENU mutagenesis platform based on the generation of three-generation pedigrees of mice carrying homozygous mutations followed by a high-throughput infection pipeline that allows us to screen numerous mice for susceptibility to either cytomegalovirus (CMV) or herpes simplex virus 1 (HSV-1) infection. We also developed genotyping tools for efficient genetic localization of the ENU mutation. We validated our mapping tools by identifying a novel mutation on the oculocutaneous albinism II gene that causes a pale coat colour and red eye phenotype. We also tested more than 264 pedigrees and 4200 progeny for viral susceptibility. Doing so, we have generated and identified six ENU pedigrees exhibiting susceptibility to HSV-1 infection and one to CMV. These families can then be used to better understand the mechanism of altered host responses against viral infection.

Introduction

Host susceptibility to infection and viral pathogenesis are highly variable, leading to rapid clearance of the pathogen burden in certain individuals or the development of severe disease in others. The resulting disease symptoms are mediated by intricate interactions between the pathogen's virulence factors, the genetic makeup of the host, and the environment. Despite this complexity, the study of Mendelian (single gene) genetic variants in humans and mice has provided important new insights into mechanisms of host resistance to infection. This forward genetic approach begins with the observation of a phenotype variation and proceeds with the identification of a causal genetic change (mutation) that allows the revelation of entirely new genes and mechanisms. The goal of

this process was to illuminate our understanding of the host response against Herpes simplex virus 1 (HSV-1) and cytomegalovirus (CMV).

HSV-1 and CMV are two large DNA viruses from the *herpesviridae* family that infect and establish latency in a large proportion of the human population. Although these pathogens produce mild to no symptoms in the majority of healthy individuals, primary infection or reactivation can cause severe diseases in patients with an immature or compromised immune system (graft recipients, HIV-infected patients, cancer patients and the elderly) (*1*, *2*).

HSV1 acute infection in healthy individuals usually provokes simple cutaneous eruptions. However, if untreated, infection in infants can cause fulminant eruptions and lethal herpes simplex encephalitis (HSE, review by Kimberlin, (*2*)). As such, HSV1 is the leading cause of viral encephalitis in the developed world. Various studies of HSE cases have shown that single gene defects can produce a severe and/or lethal infection. Mutation in either TLR3, UNC93B, TRAF3 or TBK1 can cause herpes simplex encephalitis (HSE), a severe form of HSV-1 that affects the central nervous system (*54*, *55*, *82*, *84*). The mouse model has been an essential tool that has allowed scientists to understand the genetics of host resistance to herpesviruses. Using the natural susceptibility of inbred strains, numerous loci and genes crucial to the immune response have been identified (*314*). Moreover, the usage of knock-out mice have been extremely useful in comprehending the role of human susceptibility genes in HSE (*96*, *98*, *342-344*). Moreover, resistance loci to HSV-1 in models of encephalitis (*89*, *345*) and keratitis (*346*) and cutaneous (*347*) infection identified secreted TNFα and the number of NK1.1+ cells as important modifiers of disease.

Although CMV infection causes mild to no symptoms in adults, infants and the immunocompromised can suffer from fever, mononucleosis and even neurological lesions as important as blindness and mental retardation (*108*). Genetic lesions impairing specific cell types can also cause serious herpetic infection. For instance, mutations in

GATA2, MCM4 or PRF1 result in either a reduction of NK cell (and sometimes also T cell and myeloid cell) numbers or impaired function, causing severe CMV or HSV-1 infection in affected individuals (*151*, *348-352*). Mouse models have also informed the characterization of the host response against CMV. Studies involving the naturally resistant C57BL/6 (B6) and the susceptible BALB/c mouse strains have been key for the characterization of the non-redundant role of natural killer (NK) cells in the control of infection through the interactions of activating NK receptors and viral and host proteins in a model of murine CMV (MCMV) (*162*, *163*, *169*, *353-355*).

The genetic diversity in mouse inbred strains is a limiting factor in the search for novel genes and pathways involved in viral host resistance. Chemical mutagenesis using *N*-ethyl-*N*-nitrosourea (ENU) is a productive alternative which allows for the discovery and understanding of novel genes and pathways that are involved in host resistance against viruses. ENU is a powerful mouse mutagen that creates random point mutations by creating DNA adducts that result in heritable mutations during DNA replication and cell proliferation. Although in a minority of cases small deletions have been described, the action of ENU on DNA results in nucleotide substitutions. Point mutations induced by ENU have a strong bias towards AT to TA transversions (*321*, *322*). These mutations can result in missense, nonsense or splice-site mutations that cause hypomorphic, hypermorphic or neomorphic alleles (*356*). Hence, an added advantage of ENU is that it can reveal not only information about a protein in a given process, but also about functionally important domains of a protein, improving our understanding of protein function.

One of the primary sites for the mutagenic action of ENU is the pre-meiotic spermatogonial cell. Following a period of transient sterility due to the depletion of spermatogonia by the ENU treatment, injected male mice are bred to propagate the mutation. The breeding schemes depend on the allelic characteristics required (dominant or recessive screen) and the strains required for subsequent genetic mapping. Here, we

have used a three-generation breeding scheme followed by a high-throughput pathogen challenge to scan the genome for recessive mutations which cause viral susceptibility.

The ENU mutagenesis approach has been successful at identifying viral susceptibility in mice, highlighting the role of TLR3, TLR9 and the type 1 interferon pathways, and helpful in increasing understanding of the involvement of inflammatory monocytes in the antiviral response to mouse (M)CMV (*328*, *357*). As mentioned above, we have shown the importance of the *Ptprc* gene in promoting optimal CD4-CD8 T cell interactions to clear HSV-1 infection in a murine model HSE (*66*). Using ENU mutagenesis, other groups at McGill University have also studied the importance of JAK3, USP15 and CCDC88B in susceptibility to cerebral malaria (*332*, *333*, *335*), as well as the role of USP8, STAT4 and ANK1 in resistance to salmonella infection (*336*, *337*, *358*).

In this study, we present the ENU platform we designed to identify novel mutations causing susceptibility to herpesviruses using a high-throughput infection with HSV-1 or MCMV. We developed and validated a single nucleotide polymorphism (SNP) mapping panel to localize recessive mutations in closely related C57BL/6 and C57BL/10 mice. Overall, we identified six pedigrees that segregate susceptibility to HSV-1, and one pedigree showing MCMV susceptibility. These unprecedented resources represent invaluable tools to better understand the mechanism underlying the variation in host responses against herpesviruses.

Results

Development of genetic tools used for identifying novel ENU mutations important for host resistance

In order to discover novel genes and pathways critical for resistance to herpesviruses, we have developed a recessive ENU mutagenesis platform using two different strategies. In both cases, resistant male C57BL/6 mice were injected with ENU and bred for three

generations to segregate homozygous mutations. For the HSV-1 susceptibility screen, we used a pure C57BL/6 (B6) breeding scheme to reduce the possibility of the influence of a mixed genetic background on resistance. For the MCMV screen, we used a mix C57BL/6 and C57BL/10 (B10) breeding schemes to allow mapping of the mutation using linkage analysis. The risk of the influence of a mixed genetic background on the phenotype of infected mice is lessened since MCMV is a natural mouse pathogen.

To map the mutations in a B6/B10 cross, we built a panel containing polymorphic SNP between B6 and B10. The B6 and B10 strains are closely related genetically; whereas the relatedness reduces the risk of a background effect, an obvious limitation is that it decreases the number of polymorphic markers available. Moreover, the genome sequence and genotype information on the C57BL/10 strain are limited. Thus, to generate a genotyping panel, we re-examined data previously obtained with the mouse genotyping JAX Diversity Array that contains more than 600 000 SNPs (*359*). Using this microarray we had already identified 7499 SNPs distributed in clusters between B6 and B10, although major gaps remained (*320*). To fill the gaps, we selected SNPs from the Mouse Phenome Database that are private to the C57BL/6J strain (i.e., divergent from all other C57BL strains). When the B6 SNP was different, the result was validated by Sanger sequencing using DNA from B6 and B10 mice. We tested 117 SNPs and found 43 to be polymorphic. Combined with the SNP from the JAX Diversity Array, we generated a panel containing 255 SNPs, with an average distance of 9.6 mb between markers (*66*, *320*, *332*, *360*) (Fig. 2.1 and Sup. Table 2.1). Chromosomes 2, 15 and 18 each have 1 region with a distance exceeding 25 Mb between markers, while chromosome X has 3 regions. Those uncovered gaps could reduce the significance of the linkage analysis for a deviant ENU-induced phenotype residing in those regions. With this caveat, we have built nevertheless a genotyping tool that allows us to map an ENU mutation on any chromosome.

Validation of the B6/B10 genotyping tools

To identify phenodeviant homozygote ENU mutations, we performed a three-generation breeding scheme, where G0 B6 males are injected with ENU and then outcrossed with a genetically closely related B10 female (Fig. 2.2 A) to produce G1 males. These G1 animals were bred as founders of individual pedigrees by crossing to wild-type C57BL/10 female mice; then, the daughters of this mating (generation 2 or G2) were back-crossed to the G1 father to bring ENU-induced sequence variants to homozygosity in the G3 generation. We aimed at testing at least 16 G3 offspring by pedigree for susceptibility to virus challenge considering that, should a recessive immune variant be segregating in the pedigree, we expected to observe about 4 (25%) affected mice.

During this process, we identified a pedigree, named *Tre*, where deviant animals showed light fur colour and pink eyes (Tre^{grey}, Fig. 2.2 B). Mutant mice were born with about 25 % (10/44) Mendelian frequency and were easily distinguished from their wild-type littermates at weaning. To validate the efficiency of our B6/B10 SNP panel, we genotyped 10 Tre^{grey} and 11 Tre^{wt} mice to map the causal mutation. We observed a significant peak on chromosome 7, with a logarithm of odds (LOD) score of 6.3 (Fig. 2.3 A), between marker rs32285588 (position 54.41mb) and marker rs32060039 (position 78.96mb) (Fig. 2.3 B). By querying the Mouse Genome Informatics (MGI) database, we determined that only one gene in the interval was associated with a similar phenotype: the gene for oculocutaneous albinism II (*Oca2*). Using Sanger sequencing, we sequenced all 24 exons and adjacent splice junctions. We identified the ENU mutation to be a unique A to T transversion in *Oca2* (Fig. 2.3 C) on position chr7: 56,323,725 bp. This mutation lies on the polypyrimidine splice junction downstream of exon 13 (Fig. 2.3 D), which could alter mRNA splicing and stability. This substitution was absent in all 37 strains sequenced by the Sanger Institute (http://www.sanger.ac.uk/science/data/mouse-genomes-project). This gene encodes for the OCA2 melanosomal transmembrane protein, which plays a central role in melanosome biogenesis and is associated with a defect in eye colour and coat pigmentation in both mouse and human (*361*, *362*). This result supports the efficiency of our B6/B10 SNP panel as a means of identifying novel ENU mutations.

Identification of an ENU deviant pedigree susceptible to MCMV

In order to proceed to high-throughput MCMV infections, we optimized a 7-day infection protocol. Mice were administered intravenously with a dose of 5 x 10^3 plaque forming units that is normally contained by C57BL/6 mice but results in uncontrolled replication in MCMV-susceptible BALB/c mice, which eventually succumb by day 7 post-infection (Fig. 2.4 A). Spleen index (SI), the ratio between the spleen weight and the initial mouse weight, is another phenotype distinguishing susceptibility or resistance. In C57BL/6 or C57BL/10 resistant mice, the response to MCMV leads to extra-medullary hematopoiesis taking place in the spleen, which increases their spleen weight and, by consequence, their SI (*363*) (Fig. 2.4 B). Hence, we expected susceptible animals from a deviant pedigree to show a decrease in survival by day 6 or 7 post-infection and a reduced SI. Following infection, mice were weighed and monitored daily for clinical signs. At the experimental end-point, mouse spleens and livers were harvested and weighed (Fig. 2.4 C). Pedigrees with G3 showing a decrease in survival and lower SI were considered deviant. We tested 1200 G3 mice derived from 61 pedigrees for susceptibility to MCMV (Fig. 2.5) and found that certain animals from the Glynn family succumbed before day 7 and showed a relatively low spleen index (6 susceptible mice out of 34 G3 tested), like the susceptible BALB/c control. This result demonstrates the identification of a pedigree showing MCMV susceptibility using the ENU mutagenesis platform. This family has been characterized in a subsequent study (chapter 4 of this thesis).

Identification of ENU deviant pedigrees susceptible to HSV-1

To discover novel HSV-1 susceptibility genes, we had to develop an infection pipeline allowing us to test large numbers of animals. We aimed to establish a survival screen following infection by intraperitoneal (i.p.) injection. To achieve this, we used increasingly infectious inoculums of the virus to identify the dose that better differentiates C57BL/6 and susceptible A/J mice in terms of survival (Fig. 2.6). At the lower doses ($2x10^3$ and $5x10^3$ PFU), about 20% of A/J mice survived the infection. At the higher doses ($1x10^4$

and $5x10^4$ PFU), all susceptible A/J mice succumbed to the virus and showed signs of encephalitis such as motor disturbances (circling, paralysis, lethargy) or asocial behavior. These symptoms were not observed at a lower dose. Hence, to reduce the risk of false positives we opted to use a dose of $1x10^4$ PFU to identify pedigrees showing altered response to HSV-1 in a high-throughput screen.

To screen for recessive mutations conferring susceptibility to HSV-1, we again established three-generation pedigrees. This time, however, ENU treated B6 G0 males were crossed with wild-type B6 females (Fig. 2.7 A). We used a pure B6 background to limit the residual susceptibility observed in the mixed B6/B10 background. G3 animals were infected and monitored for 14 days for clinical symptoms (Fig. 2.7 B). We tested 3020 G3 mice derived from 206 pedigrees and found an increase in susceptibility in 6 pedigrees (Fig. 2.7 C to H). All 6 families, *Keagan* (5/27; sick G3 / total G3 tested), *Dominik* (7/41), *Francesco* (4/19), *Baldwin* (4/14), *Holmes* (5/21) and *Tavon* (4/15), displayed a lower survival rate than the wild type B6 control. In each pedigree, we observed between 20 to 25% susceptible G3 mice. Studies are ongoing to identify the ENU mutations segregating in these families using next-generation sequencing. The *Keagan* pedigree is presented in a later chapter of this thesis (chapter 3).

Discussion

Infections with HSV-1 and CMV are very common and prevalent in the population. Although the majority of infections are clinically mild, primary infection with these agents during the fetal or newborn period or in immunocompromised patients can be fatal. Host genetics critically determines the outcome of infections. The identification of susceptibility genes in patients with presumed monogenic disorders has provided key insights into the pathogenesis of viral infection and host defence mechanisms, such as the TLR3-type I interferon pathway in the control of HSE as well as NK cell cytotoxic functions that curb HCMV infections (*78*, *151*). As a complement to clinical studies, random ENU

mutagenesis, combined with the use of mouse models of infection, provides a productive and unbiased approach to querying the mouse genome for antiviral mechanisms (*310*). In this study, we established an ENU mutagenesis platform, conducted high through-put screening for altered responses to CMV and HSV-1 and developed resources to identify new genes and pathways important for host resistance to herpesvirus infection. We tested 61 pedigrees for resistance to MCMV and 206 mouse pedigrees for resistance to HSV-1 (Table 2.1). One candidate pedigree with susceptibility to MCMV and 6 candidate pedigrees expressing susceptibility to HSV-1 were found.

We used a three-generation breeding scheme, where G3 animals were screened for viral susceptibility. These same G3 animals could then be used directly for the identification of the mutation via mapping or exome sequencing, according to two strategies. In the first strategy, we took advantage of the C57BL/6 and C57BL/10 strains. These two strains originated in 1921 from a common C57BL parental ancestor (*364*). Since they originate from an inbred colony, no other strains are known to have contributed to the genetic background of B6 and B10 mice (*364*). This strain combination allows us to reduce the impact of a potential modifier gene (*365*) while providing enough genetic polymorphism for efficient mapping. In the second strategy, we carried the screen in a pure B6 background.

Since the C57BL/10 strain was not sequenced, we discovered new polymorphic SNPs between B10 and B6 mice using genotyping data from the Jackson Laboratory Diversity Array (*359*) and from the Mouse Phenome Database. Validation of these SNPs yielded a success rate of 36.8%, allowing us to produce a genotyping panel that was successfully used in various studies including the ENU project (*66*, *320*, *332*). The panel contains 255 SNPs that provide genome-wide coverage, with the exception of 6 regions larger than 25 Mb on chromosomes 2, 15, 18 and X. This panel can be used to support the identification of behavioral (*366*, *367*) and immune phenotypes (*368*) distinguishing B6 and B10 strains.

The B6/B10 SNP panel was validated on a pedigree showing a visible coat colour phenotype that we identified during the production of the G3 ENU mice. We mapped a T/A to A/T transversion on a splice junction of the *Oca2* gene. This type of ENU mutation is not frequent. Most ENU induced mutations are A/T to T/A (44%) or A/T to G/C (38%) (*322*, *369*, *370*). Moreover, only 26% of mutations affect the splicing of a transcript. We are not the first group to identify an ENU mutation in *Oca2*. Four other pheno-deviant pedigrees have been characterized in previous studies (*371*). A recent review of a large panel of ENU-induced mutations identified multiple ENU-induced alleles in 43 out of 129 mutated phenovariant genes (*371*) suggested that this could result from gene size and sequence specificity.

Mutations within the *Oca2* gene (previously called *P* gene) are known to cause oculocutaneous albinism type 2, which is characterized by skin and hair hypopigmentation and ocular change, which we observed in the Tre mice (*372*). The Oca2 gene is important in melanosome biogenesis (*373*), small molecule transport across the melanomal membrane (*374*), and in regulating the melanosomal pH (*375*). Affected individuals suffer from visual inattention, nystagmus (rapid involuntary eye movement) and strabismus (abnormal eye alignment) (*376*), which we have not studied in our ENU mice. Further studies of the Tre pedigree are needed to understand the impact of the ENU mutation on *Oca2* mRNA stability and protein expression, as well as its impact on the albinism phenotype observed.

We performed an MCMV susceptibility screen on the G3 ENU mice and found one deviant pedigree. Although we tested a low number of G1 (N=61), we could quickly identify a susceptible family, which allowed us to highlight the efficiency of this type of screen. This approach has been very successful for identifying genes crucial in the innate response. MCMV has the ability to counteract and evade a variety of host resistance pathways and mechanisms, making it an excellent tool to identify genes central to host resistance (*377*). Various other ENU studies have allowed the decryption of complex TLR pathways and antiviral responses resulting from MCMV (*328*, *357*, *378*). We found that susceptible mice

from the Glynn pedigree exhibit a low spleen index, which suggests a reduction in cellularity following infection (*363*). Deep characterization of this pedigree will be performed to identify the mutated gene and its function in the immune response to MCMV (see chapter 4 in this thesis).

We also performed a susceptibility screen against HSV-1 infection and HSE. To our knowledge, we are the first group to develop an ENU platform for herpes simplex infection. The mouse model of infection has served to validate important aspects of HSV-1 pathogenesis (*96*, *98*, *342-344*). Here, we have implemented a HSV-1 model of i.p. infection which leads to HSE symptoms in susceptible mice, allowing for a high number of ENU mutated mice to be rapidly processed. An initial study in the B6/B10 cross identified 2 candidate pedigrees, one of which was carrying a mutation on *ptprc,* encoding for CD45, the mutation of which causes a severe lymphocyte deficiency (*66*). The observation of background susceptibility in various pedigrees led us to carry the HSV-1 screen in a pure B6 background. We tested families from 206 G1 and found 6 deviant pedigrees that showed clustering of HSV-1 susceptibility in terms of survival.

In the HSV-1 susceptibility screen, both the B6/B10 and the pure B6 breeding scheme produced a similar yield, with approximately 1 deviant pedigree per 30 G1 tested and 1 per 34 G1 tested, respectively. Our HSV-1 screen was also more efficient than the MCMV screen, which yielded 1 deviant pedigree per ~60 G1. The frequency of MCMV susceptibility is similar to that observed in a previous study that estimated that there were 290 genes with non-redundant function in resistance to MCMV (*379*). If we assume non-allelism among HSV-1 susceptibility pedigrees, we can deduce that there are about 580 (twice as many) critical genes for HSV-1 susceptibility in the mouse genome. Differences in life cycle and growth properties, cellular tropism and diseases caused by MCMV and HSV-1 may explain the discrepancy. It is notable, however, that an average frequency of 1 over 50 screened pedigrees has been observed in other screens at McGill University using pathogen challenge, in particular, *Salmonella Typhimurium* and *Plasmodium berghei* (*310*). Genes identified in the Salmonella screen such as *Ank1* (*336*), *Usp18*

(*358*) and *Stat4* (*337*) indicated the importance of iron homeostasis, negative type I IFN signals and NK-cell dependent IFNγ production in *Salmonella* pathogenesis. The characterization of mutations in *Ccdc88b* (*333*), *Themis* (*334*) and *Usp15* (*335*) highlighted the role of CD8+ T cell responses and type I IFN pathways in the control of resistance to cerebral malaria. Overall, these studies demonstrate the value of ENU mutagenesis to identify critical host response mechanisms against infection.

In this study, we established an infection platform to challenge high numbers of mice with MCMV and HSV-1. This work highlights the feasibility of an in vivo HSV-1 susceptibility screen performed in C57BL/6 germline mutant mice as a means of finding critical components of host resistance to HSV-1 that are required for survival. We produced and tested more than 4000 G3 mice and identified 7 deviant pedigrees. We also built genetic tools to map and identify the mutations. Thus, we developed a solid forward genetic strategy to study herpesviruses susceptibility that could also be applied to other viral agents.

Material and methods

Mouse and viruses

C57BL/6, C57BL/10, A/J and BALB/c mice were purchased from Jackson Laboratory (Bar Harbor, Maine, USA). Subsequent ENU-mutagenized animals were housed at the McGill University Life Science Complex. MCMV strain Smith (ATCC #VR1399) was produced in salivary glands and titered as previously described (*355*). HSV-1 strain 17 originates from Dr. Subak-Sharpe laboratory and was amplified and titered as described previously (*380*).

ENU mutagenesis and breeding

ENU mutagenesis was performed as described previously (*66*). Briefly, 90 mg/kg of ENU (Sigma-Aldrich) was injected IP in B6 males, which were then outcrossed with B6 or B10 females to produce G1 mice. G1 males were crossed again with a B6 or B10 females to

produce G2 progeny. Two G2 females were then backcrossed with their G1 father to generate the G3 mice used for the screens of viral susceptibility.

Mice Infections

Mice were infected IV with $4x10^3$ PFU of MCMV or IP with 10^4 PFU of HSV-1 between the age of 7 to 8 weeks. Animals weighed prior to the infection and monitored for 7 days (MCMV) or 14 days (HSV-1) for clinical signs of infection. For the MCMV infection, spleens were harvested and weighed at the experiment end-point to determine the spleen index, using this formula: SI = √([Spleen weight at the end point × 100]/Animal weight on day 0).

DNA extraction, genetic mapping and Sangers sequencing.

Whole genomic DNA was extracted using a phenol and chloroform method (*381*). Genotyping of the *Tre* pedigree was performed at the McGill University and Genome Quebec Innovation Centre (Montreal, Quebec, Canada) using the massArray platform from Sequenom. Linkage analysis was performed as described previously (*66*) using R/qtl software (version 3.3.2). The LOD score was determined using the coat colour as the phenotype. Identification and amplification of the mutation loci on *Oca2* was done by polymerase chain reaction (PCR) using primers targeting the exons (Sup. Table 2.2). PCR product was sent to Genome Quebec for Sanger sequencing and sequences were then analysed using Sequencher software (version 5.0.1)

Figures and Figure legends

Figure 2.1 – Genetics map of the B6/B10 SNP panel

255 SNP polymorphic markers between the B6 and B10 strain were selected to build a genotyping panel. Every horizontal bar represents a SNP. Coordinates can be found in the Supplemental Table 1.1.

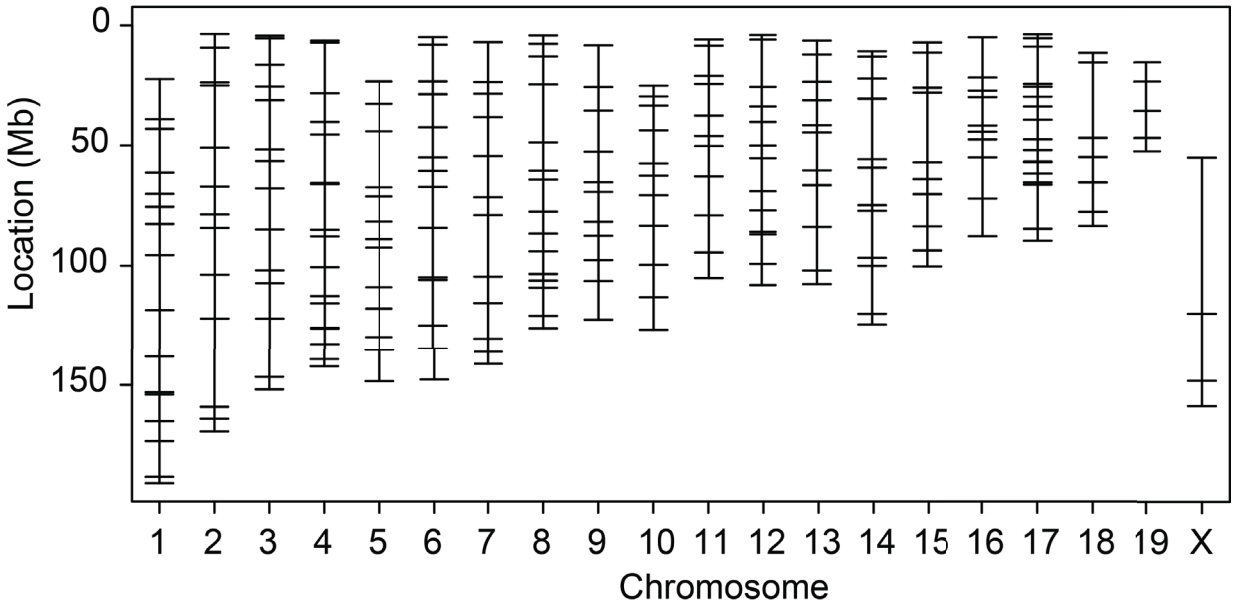
0
50
100
150
Location (Mb)
1 2 3 4 5 6 7 8 9 10 11 12 13 14 15 16 17 18 19 X
Chromosome

Figure 2.2 – Breeding strategy for the B6/B10 ENU screen and identification of grey pedigree

(A) G0 B6 males were treated with ENU and outcrossed for 2 generations with B10 females. G2 females were then backcrossed with the G1 male to produce G3 progeny that were then phenotyped. (B) Pictures of a grey mouse and a wild type mouse from the Tre pedigree identified during the production of ENU mutant mice are shown.

A

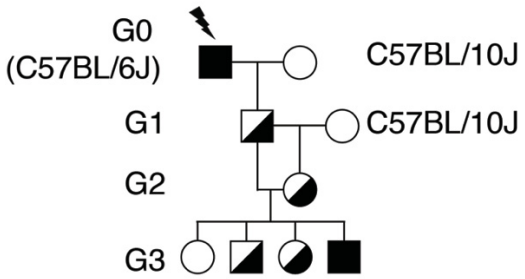

B

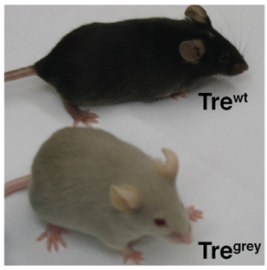

Figure 2.3 – Identification of an ENU mutation in Oca2 linked to a grey coat phenotype

(A) Genome wide linkage analysis of the Tre pedigree was performed on 21 G3. The QTL analysis led to a peak with an LOD score of 6.3 on chromosome 7. All *Trey*^{grey} G3 mice were genotyped, while only 11 *Trey*^{wt} were genotyped. (B) Haplotype of the Tre pedigree on chromosome 7. “A” represent B6 allele, “B” represent the B10 allele and “H”, a heterozygote. (C) A representative illustration of the ENU mutation on *Oca2* in the genomic DNA of *Tre*^{grey} and *Tre*^{wt} mice. (D) Schematic representation of the gene structure of Oca2. The asterisk represents the site of the ENU mutation upstream of exon 14.

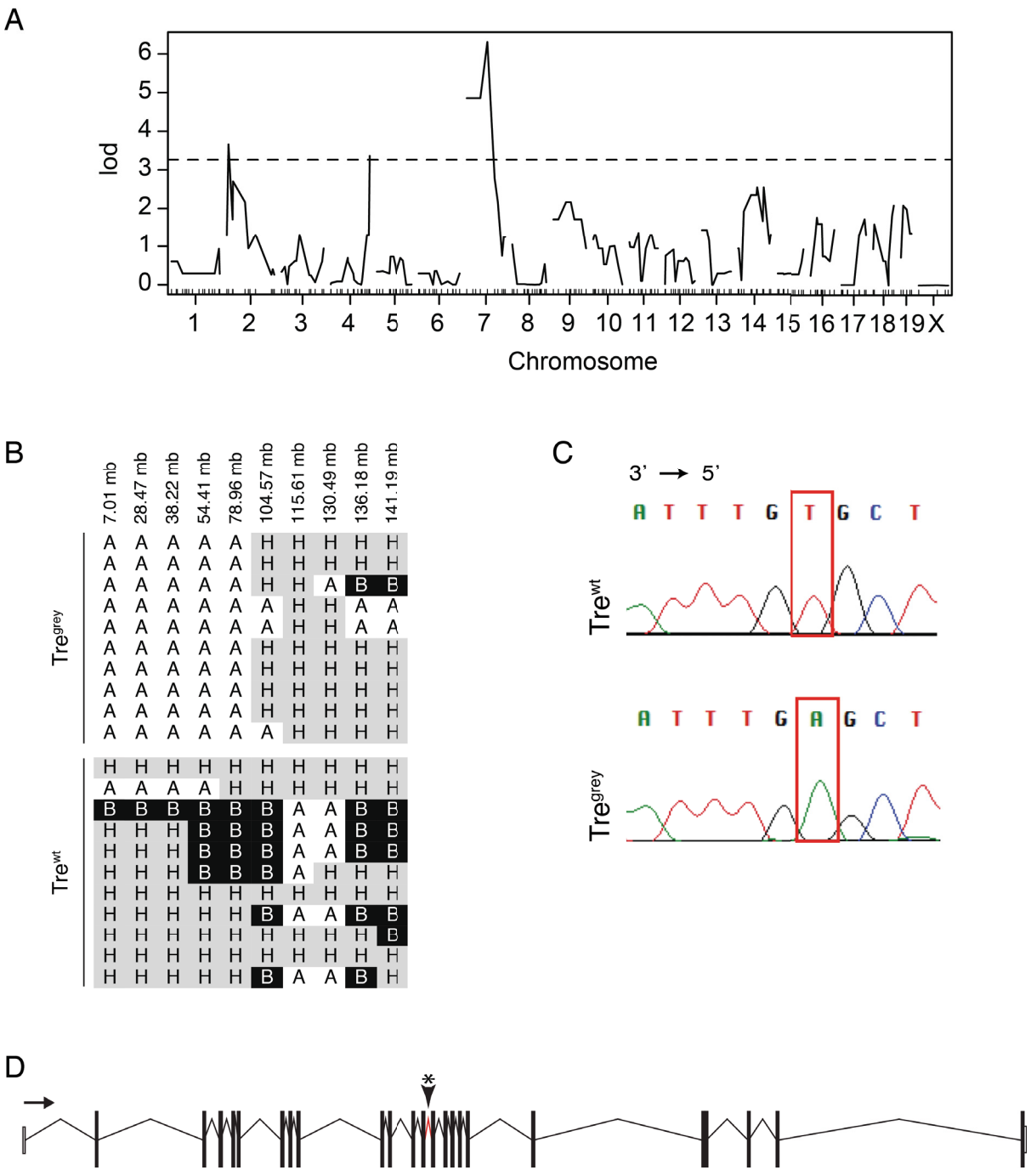
A
lod
0
1
2
3
4
5
6
1 2 3 4 5 6 7 8 9 10 11 12 13 14 15 16 17 18 19 X
Chromosome
B
7.01 mb
28.47 mb
38.22 mb
54.41 mb
78.96 mb
104.57 mb
115.61 mb
130.49 mb
136.18 mb
141.19 mb
Tre^grey
Tre^wt
C
3' → 5'
A T T T G T G C T
Tre^wt
A T T T G A G C T
Tre^grey
D

Figure 2.4 – Development of an MCMV infection pipeline

(A) ENU G3 mice were weighed, infected with MCMV and monitored for 7 days. Spleen index was determined and deviant families were selected for further studies. (B) Survival and (C) SI of the B6 or B10 resistant control and the susceptible BALB/c mice were determined following IV infection with MCMV. ****$p<0.0001$, one-way ANOVA with Tukey correction for multiple comparison.

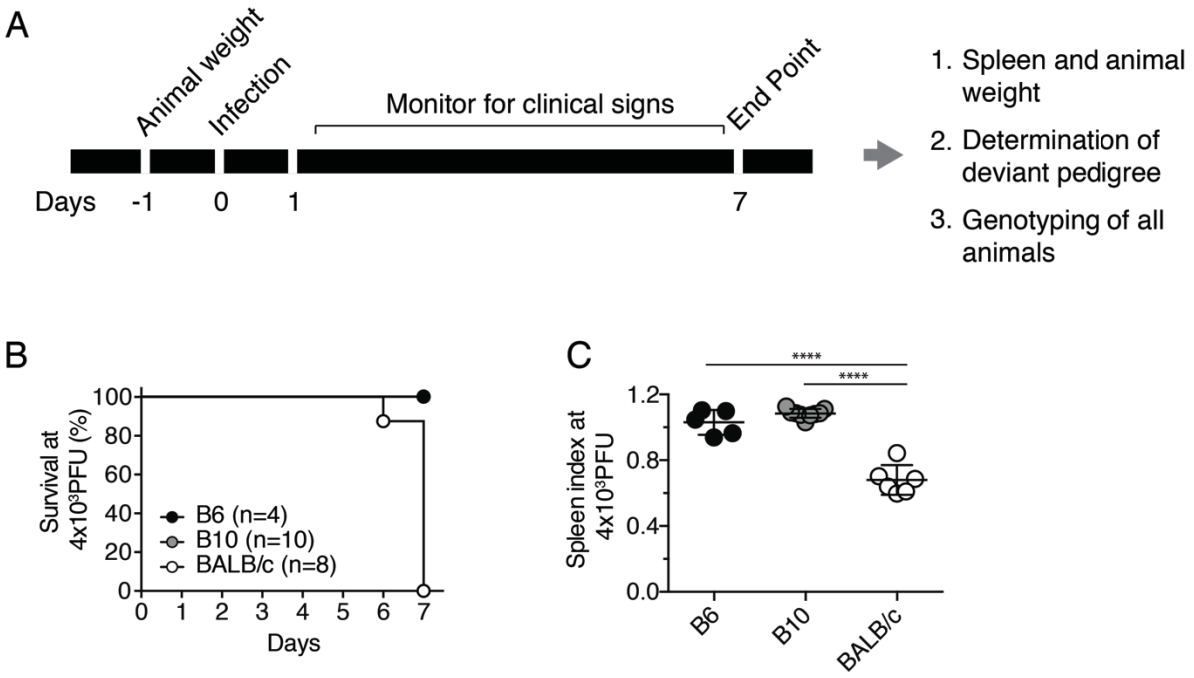
A
Animal weight
Infection
Monitor for clinical signs
End Point
Days -1 0 1 7
1. Spleen and animal weight
2. Determination of deviant pedigree
3. Genotyping of all animals
B
Survival at 4x10³PFU (%)
100
80
60
40
20
0
B6 (n=4)
B10 (n=10)
BALB/c (n=8)
0 1 2 3 4 5 6 7
Days
C
****
****
Spleen index at 4x10³PFU
1.2
0.8
0.4
0.0
B6
B10
BALB/c

Figure 2.5 – MCMV screen of the ENU mutagenized mice

G3 animals were infected with MCMV in 25 infections and the spleen index was determined at the infection end point. The spleen indexes of the susceptible mice from the Glynn pedigree that succumbed to the infection are in red. All the G1 pedigree tested are represented. The spleen indexes of all the resistant F2(B6xB10) and susceptible BALB/c controls are also displayed.

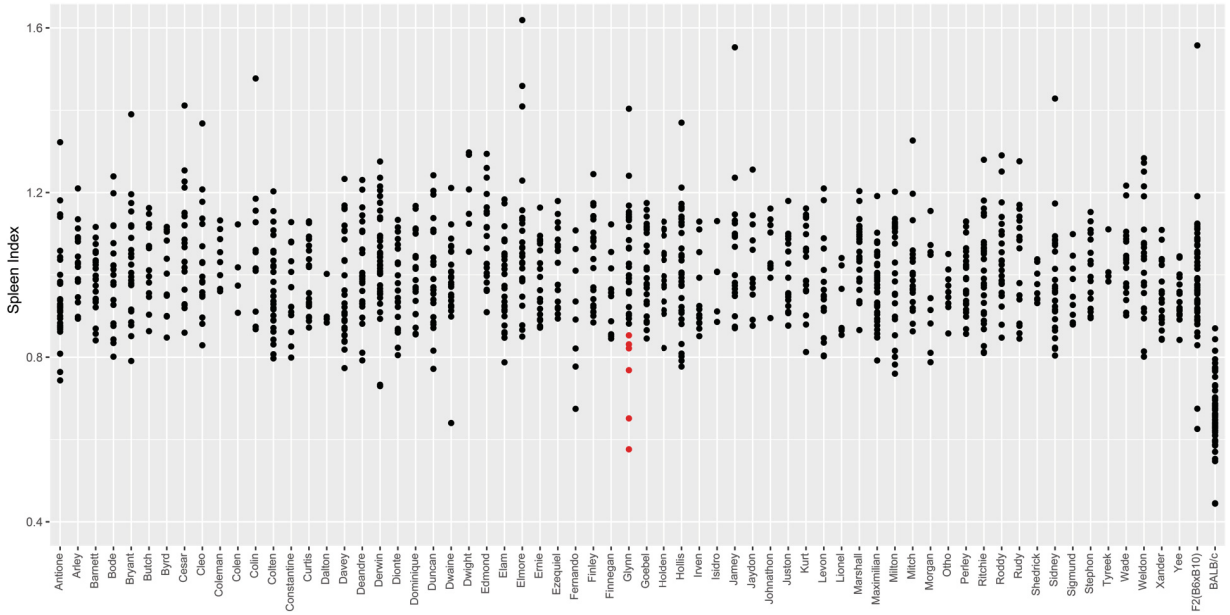
Spleen Index
1.6
1.2
0.8
0.4
Antione
Arley
Barnett
Bode
Bryant
Butch
Byrd
Cesar
Cleo
Coleman
Colen
Colin
Collen
Constantine
Curtis
Dalton
Davey
Deandre
Derwin
Dionte
Dominique
Duncan
Dwaine
Dwight
Edmond
Elam
Elmore
Ernie
Ezequiel
Fernando
Finley
Finnegan
Glynn
Goebel
Holden
Hollis
Irven
Isidro
Jamey
Jaydon
Johnathon
Juston
Kurt
Levon
Lionel
Marshall
Maximilian
Milton
Mitch
Morgan
Otho
Perley
Ritchie
Roddy
Rudy
Shedrick
Sidney
Signund
Stephon
Tyreek
Wade
Weldon
Xander
Yee
F2(B6xB10)
BALB/c

Figure 2.6 – *In vivo* titration of HSV-1

Resistant B6 or susceptible A/J mice were infected with (A) 10^3, (B) $5x10^3$, (C) 10^4 or (D) $5x10^4$ PFU IP of HSV-1. Animals were monitored for 14 days for severe signs of disease.

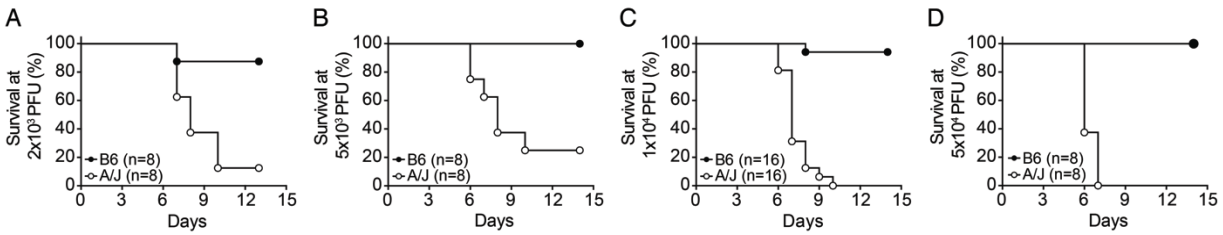
A
Survival at 2x10³ PFU (%)
B6 (n=8)
A/J (n=8)
Days
B
Survival at 5x10³ PFU (%)
B6 (n=8)
A/J (n=8)
Days
C
Survival at 1x10⁴ PFU (%)
B6 (n=16)
A/J (n=16)
Days
D
Survival at 5x10⁴ PFU (%)
B6 (n=8)
A/J (n=8)
Days

Figure 2.7 – HSV-1 screen of the ENU mutagenized mice

(A) C57BL/6 males were injected with ENU and crossed with B6 female for three generations to produce G3 progeny which carry ENU homozygote recessive mutations. (B) G3 mice were weighed, infected with 10^4 PFU of HSV-1 and monitored for 14 days. Deviant pedigrees could then be selected for further characterization. (C) Survival rates of the *Keagan*, (D) *Dominik*, (E) *Francesco*, (F) *Baldwin*, (G) *Holmes* and (H) *Tavon* pedigrees and the resistant B6 and susceptible A/J mice used during the HSV-1 screen are displayed.

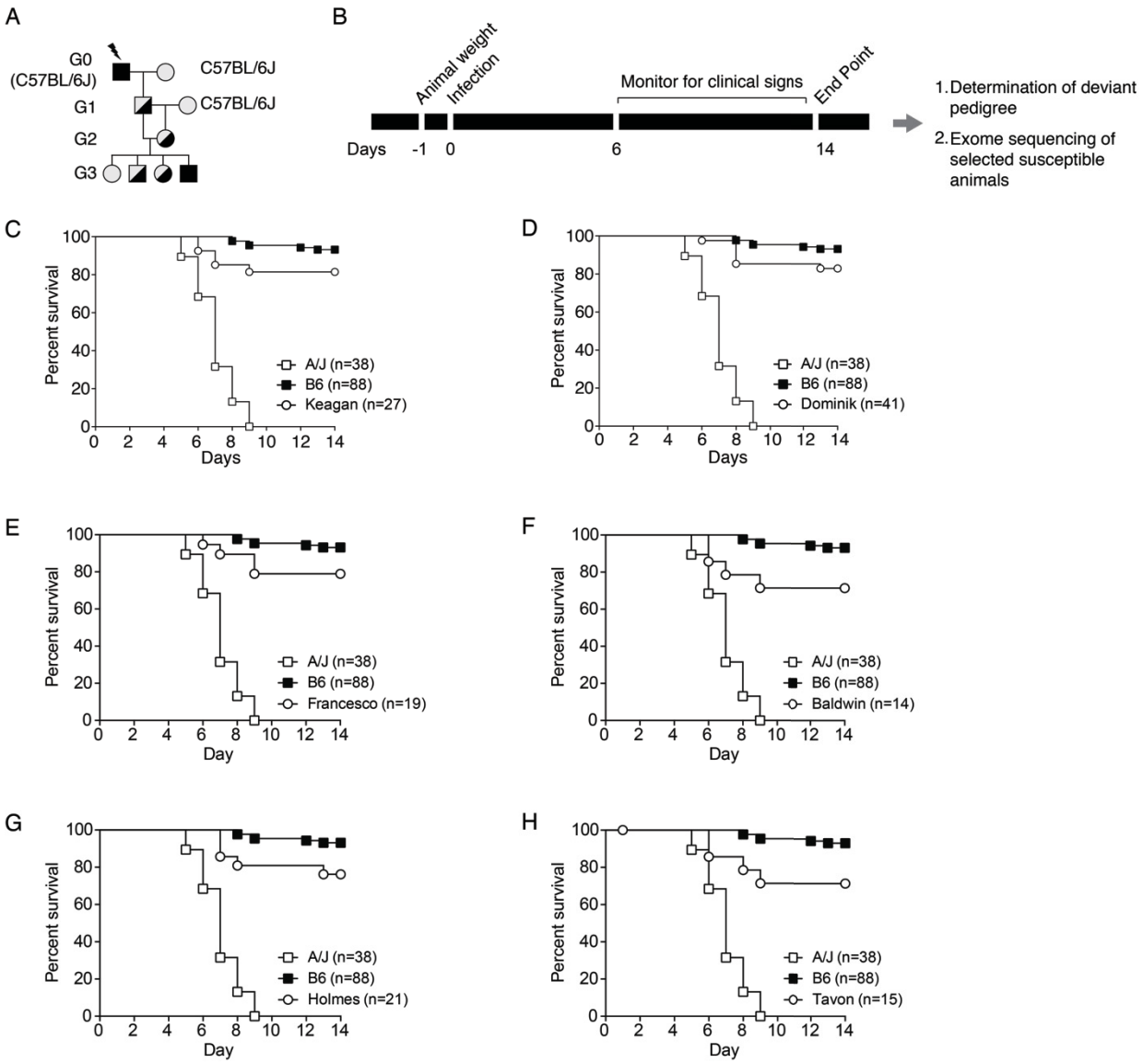
A
G0
(C57BL/6J)
C57BL/6J
G1
C57BL/6J
G2
G3
B
Animal weight
Infection
Monitor for clinical signs
End Point
Days -1 0 6 14
1. Determination of deviant pedigree
2. Exome sequencing of selected susceptible animals
C
Percent survival
A/J (n=38)
B6 (n=88)
Keagan (n=27)
Days
D
Dominik (n=41)
E
Francesco (n=19)
Day
F
Baldwin (n=14)
G
Holmes (n=21)
H
Tavon (n=15)

Table 2.1 – ENU screen for susceptibility to Herpesviruses

ENU screen	MCMV	HSV-1
Pedigrees tested	61	206
G3 animals tested	1200	3020
Candidates	1	6

Supplemental material

Supplemental Table 2.1 – Polymorphic markers between C57BL/6J and C57BL/10J mice.

Marker Name	Chromosome	Position	C57BL/6	C57BL/10
rs31652442	1	4,905,893	AA	CC
rs3708897	1	22,348,543	AA	GG
rs32737961	1	39,032,305	CC	TT
B10SNPS0005	1	43,063,842	TT	AA
rs13475886	1	61,228,463	TT	CC
rs13475913	1	70,127,169	TT	CC
B10SNP2G0002	1	75,483,331	GG	AA
rs31767016	1	82,636,707	TT	CC
B10SNP2G0015	1	95,571,814	TT	CC
B10SNP2G0019	1	118,565,405	CC	AA
rs6327099	1	131,282,938	AA	GG
rs31375526	1	138,180,275	TT	CC
rs13476148	1	144,862,429	TT	GG
B10SNPSG0013	1	152,988,092	CC	TT
rs13476182	1	153,950,459	TT	GG
rs6341208	1	165,062,830	TT	AA
B10SNPSG0020	1	173,342,737	TT	AA
B10SNPS0019	1	188,081,175	AA	GG
rs3680295	1	190,724,768	AA	GG
B10SNPS0021	2	3,582,646	AA	GG
rs13476344	2	9,314,267	TT	GG
rs33142586	2	23,743,224	CC	CC
B10SNPS0024	2	25,034,194	GG	CC
B10SNPS0026	2	50,942,492	CC	TT
rs13476554	2	67,080,320	TT	TT
rs33162749	2	78,639,333	AA	AA
B10SNPS0030	2	84,313,007	TT	CC

B10SNPS0032	2	103,735,349	CC	AA
B10SNPSG0021	2	122,094,116	TT	GG
rs13476801	2	138,305,756	GG	AA
B10SNPS0036	2	146,096,051	CC	TT
rs13476872	2	159,118,061	AA	GG
B10SNPS0037	2	164,025,160	AA	GG
rs27312411	2	169,272,130	AA	GG
B10SNPS0041	3	4,365,615	TT	CC
rs13476956	3	5,370,727	GG	AA
rs31500060	3	16,369,915	TT	CC
B10SNPS0044	3	25,440,271	CC	GG
rs30354938	3	31,168,870	AA	GG
B10SNPS0046	3	51,646,346	TT	CC
rs31596392	3	56,511,763	AA	GG
B10SNPSG0029	3	67,807,084	GG	AA
B10SNPS0050	3	84,907,155	TT	CC
rs30661719	3	101,914,952	AA	GG
B10SNPS0051	3	107,273,295	AA	GG
rs16790854	3	121,962,207	TT	CC
B10SNPSG0034	3	122,116,882	GG	AA
B10SNPS0056	3	146,593,495	CC	TT
rs31594267	3	151,882,540	AA	CC
rs32143059	4	6,301,848	AA	AA
B10SNPSG0036	4	7,149,610	CC	TT
rs32410424	4	19,603,384	TT	CC
rs13477622	4	28,249,360	AA	GG
rs32786595	4	40,225,498	TT	CC
B10SNPS0062	4	45,462,131	AA	CC
rs13477746	4	65,605,269	TT	CC
B10SNPS0064	4	66,040,938	AA	GG
rs28325196	4	85,069,930	CC	TT
B10SNPS0065	4	87,804,727	CC	AA
rs28154736	4	93,285,727	GG	AA
rs28234425	4	100,667,454	CC	GG

B10SNPS0067	4	112,653,568	TT	TT
rs6381371	4	115,708,649	CC	TT
rs4224765	4	125,991,071	CC	TT
B10SNPS0069	4	126,253,529	GG	CC
rs32203940	4	132,774,342	TT	CC
rs3661982	4	139,269,393	TT	AA
B10SNP2G0026	4	142,217,407	TT	CC
rs33367397	5	18,216,206	TT	CC
B10SNPSG0050	5	23,345,000	AA	GG
rs29779004	5	32,629,170	TT	CC
rs46835784	5	44,059,873	TT	CC
B10SNPS0079	5	67,382,789	AA	GG
rs13478320	5	71,133,300	GG	TT
rs33067522	5	81,685,659	TT	CC
B10SNPS0081	5	88,988,451	GG	AA
rs33249065	5	92,510,104	TT	CC
B10SNP2G0043	5	109,001,097	CC	AA
rs3662161	5	117,909,356	TT	CC
B10SNPS0086	5	129,799,057	TT	CC
rs13478542	5	135,358,052	GG	GG
B10SNPS0087	5	148,405,352	GG	AA
B10SNPS0089	6	4,944,845	GG	TT
rs3710142	6	8,012,701	TT	CC
B10SNPS0091	6	23,322,761	TT	AA
rs30764547	6	28,665,910	TT	AA
rs33852049	6	54,899,850	AA	GG
rs30915467	6	60,541,414	GG	AA
rs6157367	6	67,237,174	AA	TT
B10SNPS0097	6	84,280,591	CC	TT
B10SNPS0099	6	104,875,242	AA	CC
rs30421807	6	105,962,107	TT	AA
rs13478995	6	117,420,898	GG	CC
rs30215744	6	123,650,316	0	TT
B10SNPSG0065	6	125,060,262	AA	GG

rs6334723	6	134,651,968	AA	GG
B10SNPS0104	6	147,720,182	AA	GG
B10SNPS0105	7	7,014,667	TT	CC
B10SNP2G0049	7	28,467,081	TT	AA
rs31221380	7	38,216,957	TT	GG
rs32285588	7	54,410,823	GG	AA
B10SNP2G0060	7	71,519,895	GG	TT
rs32060039	7	78,961,795	GG	CC
rs31304724	7	81,933,528	TT	AA
B10SNPS0115	7	104,565,567	AA	GG
rs13479454	7	115,608,885	AA	AA
B10SNPS0118	7	130,492,865	AA	GG
rs13479522	7	136,179,208	TT	CC
rs13479540	7	141,188,625	AA	GG
B10SNPS0122	8	4,235,918	CC	TT
rs33166255	8	7,701,082	CC	GG
rs33157972	8	12,958,088	AA	GG
rs3661760	8	24,557,766	GG	TT
B10SNPS0126	8	48,705,306	GG	AA
rs30970745	8	49,539,911	CC	TT
rs13479749	8	50,761,812	TT	GG
rs33080067	8	60,422,745	AA	GG
B10SNPS0127	8	64,124,535	CC	TT
rs32729089	8	77,477,256	AA	TT
B10SNPS0130	8	86,611,947	CC	TT
rs33601490	8	94,031,516	TT	CC
rs32361852	8	103,462,818	GG	AA
B10SNPS0132	8	106,217,064	CC	AA
rs33004646	8	109,160,587	AA	GG
rs33610973	8	120,904,596	CC	TT
B10SNPS0133	8	126,154,896	AA	GG
rs29887009	9	8,307,298	GG	GG
rs13480109	9	25,697,427	AA	GG
B10SNPS0139	9	44,891,469	AA	TT

rs29644859	9	52,593,224	AA	CC
rs29640230	9	65,282,831	AA	GG
rs6396602	9	69,294,580	CC	AA
rs3673457	9	81,753,447	CC	TT
B10SNPS0144	9	87,513,872	TT	GG
rs13480362	9	97,693,921	TT	CC
B10SNPS0145	9	106,375,830	AA	GG
B10SNPS0147	9	122,496,139	TT	AA
B10SNPS0152	10	25,103,948	AA	TT
rs29336522	10	29,577,040	CC	TT
rs13480575	10	33,372,829	TT	CC
rs29356879	10	43,717,117	CC	TT
rs13480619	10	57,472,268	TT	CC
B10SNPSG0099	10	62,547,650	GG	AA
rs29344872	10	83,411,614	GG	AA
rs13480728	10	99,701,075	TT	CC
rs13480770	10	113,178,567	TT	AA
B10SNPS0162	10	126,774,961	CC	AA
B10SNPS0163	11	5,927,550	AA	GG
rs26895374	11	8,476,784	GG	TT
rs29413390	11	21,040,136	AA	GG
B10SNPS0165	11	24,352,635	GG	GG
rs6406223	11	37,583,571	TT	GG
B10SNPS0168	11	46,027,800	GG	TT
rs26979995	11	50,271,114	CC	TT
rs6268547	11	62,886,983	TT	CC
rs13481117	11	79,065,732	GG	TT
B10SNPS0171	11	83,361,835	CC	TT
rs29436909	11	94,499,650	CC	AA
B10SNPS0173	11	105,208,941	TT	GG
B10SNPS0175	12	4,035,991	CC	TT
rs29158719	12	5,967,934	GG	GG
B10SNPS0178	12	25,626,291	AA	GG
B10SNPS0179	12	33,783,681	TT	GG

rs13481403	12	40,215,580	AA	AA
rs13481439	12	50,066,538	TT	CC
B10SNPSG0101	12	55,293,511	CC	GG
rs6385807	12	56,859,360	GG	TT
rs29172987	12	69,022,193	TT	CC
rs29173065	12	76,989,416	AA	GG
B10SNPS0184	12	85,893,620	TT	CC
rs13481569	12	86,986,254	GG	AA
rs29206394	12	99,208,162	TT	GG
rs13481634	12	108,071,865	GG	GG
rs13481676	13	6,303,301	TT	CC
rs13459139	13	12,155,224	CC	TT
rs3701424	13	19,519,989	CC	TT
rs6230023	13	22,362,899	GG	AA
B10SNPS0190	13	23,458,896	TT	AA
rs13481741	13	31,195,478	CC	TT
rs3722313	13	41,538,155	TT	CC
B10SNPS0192	13	44,605,368	GG	AA
B10SNP2G0077	13	60,294,898	TT	GG
rs51679066	13	66,467,951	AG	AA
B10SNPSG0116	13	83,826,961	TT	GG
rs3702296	13	101,979,187	TT	CC
B10SNPS0198	13	107,699,046	CC	TT
rs31187642	14	10,769,899	GG	AA
B10SNPS0200	14	13,021,464	CC	TT
rs31151615	14	22,151,051	AA	GG
B10SNPS0202	14	30,518,255	GG	AA
B10SNPSG0125	14	55,673,056	TT	GG
rs30650651	14	59,200,668	TT	CC
rs30264676	14	74,815,528	AA	TT
B10SNPSG0131	14	77,195,309	CC	TT
B10SNP2G0083	14	96,734,196	GG	TT
rs31059846	14	100,024,215	TT	CC
rs3722416	14	116,406,008	GG	AA

rs3710901	14	120,021,467	AA	TT
rs31233932	14	124,508,019	GG	AA
rs13459145	15	7,117,980	CC	CC
rs32488968	15	11,377,555	TT	TT
rs32266845	15	16,094,380	TT	GG
B10SNPS0214	15	25,941,148	CC	TT
rs13482496	15	27,973,454	CC	CC
rs3702158	15	56,992,041	AA	GG
B10SNPS0218	15	63,931,032	GG	AA
rs31155407	15	64,892,362	GG	CC
rs31350865	15	70,219,592	AA	GG
B10SNPS0219	15	83,618,701	GG	AA
rs3700812	15	93,667,136	TT	CC
B10SNP2G0093	15	100,309,099	CC	TT
B10SNPSG0155	16	4,972,820	AA	GG
rs4165283	16	21,678,473	CC	CC
rs4165506	16	27,156,167	GG	AA
B10SNPS0225	16	29,856,457	AA	GG
rs3663871	16	41,688,007	AA	GG
B10SNPS0227	16	44,261,352	TT	CC
rs3687811	16	47,489,432	GG	AA
rs4187220	16	54,901,204	CC	TT
rs4201223	16	72,027,066	AA	AA
B10SNPS0232	16	87,736,505	CC	TT
B10SNPS0234	17	3,690,688	GG	AA
rs4137196	17	5,332,903	GG	GG
rs33304902	17	8,850,537	AA	GG
B10SNPS0236	17	24,310,623	TT	AA
rs29512740	17	25,523,395	GG	TT
rs33442265	17	29,663,445	AA	GG
p17.12	17	33,782,245	TT	CC
rs33334258	17	39,307,300	GG	AA
B10SNPS0237	17	47,451,200	CC	TT
P17.25	17	51,934,244	TT	AA

p17.17	17	56,679,267	TT	CC
p17.11	17	56,897,783	AA	GG
rs13483058	17	61,680,643	TT	CC
rs13483071	17	65,343,085	TT	CC
B10SNPS0239	17	66,263,080	GG	AA
B10SNPSG0168	17	84,624,403	AA	GG
rs33353857	17	89,633,195	GG	CC
rs13483208	18	11,477,238	AA	GG
rs13483221	18	15,408,257	CC	TT
rs13483296	18	35,365,919	TT	AA
B10SNPS0247	18	46,803,584	TT	CC
rs13483369	18	54,774,495	CC	CC
B10SNPS0249	18	65,425,288	GG	AA
rs13483448	18	77,559,708	TT	CC
B10SNPS0251	18	83,497,271	GG	AA
rs31112038	19	15,408,257	GG	CC
B10SNPS0255	19	23,378,788	TT	GG
rs31241164	19	35,648,431	AA	GG
B10SNPS0258	19	46,875,560	AA	GG
rs30608930	19	52,433,860	GG	GG
rs6368704	X	55,120,804	TT	CC
B10SNP2G0134	X	120,117,110	TT	AT
B10SNP2G0150	X	147,904,667	AA	GG
rs13459160	X	158,414,344	GG	TT
rs31819915	X	166,416,706	GG	TT

Supplemental Table 2.2 – Primers for sequencing Oca2 exons

Primer Name	Sequence (5’ 3’)
pOCA2.1F	GAGCCACTGAGCCTTTCAAC
pOCA2.1R	ATCTACACATTTTCAATATAGGCTTG
pOCA2.2F	AGCAGGCTGAGCAAAACAG
pOCA2.2R	TCAGACTAACAGAATGGATTTGAA
pOCA2.3F	CGGAAGGGCAGTGTTTTAAG
pOCA2.3R	TCCCATAAAATGGAGGGAAA
pOCA2.4F	AGTGCACTCCTGCAAGCAT
pOCA2.4R	GAATTCGCCATCATTTGTGA
pOCA2.54	GGCCAAGATAAGTGATTTTGAA
pOCA2.5F	TGGTGGGGAAATCTTTTGTC
pOCA2.6F	ACTGACAATCAGTATTAAGTACCACAA
pOCA2.6R	GAAGTATGGGCAAGTCTCAGG
pOCA2.7F	CATCAGAAGCTGTCCCAACA
pOCA2.7R	CTATCCGTCCCAAAGCACAC
pOCA2.8F	GCAAGCTGCTTTTAACGGTAGT
pOCA2.8R	CTCTTTAACAGGTGTAATCATTTCTG
pOCA2.9F	CATTGCTTTGTGAGCTTTCCT
pOCA2.9R	AATGGAGTTACTGCCGTTGG
pOCA2.10F	TCATTTGAGAATATTTGTTAGAGACTG
pOCA2.10R	TTCCTTATAAATCACTCAGTCTTGG
pOCA2.11F	GGGCTTTTCTGTCTGTGAGG
pOCA2.11R	TCCGTAGGAATTGCTCCTTC
pOCA2.12F	CACCCACTCATACCCCTCAT
pOCA2.12R	AAGGCATAACTGAAGACCTTGAA
pOCA2.13F	CCCCCTTGATATCTTTTTCATT
pOCA2.13R	CATCACATGAAACAATTTGAAACA
pOCA2.14F	GTAAGGGCAGCCCATTTTTA
pOCA2.14R	TCAAGAGATATGCCATCTTGACT
pOCA2.15F	GATATCCATCCAGCCAGAGC
pOCA2.15R	GCTTCCTGAAGCCATTTTGA
pOCA2.16F	TCCATATCTTGGAGTCATTAGTAAAAA
pOCA2.16R	CCCAGAACATGCATACGTCTC

pOCA2.17F	GAATCGATGTGCCTTCCTGT
pOCA2.17R	TCTCCTGATTTTCCCCTCCT
pOCA2.18F	AGCCCCTCTGTGTTTCCAG
pOCA2.18R	CTCCTGCTCATGAGAACTTCC
pOCA2.19F	CTGAGGACTGAGGGTGGAAG
pOCA2.19R	CGCAATATGTTCCTTCATGC
pOCA2.20F	GCTGTCAGTGTCACCTTGCT
pOCA2.20R	ACCGTCTGCATCCAGATACC
pOCA2.21F	GCAGCCATTAAATGCTAGGC
pOCA2.21R	CCACATCCATCTCCACACAG
pOCA2.22F	CACAGTTTGCAGTACAGCATTG
pOCA2.22R	AAAACCCGGGTCACCTTAAC
pOCA2.23F	AAGGATAACCTGTGCCTACCC
pOCA2.23R	GCAACAGAGGAGCTGGTTTC
pOCA2.24F	AAAACAAGGTTCTTTAGGTTTCG
pOCA2.24R	GAAGTCTCCAGGATTCTCCTCA
pOCA2.25F	TCACATCACAGCCTCTGAGC
pOCA2.25R	AGCATGCATTGGTGCTTTTT
pOCA2.26F	GATTCTGGGGCCACATTCT
pOCA2.26R	GGTCTTCTGCAAATCAAACTCC

Bridging statement from Chapter 2 to Chapter 3

To discover novel genes and pathways important for host resistance to HSV-1, we completed an recessive ENU mutagenesis screen and tested near 200 pedigrees for susceptibility to the virus. Doing so, we identified 6 deviant families exhibiting susceptibility to HSV-1. We selected one pedigree, named Keagan, for further analysis. In Chapter 3, we use a next-generation sequencing and linkage analysis to identify the mutation causing the phenotype in Keagan mice. We found a missense mutation in the DNA binding site of the transcription factor STAT5A, causing an altering the response to IL-2, HSV-1 and MCMV in lymphocytes.

Chapter 3 – Altered immune responses to infections with herpesviruses are associated with an *N*-ethyl-*N*-nitrosourea-induced mutation in the linker domain of STAT5A

Gabriel André Leiva-Torres[1,2], Benoit Charbonneau[1,2], Robert Eveleigh[3], Guillaume Bourque[3], Silvia M Vidal[1,2]*

Affiliations: [1]Department of Human Genetics, Centre for the Study of Host Resistance, McGill University, Montréal, Québec H3G 0B1, Canada. [2]McGill University Research Centre on Complex Traits, McGill University, Montréal, QC H3G 0B1, Canada. [3]McGill University and Genome Quebec Innovation Center, Montréal, QC, H3A 1A4, Canada.

* Corresponding author:
email: silvia.vidal@mcgill.ca

Manuscript in preparation

Abstract

Herpes Simplex virus type 1 (HSV-1) is a ubiquitous neurotropic virus that can cause severe clinical disease particularly in the setting of immunosuppression. To identify novel mechanisms important to the antiviral immune response, we characterized an *N*-ethyl-*N*-nitrosourea (ENU) mutated pedigree identified in a survival screen of mice challenged with HSV-1. Using linkage mapping and next-generation sequencing, we found an association between HSV-1 susceptibility and a locus on chromosome 11 bearing a non-synonymous single nucleotide variation (SNV) in the genes *Smurf2* (T364K) and *Stat5a* (W484G). When isolated in a homogenous C57BL/6 background, neither the combined nor individual mutations affected the survival of HSV-1 infected mice. Moreover, infection of *Smurf2*$^{-/-}$ mice further excluded a role of SMURF2 in the control of HSV-1 susceptibility. However, CD8+ T cell and NK cell responses were affected in STAT5A (W484G) mice, as their numbers were reduced following infection with HSV-1 as was the generation of antigen experienced CD44+ CD8+ T cells. Disminished cytotoxic lymphocyte responses were also observed upon infection with cytomegalovirus (CMV) compared to wild-type littermates. STAT5A is a multi-modular transcription factor essential for lymphocyte biology, the activation of which can be monitored through IL-2 and lymphocyte-specific protein tyrosine kinase/JAK3 dependent expression of IL-2R sub-units. In our mutant mice, following ex-vivo stimulation with IL-2, NK cells had reduced expression of IL-2Rβ compared to wild type mice, while the expression of IL-2Rα on CD4 and CD8 T cells was abrogated. The W484G mutation resides on the α5 helix of the STAT5A linker domain (LD) that connects the DNA binding domain and SH2 domain of the protein. Taken together, these results show that STAT5A is important to the T cell and NK cell immune responses to HSV-1 and CMV infection and a single point mutation in its LD is sufficient to compromise STAT5A function.

Introduction

Herpes virus simplex 1 (HSV-1) is a ubiquitous neurotropic dsDNA virus that latently infects 60% of the worldwide population. Although most infections are asymptomatic, primary infection or reactivation of HSV-1 can cause severe ophthalmic and neurological lesions leading to blindness, encephalitis or even death in individuals with an immature immune system or in immunocompromised patients (*2*, *90*). Numerous studies in humans and mice have highlighted the critical role of innate and cell-mediated immune responses in the control of the severity and outcome of infection with HSV-1 (*66*, *78*, *90*). Analysis of families affected with encephalitis have shown the importance of the TLR3/NF-κB/Interferon (IFN) pathway in susceptibility to HSV-1 in the central nervous system. Patients carrying mutations in either TLR3, TRAF3, UNC-93B, TRIF, NEMO, TBK-1 or STAT1 causing abnormal Interferon (IFN) α, β and λ production are predisposed to viral encephalitis (*54*, *55*, *80*, *82-84*, *382*). Studies using mouse models of infection have also contributed to a better understanding of the role of human candidate genes in the pathogenesis of HSV-1 (*96*, *97*, *343*), highlighting the importance of cellular virus sensing by innate receptors in HSV-1 resistance. In addition, multiple cell types have been shown to contribute to the control of HSV-1 in vivo. Among the most important of these cell types are natural killer (NK) cells and T cells, whose role in anti-HSV-1 immunity involves cytokine production, principally IFNγ, and the killing of virally infected cells (*66*, *383*, *384*). Hence, the frequency and severity of HSV-1 infection is markedly increased in patients with congenital NK cell or T cell immunodeficiencies, transplant recipients and AIDS patients (*385-389*). In mice, the peripheral control of HSV-1 replication via CD4+ T cell IFNγ production and the recruitment of CD8+ T lymphocytes at the site of infection has been shown to be crucial to the survival of infected mice (*66*). In addition, CD8+ T cell lymphocytes play a critical part in preventing HSV-1 reactivation, as demonstrated by the correlation between tissue persistence of HSV-1 specific CD8+ T-cells in mouse skin after viral clearance and local protection from exogenous re-inoculation (*390*, *391*).

The signal transducers and activators of transcription (STAT) proteins are important for the immune response. STATs 1 to 6 form a large family of transcription factors, all of which consist of a helical N-terminal domain, a coiled coil domain, a DNA-binding domain, a helical linker domain (LD), an Src homology 2 (SH2) domain, and a transactivation domain located in the C-terminus region (*392*). The STATs are not only central to the antiviral response; they help dictate the development, homeostasis and activation of immune cells. STAT5 is crucial for downstream signalling of IL-2 family cytokines; IL-2, IL-4, IL-7, IL-9, IL-15 and IL-21 (*393*). These cytokines are a fundamental component of T and NK cell biology (*224*). In addition, STAT5 maintains effector CD4+ and CD8+ T cells during viral infection. Activation of NK cells by IL-2 and IL-15 is also mediated by STAT5 during murine cytomegalovirus (CMV) infection (*266*, *394*).

STAT5 is comprised of two molecules, STAT5A and STAT5B, which are capable of forming homo or heterodimers, and/or tetramers following phosphorylation by JAK3 and JAK1 (*395-397*). *Stat5a*$^{-/-}$ and *Stat5b*$^{-/-}$ mice exhibit a defect in mammary gland development and lactogenesis or in a sexually dimorphic growth hormone-dependent defect (*398*, *399*). Unsurprisingly, inactivation of both STAT5A and STAT5B causes a severe increase in perinatal death (*400*). The knock-down of JAK3 or STAT5A/B causes a severe reduction of T, B and NK cells, illustrating the key role of STAT5 in lymphocyte development (*401-403*). Both the inactivation of either STAT5A/STAT5B and the blockage of their ability to produce tetramers results in a reduction of the lymphocyte population, as well as in a reduction of the expression of IL-2Rα following IL-2 stimulation, thus blocking the positive feedback loop normally occurring after activation (*231*). However, these phenotypes are not as penetrant in single mutants, underlining possible redundancy between the two molecules.

Random chemical mouse mutagenesis is a N-ethyl-N-nitrosourea (ENU)-induced mutagenesis is a powerful tool for the study of gene function and the generation of human disease models (*66*, *310*). Using a three-generation breeding scheme to isolate recessive mutations combined with an efficient phenotyping platform of mice challenged by

intraperitoneal challenge with HSV-1, we previously identified the Keagan pedigree with animals susceptible to HSV-1 infection (Chapter 2 of this thesis). In this study, we proceed to identify a novel mutation in the region overlapping the LD of the transcription factors STAT5A. We show that STAT5A W484G mutation is sufficient to compromise lymphocyte responsiveness to IL-2 *ex vivo* and to alter the NK cell and CD8+ T cell response during both HSV-1 and CMV infection *in vivo*.

Results

Identification of a novel mouse mutant with altered susceptibility to HSV1

We previously performed an ENU mutagenesis study followed by high-throughput HSV-1 infection. ENU treated B6 mice were bred for three generations to capture homozygote recessive mutations causing viral susceptibility. Doing so, we found a deviant pedigree: Keagan exhibited ~20% susceptibility to HSV-1 (Fig. 3.1 A). To identify the ENU mutation, we selected 3 susceptible animals for whole exome sequencing (WES). We found 55 ENU single nucleotide variants (SNV) unique to the Keagan pedigree (Table 3.1). Of those SNV, only 4 non-synonymous homozygote mutations were shared in at least 2 of the 3 samples. We tested for the presence of those mutations by PCR and Sanger sequencing on the mice from the Keagan pedigree and found no clear segregation of the mutations in the susceptible animals.

To clarify the mutation causing HSV-1 susceptibility in the Keagan family, we used the data from the whole-exome sequencing to perform an association study where SNV unique to that pedigree would be used to genotype the mice tested during the screening (Table 3.2). The ENU mutation would be in linkage disequilibrium and segregate in susceptible animals while resistant mice would carry the reference B6 allele or be heterozygote. We built a 55 SNP panel containing all the SNVs (synonymous and non-synonymous) unique to the Keagan pedigree (Fig. 3.1 B). Doing so, we found a significant

peak on chromosome 11 (LOD score of 3.64, $p<0.05$, Fig. 3.2 C), with two underlying mutations (Fig. 3.2 D).

The first ENU mutation was a C to A transversion at position 106,703,035 bp on chromosome (chr.) 11, within exon 11 of the gene *Smurf2*. This mutation is predicted to cause a threonine to lysine change at position 364 of the SMURF2 protein (Fig. 3.2 A). This is a highly conserved residue among vertebrates (Fig. 3.2 C). SMURF2 is an E3 ubiquitin ligase which plays a major role in the regulation of TGF-beta signalling (*404*). Although this mutation does not lie in an active domain of the protein (Fig. 3.2 B), Wiesner et al. have suggested that the region between the WW3 and the HECT domain might interact with SMAD7, regulating the expression of TGFβR on cells surface (*405*).

The second mutation at position chr.11: 100,740,662 bp was a T to G transversion in exon 13 of the *Stat5a* gene. This nucleotide change causes a tryptophan to glycine substitution at position 484, within the LD of the STAT5A protein (Fig. 3.2 E). Although the function of the LD in STAT proteins is incompletely characterized, this mutation could be of importance, as W484 is strictly conserved in STAT5A relatives from different species, suggesting a conserved structural/functional role of this residue in STAT5A activity. Moreover, W484 is conserved among all STAT family members (Fig. 3.2 G). This substantiates the potential importance of the mutation in STAT5A function. STAT5A and B are very similar and both seem to be important for the development of the immune system. *Stat5a*$^{-/-}$*Stat5b*$^{-/-}$ double mutant mice have a low survival rate and defective development of T, NK and B cells (*245*, *402*). However, these defects were not as significant in the single mutants, revealing a certain level of redundancy in the signalling of STAT5A and STAT5B.

Survival to HSV-1 infection is independent of *Smurf2*^{T363K} or *Stat5a*^{W484G}

To determine the ENU mutation causing HSV-1 susceptibility in the Keagan pedigree, we isolated the SMURF2 and STAT5A mutation by serial back-crossing and intercrossing to C57BL/6 mice. The mice were then challenged with the virus. The survival of homozygous *Smurf2*^{T364K} mice to HSV-1 infection was identical to wild-type littermates (Fig, 3.3 A). *Smurf2*^{KO} animals were also tested and no significant susceptibility was observed (Fig. 3.3 B), confirming that the ENU mutation in *Smurf2* did not cause HSV-1 susceptibility. Homozygous *Stat5a*^{W484G} were then tested, but no significant difference in mortality was observed in the mutant mice (Fig. 3.3 C). To rule out the possibility that both mutations were required for viral susceptibility, we generated *Smurf2*^{T364K}/*Stat5a*^{W484G} double mutant mice. We did not observe a decrease in survival following challenge with HSV-1 (Fig. 3.3 D). Nonetheless, STAT5 function is crucial for mounting an adequate immune response and for proper lymphocyte development. Thus, we further validated the effect of the ENU mutation on STAT5A on lymphocyte function.

Stat5a^{W484G} lymphocytes have impaired IL-2 responses

To validate the effect of the STAT5A W484G mutation on the protein function, we first quantified STAT5A expression in spleen from wild-type and mutant mice (Fig. 3.4, A and B). The ENU mutation in the LD of STAT5A reduced its expression in Stat5aW484G mice, which could impact the capacity of lymphocytes to respond to cytokine or pathogen stimuli. To answer this, we directly examined STAT5A-dependent lymphocyte phenotypes. IL-2 receptor sub-units IL-2Rβ (CD122) and IL-2Rα (CD25) are transcriptional targets of STAT5A whereas *Stat5a*-deficient lymphocytes are irresponsive to IL-2 cytokine stimulation (*406*). To test this, we stimulated *Stat5a*^{W484G} NK cells with IL-2 to stimulate proliferation and produce lymphokine activated killer cells (LAK). NK cells from *Stat5a*^{W484G} animals did not proliferate as much as the wild type littermates, and thus produced fewer LAK cells (Fig. 3.4 C). Moreover, expression levels of the IL-2Rβ (CD122) were lower in the mutant cells (Fig. 3.4 D), confirming the effect of the STAT5A ENU-

induced mutation on NK cells (*231*, *402*). We further confirmed the effect of the STAT5A mutation on CD4 and CD8 T cells by quantifying the expression of IL-2Rα (CD25) following stimulation with IL-2 and αCD3 cross-linking. Following the engagement of IL-2 to the IL-2R, JAK3 is phosphorylated, which in turn activates STAT5A and STAT5B (*407*). A reduction in the intensity of JAK3 signaling dampens the IL-2 downstream effects. Thus, *Jak3*$^{+/-}$ cells were also used as a control. The capacity of IL-2 to induce increased expression of CD25 in both CD4 and CD8 cells (Fig. 3.4, E to H) was high in wild-type cells, intermediate in *Jak3*$^{+/-}$ cells and almost completely abolished in cells from *Stat5a*^{W484G} mice, demonstrating a defect in JAK3/STAT5A signaling and confirming the effect of the W484G mutation on STAT5A function.

Stat5a^{W484G} mice show aberrant lymphocyte response following herpesviruses infection

To examine the role of *Stat5a*^{W484G} in the lymphocyte response to virus infection, we challenged animals with mouse cytomegalovirus (MCMV). NK cells are essential to the immune response to MCMV. Infection leads to the proliferation of NK cells, the direct killing of infected cells and the secretion of cytokines necessary for the activation of T cells (reviewed in (*315*)). As STAT5 is crucial to the activation of NK and T cells, we expected the ENU mutation to alter the response to the virus, as observed after IL-2 stimulation. Following MCMV infection, not only did we observe a decrease in total splenocyte numbers (Fig. 3.5, A), but we also observed a severe decrease in the total NK cell population (Fig. 3.5, B and C). Moreover, both CD4 and CD8 T cells were reduced at day 7 post-infection (p.i., Fig. 3.5, D to F). Interestingly, the low CD8 T cell number was coupled with an accumulation of naïve CD62L^{+}CD44^{-} (Fig. 3.5, H and I). Thus, the ENU mutation on the DNA binding site of STAT5A altered NK and T cell responses to MCMV infection.

The defect in lymphocyte population following infection was also confirmed using an HSV-1 infection model. In infected wild-type mice, the NK cell population increased, while a

reduction in NK cell numbers was observed at day 21 p.i. (Fig. 3.6, A and B). The mutation on STAT5A also caused a decrease in the proportion of splenic CD8 T cells, which was not observed in *Stat5a*$^{+/+}$ animals (Fig. 3.6, C and D). Moreover, following reinfection at a high viral dose two weeks after the initial infection, the CD44^{+} antigen experienced CD8 T cells were reduced by half in *Stat5a*^{W484G} mice when compared to wild-type mice. (Fig. 3.6, E and F). Thus, this mutation on the LD site of STAT5A is sufficient to alter NK and T cell responses to HSV-1 and MCMV.

Discussion

Genetic background can dictate the outcome of a viral infection. Various studies, in both humans and mice, have highlighted the importance of a single gene mutation in host resistance to HSV-1 (*54*, *66*, *78*, *80*, *90*, *98*, *342*, *343*, *408*).. In a previous study, we used ENU mutagenesis to generate mice carrying single point mutations resulting in susceptibility to HSV-1 (see Chapter 2 of this thesis). In this work, we selected the Keagan pedigree for further analysis. We used whole exome sequencing to identify the ENU mutation that causes susceptibility, but couldn't identify a mutation that segregates among the 3 susceptible animals sequenced. We then used the ENU SNVs unique to that pedigree to map the mutation and found a significant peak at chromosome 11, with *Smurf2* and *Stat5a* as candidate genes. While we could not recapitulate viral susceptibility in the different mouse strains carrying either one or both of the mutations, we pursued the analysis of the *Stat5a*^{W484G} mutant. The mice carrying the ENU mutation on STAT5A exhibited abnormal T and NK cell populations following MCMV and HSV-1 infection, as well as an incapacity to upregulate the expression of the IL2R subunits after stimulation.

We had previously injected B6 males (G0) with ENU and then bred them for 3 generations with females to produce G3 mice for phenotyping (see Chapter 2 of this thesis and (*310*)). We used a sequencing/genotyping strategy where the G3 animals were used for both phenotyping and sequencing. Although this strategy was successfully used to identify

ENU mutations in a mixed C57BL/6 – C57BL/10 breeding scheme (*66*, *332*), we found this technique to be limiting when using a pure C57BL/6 background. Due to the low amount of SNV identified during exome sequencing, genome coverage was not optimal during the subsequent genotyping step. As an alternative approach, whole genome sequencing of selected susceptible G3 mice would have allowed the discovery of more SNVs and the generation of a larger genotyping panel. This in turn would have increased coverage and genotyping efficiency while retaining a pure B6 breeding scheme. Another approach is the direct sequencing of the original G1 male. Indeed, other groups used a strategy where the whole genome of the G1 male is sequenced in order to build a large genotyping panel to be applied on animals from subsequent deviant pedigree (*328*, *409*). This method allows for quick genotyping of the susceptible G3 using all the SNVs from the parental G1 male as soon as the deviant pedigree is identified.

Although we identified an ENU mutation on the LD site of STAT5A that causes an abnormal lymphocyte response to HSV-1, this mutation does not explain the whole extent of the susceptibility we observed in the original Keagan animals. Three hypotheses could explain this discrepancy. First, in conjunction with STAT5A, a secondary gene or an alternate gene which we did not identify could be contributing to HSV-1 susceptibility. In the process of isolating the *Stat5a* mutation, we may have lost the second ENU mutation, thus losing susceptibility. This hypothesis is the most plausible, as the mutation on STAT5A altered the T cell response to the virus, and T cells are central to the control of HSV-1 infection (*35*, *66*, *73*). Second, HSV-1 susceptibility may be the result of another mutation, independent of *Stat5a*, that we could not map or sequence due to a lack of coverage and/or power. To confirm/reject either of these two hypotheses, full genome sequencing should be used to increase the number of markers, resulting in better genetic mapping. Moreover, phenotyping additional G3 animals may have helped to resolve the problem. Third, the mutation could have been on a non-coding gene such as a long non-coding RNA (lncRNA), which is known for playing a central role in the regulation of inflammatory responses, the NF-κB pathway and the function of different IFN induced genes during viral infection (*410*). The expression of more than 200 lncRNAs is modified

during HSV-1 infection (*411*). Here again, by using the technique of whole genome sequencing, we could have identified an HSV-1-susceptibility ENU mutation that impacts a non-coding gene.

Nevertheless, we have identified a single point mutation on the transcription factor STAT5A in our Keagan mice. The W484G ENU mutation lies in the LD region of STAT5A (Fig. 3.7) (*397*, *412*, *413*). Although the W484 position is strictly conserved in all STAT family members and in all species examined, the LD region of STAT proteins remains incompletely characterized (Fig. 3.2, G). For instance, a mutant in the linker domain of STAT1 (A544) failed to stimulate transcription. However, this mutant protein was normally tyrosine- and serine-phosphorylated, accumulated in the nucleus, and bound a high affinity STAT site in an electrophoretic mobility shift assay (EMSA), suggesting that the mutation abolished recruitment of transcriptional co-activators (*412*). A mutation in the linker domain of STAT3 (I563) associated with hyper immunoglobulin E syndrome was found to reduce STAT3 tyrosine phosphorylation due to conformational changes (*414*). Hence it has been proposed that the LD region of STAT proteins is involved in protein-protein interactions or inter-domain allosteric communications, which would be aberrant in STAT5A W484G mutant proteins. Moreover, previous studies have shown that STAT5A and STAT5B can form tetramers, which are critical for cytokine responses and normal T and NK cell function (*231*). STAT5 tetramers can bind to sequences with a very broad range of spacing between tandem DNA-binding motifs. It has been proposed that such binding could be facilitated by the LD region of the STAT5 protein (*415*). Thus, the W484G mutation could compromise DNA binding affinity, leading to a weaker interaction between the STAT5 tetramers and the DNA molecules, and causing the impaired lymphocyte response observed in our *Stat5a*^{W484G} mutant mice.

Although additional studies are required to understand the precise role of residue W484 in STAT5A protein function, we found that mice carrying the W484G mutation in the LD site of STAT5A display an abnormal lymphocyte response during viral infections. Previous studies have shown that STAT5A is essential for IL-2 response in T cells (*231*,

245, *402*, *406*). Here, we show that STAT5A is sufficient to abrogate IL-2 responses in both T cells and NK cells. No increase in the expression of IL-2Rα was observed following stimulation, thus indicating a defect in the positive feedback loop usually observed in IL-2 stimulated T cells (*231*, *406*), which can explain the unbalanced T cell population in HSV-1 infected mutant mice. The effect of the mutation on the capacity of T cells to restrict viral replication at the site of infection is also to be assessed. The reduction in the T cell number could have impaired the production of IFNγ by CD4 T cells at the infection site, thus reducing the recruitment and antiviral function of the CD8 T cells against HSV-1(*66*).

We showed that NK cell proliferation is compromised by the ENU mutation on STAT5A following IL-2 stimulation during MCMV or HSV-1 infection. To our knowledge, this is the first report of the importance of STAT5A for NK function during infection, independently of STAT5B. It was previously shown that impairing both STAT5A and STAT5B impairs NK development and reduces NK numbers (*231*, *402*). Also, NK cells from *Stat5b*$^{-/-}$ mice display a defect in cytotoxic activity and proliferation when stimulated with IL-2 (*246*). Here, we show that the W484 residue of the STAT5A protein is essential for proper NK proliferation following stimulation, suggesting that damaging the LD domain of STAT5A is enough to reduce the efficiency of the STAT5 signaling, even if STAT5B remains intact.

The modulation of the STAT5 pathway and subsequent NK and T cell responses is a powerful tool for the development of a novel immune therapy for cancer treatment. For instance, as CIS a negative regulator of the JAK1/STAT5 function, and GITR is a negative regulator of IL-15 activation that reduces STAT5 phosphorylation, a novel immune therapy could target CIS and GITR to increase NK and T cell functions and ameliorate clinical outcomes (*416-419*). Understanding the importance of the different domains and functional residues of STAT5A should be helpful for the development of novel, potent immunotherapeutic strategies for cancer.

Materials and Methods

Animals and viruses

ENU *Stat5a*^{W484G} mice were produced and housed in the animal facility of the Goodman Cancer Centre, McGill University. C57BL/6J and A/J were purchased from Jackson laboratories (Bar Harbor, Maine, USA). JAK3$^{-/-}$ mice were provided by Dr Phillipe Gros and SMURF2^{KO} mice were provided by Dr Jeff Wrana (Lunenfeld-Tanenbaum Research Institute). The MCMV Smith strain was obtained from ATCC (#VR1399). The virus was produced in salivary glands as previously described (*420*). HSV-1 was originally isolated by Dr. Subak-Sharpe and produced as described previously (*421*). For infection, mice of 8 to 10 weeks of age were infected i.p. with 10^4 PFU of MCMV or HSV-1. Animals were monitored daily for up to 21 days.

DNA extraction and whole-exome sequencing

Genomic DNA from tail biopsy was extracted using phenol/chloroform as described previously (*381*). Whole-exome sequencing from 3 susceptible Keagan animals was completed as previously described (*204*). Briefly, exome capture was performed using a SureSelect Mouse All Exon kit (Agilent Technologies) and parallel sequencing on an Illumina HiSeq 2000 (100-bp paired-end reads). Sequence analysis was performed through the Canadian Centre for Computational Genomics (C3G) pipeline, which follows the stepwise procedures of the Broad Institute's GATK best practices. Raw sequencing reads were trimmed using Trimmomatic (*422*) to obtain a high quality set of reads for sequence alignment. The trimmed reads were aligned to the mouse reference genome (mm10/GRCm38) using a fast, memory-efficient Burrows-Wheeler transform aligner BWA-mem (*423*). Mapped reads were further refined using the GATK (*424*) and Picard program suites (found at http://broadinstitute.github.io/picard) to improve mapping near insertions and deletions (indels: GATK indel realigner), to remove duplicate reads with the same paired start site (Picard mark duplicates), and to improve quality scores (GATK base recalibration). Variants were called using the GATK haplotype caller in gvcf mode

to allow efficient downstream merging of multiple samples into one variant file to streamline downstream variant processing procedures which included variant annotation and functional annotation with SNPeff (*425*).

Genetic Mapping

SNV that are unique to the Keagan pedigree, have a depth of read of at least 5x and were present in at least 2 of the 3 sequenced samples were selected to produce a 55 marker genotyping panel. SNP primer design and genotyping was performed at the McGill University and Génome Québec Innovation Centre using Sequenom iPLEX Gold Technology. Linkage analysis was performed with R/qtl software version 3.3.2 and the LOD score was calculated using survival as phenotype (*66*).

Protein expression analysis

STAT5A expression was measured in the spleen lysate from 8-week-old mice. Proteins were prepared using the T-Per Tissue Protein Extraction Reagent (ThermoFisher, #78510). Western blots were carried out following a standard protocol. 25µg of protein were migrated on an 8% denaturing gel and transferred onto nitrocellulose membranes. The anti-STAT5A antibody (clone E289, #ab32043) from Abcam and the anti-GAPDH antibody (clone FL335, #sc-25778) from Santa-Cruz Biotechnology were used. Bands intensities were measured using the ImageJ software (v1.50i).

Immunophenotyping

Single cell preparations from the spleen were produced and stained with different antibody cocktails. The following antibodies and reagents were acquired from eBiosciences: CD3e (145-2C11), CD8a (53-6.7), CD122 (TM-b1), CD4 (L3T4), CD62L (MEL-14), CD49b (DX5), CD44 (1M7), CD25 (PC61.5) and Fixable Viability Dye eFluor 506. All flow cytometry was performed on a BD Canto II machine and analysis was done using the FlowJo software (version 10.3).

Ex-vivo lymphocyte stimulation

For the NK/LAK proliferation assay, $15x10^6$ splenocytes were cultured for 7 days in complete RPMI containing 2000U/ml of hIL-2 (Peprotech). Media was replenished on day 3. For the stimulation of the T cells, 10^6 splenocytes were cultured in 1ml of complete RMPI and stimulated with 10ug/ml plate bound αCD3 (145-2C11, eBioscience) and 1000 U/ml of hIL-2 for 72 hours. Cells were then prepared for flow cytometry analysis.

STAT5A structure and protein sequence alignment

STAT5A protein structure was obtained from the RCSB Protein Data Bank, as described by Neculai et al. (*66*). Analysis of the structure was performed using USCF Chimera software (version 1.11.2). Protein sequences were obtained from the Uniprot Protein Knowledgebase or the NCBI Protein Database. Alignments were performed using the ClustalW2 alignment tool or the CLC Sequence Viewer software (version 6.8.1).

Figures and Figures legends

Figure 3.1- Mapping the susceptibility mutation in the Keagan pedigree

(A) Mice from the Keagan pedigree were weighed, infected with 10^4 PFU of HSV-1 and monitored for 14 days. Survival rates of the Keagan mice and the resistant B6 and susceptible A/J mice used during the HSV-1 screen are displayed. (B) Homozygote SNVs unique to the Keagan pedigree were used to produce a panel with 55 polymorphic markers. (C) A QTL analysis was performed on the G3 from the Keagan pedigree. The dash line represents the α threshold of 0.05. (D) Haplotypes of chromosome 11 showing the segregation of the ENU mutation (A), the reference C57BL/6 allele (B) or heterozygote genotype (H).

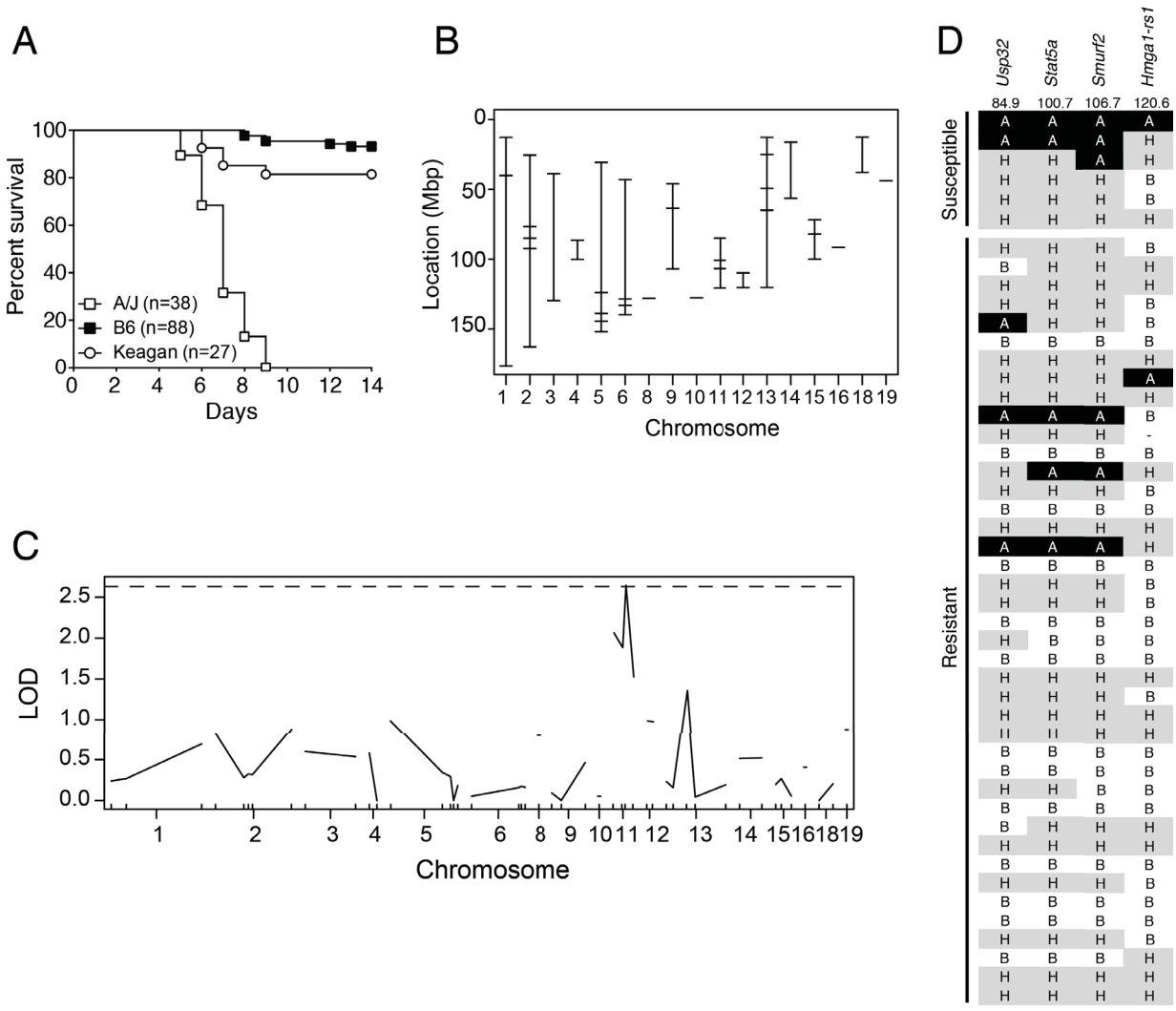
A
Percent survival
Days
A/J (n=38)
B6 (n=88)
Keagan (n=27)
B
Location (Mbp)
Chromosome
C
LOD
Chromosome
D
Usp32
Stat5a
Smurf2
Hmga1-rs1
84.9
100.7
106.7
120.6
Susceptible
Resistant

Figure 3.2 - Genetic location of the *Smurf2* and the *Stat5a* ENU mutations

(A) Diagram of the ENU mutation on Smurf2 showing the amino acid substitution. (B) Protein structure of SMURF2. (C) Alignment of Smurf2 on the mutation site. Accession numbers: Mouse – NP_079757.2, Human – NP_073576.1, Rhesus Macaque – AFE71357.1, Common chimpanzee – JAA29960.1, Rat – 157818165, Cattle – DAA18293.1, Green Sea turtle – EMP40178.1, Wild duck – EOB06683.1, Tupaia – ELW67486.1, African clawed frog – AAG50422.1. (D) Diagram of the ENU mutation on Stat5a showing the amino acid substitution. (E) Protein structure of STAT5A showing the location of the ENU mutation. (F) Alignment of STAT5A and STAT5B at the site of the ENU mutation. Uniprot entry numbers: Mouse – P42230, Human – P42229, Bovin – Q95115, Rat – Q62771, Sheep – P42231, Pig – Q9TUZ1, Zebrafish – Q68SP3, STAT5B Mouse – P42232, STAT5B Human – P51692. (G) Alignment of the murine STATs in the region in which the linker domain overlaps with the DNA domain of STAT5A (positions 475 to 583). The W484 residue is highlighted in grey. The bar plot represents the conservation level of each residue. Uniprot identifier numbers: STAT1 – P42225, STAT2 – Q9WVL2, STAT3 – P42227, STAT4 – P42228, STAT5A – P42230, STAT5B – P42232 and STAT6 – P52633.

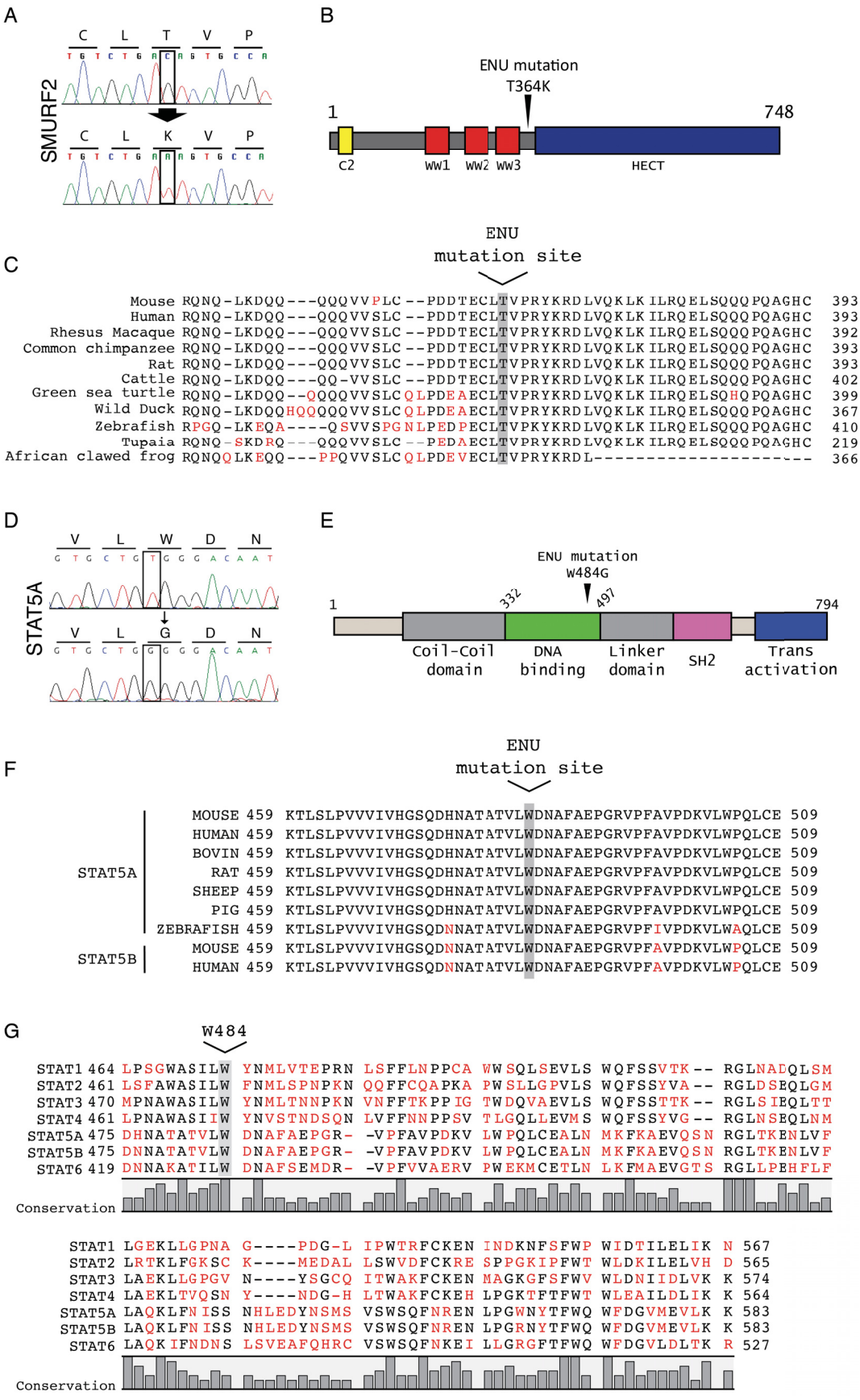
A
SMURF2
C L T V P
C L K V P
B
ENU mutation
T364K
1
748
C2
WW1
WW2
WW3
HECT
C
ENU
mutation site
Mouse RQNQ-LKDQQ---QQQVVPLC--PDDTECLTVPRYKRDLVQKLKILRQELSQQQPQAGHC 393
Human RQNQ-LKDQQ---QQQVVSLC--PDDTECLTVPRYKRDLVQKLKILRQELSQQQPQAGHC 393
Rhesus Macaque RQNQ-LKDQQ---QQQVVSLC--PDDTECLTVPRYKRDLVQKLKILRQELSQQQPQAGHC 392
Common chimpanzee RQNQ-LKDQQ---QQQVVSLC--PDDTECLTVPRYKRDLVQKLKILRQELSQQQPQAGHC 393
Rat RQNQ-LKDQQ---QQQVVSLC--PDDTECLTVPRYKRDLVQKLKILRQELSQQQPQAGHC 393
Cattle RQNQ-LKDQQ---QQ-VVSLC--PDDTECLTVPRYKRDLVQKLKILRQELSQQQPQAGHC 402
Green sea turtle RQNQ-LKDQQ--QQQQVVSLCQLPDEAECLTVPRYKRDLVQKLKILRQELSQHQPQAGHC 399
Wild Duck RQNQ-LKDQQHQQQQQVVSLCQLPDEAECLTVPRYKRDLVQKLKILRQELSQQQPQAGHC 367
Zebrafish RPGQ-LKEQA----QSVVSPGNLPEDPECLTVPKYKRDLVQKLKILRQELSQQQPQAGHC 410
Tupaia RQNQ-SKDRQ---QQQVVSLC--PEDAECLTVPRYKRDLVQKLKILRQELSQQQPQAGHC 219
African clawed frog RQNQQLKEQQ---PPQVVSLCQLPDEVECLTVPRYKRDL---------- 366
D
STAT5A
V L W D N
V L G D N
E
ENU mutation
W484G
1
332
497
794
Coil-Coil domain
DNA binding
Linker domain
SH2
Trans activation
F
ENU
mutation site
STAT5A
MOUSE 459 KTLSLPVVVIVHGSQDHNATATVLWDNAFAEPGRVPFAVPDKVLWPQLCE 509
HUMAN 459 KTLSLPVVVIVHGSQDHNATATVLWDNAFAEPGRVPFAVPDKVLWPQLCE 509
BOVIN 459 KTLSLPVVVIVHGSQDHNATATVLWDNAFAEPGRVPFAVPDKVLWPQLCE 509
RAT 459 KTLSLPVVVIVHGSQDHNATATVLWDNAFAEPGRVPFAVPDKVLWPQLCE 509
SHEEP 459 KTLSLPVVVIVHGSQDHNATATVLWDNAFAEPGRVPFAVPDKVLWPQLCE 509
PIG 459 KTLSLPVVVIVHGSQDHNATATVLWDNAFAEPGRVPFAVPDKVLWPQLCE 509
ZEBRAFISH 459 KTLSLPVVVIVHGSQDNNATATVLWDNAFAEPGRVPFIVPDKVLWAQLCE 509
STAT5B
MOUSE 459 KTLSLPVVVIVHGSQDNNATATVLWDNAFAEPGRVPFAVPDKVLWPQLCE 509
HUMAN 459 KTLSLPVVVIVHGSQDNNATATVLWDNAFAEPGRVPFAVPDKVLWPQLCE 509
G
W484
STAT1 464 LPSGWASILW YNMLVTEPRN LSFFLNPPCA WWSQLSEVLS WQFSSVTK-- RGLNADQLSM
STAT2 461 LSFAWASILW FNMLSPNPKN QQFFCQAPKA PWSLLGPVLS WQFSSYVA-- RGLDSEQLGM
STAT3 470 MPNAWASILW YNMLTNNPKN VNFFTKPPIG TWDQVAEVLS WQFSSTTK-- RGLSIEQLTT
STAT4 461 LPNAWASIIW YNVSTNDSQN LVFFNNPPSV TLGQLLEVMS WQFSSYVG-- RGLNSEQLNM
STAT5A 475 DHNATATVLW DNAFAEPGR- -VPFAVPDKV LWPQLCEALN MKFKAEVQSN RGLTKENLVF
STAT5B 475 DNNATATVLW DNAFAEPGR- -VPFAVPDKV LWPQLCEALN MKFKAEVQSN RGLTKENLVF
STAT6 419 DNNAKATILW DNAFSEMDR- -VPFVVAERV PWEKMCETLN LKFMAEVGTS RGLLPEHFLF
Conservation
STAT1 LGEKLLGPNA G-----PDG-L IPWTRFCKEN INDKNFSFWP WIDTILELIK N 567
STAT2 LRTKLFGKSC K-----MEDAL LSWVDFCKRE SPPGKIPFWT WLDKILELVH D 565
STAT3 LAEKLLGPGV N-----YSGCQ ITWAKFCKEN MAGKGFSFWV WLDNIIDLVK K 574
STAT4 LAEKLTVQSN Y-----NDG-H LTWAKFCKEH LPGKTFTFWT WLEAILDLIK K 564
STAT5A LAQKLFNISS NHLEDYNSMS VSWSQFNREN LPGWNYTFWQ WFDGVMEVLK K 583
STAT5B LAQKLFNISS NHLEDYNSMS VSWSQFNREN LPGRNYTFWQ WFDGVMEVLK K 583
STAT6 LAQKIFNDNS LSVEAFQHRC VSWSQFNKEI LLGRGFTFWQ WFDGVLDLTK R 527
Conservation

Figure 3.3 - HSV-1 susceptibility of SMURF2 and STAT5A mutants

(A) *Smurf2*^{T364K}, (B) *Smurf2*^{KO}, (C) *Stat5a*^{W484G} and (D) *Smurf2*^{T364K}/*Stat5a*^{W484G} double mutant mice were infected with HSV-1 with 10^4 PFU IP. Wild-type littermates, resistant B6 and susceptible A/J mice were also infected. Animals were monitored for 14 days for clinical signs. Statistics: Log-rank (Mantel-Cox) test.

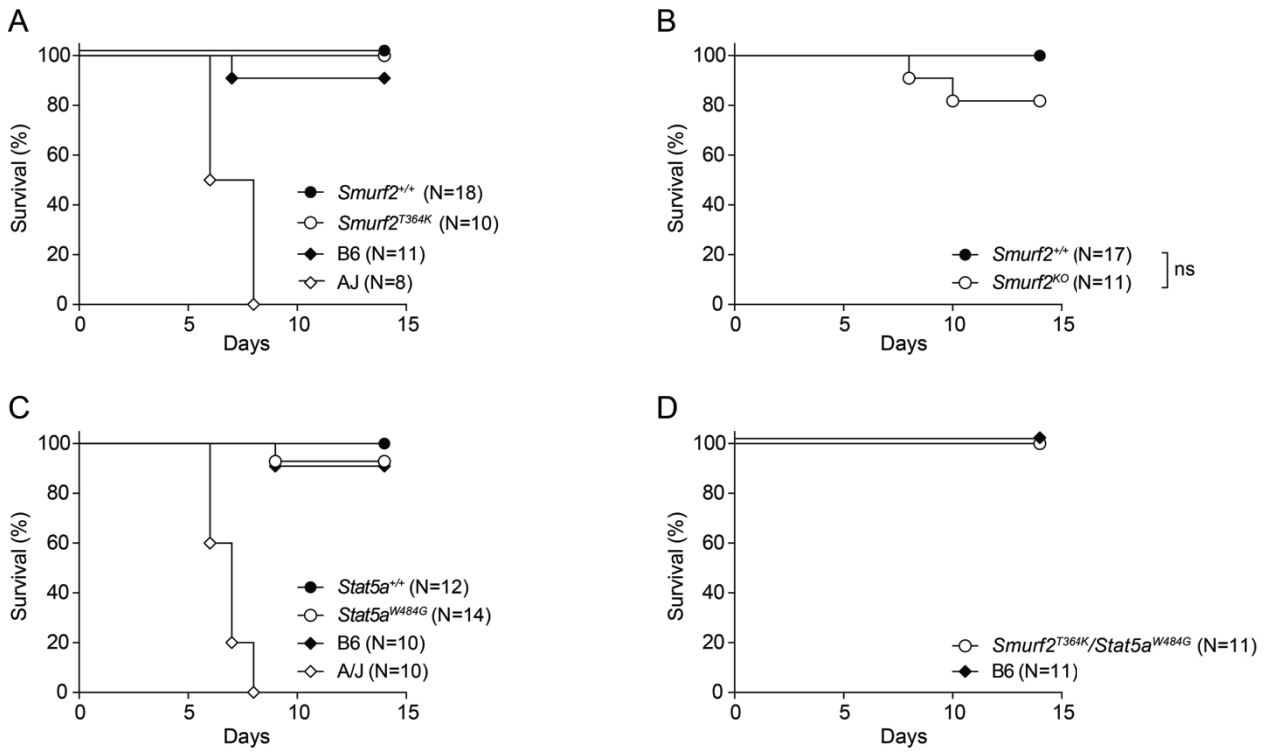
A
Survival (%)
Days
Smurf2+/+ (N=18)
Smurf2T364K (N=10)
B6 (N=11)
AJ (N=8)
B
Survival (%)
Days
Smurf2+/+ (N=17)
Smurf2KO (N=11)
ns
C
Survival (%)
Days
Stat5a+/+ (N=12)
Stat5aW484G (N=14)
B6 (N=10)
A/J (N=10)
D
Survival (%)
Days
Smurf2T364K/Stat5aW484G (N=11)
B6 (N=11)

Figure 3.4 – *Stat5a*^{W484G} lymphocyte response to IL-2

(A) STAT5A expression in spleen lysates from *Stat5a*$^{+/+}$ and *Stat5a*^{W484G} mice was probed by Western blot. The relative band expression (N=3) of STAT5A is shown in (B). (C) Fifteen million splenocytes from wild type and *Stat5a*^{W484G} mice were stimulated with 2000U/ml of IL-2 for 7 days to produce LAK cells. NK1.1+CD3- cells were then analyzed by FACS and counted. (D) The mean fluorescence intensity of CD122 was measured on these LAK cells by FACS. A representative histogram plot of CD122 expression of mutant and wild-type cells is shown. (E) 10^6 splenocytes were stimulated for 72h with 10^3 U/ml IL-2 and/or plate-bound CD3. Expression levels of CD25 were measured in CD4+CD3+ cells. (F) Representative histogram of CD25 expression in CD4 T cells. (G) CD25 expression level was also measured in CD8+CD3+ cells after IL-2/CD3 stimulation (H) A representative histogram of CD25 expression is also displayed. Statistics: *: $p<0.05$, **: $p<0.01$, ***: $p<0.001$, ****:$p<0.0001$ (Student T test or two-way ANOVA).

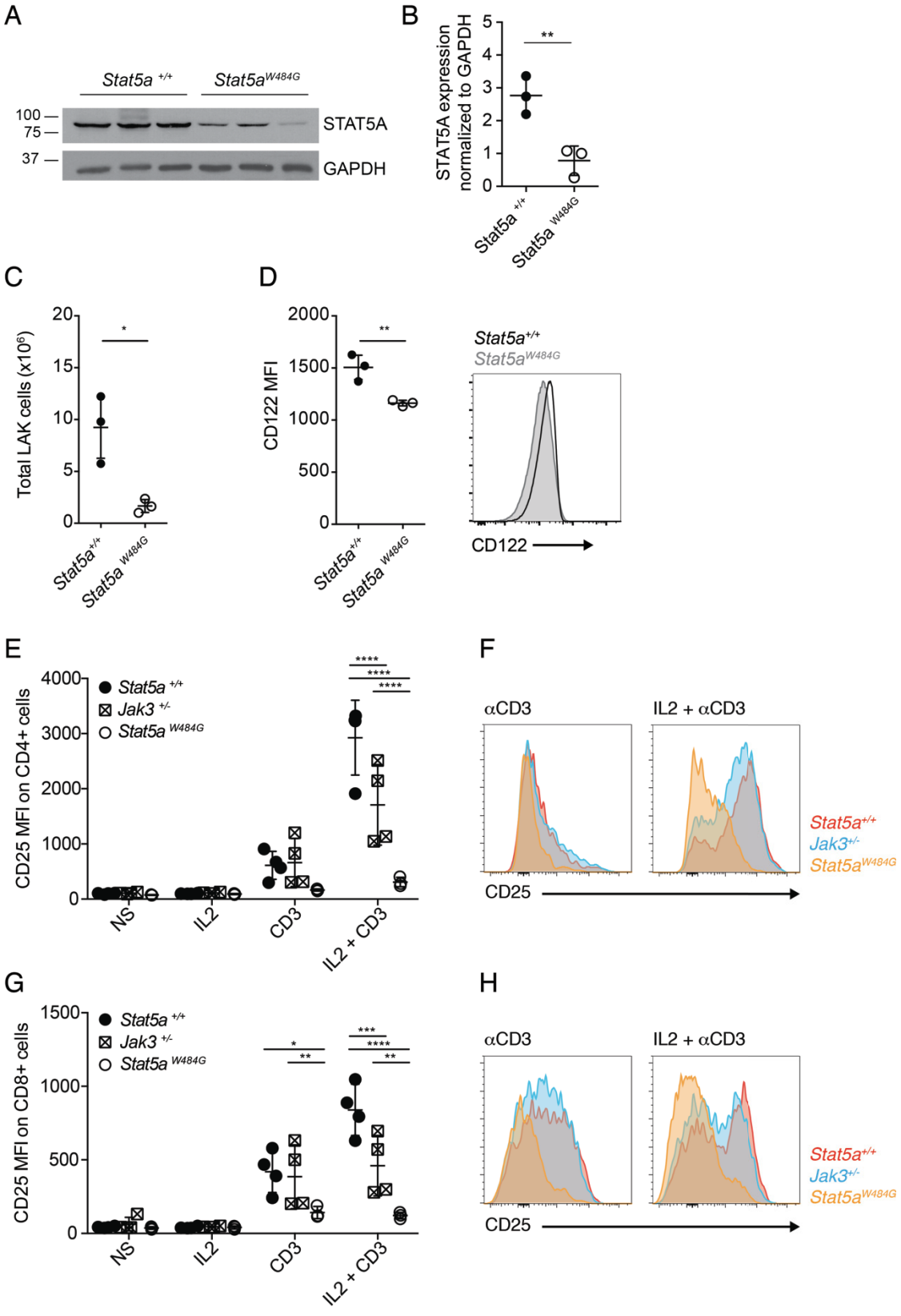
A
Stat5a +/+
Stat5a W484G
100
75
37
STAT5A
GAPDH
B
STAT5A expression normalized to GAPDH
Stat5a +/+
Stat5a W484G
C
Total LAK cells (x10^6)
D
CD122 MFI
Stat5a+/+
Stat5aW484G
CD122
E
CD25 MFI on CD4+ cells
Jak3 +/-
NS
IL2
CD3
IL2 + CD3
F
αCD3
IL2 + αCD3
Jak3+/-
CD25
G
CD25 MFI on CD8+ cells
H

Figure 3.5 – *Stat5a*^{W484G} lymphocyte response to MCMV infection

(A) Total splenocyte number was determined in uninfected (PBS) animals and infected mice at day 5 and 7 p.i. (B) Total NK cell numbers were also quantified via the expression of DX5 and CD3. (C) Representative plot of $DX5^{+}CD3^{-}$ NK cells from splenocytes of infected mice at day 7. (D) Total CD4+CD3+ and (E) CD8+CD3+ splenocytes were quantified at day 5, day 7 or in uninfected (PBS) animals. (F) Representative plot of CD4+ and CD8+ in CD3+ splenocytes at day 7 p.i. (G) Expression of CD62L and CD44 were measured in $CD4^{+}CD3^{+}$ and (H) $CD8^{+}CD3^{+}$ cells. (I) CD62L and CD44 on CD8+CD3+ cells at day 7 p.i. Statistics: *: $p<0.05$, **: $p<0.01$, ****:$p<0.0001$ (two-way ANOVA).

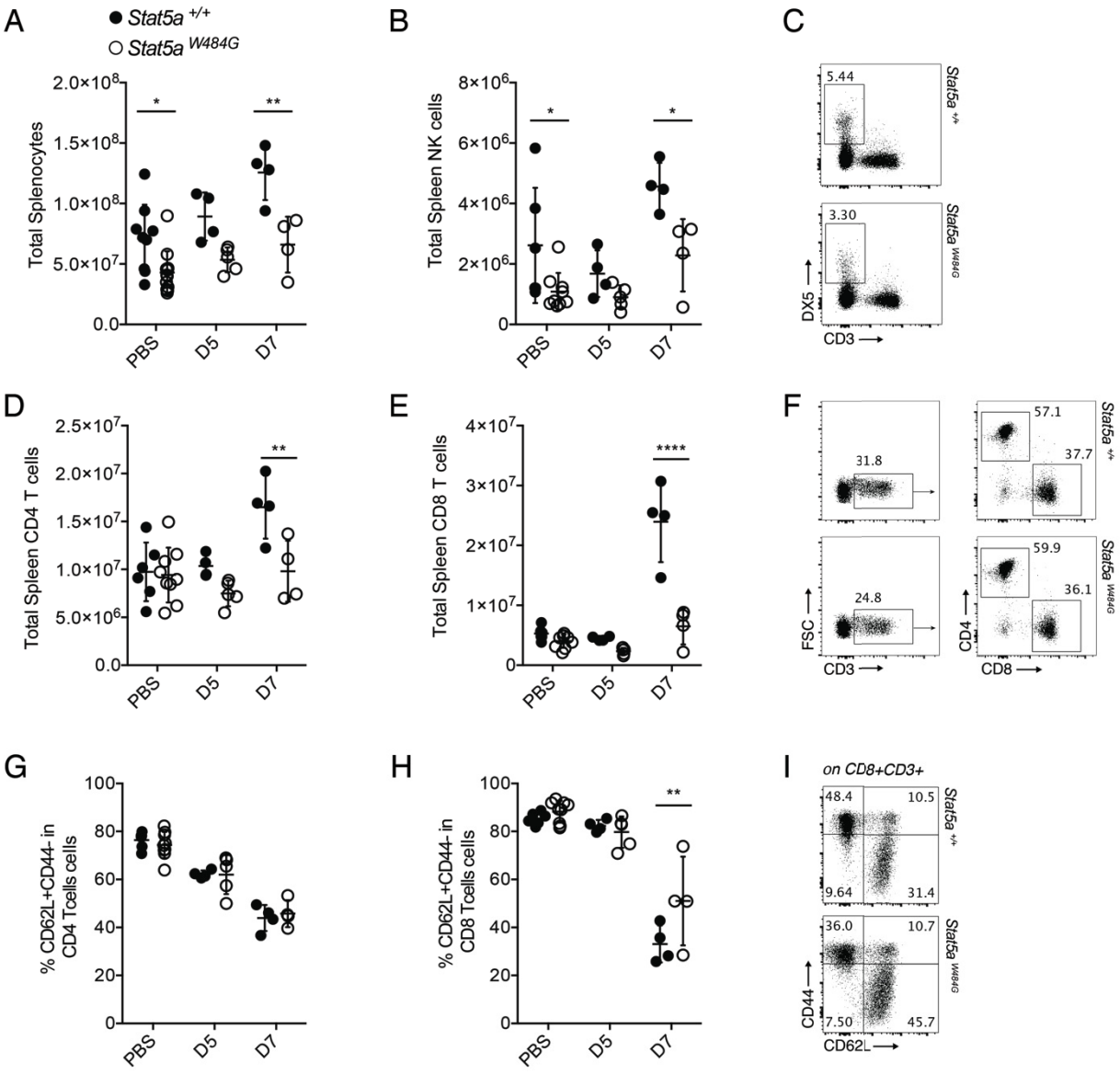
A
Stat5a +/+
Stat5a W484G
Total Splenocytes
2.0×10^8
1.5×10^8
1.0×10^8
5.0×10^7
0.0
*
**
PBS
D5
D7
B
Total Spleen NK cells
8×10^6
6×10^6
4×10^6
2×10^6
0
*
*
PBS
D5
D7
C
5.44
Stat5a +/+
3.30
Stat5a W484G
DX5
CD3
D
Total Spleen CD4 T cells
2.5×10^7
2.0×10^7
1.5×10^7
1.0×10^7
5.0×10^6
0.0
**
PBS
D5
D7
E
Total Spleen CD8 T cells
4×10^7
3×10^7
2×10^7
1×10^7
0
****
PBS
D5
D7
F
31.8
57.1
37.7
Stat5a +/+
24.8
59.9
36.1
Stat5a W484G
FSC
CD3
CD4
CD8
G
% CD62L+CD44- in CD4 Tcells cells
100
80
60
40
20
0
PBS
D5
D7
H
% CD62L+CD44- in CD8 Tcells cells
100
80
60
40
20
0
**
PBS
D5
D7
I
on CD8+CD3+
48.4
10.5
Stat5a +/+
9.64
31.4
36.0
10.7
Stat5a W484G
7.50
45.7
CD44
CD62L

Figure 3.6 – *Stat5a*^{W484G} lymphocytes response to HSV-1 infection

(A) NK cell were quantified in the spleen at day 7, 14 and 21 p.i. with 10^4 PFU of HSV-1. (B) Representative flow cytometric dot plots showing $DX5^+CD3^-$ NK cells from *Stat5a*^{W484G} and *Stat5a*$^{+/+}$ mice at day 21 p.i. (C) Frequency of CD8 T cells in wild-type and mutant mice from day 7 to 21 p.i. (D) Representative flow cytometric dot plots showing $CD3^+CD8^+$ T cells at day 21 p.i. (E) CD44 proportion in CD8 T cells at day 28 p.i., following a re-infection at day 23 with $5x10^4$ PFU. (F) Representative FACS plot of $CD44^+$ in $CD3^+CD8^+$ spleen cells at day 28 p.i. Statistics: *: $p<0.05$, **: $p<0.01$ (two-way ANOVA).

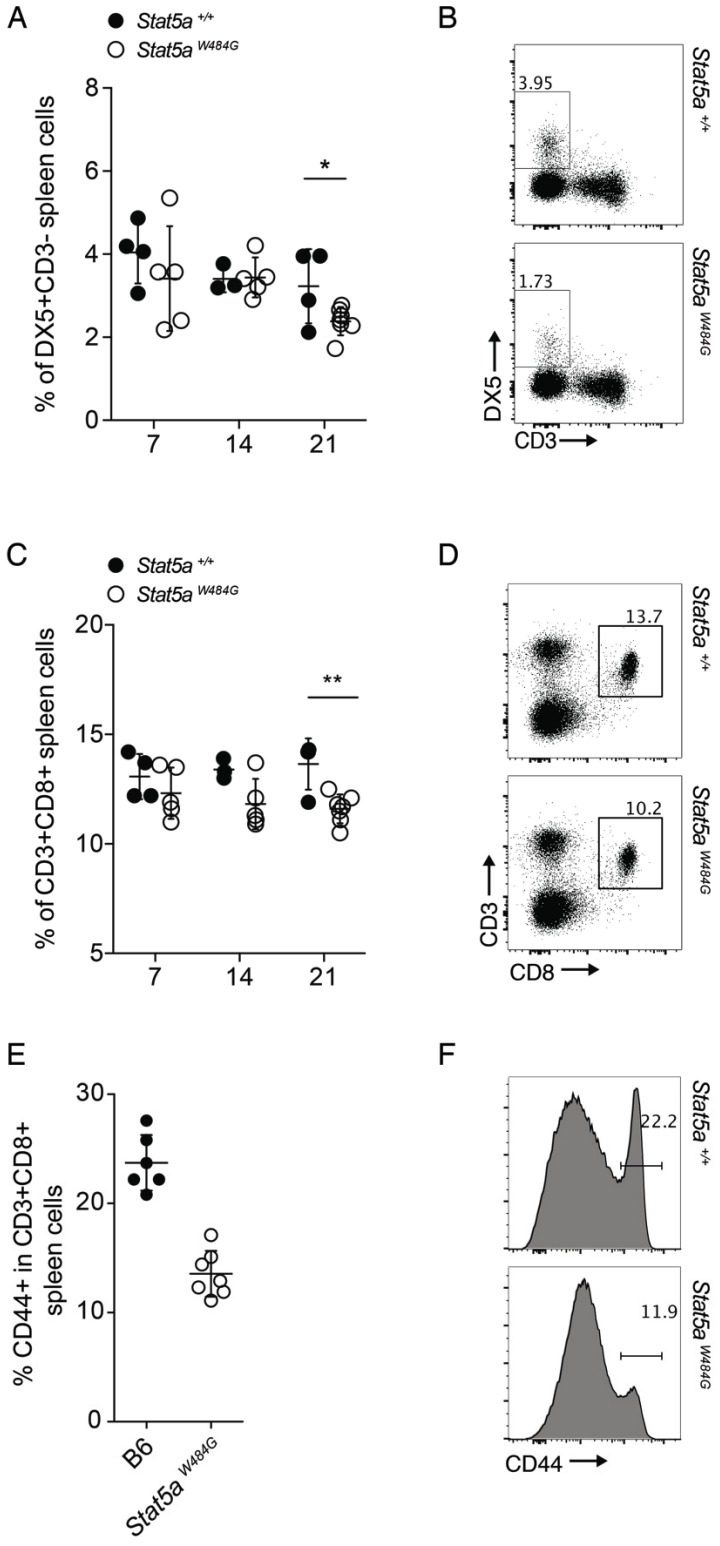
A
Stat5a +/+
Stat5a W484G
% of DX5+CD3- spleen cells
8
6
4
2
0
7
14
21
*
B
3.95
1.73
Stat5a +/+
Stat5a W484G
DX5
CD3
C
Stat5a +/+
Stat5a W484G
% of CD3+CD8+ spleen cells
20
15
10
5
7
14
21
**
D
13.7
10.2
Stat5a +/+
Stat5a W484G
CD3
CD8
E
% CD44+ in CD3+CD8+ spleen cells
30
20
10
0
B6
Stat5a W484G
F
22.2
11.9
Stat5a +/+
Stat5a W484G
CD44

Figure 3.7 – Molecular modelling of wild-type W484 residue on the three-dimensional structure of STAT5A homodimer

The STAT5A DNA binding domain is illustrated in blue. The portion of the linker domain overlapping in function with DNA binding domain is coloured in green. The rest of the linker domain is in yellow. The tryptophan residue on position 484 is in red.

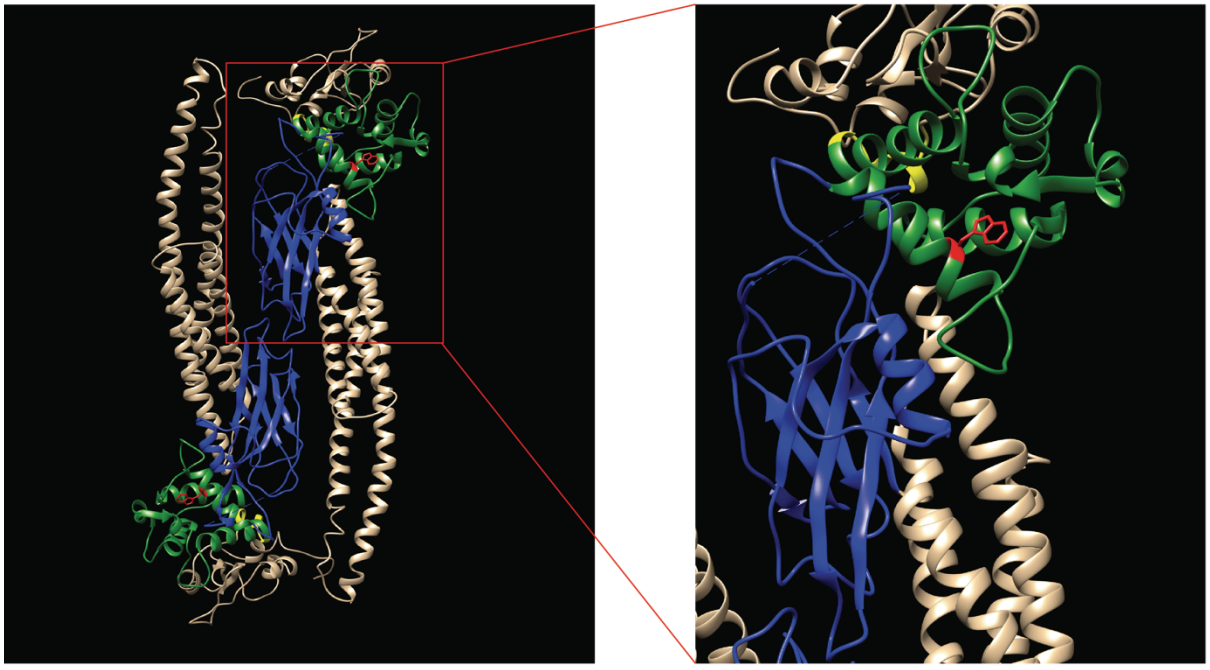

Table 3.1 – Exome sequencing analysis of susceptible Keagan mice

Criteria	SNV
In 2 of 3 samples, Depth Read ≥ 5	55
Missense or Nonsense	40
Homozygote mutant in at least 1 sample	14
Homozygote mutant in at least 2 sample	4

Table 3.2 – List of ENU SNV unique to the Keagan pedigree

Chr	Position	Ref Allele	Alt Allele	Gene	Avg Depth	Effect Type	Codon Change	AA Change	# Sample	Alt Homo	Alt Het
1	12,832,900	G	A	Sulf1	27	Nonsense	tGg/tAg	W759*	2	0	2
1	40,040,105	C	T	Map4k4	101	Silent	taC/taT	Y210	2	0	2
1	145,493,559	A	T	B3galt2	45	Missense	aAc/aTc	N101I	3	0	3
1	176,299,295	T	G	Olfr417	131	Missense	gaT/gaG	D82E	3	0	3
2	25,448,389	G	A	B230208H17Rik	28	Missense	cCa/cTa	P166L	2	0	2
2	76,582,914	G	T	Ttn	55	Missense	Cag/Aag	Q14351K	2	0	2
2	84,898,400	A	G	Tnks1bp1	356	Missense	Agc/Ggc	S305G	2	0	2
2	92,253,259	G	T	Cry2	118	Missense	Ccc/Acc	P465T	2	0	2
2	162,774,355	T	A	L3mbtl1	27	Missense	tTc/tAc	F196Y	3	0	3
3	38,790,604	T	A	Fat4	85	Missense	Ttt/Att	F1575I	2	0	2
3	86,802,687	T	A	Cd1d1	72	Missense	Acg/Tcg	T68S	2	1	1
3	129,565,046	A	T	Cfi	97	Splice site			2	0	2
4	86,471,687	C	T	Dennd4c	3	Silent	acC/acT	T1287	2	2	0
4	100,151,578	A	T	Ube2u	5	Start gained			2	2	0
4	145,730,520	G	A	Gm13251	5	Missense	Cat/Tat	H566Y	2	0	2
5	30,666,775	T	C	Ccdc164	33	Splice site			2	1	1
5	123,897,556	T	C	Mlxip	56	Silent	ggT/ggC	G233	3	0	3
5	138,749,767	A	C	Stag3	49	Silent	acA/acC	T1117	3	0	3
5	144,309,947	T	C	2810453I06Rik	6	Missense	aTc/aCc	I44T	2	2	0
5	151,847,890	T	C	Stard13	42	Missense	cAc/cGc	H948R	3	1	2
6	43,065,879	T	C	Olfr441	245	Missense	gTa/gCa	V46A	2	0	2
6	128,383,150	A	G	Fkbp4	79	Missense	Tca/Cca	S336P	2	0	2
6	133,005,534	T	C	Tas2r140	17	Missense	aAt/aGt	N93S	2	0	2
6	139,717,282	A	G	Pik3c2g	144	Missense	gAc/gGc	D775G	2	0	2
7	49,918,065	C	T	Gm5595	5	Missense	Ggt/Agt	G165S	2	0	2
8	128,006,012	A	G	Sipa1l2	86	Missense	gTg/gCg	V519A	3	1	2
9	3,004,860	A	T	Gm11168	23	Missense	Aca/Tca	T134S	2	0	2
9	46,018,657	A	G	Sik3	43	Missense	Acc/Gcc	T784A	2	1	1
9	63,515,384	T	A	Smad3	75	Missense	Acc/Tcc	T144S	2	1	1
9	106,926,106	T	C	Dock3	183	Silent	tcA/tcG	S330	2	1	1
10	127,558,220	T	G	Baz2a	79	Missense	aaT/aaG	N925K	2	0	2
11	84,872,662	A	G	Usp32	16	Missense	gTt/gCt	V224A	3	1	2
11	100,740,662	T	G	Stat5a	162	Missense	Tgg/Ggg	W484G	3	1	2
11	106,703,035	G	T	Smurf2	39	Missense	aCa/aAa	T351K	3	2	1
11	120,624,402	A	C	Hmga1-rs1	23	Missense	aAg/aCg	K67T	2	0	2
12	109,751,230	G	A	Eml1	167	Missense	Gtg/Atg	V320M	3	2	1
12	120,188,582	A	T	Abcb5	16	Missense	aaT/aaA	N79K	2	2	0
13	12,794,807	T	C	Gm2399	26	Missense	aTc/aCc	I60T	2	0	2
13	25,035,571	A	C	Gpld1	26	Missense	cAt/cCt	H29P	2	0	2
13	27,667,431	T	C	Prl8a1	28	Missense	aAc/aGc	N164S	2	0	2
13	41,198,558	G	A	Gcm2	40	Silent	aaC/aaT	N361	2	0	2

13	49,303,414	G	A	1110007C09Rik	79	Missense	Cgt/Tgt	R37C	3	0	3
13	64,895,591	A	C	Cntnap3	25	Missense	aTt/aGt	I211S	2	0	2
13	120,146,372	T	C	Nnt	59	Missense	gAa/gGa	E546G	2	0	2
14	16,191,054	A	G	Lrrc3b	29	Missense	gTa/gCa	V22A	3	0	3
14	56,388,654	C	T	Adcy4	111	Silent	tcG/tcA	S979	2	0	2
15	71,743,197	T	C	Col22a1	105	Silent	acA/acG	T758	3	1	2
15	81,900,685	A	G	Mei1	15	Missense	cAc/cGc	H87R	3	1	2
15	100,001,570	A	G	Dip2b	60	Missense	cAt/cGt	H344R	3	1	2
16	10,741,929	G	C	Clec16a	58	Frame shift			2	0	2
16	91,495,676	A	G	Ifnar1	73	Missense	gAa/gGa	E191G	2	0	2
17	34,020,175	C	A	Kifc1	39	Missense	Gtt/Ttt	V407F	2	0	2
18	12,623,987	T	C	Lama3	21	Missense	Tct/Cct	S981P	3	2	1
18	37,902,070	T	A	Pcdhgc5	94	Missense	cTg/cAg	L59Q	2	2	0
19	43,889,250	G	A	Abcc2	35	Silent	ttG/ttA	L678	2	0	2

Abbreviations: Chr - Chromosome, Ref - Reference allele, Alt - Alternative allelle, Avg - Average, AA - Amino acid, Homo - Homozygote, Het - Heterozygote.

Bridging statement from Chapter 3 to Chapter 4

In Chapter 2, we presented the ENU mutagenesis screen that we performed to discover novel genes and pathways important for host resistance to herpesviruses. We found 6 deviant pedigree susceptible to HSV-1 and 1 susceptible to MCMV. In Chapter 3, we analysed the Keagan family, a family originally susceptible to HSV-1, identified a mutation in DNA binding site STAT5A. In the next chapter, we studied the deviant family susceptible to MCMV: Glynn. Using linkage analysis and whole-exome sequencing, we identify a non-sense mutation abrogating the expression of the GTPase GNL1. We found that the GNL1 mutation causes severe NK cells deficiency in mice. NK cells from GNL1 mutant mice were unable to respond to IL-2 and IL-15, hindering their homeostasis and increasing NK cells death. We also found that inactivation of p53 rescue the NK cell deficiency and cell death.

Chapter 4 - An ENU induced mutation in the GNL1 GTPase causes a p53-dependent NK cells deficiency

Gabriel André Leiva-Torres[1,2], Benoit Charbonneau[1,2], Natasha Barone[1], Mathieu Mancini[1], Rob Sladek[2] and Silvia Vidal[1,2*]

1. Dept of Human Genetics, McGill University, Montréal, Québec, Canada; 2. McGill University Research Centre on Complex Traits, McGill University, Montréal, Québec, Canada; 3. Genome Quebec Innovation Center, Montréal, Québec, Canada.

*Corresponding author:
Email: silvia.vidal@mcgill.ca

Paper submitted

Abstract

To identify novel genes and pathways central to host resistance to mouse cytomegalovirus (MCMV), we used random chemical mutagenesis with N-Ethyl-N-Nitrosourea and found a critical mutation on the highly conversed GTPase GNL1. The GNL1 mutant mice were highly susceptible to MCMV. Classical bone-marrow derived NK cells, which play a non-redundant role in viral resistance, but not tissue resident NK cells, were drastically reduced, causing viral susceptibility. NK cells missing GNL1 showed increased apoptosis and lacked homeostatic proliferation *in vivo*. In culture, explanted NK cells showed cell cycle blockage after stimulation with IL-2 and IL-15, two cytokines critical for NK cell development, homeostasis and survival. The inactivation of p53 in GNL1 mutant mice rescued both the increased cell death and the NK deficiency. We show that GNL1 is crucial for NK cell homeostasis and that GNL1 inactivation leads to a p53 dependent NK deficiency and MCMV susceptibility.

Introduction

Natural Killer (NK) cells are innate lymphocytes that play a crucial role in the control of viral infections, in particular of herpesviruses such as cytomegalovirus (*141*). NK cell activation is tightly regulated by the sum of inhibitory and activating signals emanating from a wide array of germ-line encoded receptors that allow NK cells to sense and rapidly respond to their environment (*56*, *154*). Inhibitory receptors, most of which bind MHC class I molecules, provide a dominant signal that protects “self” from NK cells attack and include the Killer Immunoglobulin Receptors (KIRs) in humans and Ly49s in mice. Activating receptors elicit signals that promote cytotoxic granule mobilization, cytokine secretion as well NK cell proliferation.

The model of infection with mouse cytomegalovirus (MCMV) has been very useful to delineate NK cell functions during the host response against the virus. NK cells contribute

to the control of MCMV infection by directly eliminating virus infected cells. In the C57BL/6 (B6) mouse strain, MCMV resistance depends on the activating Ly49H NK cell receptor recognizing its ligand, the viral protein m157, on infected cells (*159*, *162*, *163*). The antigen-specific recognition leads to Ly49H+ NK cell activation and expansion, which are sustained by pro-inflammatory cytokines IL-2, IL-18 and IL-33 (*148*, *167*, *426*). NK cells also impact the outcome of infections through regulatory functions whereby NK cells regulate the maturation of dendritic cells (*427*) and, depending on the cytokine milieu, can either dampen (IL-10 production) (*428*) or boost (IFNγ and TNFα) the adaptive T cell antiviral response cell response (*429*).

NK cells develop from a common lymphoid progenitor in the bone marrow; however, individual tissues contain phenotypically and functionally distinct subsets (*215*). Moreover, certain tissue resident NK cells have different developmental requirements. It is the case of thymus NK cells which differ from conventional bone-marrow derived NK cells by requiring IL-7 signals for their development (*219*), whereas liver NK cells express TRAIL and CD49a (*217*, *218*).

IL-2 and IL-15 are central to NK survival, proliferation and differentiation. Receptors of both cytokines share two subunits: γc and IL-2Rβ (also named CD122) (*430*)**.** Triggering of the receptor activates the JAK3/STAT5, the RAS/MEK/ERK and the PI3K/mTOR/AKT signaling pathways leading to NK cell differentiation, proliferation, survival and activation (*240*, *248*, *250*, *431*, *432*). This signal also increases the expression of CD122 on the cell surface, creating a positive feedback loop (*250*). Consequently, the absence of the γc subunit causes severe NK deficiency in mice (*433*).

In humans, inherited NK cell deficiency (NKD), in which NK cell counts are below 100 cells/ul, are often associated with a lack of other lymphoid cells, as with SCID patients who also lack T cells and B cells (*151*). There are combined NKDs associated with normal T cell count but low levels of myeloid cells. This is the case of the first reported non-T cell NK cell-deficiency associated with increased susceptibility to the Varicella-Zoster Virus,

Herpes simplex virus 1 (HSV-1) and CMV infections (*385*). Autosomal dominant mutations in the *Gata2* gene, a hematopoietic transcription factor, were found to lead to NK and B cell deficiency with monocytopenia (*434*). Both development and cytotoxic NK cell function are perturbed, although the latter can be partially compensated by type I IFN treatment (*348*). Compound heterozygous rare mutations in Go-Ichi-Ni-San complex subunit 1 (GINS1), which is essential for DNA replication, were found associated with chronic neutropenia and NK cell deficiency (*435*). By contrast, only patients with autosomal recessive mutations in the minichromosomal maintenance (MCM)4, a member of the hexameric complex involved in DNA replication, have normal T and B cell counts but very few circulating NK cells (*351*, *436*). The NK cells left displayed a strong proliferation defect in response to IL-2 or IL-15 stimulation and an excess of spontaneous apoptosis (*351*).

To decipher the pathways crucial for host resistance, we have used a forward genetics approach. N-Ethyl-N-Nitrosourea (ENU) mutagenesis is a powerful mutagen used to introduce random point mutations in spermatogonial stem cells, allowing us to generate mice showing a large spectrum of phenotypes (*325*). Following a large throughput screen against a pathogen, this unbiased system can be used to identify novel genes and pathways crucial for host resistance. ENU mutagenesis was previously used to identify novel genes and pathways important for NK cells immune response to MCMV, among which Itgb2 (*437*), Unc13d (*438*) and Stat1 (*379*).

In this study, we generated an ENU pedigree carrying a critical mutation on the uncharacterized GTPase guanine nucleotide binding protein-like 1 (GNL1) which renders the mice highly susceptible to MCMV infection. GNL1 is part of the HSR1-MMR1 family of large GTPases, which are known to be important for cell cycle progression, development and ribosome biogenesis (*439-444*). For instance, GNL2 and GNL3 are crucial for ribosome biogenesis and their disruption causes MDM2-mediated activation of p53 (*420*). GNL3L disruption also causes a p53 dependent cell cycle arrest (*445*). We found that animals bearing the critical ENU mutation on GNL1 were NK deficient due to

the inability of these cells to respond to IL-2 and IL-15 stimulation, causing a cell cycle arrest and increased cell death. The inactivation of p53 rescues the NK deficiency and cell death observed in the GNL1 mutant mice.

Results

Identification of a deviant pedigree

To identify novel genes crucial for viral resistance and the immune compartment, we used a forward genetics approach. We mutagenized and screened a large cohort of mice for susceptibility to MCMV. We used ENU, a powerful mutagen able to produce random point mutations in spermatogonial stem cells. We started by injecting Generation 0 (G0) B6 male mice with ENU and mating them with C57BL/10J (B10) females to produce G1 males, which were used as the founder of a given pedigree. We used a three-generation breeding scheme to capture recessive mutations in G3 mice (*66*) (Fig. 4.1 A), where homozygote mutations are expected to segregate in about 25% of animals. G3 mice were then infected intravenously with $4x10^3$ pfu of MCMV and monitored for 7 days for clinical signs, at which point the mice were sacrificed and spleens were weighed. Doing so, we found one pedigree, named Glynn, with a lower survival rate than the resistant control F1 (B6xB10) mice (Fig. 4.1 B). Susceptible animals within the pedigree (*Glynn*^{S}) also had a low spleen index, comparable to the BALB/c susceptible control (Fig. 4.1 C). Splenomegaly caused by extra-medullary hematopoiesis will take place in the spleen of resistant mice, increasing its weight and, by consequence, the spleen index. Susceptible mice will not show this increase (*363*), which is what we observed in the *Glynn*^{S} animals. Uninfected *Glynn*^{S} mice were also smaller in weight (Fig. 4.1 D) and size (Fig. 4.1 E) when compared to littermates, thereby leading us to believe that the ENU mutation could affect a gene important for mouse development.

Identification of an ENU mutation causing MCMV susceptibility

To identify the ENU mutation in the Glynn pedigree, we took advantage of the B6/B10 mixed background to perform a linkage analysis on the G3 mice using survival as the phenotype. Using a panel of 255 SNP polymorphic between the B6 and B10 strains (*332*), we found a significant quantitative trait loci (QTL) on chromosome 17 from 29.66 Mb (rs33442265) to 47.45 Mb (B10SNPS0237, from (*360*)) with a logarithm of odds score of 6.1 (Fig. 4.2, A and B). In that interval, the B6 allele carrying the ENU mutation clearly segregated in the susceptible animals while resistant mice were either heterozygote or had the wild type B10 allele.

This region of chromosome 17 is very dense, with over 461 genes (according to the Mouse Genome Informatics database), including H2 genes. To identify the mutation causing MCMV susceptibility, we performed whole-exome sequencing on the genomic DNA of two susceptible animals. Eleven novel ENU homozygote mutations were shared between the two samples (Table 4.1), of which only 2 encoded for a damaging mutation. The first one caused a frame shift on the predicted gene *Gm17647* on chromosome 2. Since no linkage was found on that chromosome, we excluded this mutation as a potential candidate. The second mutation was the only one located on chromosome 17 and was found directly underneath our QTL loci at position 36,120,530. We identified a T to A mutation on the 8th exon of the gene *Gnl1* (Fig. 4.2 C), changing the Cysteine on position 365 (of a 607 amino acid protein) to a premature stop codon (C365X). The presence of the mutation was confirmed by Sanger sequencing on all animals used during the screening. All susceptible animals carried the C365X homozygous mutation, while resistant mice were either heterozygote or homozygote wild type (Fig. 4.2 D). Animals were then backcrossed twice to the parent strain B6 and intercrossed to isolate the *Gnl1* mutation.

GNL1 function is not well defined. It belongs to the HSR1-MMR1 family of large GTPase (*439*). The GTPase site takes the form of five permutated circular motifs (G5-G4-G1-G2-G3). GNL1 has been shown to be important for cell cycle progression (*446*). Other genes

from that same family are known to be important for controlling cell cycle, for stem-cell biology, embryonic development and ribogenesis (*420*, *440-442*, *445*, *447*). Interestingly, GNL1 is highly conserved among vertebrates and insects (Fig. 4.2 E). Our mutation lies in a very conserved region of the protein, impairing its GTPase domain.

GNL1 is highly expressed in immune organs

To better understand the role of GNL1 in MCMV susceptibility, we started by examining *Gnl1* mRNA expression in wild type animals using *in situ* hybridization. *Gnl1* is expressed throughout the body, with high expression levels in the brain and immune organs such as the thymus, spleen and bone marrow (Fig. 4.3 A). This was corroborated by real time PCR analysis to measure the relative expression of Gnl1 transcripts (Fig. 4.3 B). Our results confirmed the results found by Lara-Astiago et al. (*448*) that showed, using RNAseq, that *Gnl1* was highly expressed in immune cells and hematopoietic stem cells. Our ENU mutant mice (named $Gnl1^{C365X}$) expressed lower levels of the messenger than the wild type littermates (Fig. 4.3 C). Moreover, we could not detect the full-size protein using an N-terminal specific antibody, nor could we detect a truncated version in $Gnl1^{C365X}$ mice (Fig. 4.3 D), showing that our ENU mice are null mutants.

$Gnl1^{C365X}$ mice are susceptible to MCMV, but the NK cell response is normal

To confirm the importance of GNL1 in host resistance to MCMV, we performed an infection time-course on our mutant mice. From days 2 to 5 post-infection (p.i.), $Gnl1^{C365X}$ mice show very low spleen index when compared to their wild type littermates, as well as high splenic viral load (Fig. 4.4, A and B). $Gnl1^{C365X}$ mice succumb to the infection between day 5 and day 7. Since NK cells play a critical role in early host resistance, we verified if these cells could respond to the viral infection. IFNγ is critical for establishing an adequate anti-MCMV early response (*421*). We first quantified the intracellular production of IFNγ by NK cells on day 2 p.i. after re-stimulation (Fig. 4.4 C). No defect in the production of type 2 interferon was detected. NK cells from mutant mice produced

IFNγ at very high levels, which correlates with the high viral load observed in *Gnl1*^{C365X} mice. We then verified if the NK maturation program was normal in *Gnl1*^{C365X} mice during the peak of viral replication (on day 4). We measured the expression of CD11b and CD27 to separate the NK cells into four populations (double negative (DN); CD27 single positive (SP); double positive (DP) and CD11b SP), from the less mature but proliferative CD27^{-} CD11b^{-} cells to the highly cytotoxic CD11b^{+}CD27^{-} NK cells (*204*). No significant difference was observed between mutant and wild type mice, showing that the susceptibility of *Gnl1*^{C365X} to MCMV is not due to a maturation defect following infection (Fig. 4.4 D). We also confirmed that the activation of NKs was normal in the mutant mice by quantifying the expression of CD69 and KLRG1 (Fig. 4.4 E). Both *Gnl1*$^{+/+}$ and *Gnl1*^{C365X} NK cells show similar activation levels following infection. Thus, the inability of *Gnl1*^{C365X} mice to control infection is not due to a lack of activation of the NK cells.

Recognition of viral components by NK cells is crucial for host resistance. Indeed, the activating receptor Ly49H is central to the recognition of infected cells via its interaction with the viral protein m157. We assessed the capacity of Ly49H^{+} NK cells to proliferate following infection. Mice were infected with MCMV for 5 days and then injected with BrdU 3 hours prior to the sacrifice. Proliferating cells were determined by quantifying the incorporation of BrdU in Ly49H^{+} NK cells. No proliferation defect was observed in *Gnl1*^{C365X} (Fig. 4.4 F). In fact, NK proliferation levels were higher in mutant mice: These levels seem to be driven by the high viral load found in these mice (Fig. 4.4 B). Interestingly, although the Ly49H^{+} NK proliferation was strong in *Gnl1*^{C365X} mice, the NK population was smaller in mutant mice than in their wild type litter, in both infected and PBS treated animals (Fig. 4.4 G). This led us to believe that our ENU mutant mice could have a reduced NK population.

The viral load in *Gnl1*^{C365X} mice is higher than in wild type mice, limiting our ability to measure NK function in an inflammatory environment equivalent to wild type mice. To validate that *Gnl1*^{C365X} NK cells behave like wild type cells in a similar environment, we took advantage of *Ly49h*$^{-/-}$ mice, which lack Ly49H^{+} NK cells, and performed an adoptive

transfer. Splenocytes from either *Gnl1*$^{+/+}$ or *Gnl1*^{C365X} mice were transferred into *Ly49h*$^{-/-}$ mice followed by MCMV infection. In this context, splenic viral load was similar between both groups (*Gnl1*$^{+/+}$: 5.15±0.93, *Gnl1*^{C365X}: 5.28±0.69, Mean±SD Log_{10} PFU/g). No difference was observed in the proliferation (via BrdU incorporation) between the wild type and the mutant Ly49H^{+} NK (Fig. 4.4 H). Thus, in comparable environments, no differences in NK response was observed between the groups.

GNL1 deficiency affects the integrity of the main immune organs

Although no critical defect was observed in the NK function in the *Gnl1*^{C365X} mice, the reduction in NK proportion observed during the proliferation assay (Fig. 4.4 B) led us to believe that the composition of the immune compartment could be compromised in these animals. We performed a hematology analysis of wild type and mutant mice and did not observe a significant decrease in the white blood cell count (Fig. 4.5 A). However, *Gnl1*^{C365X} show signs of anemia, as the red blood cells, hemoglobin and hematocrit values were low. We previously observed that uninfected *Gnl1*^{C365X} mice are smaller than their wild type littermates (Fig. 4.1 E). This size difference is also reflected in the size of immune organs and overall blood cell number, which were both reduced in the mutant animals (Fig. 4.5, B and C). Moreover, the proportion of *Gnl1*^{C365X} animals per litter is smaller than normal. At weaning age (3 weeks old), only 12–15% of the animals are homozygous mutants, instead of the expected 25% Mendelian ratio. This suggests either an in utero or perinatal developmental problem. Consequently, the ENU mutation on GNL1 seems to have a pleiotropic impact on the animals.

Knowing that the size of the immune compartment was reduced, we further examined cell repertoires in the spleen and thymus. We first observed a reduced proportion of splenic B220^{+} cells in the mutant mice (Fig. 4.5 D). No significant difference was observed in the frequency of monocytes and macrophages in the *Gnl1*^{C365X} mice (Fig. S4.1, A and B). Thymus T cell populations were also similar between the mutant and the wild type mice (Fig. 4.5 E). Splenic T cell proportions in *Gnl1*^{C365X} mice were equal to wild type animals (Fig. 4.5 F). However, a reduction in the CD44^{+} CD4 T cells sub group was noticed in the

Gnl1^{C365X} mice (Fig. 4.5 G). To verify if the difference in effector CD4 T cells could impact T cell function and the antiviral response, *Gnl1*^{C365X} mice were challenged with HSV-1. We have previously shown that T cells, but not NK cells, are critical mediators of the antiviral response against HSV-1 and herpes simplex encephalitis (*66*). However, no significant increase in mortality was observed in *Gnl1*^{C365X} mice (Fig. 4.5 H), showing that the difference observed in T cell subpopulations does not impact the capacity of these cells to mount an appropriate antiviral response. *Gnl1*^{C365X} are resistant to HSV-1, a pathogen primordially controlled by T cells, while being susceptible to MCMV, a virus primarily controlled by NK cells. Thus, MCMV susceptibility seems to be driven by a cell specific defect.

The absence of GNL1 leads to a NK deficiency

Although interesting differences were observed in the adaptive compartment of the GNL1 mutant animals, the timeframe of the susceptibility to MCMV observed previously led us to believe that a deregulation of innate immunity could explain this phenotype. Knowing the importance of NK cells in the resistance to MCMV, splenic DX5^{+}CD3^{-} cells were quantified. Flow cytometry analysis showed that the NK cell compartment is greatly reduced in mutant mice, in both proportion and cell numbers (Fig. 4.6, A and B). A similar reduction was observed in the blood compartment (Fig 4.6 C). These low NK numbers are comparable to the ones observed in NK deficient human patients (*151*), who tend to suffer from severe herpesvirus infection. The reduction is also observed when using NK1.1 to detect NK cells in the spleen, bone marrow and lymph nodes (Fig. 4.6, D and E). However, this phenotype was not observed in the thymus. NK cell deficiency is not observed in thymic NK cells, which can be explained by the fact that conventional NK (cNK) cells use a developmental pathway which is distinct from that of thymic NK cells (*172*). To further understand the extent of the deficiency, liver conventional NK cells (DX5^{+}, CD49a^{-} NK1.1^{+} and CD3^{-}) and liver resident NK cells (DX5^{-}, CD49a^{+}, NK1.1^{+} and CD3^{-}) were quantified (Fig. 4.6, F and G). As expected, cNKs were greatly reduced in the liver of *Gnl1*^{C365X} mice. Comparatively, no deficiency was observed in the liver-resident NK cell population. Indeed, DX5- liver-resident NK cells proportion was similar in wild-

type and mutant mice. The absence of phenotype in the tissue resident NK compartment could also be due to the origin of the liver-resident NK cells, which differs from that of the cNK cells (*449*). Hence, GNL1 deficiency leads to a reduction in the numbers of various cells types, but the most dramatic deficiency was observed in the cNK population.

To verify that NK deficiency affects the killing ability of the NK compartment, thus causing viral susceptibility, we performed a rejection assay. Normally educated NK cells rapidly eliminate MHC-1$^{-/-}$ cells, while leaving MHC-1$^{+/+}$ self-cells unarmed. Differentially stained splenocytes from MHC-1$^{-/-}$ mice and from either *Gnl1*$^{+/+}$ or *Gnl1*^{C365X} mice were injected into *Gnl1*$^{+/+}$ or *Gnl1*^{C365X} animals. Eighteen hours post injections, spleen cells were harvested and quantified by flow cytometry (Fig. 4.6 H). Although *Gnl1*^{C365X} showed a lower killing than wild-type (although not significant), mutant NK cells were able to kill the MHC-1 $^{-/-}$ cells. To confirm that cell rejection is NK dependent, mice were treated with anti-asialo GM1 prior to the injection in order to deplete NK cells. No killing was observed, confirming that NK cells drove the MHC-H1$^{-/-}$ splenocyte killing. Hence, the cytotoxic activity of *Gnl1*^{C365X} NK cells was not abrogated by the low NK cell numbers.

To better understand the cause of NK deficiency, NK maturation was analyzed in uninfected *Gnl1*^{C365X} mice using the expression of CD27 and CD11b. GNL1 is important for the maturation of NK cells (Fig. 4.7 A). Indeed, an accumulation of the less mature double negative NK cells coupled with a reduction of the most mature CD11b+ single positive cells was observed in the mutant animals. This defect in maturation was also reflected in the expression of NK receptors. *Gnl1*^{C365X} mice had lower amounts of NKs expressing the activating receptor Ly49H and Ly49G2, while no difference was observed in the expression of the inhibitory receptor Ly49A and Ly49I/C (Fig. 4.7 B). Interestingly, although their numbers were reduced, Ly49H^{+} NK cells could respond to MCMV infection (Fig. 4.4 G). Moreover, following infection, Ly49H^{+} NK cell proportions in mutant mice were higher than in wild type mice (Fig. S4.2 A). Nonetheless, in a steady state context, the absence of GNL1 caused a delay in NK maturation as well as a reduction in the expression of activating receptors.

To confirm that NK deficiency directly causes viral susceptibility, $2x10^5$ wild type NK cells were adoptively transferred into *Gnl1*^{C365X} mice and were then challenged with the virus. As expected, when NK numbers are increased, *Gnl1*^{C365X} mice regain resistance (Fig. 4.7 C). In contrast, mutant mice remain susceptible when incompetent *Ly49h*$^{-/-}$ NK cells that do not recognize MCMV are transferred, confirming that the NK deficiency led to the viral susceptibility observed in *Gnl1*^{C365X} mice.

GNL1 is important for NK cell survival

Members of the MMR1-HSR1 family of large GTPase are known to play an important role in the cell cycle progression (*440*, *441*, *445*, *446*). An absence of GNL1 could compromise cell proliferation, thereby resulting in the NK deficiency that we observed in the ENU animals. Cell proliferation was measured in *Gnl1*^{C365X} NK cells by quantifying the expression of intracellular Ki67; no reduction was detected (Fig. 4.7 D). To understand the impact of the GNL1 mutation on NK cell survival, the activity of caspase-3 was measured. A significant increase in cleaved caspase-3 activity of splenic NKs was observed in mutant mice (Fig. 4.7 E). No increase was observed in T and B cells (Fig. S2 B to D). This increase in apoptotic NK cells was reflected in a drastic increase in NK cell mortality in *Gnl1*^{C365X} mice (Fig. 4.7 F), showing that the absence of GNL1 leads to an increase in NK cell death, which suggests a defect in NK homeostasis and could contribute to the NK deficiency observed in the mutant mice.

NK cell homeostasis is compromised in the absence of GNL1

Our hypothesis is that GNL1 could be important for the homeostasis of NK cells. To test this, we performed a competitive homeostatic proliferation assay between *Gnl1*^{C365X} (expressing CD45.2) and B6$^{CD45.1}$ (expressing CD45.1) NK cells. We adoptively transferred equal amounts of enriched NK cells of each genotype into lymphopenic *Rag2* $^{-/-}\gamma c^{-/-}$ (Fig. 4.8 A). Five days later, 75% of the splenic NK cells harvested expressed

CD45.1, suggesting that *Gnl1*^{C365X} NK cells are unable to proliferate as efficiently as wild-type cells in a homeostatic condition.

IL-2 and IL-15 are crucial cytokines known to play a central role in NK development, proliferation and survival (*450*). Both cytokine receptors share common subunits (γc and IL-2Rβ) that lead to the phosphorylation of STAT5 (*451*). To verify if the reduction in homeostatic proliferation is caused by an inadequate response to these cytokines, we quantified the expression of CD122 (IL-2Rβ) on bone marrow and spleen NK cells. In both organs, expression of CD122 on the surface of NK cells was reduced (Fig. 4.8, B and C). This defect could influence the capacity of NK cells to respond to IL-2 and IL-15. Thus, enriched NK cells were stimulated *ex-vivo* and cell cycle progression was measured. When stimulated with either IL-2 or IL-15, NK cells missing GNL1 proliferated at significantly lower levels than wild type cells (Fig. 4.8, D and F respectively). We examined cell cycle progression in cytokine stimulated cells using flow cytometry with propidium iodide DNA staining and the proliferation marker Ki67. We observed that mutant cells were mostly blocked at the G0 stage, while wild type NK cells could progress through the cell cycle (Fig. 4.8, E and G). However, this wasn't a full blockage, since a low number of NK cells were able to enter the G1 and S/G2/M phases.

To verify that the lack of response to IL-2 and IL-15 is NK specific and not due to a generalized defect directly downstream of the shared chains of the IL2/IL15 receptor, we tested the responsiveness of the IL-2Rβ pathway in T cells. CD4 and CD8 T cells were stimulated with IL-7, which increases T cell survival and expansion via IL-2Rβ and STAT5 (*452*). No difference between wild-type and mutant cells was observed in the number of T cells produced following stimulation for both CD4 and CD8 T cells (Fig. 4.8 H). Thus, the defect observed in NK cells is not present in the adaptive T cell compartment. Overall, in the absence of GNL1, NK cells are unable to properly respond to IL-2 and IL-15, leading to a partial cell cycle blockage and a decrease in survival.

p53 mediates the NK deficiency observed in *Gnl1*^{C365X} mice

One key regulator of survival and homeostasis is the pro-apoptotic p53. Its activation triggers the cleavage of caspase 3, causing cell cycle arrest and apoptosis. As such, GNL3 and GNL3L, members of the MMR1-HSR1 family of GTPase, regulate p53 via the inhibition of MDM2, a E3 ubiquitin ligase that targets p53 (*440*, *445*, *453*). Ribosomal stress is also known to cause activation of p53 via the inhibition of MDM2 by the ribosomal protein L5 and L11 (review in (*454*)). The large GTPases Yqlf (a bacterial orthologs of GNL1 also named RbgA), Lsg1, GNL2 and GNL3 belong to the MMR1-HSR1 family and are important for ribogenesis (*420*, *443*, *444*, *455*, *456*). Abnormal expression of these proteins causes cell cycle arrest and/or cell death. Thus, we hypothesize that the abnormal homeostasis observed in *Gnl1*^{C365X} NK cells could be mediated via p53.

To test the involvement of p53 in the increased cell death observed in *Gnl1*^{C365X} NK cells, we took advantage of p53 deficient mice and generated *p53*$^{-/-}$x*Gnl1*^{C365X} double mutant mice. Inactivation of p53 significantly increased the total splenocyte count previously observed in *Gnl1*^{C365X} animals (Fig. 4.9 A). More interestingly, the NK deficiency is rescued in the *p53*$^{-/-}$x*Gnl1*^{C365X} double mutant, in both proportion and total NK cell numbers, showing the potential interplay between p53 and GNL1 (Fig. 4.9, B and C). As such, active Caspase 3 level of *p53*$^{-/-}$x*Gnl1*^{C365X} NK cells were similar to the ones observed in wild-type cells (Fig 4.9. D). CD122 expression was also increased in the double mutant cells, highlighting the involvement of p53 in the homeostasis observed in *Gnl1*^{C365X} NK cells (Fig. 4.9 E). Thus, the NK deficiency observed in the *Gnl1*^{C365X} is mediated by p53.

Discussion

In this study, we report an ENU mutation on GNL1 causing severe MCMV infection and delineating a novel NK deficiency. Although the remaining NK cells could respond to an inflammatory environment, they are prone to cell death at steady state. This imbalance in

homeostasis is due to an inability of NK cells to respond appropriately to IL-2 and IL-15, leading to cell cycle arrest. The inactivation of p53 rescues the cell death and NK deficiency observed in *Gnl1*^{C365X} animals. Interestingly, although NK cells were greatly reduced, T cell proportions remained normal. Following IL7 stimulation, *Gnl1*^{C365X} T cells proliferated similarly as wild type cells. Moreover, mutant mice resisted HSV-1 infection, where T cells, but not NK cells, are essential (*66*). Numbers of monocytes and neutrophils in blood and spleen were normal. However, further experiments must be conducted to establish the integrity of the myeloid compartment.

We have found that the absence of GNL1 expression led to a reduction in B cell population and an NK deficiency, while still retaining normal T and tissue-resident NK cell numbers. No reduction was observed in the myeloid lineage, which suggested a lineage specific role of GNL1 in hematopoiesis. As such, cNK cells follow a developmental route different than tissue resident NK cells (*219*, *457*). In *Gnl1*^{C365X} mice, the NK deficiency was only observed in conventional NK cells, while thymus and liver tissue-resident NK cells remained normal, reinforcing the lineage specificity of GNL1 function. However, this does not exclude the possibility that GNL1 could also be crucial for other cell types. Indeed, *Gnl1*^{C365X} mice are smaller than wild-type mice, suggesting a possible role in development. Interestingly, this type of NK deficiency has also been observed in human patients. Indeed, individuals carrying a mutation on MCM4, a protein involved in DNA replication, are NK deficient and highly susceptible to herpesviruses (*351*). Moreover, mutations in MCM4 also lead to short stature, which we observed in *Gnl1*^{C365X} mice (*436*). Mutations in GATA2, also cause NK deficiency, B cell lymphopenia and monocytopenia (*348*) in humans. Similar to our GNL1 mutant, patients carrying the mutated GATA2 allele have a reduced mature CD56^{dim} NK cell population, showing a maturation delay. Again, these patients suffered from recurrent infection with VZV, HSV and CMV (*349*). However, our *Gnl1*^{C365X} mice were not susceptible to HSV-1 infection.

Without GNL1 expression, NK cell homeostasis is unbalanced. This is caused by an inability to respond to IL-2 and IL-15, leading to an important cell cycle arrest.

Interestingly, a previous study has shown that GNL1 localization in HeLa cells is cell cycle-dependent and that its overexpression promotes G2/M transition (*446*). Similarly, we have found that following IL-2 or IL-15 stimulation, most *Gnl1*^{C365X} NK cells stay at G0 stage, confirming the importance of GNL1 in the cell cycle progression. To our knowledge, this is the first report of a cell cycle control by GNL1 in immune cells. Other members of the HSR1-MMR1 family have also been implicated in the control of the cell cycle. Indeed, GNL2 has been reported to be crucial to cell cycle exit (*441*), GNL3 controls cell cycle via MDM2 and p53 (*440*) and GNL3L promotes G2/M transition (*445*).

We showed that the Gnl1^{C365X} NK deficiency is mediated by p53, as its inactivation restored NK numbers as well as reducing cell death. The involvement of p53 in GNL1's function is not surprising, as GNL2, GNL3 and GNL3L inactivation increases p53 activation, causing cell death (*441*, *445*), which is mediated by the destabilization of the MDM2/p53 complex. GNL3 disruption causes an increase in p53 activity and cell cycle blockage via the inhibition of MDM2 in a L5/L11 dependent manner (*420*, *453*).

Our results suggest a similar role for GNL1 (Fig. 4.9 F). In wild type cells, following the binding of IL2 or IL15 to their receptor, the cell cycle is initiated to promote translation and cell division. Signaling via mTOR also stimulates an increase in translation and ribosome biogenesis (*252*). We suggest that GNL1 could play a role in ribosome biogenesis or in maintaining ribosome/polysome integrity. In a wild type context, p53 is inhibited by MDM2 as no ribosomal stress is present and the NK cell can normally divide. In the absence of GNL1, NK cell stimulation by IL2/IL15 does not result in a normal cell cycle progression, as translation is compromised. Without GNL1, ribosome biogenesis or ribosome integrity is aberrant, leading to the inhibition of MDM2 (possibly by L5 and L11) and the subsequent activation of p53. This induces a cell cycle arrest and cell death.

Although this model explains the increased apoptosis and cell cycle blockage observed in *Gnl1*^{C365X} NK cells, a question remains: Why is this cell deficiency and homeostasis defect specific to the NK cells? One explanation is that ribosomes and polysomes have

a level of heterogeneity that remains to be fully appreciated. Indeed, the protein composition of ribosomes varies according to their subcellular location (*458*). These ribosome associated proteins are linked to different functions, such as cell cycle and metabolism. It has been proposed that the different varieties of ribosome associate proteins provide ribosomes with a preference for certain pools of mRNA. As a result, different ribosome pools have preferences for different types of transcripts. (*459*). It is possible that the GNL1 function is specific to certain "pools" of ribosomes specific to the NK lineage. The absence of GNL1 would impact the NK cells, while minimizing the effect on other cell types. Another explanation is that GNL1 regulates the expression or the stability of ribosomal protein specific to the NK cell lineage commitment. This mechanism was observed in T cells, where the ablation of the ribosomal protein L22 impairs the development of $\alpha\beta$ T cells and leads to a p53 induced cell death while sparing $\gamma\delta$ T cells (*460*). Although both cell types share a common progenitor, L22 inactivation only affected $\alpha\beta$ T cells. Similarly, ablation of GNL1 could impact a ribosomal protein that is specifically important for the homeostasis of the NK lineage, causing the NK deficiency observed while leaving other lineages untouched (T cells) or mildly affected (B cells).

We also have to account for the possibility that GNL1 could play a role in the development and/or the lineage commitment of NK progenitors, contributing to the NK deficiency of *Gnl1*^{C365X} mice. Indeed, the low cell number observed in the bone marrow of the mutant mice suggests a defect in hematopoiesis. Further study of GNL1 will be necessary to clarify its role in NK cell homeostasis and its interplay with p53.

In sum, our MCMV screen of ENU mutated mice allowed us to identify a critical mutation on the uncharacterized *Gnl1* gene. Our findings show that GNL1 is crucial to the proper cell cycle progression in NK cells following IL-2 and IL-15 stimulation and help to better understand the cellular mechanism regulating NK cell biology and homeostasis in a p53 dependent manner. Study of the ribosome biogenesis and ribosome/polysome integrity of GNL1 deficient mice will provide a better understanding of the specific role of GNL1 in NK cells.

Materials and Methods

Animals and virus

C57BL/6J, C57BL/10J, A/J, BALB/c mice were purchased from the Jackson laboratories (Bar Harbor, Maine, USA). ENU-mutagenized mice were bred in the animal facility of the Goodman Cancer Centre, McGill University. Hematology analysis was performed by the McGill Comparative Medicine and Animal Resources Centre. The Smith strain of MCMV was kindly provided by Dr. Seung-Hwang Lee (University of Ottawa) and produced in salivary glands and titered as described previously (*355*). HSV-1 strain 17 was originally from Dr. Subak-Sharpe and was amplified as described previously (*380*).

ENU mutagenesis and breeding

ENU mutagenesis was performed as described previously (*66*). Briefly, G0 B6 male mice were mutagenized with three i.p. injection of 90 mg/kg of ENU (Sigma). These males were then outcrossed with female B10 mice to produce G1 mice. Males from those F1 hybrid mice were outcrossed again with female B10 mice to produce G2 animals, which inherit 50% of the B6 sequence variants in the G1 mice. Two G2 females were then backcrossed with their G1 father to generate G3 animals, which were then screened for susceptibility to MCMV.

Mice infection and virus load

Mice of 7 to 8 weeks of age were infected intravenously with $4x10^3$ pfu of MCMV or intraperitoneally with 10^4 pfu of HSV-1. Mice were monitored daily up to 7 days for MCMV infection and 15 days for HSV-1 infection. Animals that succumb to the infection were considered susceptible. To evaluate MCMV viral load, spleens and livers were harvested in RPMI 1640 and homogenized through a 70μm cell strainer or by using a Roche MagNA lyser and 1.4 mm ceramic beads. Five-fold dilutions of the homogenates were produced in DMEM and plated in MEF for a plaque forming assay as described previously (*316*).

MEFs from BALB/c mice were prepared as described previously (*316*). Splenomegaly was determined by the spleen index (SI) following infection using the following formula: SI = √([Spleen weight at the end point × 100]/Animal weight on day 0).

In vitro infection time course

The MCMV time course was performed as described by Jurak et al. (*461*). Briefly, $5x10^4$ MEF were infected at an MOI of 0.1 in a volume of 2ml. At 24, 48 and 72 hours p.i., 300ul of supernatant was taken out and replaced with fresh media. Virus load was determined as explained by Desrosiers et al. (*316*).The HSV-1 time course was done as described previously (*380*). We infected $2.5x10^4$ MEF with HSV-1 at a MOI of 0.1. All supernatants and cells were harvested at 6, 12 and 24 hours p.i. For viral load determinations, samples were frozen and thawed three times to release all cell-associated virus. Viral titering was performed as described by (*380*).

DNA extraction and genetic mapping

Genomic DNA from the tail biopsy was extracted using phenol and chloroform as described previously (*381*). The genome scan was performed at the McGill University and Genome Quebec Innovation Centre (Montreal, Quebec, Canada). DNA from 6 susceptible mice and 28 resistant animals from the Glynn pedigree were genotyped using a panel of 255 B6/B10 polymorphic SNPs; QTL analysis was performed with R/qtl software version 2.12.2; and LOD score was calculated using survival as phenotype as described previously (*66*).

Whole-exome sequencing

Whole-exome sequencing of the genomic DNA samples from two susceptible animals was performed as described by Caignard et al (*66*). Capture was performed using the SureSelect Mouse Exon kit (Agilent Technologies, USA) and sequenced using Illumina HiSeq 2000 (100-bp paired end reads) at The Centre for Applied Genomics (Hospital for Sick Children, Toronto, Canada). The analysis was performed at the Genome Quebec Innovation Centre (Montréal, Canada). The pipeline Canadian Centre for Computational

Genomics (C3G) follows the stepwise procedures of the BROAD Institute GATK best practices. Raw sequencing reads were trimmed using Trimmomatic (*422*) to obtain a high quality set of reads for sequence alignment. The trimmed reads are aligned to a reference genome (build (mm10/GRCm38) using a fast, memory-efficient Burrows-Wheeler transform aligner, BWA-MEM (*423*). Mapped reads are further refined using the GATK (*424*) and Picard program suites (http://broadinstitute.github.io/picard) to improve mapping near insertions and deletions (indels: GATK indel realigner); to remove duplicate reads with the same paired start site (Picard mark duplicates); and to improve quality scores (GATK base recalibration). Variants are called using the GATK haplotype caller in gvcf mode to allow efficient downstream merging of multiple samples into one variant file to streamline downstream variant processing procedures, which include variant annotation and functional annotation with SNPeff (*425*).

RNA and protein expression.

Expression of the *Gnl1* gene was detected whole-mount in situ hybridization as described by Kennedy et al. (*333*). PCR amplification of the *Gnl1* mRNA was performed using these primers: 5'- GCGCTATAATACGACTCACTATAGGGAGA-GGAATCCGTGACCCATCA TATC-3' and 5'- GCATTAATTTAGGTGACACTATAGAAGCG-GAGGGAAAGAGGTG AACAAGAC-3', which contain embedded T7 and SP6 polymerase promoter sites. Total organ RNA was extracted as described by Caignard et al (*66*). Quantitative reverse transcription PCR of *Gnl1* was performed using these primers: 5'-GTATGTAACTGGAGAGCTTGGG-3' and 5'-CGAGGGAAAGAGGTGAACAAG-3'. Total organ or cell RNA was reverse transcribed to cDNA using random hexamer and M-MuLV reverse transcriptase (Invitrogen) followed by an amplification with the Platinum SYBR Green SuperMix-UDG (Invitrogen). Detection of GNL1 protein was performed via immunoblotting, using a rabbit antibody specific for the N-terminal region of GNL1 (Sigma-Aldrich, SAB4501227).

Immunophenotyping

Single cell preparations from spleen, bone marrow, liver and lymph nodes were prepared and stained with various cocktails of antibodies. Antibody specific for B220 (RA3-6B2), CD3e (145-2C11), CD11b (M1/70), CD4 (L3T4), CD8a (53-6.7), CD122 (TM-b1), cKit (ACK2), CD127 (A7R34), CD62L (MEL-14), Gr1 (RB6-8C5), CD49b (DX5), CD44 (1M7), FLT3 (A2F10), Ly49H (3D10), Ly49G2 (eBio4D11), Sca1 (D7), CD69 (H1.2F3), KLRG1 (2F1), NK1.1 (PK136) the Fixable Viability Dye eFluor 506 and the Cell Proliferation Dye eFluor 450 were from eBioscience. Antibodies against CD27 (LG.3A10), IFNγ, CD49a (Ha31/8) and Ly49A (YE1/48.10.6) were from BD Bioscience. Intracellular staining was performed using the Foxp3/Transcription Factor Fixation/Permeabilization kit (eBioscience). Caspase 3 activity was detected with the CaspGow fluorescein active Caspase-3 Staining Kit (eBioscience). All flow cytometry analysis was performed on a BD Canto II machine and using the FlowJo software (version 10.4). For the BrdU incorporation assay, mice were injected with 2mg i.p. of BrdU 3 hours prior to the sacrifice. Incorporation was measured using the FITC BrdU Flow Kit (BD Biosciences).

Ex-vivo cell stimulation

Splenic NK cells were enriched using the NK Cell Isolation Kit II on the MS separation column (Miltenyi). NK cells were enriched up to 88% for wild-type mice and 60% for *Gnl1*^{C365X} animals. Splenocytes or enriched NK cells were stimulated with murine IL12, IL-15 or IL18 (Peprotech); human IL-2 (Peprotech) was used for cell cycle analysis; PMA and Ionomicyn (Sigma) were used for IFNγ detection or cell cycle analysis.

Cell-cycle analysis

Stimulated NK and T cells cells were stained with the appropriate antibodies cocktail followed an anti-Ki67 antibody (clone SolA15, eBioscience) and 7AAD (BD Bioscience) according to manufacturers protocol. Cells were acquired on a BD Canto II machine and analyzed using the FlowJo software (version 10.4). Analysis was performed as described previously (*462*, *463*). Briefly, 7AAD^{low}Ki67^{-} were considered in G0, 7AAD^{low}Ki67^{+} were considered in G1 and 7AAD^{int}Ki67^{+} were considered in S-G2-M.

Killing assay and adoptive transfer

The killing assay was performed as described previously (*171*, *464*, *465*). MHC-1$^{-/-}$ or host splenocytes were stained with a high dose of CFSE (Invitrogen, 20 µl, 10mM) or eFluor 670 proliferation dye (eBioscience; 5 µl, 5 mM) prior to i.v. injection into wild type or mutant mice. Splenocytes were harvested 18 hours after the injection for analysis by flow cytometry. Adoptive transfer into Rag2$^{-/-}\gamma c^{-/-}$ mice was performed as described by Sun et al. (*466*). Equal numbers (10^5 cells) of B6$^{CD45.1}$ and *Gnl1*^{C365X} enriched NK cells were stained with eFluor 450 proliferation dye (eBioscience) prior to the i.v. injection. Five days after the injection, spleen cells were harvested for FACS analysis.

Statistics

Statistics were calculated using GraphPad Prism software version 6.0. Statistical tests employed for *in vivo* and *ex vivo* experiments are indicated in the figure legends. All data are displayed as the mean ± standard deviation.

Figures and Figure legends

Figure 4.1 – Identification of an ENU mutated pedigree susceptible to MCMV infection

(A) G0 mice were produced by injecting C57BL/6J (B6) mice with ENU and crossing them in a three-generation breeding scheme with the closely related strain C57BL/10J (B10) to enrich for homozygote recessive mutations. (B) Survival following MCMV infections of the Glynn pedigree (N=34), the F1 (B6xB10) resistant control (N=21) and the BALB/c susceptible control (N=19). (C) Spleen index of the resistant and susceptible animals of the Glynn pedigree, the F1 (B6xB10) resistant control and the BALB/c susceptible control from the survival screen (****p <0.0001 two-way ANOVA). (D) Body weight of 7- to 8-week old male and female from the Glynn pedigree was measured in uninfected animals. Pooled data from 4 experiments are shown (*n* = 13–24 per group, ****p <0.0001 two-way ANOVA) (E) Representative images showing the size of a 7-week-old male $Glynn^{R}$ and $Glynn^{S}$.

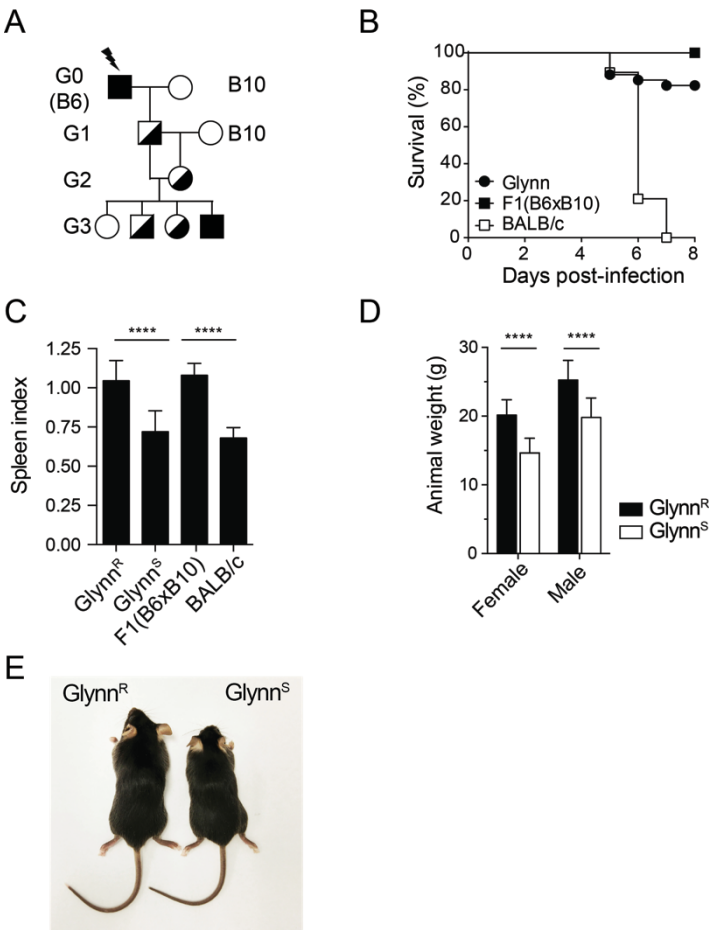
A
G0
(B6)
B10
G1
B10
G2
G3
B
Survival (%)
100
80
60
40
20
0
Glynn
F1(B6xB10)
BALB/c
0
2
4
6
8
Days post-infection
C
Spleen index
1.25
1.00
0.75
0.50
0.25
0.00
****
****
GlynnR
GlynnS
F1(B6xB10)
BALB/c
D
Animal weight (g)
30
20
10
0
****
****
GlynnR
GlynnS
Female
Male
E
GlynnR
GlynnS

Figure 4.2 – Identification of a critical mutation on the *Gnl1* gene causing MCMV susceptibility.

(A) Genome wide linkage analysis of the Glynn pedigree was performed on 34 animals (6 susceptible and 28 resistant) using polymorphic SNP markers between the B6 and B10 genetic strains. QTL mapping led to a peak LOD score of 6.096 on chromosome 17. (B) Haplotypes of the median region of chromosome 17 showing the segregation of the C57BL/6 allele (A) in a (C57BL/10xC57BL/6 ENU) F2 cohort. (C) Genomic DNA of a $Glynn^{R}$ and $Glynn^{S}$ was amplified by polymerase chain reaction and analyzed by Sanger sequencing. The red box indicated the location of the C365X ENU mutation on GNL1. (D) Survival of the $Gnl1^{C365X}$, $Gnl1^{+/C365X}$ and $Gnl1^{+/+}$ animals from the MCMV screen. (E) Structure of GNL1 including the GTPase domain (G1 to G5), the nuclear location signal (NLS) and the ENU mutation. The alignment of GNL1 showing the conservation of the C365 residue was performed using a CLC Sequence viewer. Ascension number: Human - NP_005266.2, Chimpanzee - NP_001065264.1, Rhesus macaque - NP_001040604.1, Wolf - XP_848324.1, Cattle - NP_001096742.1, Mouse - NP_032162.2, Rat - NP_997665.1, Zebrafish - NP_001070721.1, Drosophila - NP_610055.1, Mosquito - XP_317131.4, Frog - NP_001072441.1.

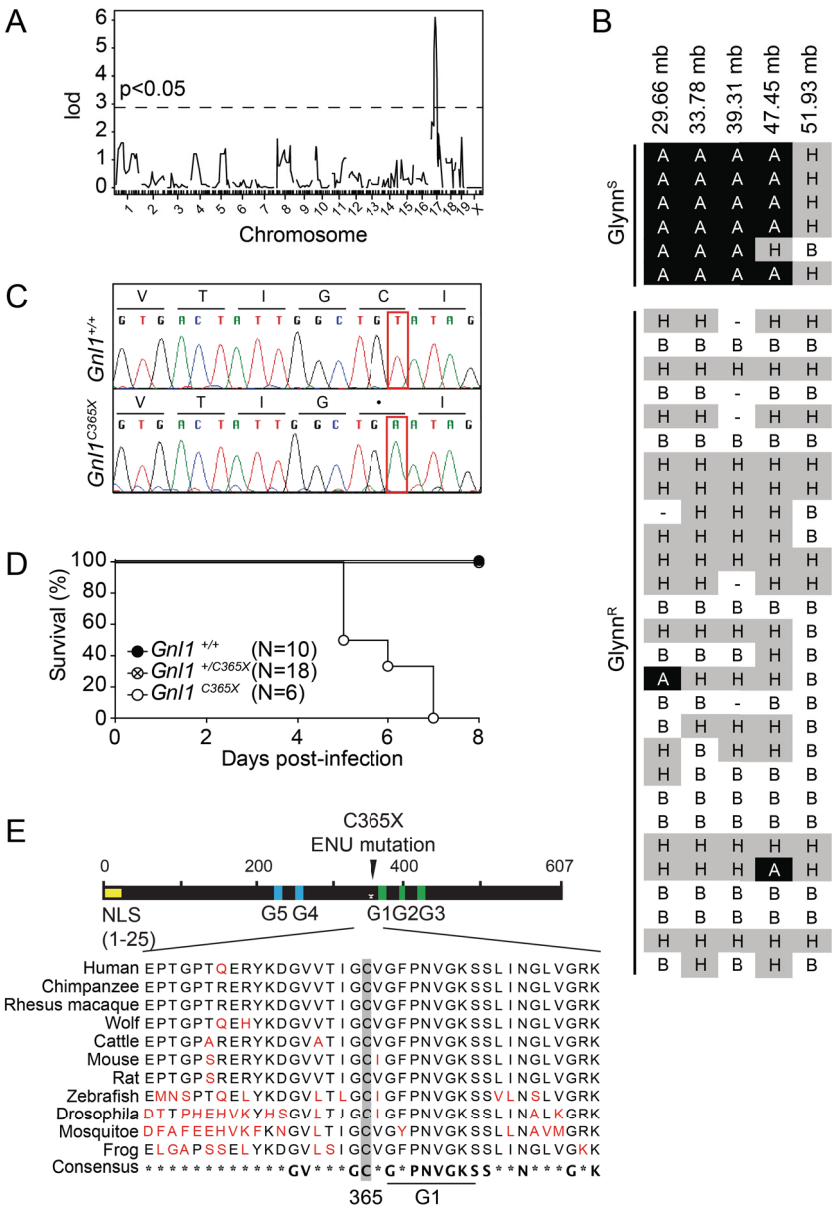
A
lod
p<0.05
Chromosome
B
29.66 mb
33.78 mb
39.31 mb
47.45 mb
51.93 mb
Glynn^S
Glynn^R
C
Gnl1+/+
Gnl1C365X
D
Survival (%)
Gnl1 +/+ (N=10)
Gnl1 +/C365X (N=18)
Gnl1 C365X (N=6)
Days post-infection
E
C365X
ENU mutation
NLS
(1-25)
G5 G4
G1G2G3
Human EPTGPTQERYKDGVVTIGCVGFPNVGKSSLINGLVGRK
Chimpanzee EPTGPTRERYKDGVVTIGCVGFPNVGKSSLINGLVGRK
Rhesus macaque EPTGPTRERYKDGVVTIGCVGFPNVGKSSLINGLVGRK
Wolf EPTGPTQEHYKDGVVTIGCVGFPNVGKSSLINGLVGRK
Cattle EPTGPARERYKDGVATIGCVGFPNVGKSSLINGLVGRK
Mouse EPTGPSRERYKDGVVTIGCIGFPNVGKSSLINGLVGRK
Rat EPTGPSRERYKDGVVTIGCVGFPNVGKSSLINGLVGRK
Zebrafish EMNSPTQELYKDGVLTLGCIGFPNVGKSSVLNSLVGRK
Drosophila DTTPHEHVKYHSGVLTIGCIGFPNVGKSSLINALKGRK
Mosquitoe DFAFEEHVKFKNGVLTIGCVGYPNVGKSSLLNAVMGRK
Frog ELGAPSSELYKDGVLSIGCVGFPNVGKSSLINGLVGKK
Consensus ***********GV***GC*G*PNVGKSS**N***G*K
365
G1

Figure 4.3 - Expression of *Gnl1* in wild type and mutated mice

(A) X-ray film autoradiography following antisense in situ hybridization showing bright labeling under dark field illumination in young mouse on p10. Parallel sections were stained with cresyl violet (cv), an antisense (as) or sense (s) probe to detect the *Gnl1* mRNA in the aorta (A), bone marrow (BM), cerebellum (Cb), cerebral cortex (Cx), dorsal root ganglia (DRG), epidydimis (Ep), hippocampus (Hi), kidney (Ki), liver (Li), lung (Lu), pelvic bone (PB), salivary gland (SG), small intestine (SIn), spleen (Sp), testis (Te), trigeminal ganglion (TG) and thymus (Th). (B) The expression of *Gnl1* messenger in various organs from three wild type B6 mice was quantified by qPCR. Data representing mean expression levels normalized to *Hprt* expression are shown ± SD (C) Expression of *Gnl1* mRNA from wild type and mutant brain tissue. Data representing mean expression levels normalized to *Hprt* expression are shown ± SD (4 repeats, *p <0.05). (D) Expression of the GNL1 protein in $Gnl1^{+/+}$ and $Gnl1^{C365X}$ mice was detected by western blot.

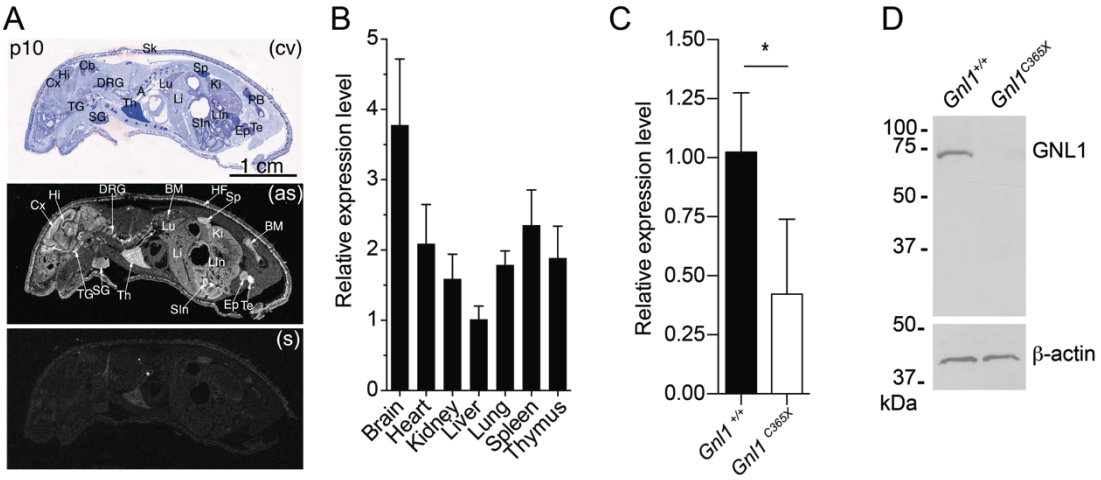
A
p10
(cv)
Sk
Cb
Hi
Cx
DRG
A
Lu
Sp
Ki
Li
PB
Th
TG
SG
Lln
Sln
EpTe
1 cm
(as)
BM
HF
Sp
Lu
Ki
Li
Lln
Th
Sln
Ep
Te
(s)
B
Relative expression level
Brain
Heart
Kidney
Liver
Lung
Spleen
Thymus
C
Relative expression level
*
Gnl1 +/+
Gnl1 C365X
D
Gnl1+/+
Gnl1C365X
GNL1
β-actin
kDa

Figure 4.4 – NK response to MCMV infection in *Gnl1*^{C365X} mice

(A) Wild type and mutant mice were infected i.v. with 4x10^3 PFU of MCMV. Spleen index and (B) splenic viral load were quantified at day 2, 4 and 5 p.i. (C) Intracellular IFNγ production in NK cells (NK1.1$^+$, CD3$^-$) was quantified by flow cytometry at day 2 p.i. (D) The 4-stage maturation program (using the expression of CD11b and CD27) was measured on splenic NK cells on day 4 p.i. Representative plots of the CD11b and CD27 expression on NK1.1$^+$CD3$^-$ cells are shown. (E) The expression of activation markers CD69 and KLRG1 was also measured on splenic NK cells (NK1.1$^+$, CD3$^-$) at day 4 p.i. A representative histogram of their expression on NK1.1$^+$CD3$^-$ cells from *Gnl1*$^{+/+}$ and *Gnl1*^{C365X} animals is shown. (F) Mice were injected i.v. with PBS or 4x10^3 PFU of MCMV. Proliferation ability of NK cells was determined at day 5 p.i. BrdU was injected 3 hours prior to the sacrifice and incorporation was quantified in splenic Ly49H$^+$ NK cells. A representative histogram of BrdU detection in NK1.1$^+$CD3$^-$ cells from infected mice is displayed. (G) Expansion of the NK compartment was also measured at day 5 p.i. in infected and uninfected animals using the expression of DX5 and CD3. Combined data from 2 or 3 experiments are shown (n = 5–13 per group). (H) 20x10^6 splenocytes from *Gnl1*$^{+/+}$ or *Gnl1*^{C365X} mice were adoptively transfered into *Ly49h*$^{-/-}$ mice. Animals were infected with MCMV. At 5 days p.i., splenic Ly49H$^+$ NK proliferation was also measured via the incorporation of BrdU. *p <0.05, **p <0.01, ***p <0.001, ****p <0.0001 (Two-way ANOVA).

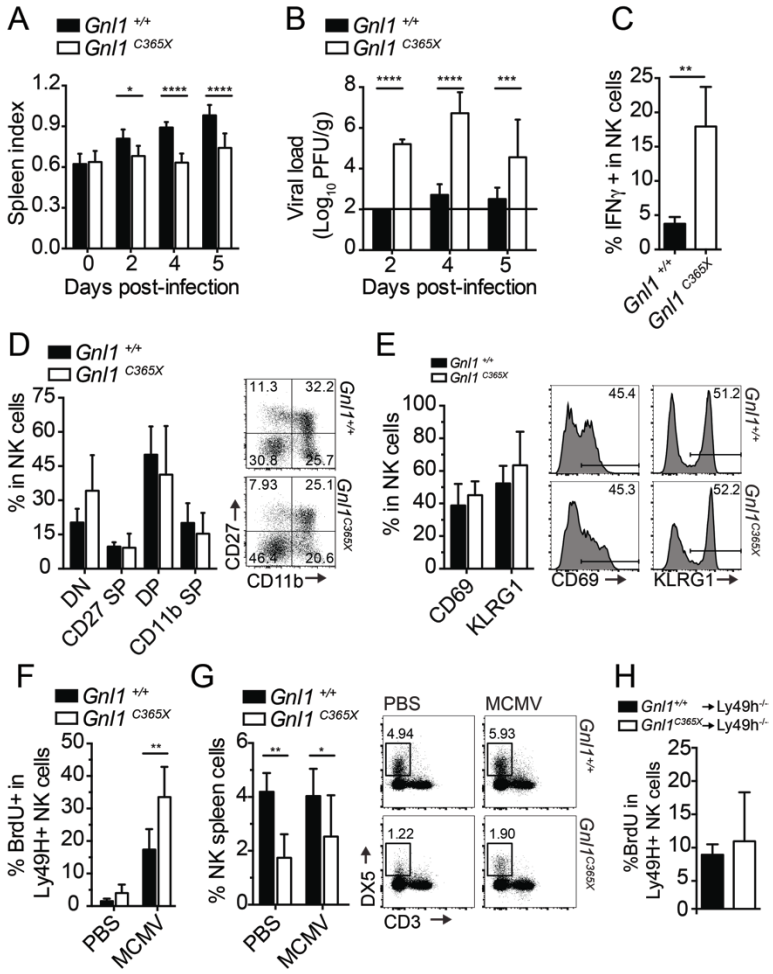
A
Gnl1 +/+
Gnl1 C365X
Spleen index
Days post-infection
B
Viral load (Log10 PFU/g)
Days post-infection
C
% IFNγ + in NK cells
D
% in NK cells
DN
CD27 SP
DP
CD11b SP
CD27
CD11b
E
% in NK cells
CD69
KLRG1
F
% BrdU+ in Ly49H+ NK cells
PBS
MCMV
G
% NK spleen cells
PBS
MCMV
DX5
CD3
H
Gnl1+/+ → Ly49h-/-
Gnl1C365X → Ly49h-/-
%BrdU in Ly49H+ NK cells

Figure 4.5 – Immune populations are reduced in *Gnl1*^{C365X} mice

(A) Blood from *Gnl1*$^{+/+}$ and *Gnl1*^{C365X} mice was collected. White blood cells (WBC), platelets, red blood cells (RBC) were quantified, as well as hemoglobin and hematocrit levels. Results are representative of three independent experiments. **p<0.01, ***p <0.001 (two-tailed Students t-test). (B) Representative picture of the thymus and spleen from 7 week old *Gnl1*$^{+/+}$ and *Gnl1*^{C365X} mice. (C) Immune organs from 7- to 9-week old mice were harvested and cells were counted. Combined data from at least three experiments are shown (*n* = 16 to 30 per group). ****p <0.0001 (Two-way ANOVA) (D) B220 expression was also measured on spleen cells. A representative histogram of each group is shown. (*n* = 9–12 per group from 3 independent experiments). ***p <0.001 (two-tailed Students t-test). (E) Expression of CD4 and CD8 was analyzed on thymus cells by FACS to quantify double negative (DN), double positive (DP), CD4 simple positive (CD4+ SP) and CD8 simple positive (CD8+ SP) thymocytes. Data from three independent experiments are shown (*n* = 8–13 per group). The dot plots showing the T cell population for each group is shown. (F) Expression of CD4 and CD8 was measured on CD3+ spleen cells to quantify splenic T cells (*n* = 9–12 per group from 3 independent experiments) (G) CD44 expression was quantified on CD4+CD3+ and CD8+CD3+ spleen cells. Representative histograms of the expression of CD44 is shown. Data represent two independent experiments combined (*n* = 9 per group). **p <0.01 (Two-way ANOVA). (H) *Gnl1*$^{+/+}$, *Gnl1*^{C365X}, resistant B6 and susceptible A/J mice were infected with 10^4 PFU i.p. of HSV-1. Mice were monitored for 15 days. Survival curves were analyzed using the Log-rank (Mantel-Cox) test.

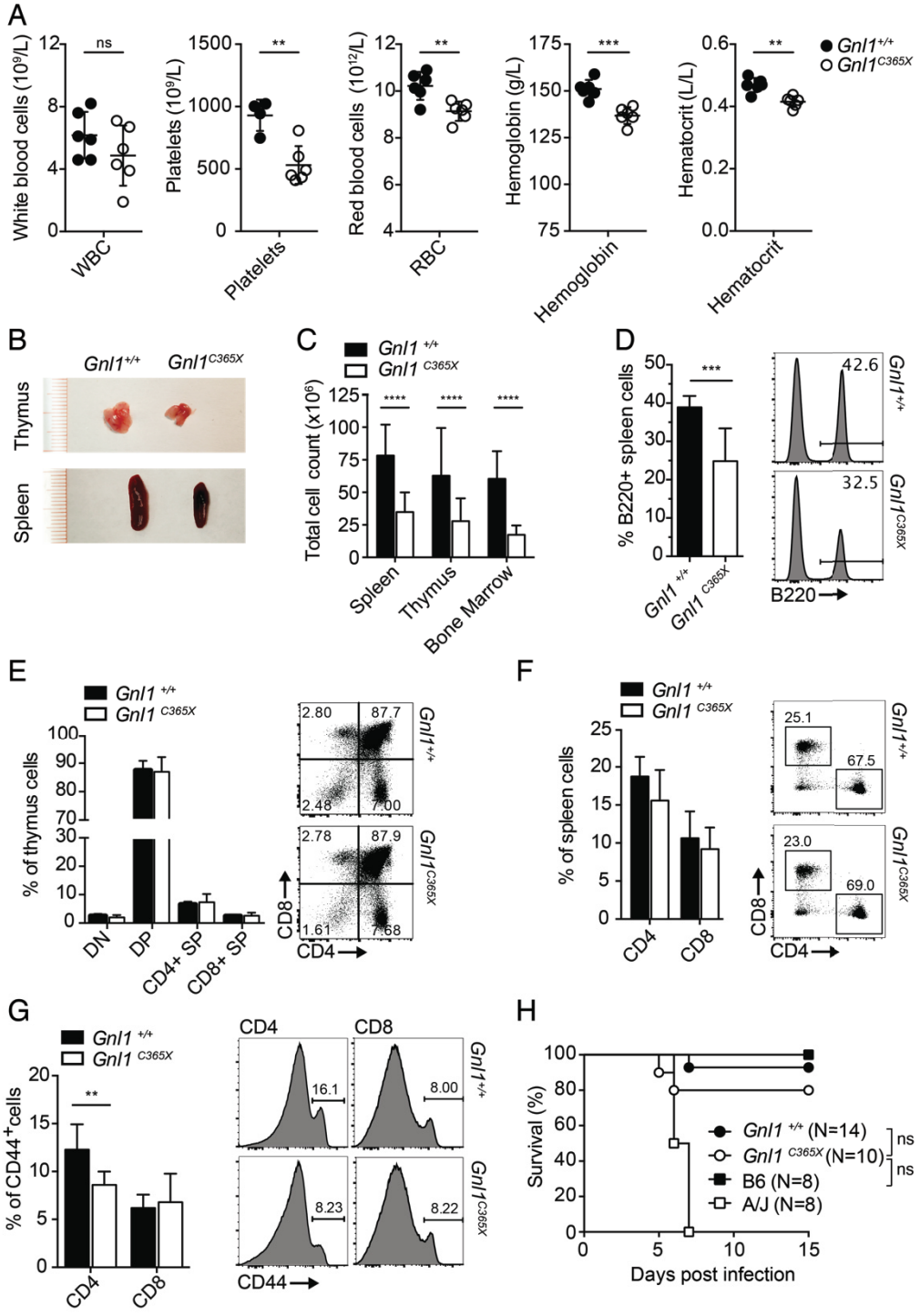
A
White blood cells (10⁹/L)
ns
WBC
Platelets (10⁹/L)
**
Platelets
Red blood cells (10¹²/L)
**
RBC
Hemoglobin (g/L)
***
Hemoglobin
Hematocrit (L/L)
**
Hematocrit
Gnl1+/+
Gnl1C365X
B
Gnl1+/+
Gnl1C365X
Thymus
Spleen
C
Gnl1 +/+
Gnl1 C365X
Total cell count (x10⁶)
****
Spleen
Thymus
Bone Marrow
D
% B220+ spleen cells
***
Gnl1 +/+
Gnl1 C365X
42.6
32.5
B220
E
Gnl1 +/+
Gnl1 C365X
% of thymus cells
DN
DP
CD4+ SP
CD8+ SP
2.80
87.7
2.48
7.00
2.78
87.9
1.61
7.68
CD8
CD4
F
Gnl1 +/+
Gnl1 C365X
% of spleen cells
CD4
CD8
25.1
67.5
23.0
69.0
G
Gnl1 +/+
Gnl1 C365X
% of CD44+cells
**
CD4
CD8
16.1
8.00
8.23
8.22
CD44
H
Survival (%)
Gnl1 +/+ (N=14)
Gnl1 C365X (N=10)
B6 (N=8)
A/J (N=8)
ns
ns
Days post infection

Figure 4.6 - NK deficiency in *Gnl1*^{C365X} animals

(A) The dot plots are representative of the DX5^{+}CD3^{-} NK cells from the spleen *Gnl1*$^{+/+}$ and *Gnl1*^{C365X} mice. NK cell proportions were quantified by FACS. Data are combined from 4 independent experiments (n = 14 per group). (B) Total spleen NK cell count was determined using DX5 and CD3 staining. (C) Blood DX5^{+}CD3^{-} NK cells from mutant or wild type mice were quantified by flow cytometry. (D) Representative dot plots from spleen, bone marrow, lymph nodes and thymus showing NK cells. (E) NK1.1^{+}CD3^{-} NK cells were quantified by FACS. Graphs represent data from at least 2 independent experiments (n = 6–15 per group). *p <0.05, **p <0.01, ***<0.001, ****p <0.0001 (two-tail Students t-test). (F) Conventional NK cells (cNK: DX5^{+}, CD49a^{-}, NK1.1^{+} and CD3^{-}) and liver-resident NK (CD49a^{+}, DX5^{-}, NK1.1^{+} and CD3^{-}) were detected by FACS. A representative plot of cNK and liver resident NK is shown for each genotype. (G) Liver cNK and liver-resident NK cells were quantified in *Gnl1*^{C365X} and *Gnl1*$^{+/+}$ mice. Pooled data from two independent experiments are shown (n = 8 per group). ****p<0.0001 (Two-way ANOVA). (H) Equal amounts of MHC$^{-/-}$ splenocytes (stained with CFSE) and *Gnl1*$^{+/+}$ or *Gnl1*^{C365X} (stained with efluor 670 dye) were injected in wild type or mutant mice. 18 hours later, all splenocytes were analyzed by flow cytometry for presence of dyed cells. Surviving MHC-1$^{-/-}$ splenocytes were quantified and normalized to the self-cells. One day prior to the injection, certain animals were treated with anti-asialo GM1. Combined data shown are from two independent experiments.

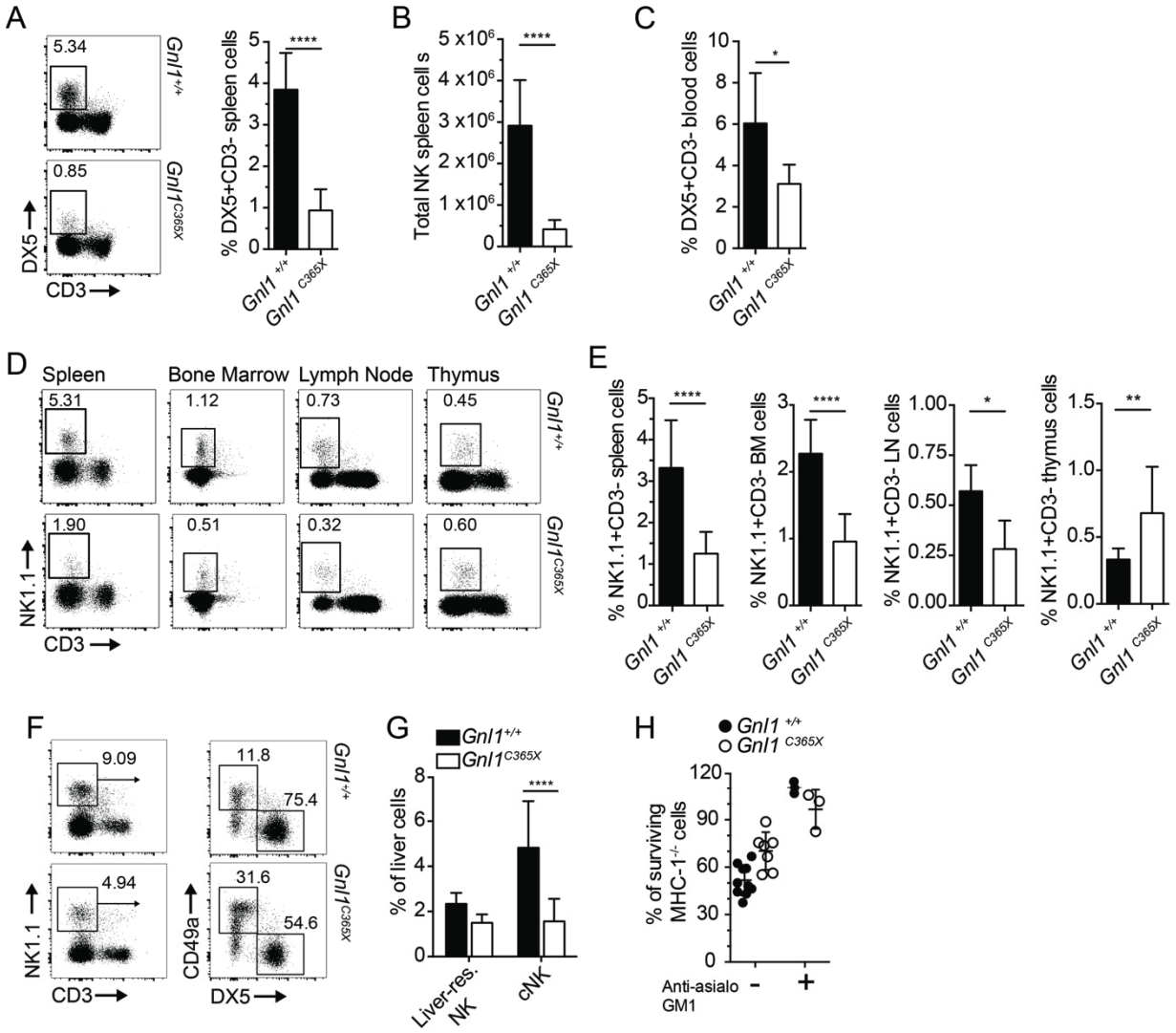
A
5.34
0.85
Gnl1+/+
Gnl1C365X
DX5
CD3
% DX5+CD3- spleen cells
****
Gnl1 +/+
Gnl1 C365X
B
Total NK spleen cell s
5 x10^6
4 x10^6
3 x10^6
2 x10^6
1 x10^6
****
C
% DX5+CD3- blood cells
*
D
Spleen
Bone Marrow
Lymph Node
Thymus
5.31
1.12
0.73
0.45
1.90
0.51
0.32
0.60
NK1.1
CD3
E
% NK1.1+CD3- spleen cells
% NK1.1+CD3- BM cells
% NK1.1+CD3- LN cells
% NK1.1+CD3- thymus cells
F
9.09
11.8
75.4
4.94
31.6
54.6
CD49a
DX5
G
Gnl1+/+
Gnl1C365X
% of liver cells
Liver-res. NK
cNK
H
Gnl1 +/+
Gnl1 C365X
% of surviving MHC-1-/- cells
Anti-asialo GM1
-
+

Figure 4.7 - NK cell maturation and survival in uninfected *Gnl1*^{C365X} mice

(A) A representative plot of each genotype showing the expression of CD11b and CD27 on NK1.1^{+}CD3^{-} spleens. The four-stage maturation program was measured by FACS. Combined data from 3 independent experiments are shown (*n* = 10–13 per group). **p <0.01, ****p <0.0001 (two-way ANOVA) (B) Expression of Ly49H, Ly49G2, Ly49A and Ly49 I/C on NK1.1^{+}CD3^{-} NK cells from *Gnl1*$^{+/+}$ and *Gnl1*^{C365X} spleens. Pooled data from at least 2 independent experiments are shown (*n* = 8–13 per group). **p <0.01 (two-tail Students t-test). (C) 2x10^{5} enriched NK cells form *Ly49h*$^{-/-}$ or B6 mice were adoptively transferred into *Gnl1*^{C365X} mice and then challenged with MCMV. Resistant control *Gnl1*$^{+/+}$ were injected with PBS prior to the infection. Mice were monitored for 14 days for clinical signs. **p<0.01 (Log-rank Mantel-Cox test). (D) Expression of Ki67 in NK1.1^{+}CD3^{-} NK cells from the spleen of wild-type and mutant mice. Data from 2 independent experiments were combined (*n* = 6–7 per group). Representative histograms of the Ki67 expression in spleen NK cells from *Gnl1*$^{+/+}$ (red) and *Gnl1*^{C365X} (blue) mice. (E) Spleen active Caspase-3 levels in NK1.1^{+}CD3^{-} NK cells were determined by FACS by measuring the binding of DEVD-FMK (conjugated to FITC) to the active Caspase-3. Combined data from at least 2 experiments are shown (*n* = 7–9 per group). A representative histogram of the active Caspase-3 expression in spleen NK cells from *Gnl1*$^{+/+}$ (red) and *Gnl1*^{C365X} (blue) mice are shown. (F) Dead NK1.1^{+}CD3^{-} spleen cells were quantified by FACS using a Fixable Viability Dye eFlour 506. Pooled data from 4 independent experiments are displayed (*n* = 15–16 per group). ****p <0.0001 (two-tails Students t-test).

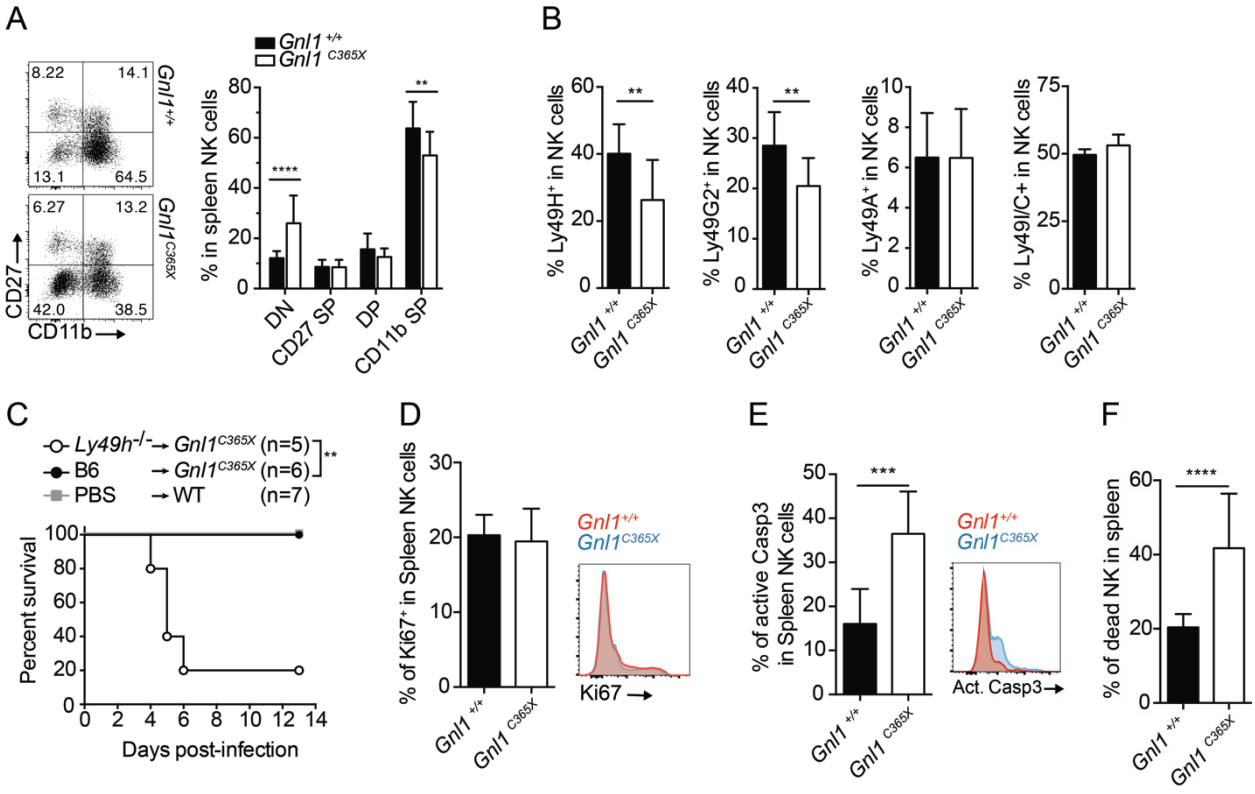
A
B
C
D
E
F
Gnl1 +/+
Gnl1 C365X
8.22
14.1
13.1
64.5
6.27
13.2
42.0
38.5
CD27
CD11b
% in spleen NK cells
DN
CD27 SP
DP
CD11b SP
% Ly49H+ in NK cells
% Ly49G2+ in NK cells
% Ly49A+ in NK cells
% Ly49I/C+ in NK cells
Ly49h-/- → Gnl1C365X (n=5)
B6 → Gnl1C365X (n=6)
PBS → WT (n=7)
Percent survival
Days post-infection
% of Ki67+ in Spleen NK cells
Ki67
% of active Casp3 in Spleen NK cells
Act. Casp3
% of dead NK in spleen

Figure 4.8 – NK cell homeostasis in *Gnl1*^{C365X} mice

(A) Equal amounts of NK cells (10^5 cells) from B6$^{CD45.1}$ and *Gnl1*^{C365X} were adoptively transferred into *Rag2*$^{-/-}\gamma c^{-/-}$ mice. Five days later, spleens were harvested and NK cells were quantified by FACS using antibodies against CD45.1 or CD45.2. ****p<0.000.1 (two-tails Student t-test, N=4). (B) CD122 median fluorescence intensity was measured on bone marrow (left) and spleen (right) NK1.1$^+$, CD122$^+$, CD3$^-$ cells. **p <0.01 (two-tails Students t-test). (C) Representative expression of CD122 on bone marrow and spleen NK1.1$^+$ CD122$^+$ CD3$^-$ cells from wild type and mutant mice. (D) We stimulated 25000 enriched NK cells with 2000U/ml of IL-2 (represented by the red arrow). At day 3 p.i., total NK1.1$^+$CD3$^-$ NK cells were counted. *p <0.05 (two-tails Students t-test). (E) The cells cycle progression was determined using Ki67 and 7AAD staining by FACS. ***p <0.01 (Two-way ANOVA). (F) We stimulated 25000 enriched NK cells with 25ng/ml IL-15 (represented by the red arrow). At day 3 NK1.1$^+$CD3$^-$ cells were counted. **p <0.01 (two-tails Students t-test). (G) The cells cycle progression was also determined using Ki67 and 7AAD at day 3 p.i. ***p <0.001, ****p <0.0001 (Two-way ANOVA). (H) We stimulated 25000 CD4 T cells or CD8 T cells with 25ng/ml of IL7 (represented by the red arrow). At day 3 p.i., total CD4$^+$CD3$^+$ and CD8$^+$CD3$^+$ cells were counted. Data are representative of at least 2 independent experiments.

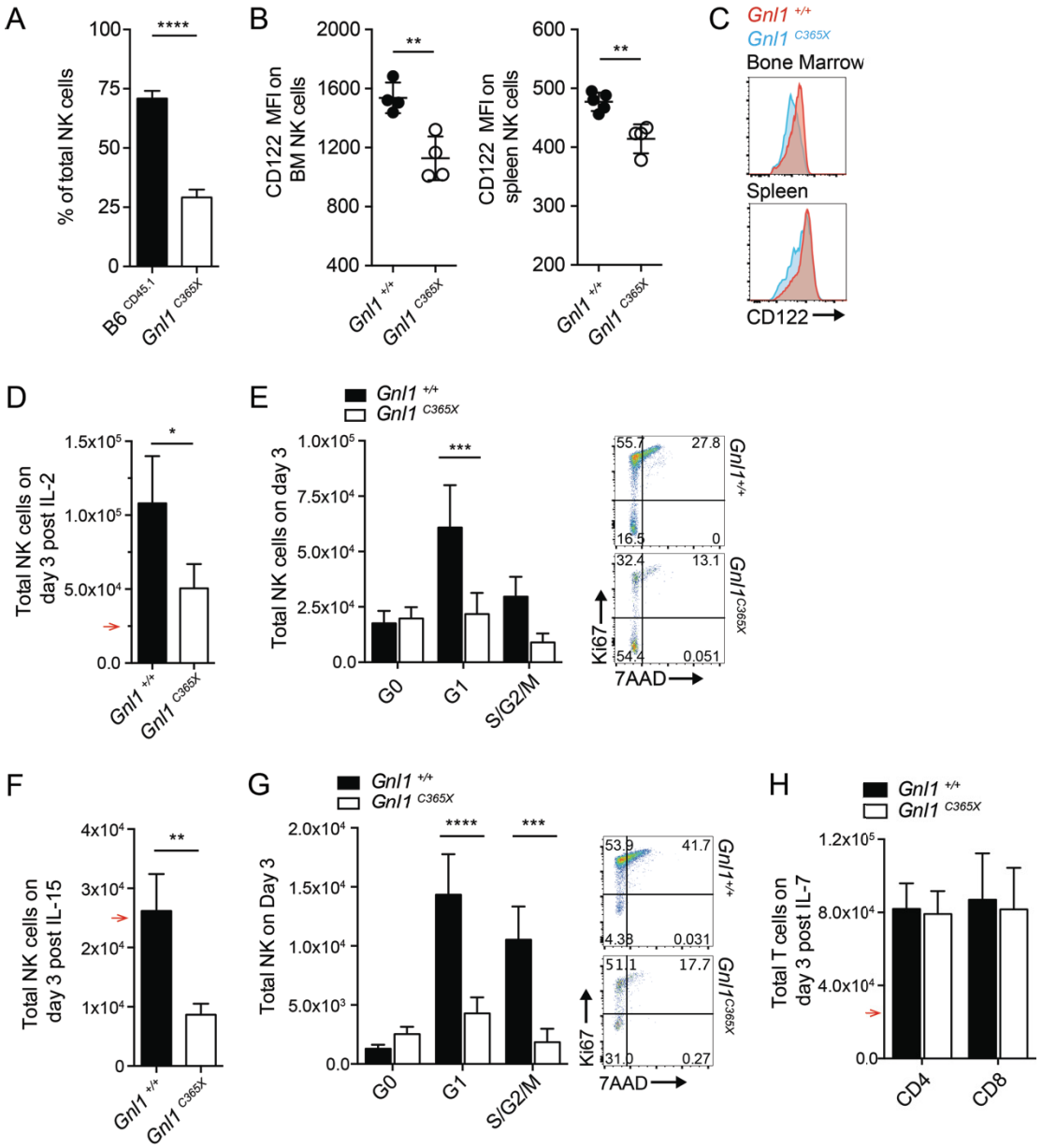
A
% of total NK cells
100
75
50
25
0
****
B6 CD45.1
Gnl1 C365X
B
CD122 MFI on BM NK cells
2000
1600
1200
800
400
**
Gnl1 +/+
Gnl1 C365X
CD122 MFI on spleen NK cells
600
500
400
300
200
**
Gnl1 +/+
Gnl1 C365X
C
Gnl1 +/+
Gnl1 C365X
Bone Marrow
Spleen
CD122
D
Total NK cells on day 3 post IL-2
1.5x10^5
1.0x10^5
5.0x10^4
0.0
*
Gnl1 +/+
Gnl1 C365X
E
Gnl1 +/+
Gnl1 C365X
Total NK cells on day 3
1.0x10^5
7.5x10^4
5.0x10^4
2.5x10^4
0.0
***
G0
G1
S/G2/M
55.7
27.8
16.5
0
Gnl1+/+
32.4
13.1
54.4
0.051
Gnl1C365X
Ki67
7AAD
F
Total NK cells on day 3 post IL-15
4x10^4
3x10^4
2x10^4
1x10^4
0
**
Gnl1 +/+
Gnl1 C365X
G
Gnl1 +/+
Gnl1 C365X
Total NK on Day 3
2.0x10^4
1.5x10^4
1.0x10^4
5.0x10^3
0.0
****
***
G0
G1
S/G2/M
53.9
41.7
4.38
0.031
Gnl1+/+
51.1
17.7
31.0
0.27
Gnl1C365X
Ki67
7AAD
H
Gnl1 +/+
Gnl1 C365X
Total T cells on day 3 post IL-7
1.2x10^5
8.0x10^4
4.0x10^4
0.0
CD4
CD8

Figure 4.9 – Inactivation of p53 rescues the GNL1^{C356X} NK deficiency

(A) Spleen from from *Gnl1*^{C365X} and *p53*$^{-/-}$ single and double mutant mice were harvested and total splenocytes were quantified. (B) Splenic NK cell proportions were determined using NK1.1 and CD3. A representative dot plot of each group is shown. (C) Total splenic NK cell counts were also determined, using NK1.1 and CD3. (D) Active Caspase-3 levels in NK1.1^{+}CD3^{-} NK cells were determined by FACS by measuring the binding of DEVD-FMK (conjugated to FITC) to the active Caspase-3. A representative histogram of each genotype is displayed. (E) Expression of CD122 on NK1.1+CD3- cells was determined by measuring the median fluorescence intensity. A representative histogram of the expression of CD122 on NK1.1^{+}CD122^{+}CD3^{-} cells is shown. (F) In the presence of GNL1, IL-2 or IL-15, stimulation leads to the initiation of the cell cycle and the increase in translation leading to cell division. At this point, MDM2 is bound to p53, allowing for cell survival and division. GNL1 could be beneficial by allowing for ribosome and polysome integrity. In the absence of GNL1, ribosomes and polysomes are compromised, leading to the sequestration of MDM2 by ribosomal proteins. This induces the release of p53, causing an increase in Caspase-3 activity and cell death. *p<0.05, **p<0.01, ***p0.001 (Two-way ANOVA). Data are representative of 2 independent experiments.

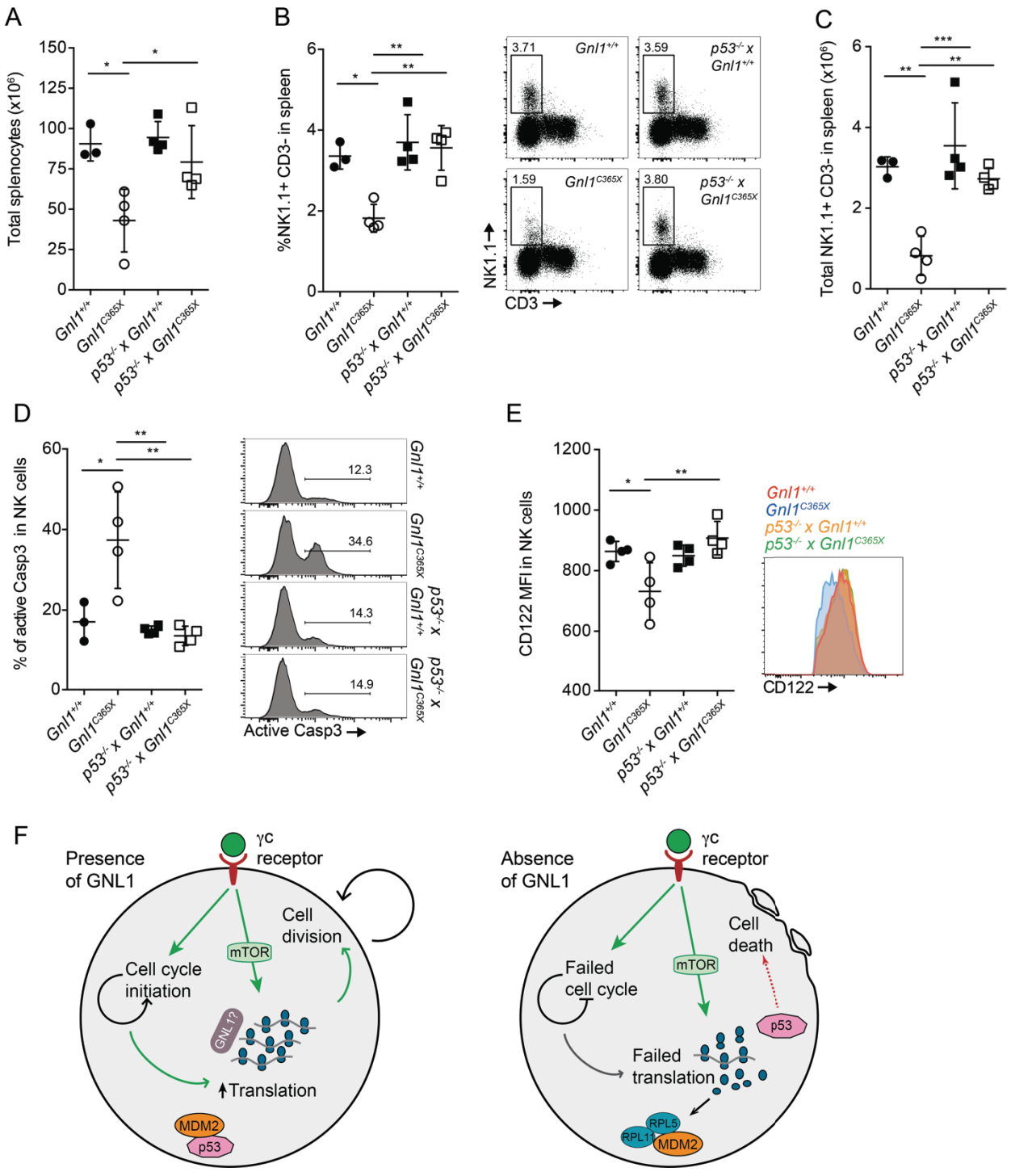
A
Total splenocytes (x10⁶)
150
125
100
75
50
25
0
*
*
Gnl1+/+
Gnl1C365X
p53-/- x Gnl1+/+
p53-/- x Gnl1C365X
B
%NK1.1+ CD3- in spleen
6
4
2
0
**
*
**
Gnl1+/+
Gnl1C365X
p53-/- x Gnl1+/+
p53-/- x Gnl1C365X
3.71
Gnl1+/+
3.59
p53-/- x Gnl1+/+
1.59
Gnl1C365X
3.80
p53-/- x Gnl1C365X
NK1.1
CD3
C
Total NK1.1+ CD3- in spleen (x10⁶)
6
4
2
0
***
**
**
Gnl1+/+
Gnl1C365X
p53-/- x Gnl1+/+
p53-/- x Gnl1C365X
D
% of active Casp3 in NK cells
60
40
20
0
**
*
**
Gnl1+/+
Gnl1C365X
p53-/- x Gnl1+/+
p53-/- x Gnl1C365X
12.3
34.6
14.3
14.9
Gnl1+/+
Gnl1C365X
p53-/- x Gnl1+/+
p53-/- x Gnl1C365X
Active Casp3
E
CD122 MFI in NK cells
1200
1000
800
600
400
*
**
Gnl1+/+
Gnl1C365X
p53-/- x Gnl1+/+
p53-/- x Gnl1C365X
Gnl1+/+
Gnl1C365X
p53-/- x Gnl1+/+
p53-/- x Gnl1C365X
CD122
F
Presence of GNL1
γc receptor
Cell division
mTOR
Cell cycle initiation
GNL1?
Translation
MDM2
p53
Absence of GNL1
γc receptor
Cell death
mTOR
Failed cell cycle
p53
Failed translation
RPL5
RPL11
MDM2

Table 4.1 - Whole-exome sequencing analysis

Shared mutation by sample 1 and 2	
Total shared mutations	73
Homozygote mutations	11
Synonymous/Nonsense/Damaging	5/4/2
Located on chr17: 29.66-47.45mb	1
Damaging	1

Supplemental material

Figure S4.1 – Myeloid cell and NK cell population in *Gnl1*^{C365X} mice

(A) Monocytes (Gr1^{+}CD11B^{+}) and (B) macrophage (F4/80^{+}CD11B^{+}) frequencies were measured in the spleen of uninfected 7–8 week old animals. Data are representative of three independent experiments (*n*=4 per groups per experiment).

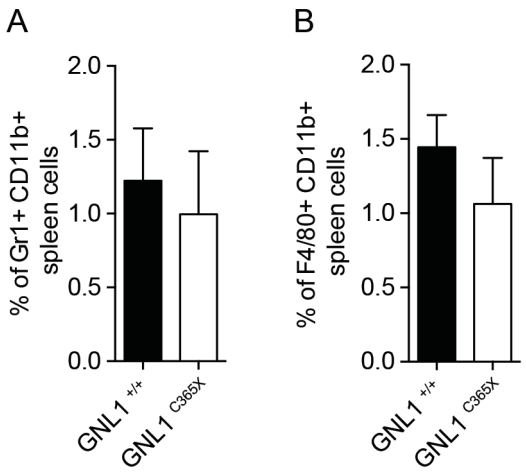
A
% of Gr1+ CD11b+ spleen cells
2.0
1.5
1.0
0.5
0.0
GNL1 +/+
GNL1 C365X
B
% of F4/80+ CD11b+ spleen cells
2.0
1.5
1.0
0.5
0.0
GNL1 +/+
GNL1 C365X

Figure S4.2 – Cell survival is not decreased in *Gnl1*^{C365X} B and T cells

(A) Splenic Ly49H+ NK cells were quantified at day 4 and 5 following MCMV infection. Combined data from at least three experiments are shown (n = 16 to 30 per group). ****p <0.0001 (Two-way ANOVA). (B) Splenocyte from *Gnl1*$^{+/+}$ and *Gnl1*^{C365X} mice were collected and active Caspase-3 was measured by the binding of DEVD-FMK (conjugated to FITC) in B cells (C) CD4 T cells and (D) CD8 T cells. Pooled data from two experiments are shown (n = 7–9 per groups).

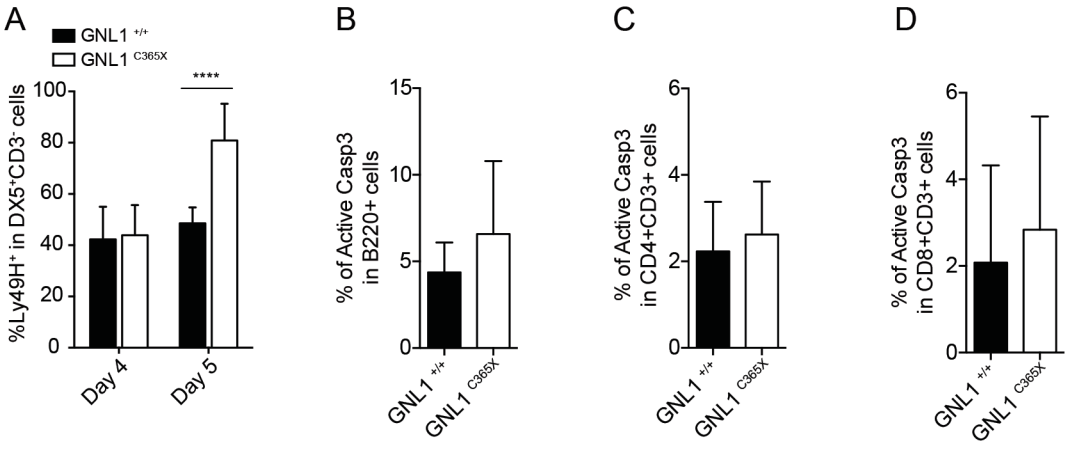
A
GNL1 +/+
GNL1 C365X
****
%Ly49H+ in DX5+CD3- cells
100
80
60
40
20
0
Day 4
Day 5
B
% of Active Casp3 in B220+ cells
15
10
5
0
GNL1 +/+
GNL1 C365X
C
% of Active Casp3 in CD4+CD3+ cells
6
4
2
0
GNL1 +/+
GNL1 C365X
D
% of Active Casp3 in CD8+CD3+ cells
6
4
2
0
GNL1 +/+
GNL1 C365X

Conclusions and general discussion

Herpesviruses are very successful pathogens. A key component of their success is their ability to infect a given host without causing a life-threatening infection which would hinder their transmission ability. Although symptoms of both HSV-1 and CMV tend to be mild, cases of patients suffering from severe herpetic infection resulting from single gene mutations have been reported (reviewed in (*78*, *151*)). Host genetics plays a crucial role in resistance to the viruses. The study of human immunity to herpesviruses is limited to the number and variety of cases that have occurred; thus the quantity of tissue and cell types available are limited. As an alternative, mouse models are a fundamental tool for studying disease. Infection of different inbred mouse strains have allowed the dissection of the genetic architecture of host resistance. To discover new genes and pathways important for the HSV-1 and CMV immune response, we used ENU chemical mutagenesis coupled with a high throughput infection platform. Following the production and testing of over 261 pedigrees, we found seven deviant families susceptible to HSV-1 or MCMV. We identified a mutation on the DNA binding site of STAT5A which alters viral lymphocyte responses and IL-2. We also observed a mutation which inhibits the expression of the GTPase GNL1, leading to an NK deficiency.

The ENU approach

ENU is a powerful tool which produces random single nucleotide mutations that can be propagated and isolated for further analysis. Compared to other commonly used mutagens, such as x-rays or chlorambucil, ENU has three main advantages (*322-324*). First, it is very efficient: ENU induces loss-of-function mutation at a given locus in approximately 1 sperm in 1000 and about one point mutation for every 1-2 Mb of genomic DNA. This rate is about 100-fold higher than the spontaneous mutation rate and 3-fold higher than X-radiation. Second, ENU induces single point mutations rather than large deletions or complex multi-locus chromosomal re-arrangements as produced by X-ray or

chlorambucil treatment. Third, unlike chlorambucil, which targets post-meiotic cells, ENU induces mutations in pre-meiotic spermatogonial cells, allowing ENU-treated male mice to sire mutant offspring for extended periods of time. These advantages have made ENU the preferred method for genetic screens in the mouse.

The ENU mutations can be propagated following different breeding schemes that make it possible to segregate either dominant or recessive mutations. Theoretically, mice can carry mutations in any type of gene and pathway, which can be probed for their role in the host response to virus infection by assessing viral susceptibility. This allows for the isolation of a mutation of interest and the generation of a monogenic model of infection. The *Gnl1* and *Stat5a* mutant mice that we discussed in chapters 3 and 4 of this thesis are good examples of this.

To discover new genes important for host resistance, we used a very stringent phenotype: survival. This method had the benefit of ensuring that the mutation found would have a critical function in disease pathogenesis. Of course, using such a severe phenotype has one major caveat: we might find mutations that influence genes with a central role in the immune system, and which, as a result, affect many different cell types and compartments. Moreover, we expected that a certain proportion of such genes would have already been identified and characterized. The identification of *ptprc* (CD45) during an HSV-1 susceptibility screen is an excellent example of a mutation on a known gene, where the abrogation of CD45 causes severe T cell and NK cell lymphopenia (*66*). Nonetheless, discovery of that mutation allowed for a better understanding of the anti-HSV-1 T cell response and the interplay between CD4 and CD8 T cells during infection. The $STAT5A^{W484G}$ pedigree is another example of an ENU mutation on a well-characterized gene. However, the study of $STAT5^{W484G}$ mice allowed for the study of the STAT5 protein linker domain in T and NK cell responses, which revealed the role of a specific residue on protein function. Although the search for novel uncharacterized genes using a strong phenotype for screening represents a challenge, we were able to identify a mutation on the GTPase GNL1 that causes a severe susceptibility to MCMV. Prior to

our work, no clear function was reported for GNL1 in metazoans, whereas we have now established its crucial role in the fate of NK cells. Altogether, our data illustrate that ENU mutagenesis can not only identify the function of previously uncharacterized genes: It can also shed new light on known pathways and reveal protein functions that could not be identified through gene-targeting studies. Moreover, since ENU causes point mutations, it can better mirror the type of variation most frequently observed in the human population, and thus can produce more accurate models for the study of diseases.

The type of phenotypic screen used will dictate the pathway investigated and will allow for further characterization. Hence various consortia worldwide have developed ENU screens focused on their own particular area of biological interest, from behaviour to development (*467-469*). The laboratories of Chris Goodnow and Bruce Beutler have also applied this approach to dissect the molecular regulation of the immune system. Some immunological screens have tested the integrity of TLR signaling in macrophages; the ability to mount a humoral response to antigenic challenge; and effectiveness in resisting MCMV infection (*357*, *470*). The extent of the success of this technique has been quite impressive, as seen in the Mutagenetix database, which compiles discovered ENU-induced phenotypes and mutations. The database currently contains 116 mutations affecting 75 genes that have been linked to immune-phenotypes (*330*, *331*). Notable discoveries include the identification of new components of TLR signal transduction pathways such as the polytopic membrane protein, UNC93B (which is involved in the intracellular transport of nucleotide-sensing TLR3, TLR7/8 and TLR9), and the amino acid transporter, SLC15A4 (required for TLR7 and TLR9 signaling in dendritic cells), which have in turn provided tremendous insight into the system. Another example is the discovery of a key regulator of antibody responses, CARD11 (*471*). In this case, a single amino acid substitution revealed separate roles in lymphocyte activation and in immune-regulation, a phenotype not observed in knock-out mice. Our in vivo screen for HSV-1 susceptibility isolated 5 independent HSE families; additional work is required to validate these families. However, we can expect that their study will contribute to the identification of genes crucial to the immune response.

The vast majority of ENU mutations identified to date are coding, frameshift, nonsense, and critical splicing mutations affecting protein function, which can be discovered using whole-exome sequencing. This approach, however, neglects a large part of the genome that does not code for proteins yet is critical for the regulation of pathogenesis (*472*), including regulatory RNAs (*473*). For instance, as well as directly regulating viral replication, microRNAs can play a determinant role on the regulation of the immune system (*410*, *411*).. As discussed in chapter 3, whole genome sequencing of ENU deviant mice could cover the non-coding genome. Another alternative would be the usage of high-throughput RNA sequencing (RNAseq). This next-generation sequencing method can be applied to sequencing both the mRNA and the non-coding RNAs, as well as their quantification. This technique was used in a study of human nasopharyngeal carcinoma, using *ex-vivo* cultures of healthy and malignant tissue (*474*). This approach would also permit for the integration of both host and viral transcriptomes to better define the pathways involved in the interplay between the host and the pathogen. RNA sequencing could also be used for the direct identification of coding mutations, as it gives both the sequence information and the expression levels. However, this technique demands that the mutated transcript be expressed and that the mutation lies directly in an exon. That would not have been optimal for the study of the GNL1^{C365X} mutants (reduced transcript level) or the Tre pedigrees (mutation in a splice junction region). RNA sequencing could be used in conjunction with a linkage analysis, as it will allow for a better mapping and identification of the mutation. Regardless of the method used, selecting the right tissue is crucial for success (e.g. brain tissue for HSE model and spleen for CMV model).

The advent of next-generation sequencing has rendered the ENU mutagenesis approach much more efficient and expanded its applications. For example, the Beutler group has developed a mutagenesis pipeline where mutations that cause phenovariance and the phenotype they cause are discovered simultaneously. For this, all G1 males are sequenced using WES to call all ENU-induced coding mutations (*313*, *328*). Each G1 is used to establish a pedigree, whereas WES information is used to generate genotyping

panels based on the discovered ENU-induced SNVs present in the G1. Using these panels, G2 and G3 animals are genotyped prior to phenotyping. Cohorts of 30-50 G3s are passed through a phenotyping panel using blood cells, and then through in vivo challenges. Mouse phenotype data is then used to map the causative mutation. This method allows for the identification of the ENU mutation as soon as a deviant pedigree is identified (in "real time"). This approach also has the advantage of reducing the time between the phenotyping and the identification of the mutation, as well as giving a complete overview of all mutations, including incidental mutations which are not associated with the phenotype. However, it is costly, demands quick access to genomic platforms and in-house competence in animal care, *in-vivo* and *in-vitro* expertise with pathogens and an efficient bioinformatics team.

As the availability of whole-exome sequencing increases and costs are reduced, the sequencing of human patients suffering from unexplained infections and/or diseases will become more common. The identification of genes underlying primary immunodeficiencies that result in severe disease has greatly benefited from this technology (*475*). Initiatives such as the 100,000 Genome Project in England leverage the increased availability of next-generation sequencing to identify damaging mutations in rare diseases and cancer (*476*). Another example of the use of whole-exome sequencing for diagnostics was the discovery of compound heterozygote mutations in IRF7 which cause life-threatening flu infections in children (*308*). Although very useful, next-generation sequencing still requires many steps of bioinformatic validation as well as *in-vitro* and *in-vivo* confirmation. This approach relies on the detection and accurate diagnosis of affected patients, and their families' collaboration. Increased usage and awareness of these technologies should help to facilitate their application.

To better understand the genetic determinants of host resistance and the numerous pathways involved in the immune response to viruses, the mouse model still remains a powerful and versatile tool. When used in a forward genetics project, like the one described in this thesis, the mouse model allows for the dissection of the different genes

and pathways crucial to the innate and adaptive response to a given pathogen. The capacity to randomly create and isolate different mutations on different regions of any gene allows for a better understanding of their functions. The mouse model also allows for a global overview of the immune response. This versatility and scope is not possible in human studies, as they rely on the natural occurrence of phenovariant mutations. The mouse model gives access to the analysis of the pathogenesis in a diversity of organs that are not accessible in human studies. The high variety of immunological and genetic testing applicable to the mouse model also makes it a powerful tool to dissect the complexity of the immune response. Thus, it is necessary to combine the patient-driven and the mouse model approaches to contextualize the different findings of both models.

The development of CRISPR-Cas9 technology, which makes it possible to edit a given gene and generate a subsequent mouse or cells line, has also become an important tool for the study of host resistance (*477*, *478*). The availability of commercial solutions facilitates the validation and analysis of candidate genes from ENU and human studies. CRISPR-based mutagenesis has become a very efficient method of producing organisms carrying loss-of-function alleles, and powerful tools are being created to rapidly produce new CRISPR-based alleles in genome-wide and gene-focused applications in cells (*479*). ENU mutagenesis, however, remains advantageous for in vivo screens as well as for generating a variety of alleles allowing for an in-depth characterization of a gene. As such, both methods play complementary roles in achieving a better understanding of the immunological mechanisms involved in resistance to CMV and HSE.

Susceptibility to HSE

HSV-1 is a highly successful virus: between 60 and 100% of the population is seropositive for the virus. HSV-1 can cause severe encephalitis, which results in long-term damage even when treated. The high prevalence of this virus, as opposed to the rarity of HSE cases, suggests that there is an important genetic component to the disease. Therefore, the interplay between the host response and the virus dictates the outcome of the

infection, whereby host genetic polymorphisms play a critically determining role in the effectiveness and magnitude of the immune response.

Various human studies have shown the importance of the TLR3-IFN-α/β pathway in the resistance to HSE. Young children carrying Mendelian mutations affecting this pathway suffered from severe HSE (*78*, *480*). These studies highlight the importance of cell intrinsic innate immunity in the control of the viral infection. However, these findings do not represent the whole extent of the causes of the disease; as of yet many cases of childhood HSE remain to be resolved. 90% of HSE is caused by HSV-1 (the other 10% by HSV-2) and only one third of those HSE cases affect children between 6 months and 20 years old (*24*, *25*). For example, HSE cases in neonates are mainly caused by HSV-2, from mothers affected by a primary infection (*26*, *27*). Moreover, approximately 50% of HSE cases are found in individuals over the age of 50; a population which tends to have been previously exposed to HSV-1 in their lifetime (*24*). Interestingly, the disease in those patients does not originate from the latent virus but rather from a novel primary infection, as the viral strain in the CNS is different than the one found in the periphery (*481*). These observations suggest the involvement of an immune mechanism other than cell- intrinsic innate immunity to the development of HSE.

Whereas an intact cell-intrinsic TLR3 pathway is crucial to HSE resistance in children, a large proportion of HSE cases remain unexplained (*482-484*), adult cases in particular. The use of mouse models supports a key role for adaptive T cell functions in the control of CNS infection and the development of HSE. For example, in our laboratory, we have identified an ENU mutation in *ptprc* (encoding for CD45) during an HSV-1 resistance screen (*66*). This mutation caused lymphopenia, which leads to HSE even in the presence of a functional TLR3 pathway. In this thesis, I have described a mutation in STAT5A found during an HSV-1 screen which alters T and NK cell responses to the virus. We observed that T cells and NK cells bearing the mutation lack responsiveness to cytokines and the capacity to proliferate in response to pathogen challenge. More recently, our group also found a mutation during another ENU project in c-Rel, one of the five sub-units of NF-κB.

This mutation impacts both the stromal cells and T cells from the hematopoietic compartment (*338*). Taken together, these ENU mutants highlight the importance of adaptive immunity in the resistance to HSV-1 infection, and ultimately HSE.

Questions regarding the type of HSE the mouse model replicates were raised. As the mutations found in ENU studies differ from the pathway described in children affected with HSE, one hypothesis is that the mouse model is better suited to describe the pathology observed in older patients. The two immune pathways or compartments would be critical at different points of human development: Cell intrinsic immunity appears to be more critical in newborns and young children, whereas adaptive immunity is vital to control adult HSE. After remission, children previously affected with HSE did not have increased recurrent labial infections and relapses were rare (*408*). Moreover, children with severe combined immunodeficiency (no T and B cells) are not more prone to HSE, but are susceptible to recurrent labial infections (*485*). In a more recent study, patient with severe HSE exhibit a normal T cell compartment, even if cell-intrinsic innate immunity was altered (*486*). A recent study by Koyanagi et al. has also showed that CD8 T cell accumulation in the CNS is crucial to resistance to HSE (*487*). HSV-1 has indeed developed a mechanism where the expression of the chemokine CXCL9 is downregulated by the viral protein UL13, thus promoting viral evasion. However, the recruitment of immune cells to the brain has to be balanced, as the transmigration of too many cells can lead to detrimental neuroinflammation (*488*).

We found that the STAT5A linker domain is important for the modulation of the T cell response following HSV-1 infection. The direct effect of our ENU mutation remains to be defined: whether or not this mutation impacts on the control of the viral replication or CNS neuroinflamation has yet to be determined. The intracranial model of infection, where the virus is injected in the brain, would be an appropriate method in this case, as the immune response to the virus in the brain could be measured (*98*). A better understanding of STAT5A functions will allow for the development of new treatments that either increase or decrease T cell response during infection. The modulation of STAT5A function by

targeting the linker domain could be a possible therapeutic avenue, allowing for the control of the T cell response, which in turn will influence viral replication and neuro-inflammation.

Susceptibility to CMV and NK cells

MCMV is a powerful model for the study of the biology of NK cells. Although these cells were first characterized in studies involving tumor suppression, it is in the context of MCMV infection that many of their functions and mechanisms were defined (*175*, *176*, *315*, *489*). NK cells are essential, non-redundant lymphocytes for resistance to the virus. This central role of NK cells in the anti-MCMV response has been exploited in many studies, allowing for a better understanding of recognition/activation mechanisms, cytotoxicity and cytokine production (*315*, *490*). NK cells will not only directly kill infected cells, but also secrete IFNγ, which activates T cells, specifically CD8 T cells. This activation is crucial to the subsequent control of MCMV infection (*491*). NK deficiency observed in *Gnl1*^{C365X} mice could impact the T cell response to the virus. We could not measure the T cell response at a later stage of infection, since the animals succumb to the infection before the expansion of CD8 T cells (starting at day 4) (*140*, *492*). Infection at a lower dose could facilitate the analysis of the T cell response, as mice would survive the infection. This approach will also allow us to study the memory-like NK cells that should be generated following the infection to verify the role of GNL1 in this process.

During our ENU screen we found a nonsense mutation in the *Gnl1* gene that completely abolished GNL1 protein expression and caused an NK deficiency. This specificity in the NK deficiency is interesting, since NK deficiency tends to be coupled with a reduction in lymphocytes and/or myeloid cells and general immunodeficiency (*151*). For instance, although mutations in *Gata2* have been linked to NK cell-lymphopenia and susceptibility to viral infections, *Gata2*-deficiecy is also coupled with profound B-cell and monocytopenia leading to severe bacterial and fungal infections (*350*, *434*, *493*). Other ENU studies for susceptibility to MCMV have also found mutations in genes causing an NK deficiency. The Mutagenetix database reports 8 genes that, when mutated, can lead

to decreased NK cell numbers (*330*). These mutations also cause a reduction in T and B cell populations or affect NK function (*330*). One mutation in *Flt3* dramatically reduced NK cell numbers, however the effect was due in part to a cell deficit in dendritic cells, which also impaired NK activation following infection. To our knowledge, the GNL1 phenotype that we have observed is similar to the one observed in patients who carry mutations in MCM4, a protein important for DNA replication; patients with *MCM4* mutations have severely reduced NK cell numbers and severe susceptibility to herpesviruses, despite the fact that other immune cell populations, such lymphocytes and myeloid cells, appear normal (*351*, *436*). However, a number of developmental problems were observed in MCM4 patients. Our screen for MCMV-susceptibility led to the characterization of *Gnl1*, which is crucial to NK cell homeostasis and survival. While it showed NK cell specificity, the mutation did not impair their activation or cytotoxic activity, suggesting that GNL1 can be used as a new entry point to exploit NK cells for the management of patients in clinics.

The therapeutic potential of GNL1

The newly discovered GNL1 role in NK cells we have described will allow for the development of new therapeutic strategies. The modulation of NK proliferation by GNL1 expression could be applied in different contexts. Although I will describe approaches that leverage GNL1, the modulation of NK proliferation could also be applied to other genes that are important for NK cell homeostasis and proliferation.

Using Gnl1 as a marker for viral susceptibility. As NK cells play a key role in viral resistance, deficiency in these cells can cause severe herpetic, fungi or bacterial infections (*151*). For instance, a defect in *Gata2* and *Mcm4* leads to a reduction in NK cell numbers, causing severe herpetic infection in humans (*348*, *436*). However, the genetic causes for other types of NK deficiencies causing CMV and herpesvirus susceptibility remain unknown. Using *Gnl1* as a novel genetic marker for NK deficiency and/or immune defect can benefit patients: It can lead to a better description of the cause of the disease, with the end goal of facilitating treatment.

Gnl1-deficient mice as model to study inflammatory disease. NK cells are known to play an important role in inflammatory diseases; these can either be beneficial or detrimental. For instance, Systemic Lupus Erythematosus, rheumatoid arthritis, antiphospholipid syndrome and multiple sclerosis have been associated with an increase or a decrease in NK cell number, although the mechanism leading to this remains unclear (*494*). Moreover, a polymorphism in *Gnl1* was associated with rheumatoid arthritis in two different GWAS (*495*, *496*). Thus, mice carrying *Gnl1*-deficient isoforms or novel *Gnl1*-knock-in or *Gnl1*-conditional alleles could be used to study the effect of the mutation in models of inflammatory diseases such as collagen-induced arthritis or experimental autoimmune encephalitis. It would also be pertinent to assess the importance of *Gnl1* in the generation of memory NK cells, as cytokine-induced memory-like NK cells are prone to respond to an inflammatory environment (*280*) and could influence the outcome of this type of disease. Such studies would help increase the understanding of these illnesses and the development of new therapies.

GNL1 as a target for therapeutic modulations of NK cell populations. Over 177 clinical trials targeting NK cells were reported during the last four years in North America and Europe (according to www.clinicaltrials.gov). As such, the production of NK cells as an adjuvant for the treatment of cancer is promising. One approach used for the treatment of leukemia patients is the pre-treatment of a graft with IL-2 in order to increase NK cell numbers and produce lymphokine-activated killer cells. These cells can then attack the remaining tumor cells and reduce the risk of relapse (review in (*497*)). However, this procedure increases T cell numbers as well. This increase can be detrimental to the patient, as it carries the potential risk of graft-versus-host disease. Moreover, regular injections of IL-2 are necessary, as these NK cells have a short lifespan. The other approach used is the blocking of inhibitory KIR receptors in order to increase the activation of NK cells and their cytotoxic activity (*498*). The increased expression of the NK-stimulating ligand NKG2D on tumor cells by chemotherapeutic agents (such as 5-FU, Ara-C, cisplatin) can also be used to achieve the same end goal (*499*). However, neither

technique increases the NK pool, but rather modifies their function, which could lead to adverse effects.

By modulating GNL1 expression, the NK cell population could be increased, while leaving their main function untouched. This could be achieved by increasing GNL1 expression or function in NK cells, or by using an expression construct carrying *Gnl1* cDNA. This technique could also be used to increase NK cell numbers of patients affected with severe herpetic infection, while avoiding the long-term toxicity of classical drugs and decreasing the risk of drug resistance. Although promising, the modulation of GNL1 expression demands many studies, trials and much optimization.

Final conclusion

For my thesis, we aimed to use chemical mutagenesis to dissect the genetic factors involved in host resistance to viral infection, paving the way for the development of new therapies. Usage of ENU mutagenesis allows a better understanding of the immune response in three ways.

1- *Discovery of novel genes and pathways*. The characterization of *Gnl1*'s function and its role in NK cell homeostasis via p53 and its importance in the IL-2/IL-15 response is a great example of the effectiveness of ENU.
2- *Discovery of novel functions of known genes*. During my thesis, I closely collaborated on two other ENU screens that led to the identification of *ptprc* and *REL* as crucial genes for an efficient innate and adaptive response to HSE (*66*, *338*).
3- *Dissection of the specific protein region and its importance in the immune response*. I generated an ENU mutation in the linker domain of the DNA binding site of STAT5A and described the importance of that region for T and NK cell responses to IL-2 and viral infection.

Although the aims of the project were ambitious, we can conclude that this ENU project was successful. During my thesis project, we identified known and novel genes that are important for antiviral immunity. These discoveries, which allow for a better understanding of the mechanism governing the regulation of the immune system, should ultimately help in the elaboration of antiviral and immune-mediated treatments.

References

1. J. Sinclair, Latency and reactivation of human cytomegalovirus. *J. Gen. Virol.* **87**, 1763–1779 (2006).
2. D. Kimberlin, Herpes simplex virus, meningitis and encephalitis in neonates. *Herpes : the journal of the IHMF*. **11 Suppl 2**, 65A–76A (2004).
3. D. Z. Rechenchoski, L. C. Faccin-Galhardi, R. E. C. Linhares, C. Nozawa, Herpesvirus: an underestimated virus. *Folia Microbiol*. **62**, 151–156 (2016).
4. B. Roizman, D. M. Knipe, R. J. Whitley, in *Fields Virology*, D. M. Knipe, P. M. Howley, Eds. (ed. 5, 2007), vol. 2, pp. 2501–2601.
5. M. Ho, The history of cytomegalovirus and its diseases. *Med. Microbiol. Immunol.* **197**, 65–73 (2008).
6. E. S. Mocarski, T. Shenk, R. F. Pass, in *Fields Virology*, D. M. Knipe, P. M. Howley, Eds. (Lippincott Williams & Wilkins, ed. 5, 2007), vol. 2.
7. B. Roizmann *et al.*, The Family Herpesviridae - an Update. *Arch Virol*. **123**, 425–449 (1992).
8. J. H. Subak-Sharpe, D. J. Dargan, HSV molecular biology: general aspects of herpes simplex virus molecular biology. *Virus genes*. **16**, 239–251 (1998).
9. A. J. Davison, Evolution of the herpesviruses. *Veterinary microbiology*. **86**, 69–88 (2002).
10. R. D. Everett, HSV-1 biology and life cycle. *Methods Mol. Biol.* **1144**, 1–17 (2014).
11. P. M. Jean Beltran, I. M. Cristea, The life cycle and pathogenesis of human cytomegalovirus infection: lessons from proteomics. *Expert Rev Proteomics*. **11**, 697–711 (2014).
12. E. Murphy, I. Rigoutsos, T. Shibuya, T. E. Shenk, Reevaluation of human cytomegalovirus coding potential. *Proc. Natl. Acad. Sci. U.S.A.* **100**, 13585–13590 (2003).
13. M. K. Kukhanova, A. N. Korovina, S. N. Kochetkov, Human herpes simplex virus: life cycle and development of inhibitors. *Biochemistry Mosc.* **79**, 1635–1652 (2014).
14. L. J. Perry, D. J. McGeoch, The DNA sequences of the long repeat region and adjoining parts of the long unique region in the genome of herpes simplex virus type 1. *J. Gen. Virol.* **69 (Pt 11)**, 2831–2846 (1988).
15. E. Murphy *et al.*, Coding potential of laboratory and clinical strains of human cytomegalovirus. *Proc. Natl. Acad. Sci. U.S.A.* **100**, 14976–14981 (2003).
16. S. A. Staras *et al.*, Seroprevalence of cytomegalovirus infection in the United States, 1988-1994. *Clinical infectious diseases : an official publication of the Infectious Diseases Society of America*. **43**, 1143–1151 (2006).

17. R. J. Whitley, D. W. Kimberlin, B. Roizman, Herpes simplex viruses. *Clinical infectious diseases : an official publication of the Infectious Diseases Society of America*. **26**, 541–53– quiz 554–5 (1998).
18. M. J. Levin, A. Weinberg, D. S. Schmid, Herpes Simplex Virus and Varicella-Zoster Virus. *Microbiol Spectr*. **4** (2016), doi:10.1128/microbiolspec.DMIH2-0017-2015.
19. M. J. Groves, Genital Herpes: A Review. *Am Fam Physician*. **93**, 928–934 (2016).
20. J. T. Schiffer, A. Wald, S. Selke, L. Corey, A. Magaret, The Kinetics of Mucosal Herpes Simplex Virus–2 Infection in Humans: Evidence for Rapid Viral-Host Interactions. *J. Infect. Dis.* **204**, 554–561 (2011).
21. P. T. Ohara, M. S. Chin, J. H. LaVail, The spread of herpes simplex virus type 1 from trigeminal neurons to the murine cornea: an immunoelectron microscopy study. *J. Virol.* **74**, 4776–4786 (2000).
22. H. S. Toma *et al.*, Ocular HSV-1 latency, reactivation and recurrent disease. *Semin Ophthalmol*. **23**, 249–273 (2008).
23. J. W. Gnann, R. J. Whitley, Herpes Simplex Encephalitis: an Update. *Curr Infect Dis Rep*. **19**, 13 (2017).
24. R. J. Whitley, Herpes simplex encephalitis: adolescents and adults. *Antiviral Res.* **71**, 141–148 (2006).
25. I. Steiner, F. Benninger, Update on herpes virus infections of the nervous system. *Curr Neurol Neurosci Rep*. **13**, 414 (2013).
26. S. H. James, D. W. Kimberlin, R. J. Whitley, Antiviral therapy for herpesvirus central nervous system infections: neonatal herpes simplex virus infection, herpes simplex encephalitis, and congenital cytomegalovirus infection. *Antiviral Res.* **83**, 207–213 (2009).
27. C. Thompson, R. Whitley, Neonatal herpes simplex virus infections: where are we now? *Adv. Exp. Med. Biol.* **697**, 221–230 (2011).
28. G. B. Elion *et al.*, Selectivity of action of an antiherpetic agent, 9-(2-hydroxyethoxymethyl) guanine. *Proc. Natl. Acad. Sci. U.S.A.* **74**, 5716–5720 (1977).
29. F. Morfin, D. Thouvenot, Herpes simplex virus resistance to antiviral drugs. *J. Clin. Virol.* **26**, 29–37 (2003).
30. D. M. Coen, in *Antiviral Research* (American Society of Microbiology, 2009), pp. 1–18.
31. S. Efstathiou, C. M. Preston, Towards an understanding of the molecular basis of herpes simplex virus latency. *Virus Res.* **111**, 108–119 (2005).
32. M. L. Cook, J. G. Stevens, Pathogenesis of herpetic neuritis and ganglionitis in mice: evidence for intra-axonal transport of infection. *Infect. Immun.* **7**, 272–288 (1973).
33. G. A. Smith, S. P. Gross, L. W. Enquist, Herpesviruses use bidirectional fast-

axonal transport to spread in sensory neurons. *Proc. Natl. Acad. Sci. U.S.A.* **98**, 3466–3470 (2001).

34. K. M. Khanna, R. H. Bonneau, P. R. Kinchington, R. L. Hendricks, Herpes simplex virus-specific memory CD8+ T cells are selectively activated and retained in latently infected sensory ganglia. *Immunity*. **18**, 593–603 (2003).
35. T. Liu, K. M. Khanna, X. Chen, D. J. Fink, R. L. Hendricks, CD8(+) T cells can block herpes simplex virus type 1 (HSV-1) reactivation from latency in sensory neurons. *Journal of Experimental Medicine*. **191**, 1459–1466 (2000).
36. J. G. Stevens, E. K. Wagner, G. B. Devi-Rao, M. L. Cook, L. T. Feldman, RNA complementary to a herpesvirus alpha gene mRNA is prominent in latently infected neurons. *Science*. **235**, 1056–1059 (1987).
37. T. J. Hill, W. A. Blyth, D. A. Harbour, E. L. Berrie, A. B. Tullo, Latency and other consequences of infection of the nervous system with herpes simplex virus. *Prog. Brain Res.* **59**, 173–184 (1983).
38. C. S. Miller, R. J. Danaher, R. J. Jacob, Molecular aspects of herpes simplex virus I latency, reactivation, and recurrence. *Crit. Rev. Oral Biol. Med.* **9**, 541–562 (1998).
39. I. Gresser, M. G. Tovey, C. Maury, M. T. Bandu, Role of interferon in the pathogenesis of virus diseases in mice as demonstrated by the use of anti-interferon serum. II. Studies with herpes simplex, Moloney sarcoma, vesicular stomatitis, Newcastle disease, and influenza viruses. *Journal of Experimental Medicine*. **144**, 1316–1323 (1976).
40. R. Zawatzky, H. Kirchner, J. DeMaeyer-Guignard, E. DeMaeyer, An X-linked locus influences the amount of circulating interferon induced in the mouse by herpes simplex virus type 1. *J. Gen. Virol.* **63**, 325–332 (1982).
41. D. A. Leib *et al.*, Interferons Regulate the Phenotype of Wild-type and Mutant Herpes Simplex Viruses In Vivo. *Journal of Experimental Medicine*. **189**, 663–672 (1999).
42. S. Luecke, S. R. Paludan, Innate recognition of alphaherpesvirus DNA. *Adv. Virus Res.* **92**, 63–100 (2015).
43. K. P. Egan, S. Wu, B. Wigdahl, S. R. Jennings, Immunological control of herpes simplex virus infections. *J. Neurovirol.* **19**, 328–345 (2013).
44. Z. Wang *et al.*, Regulation of innate immune responses by DAI (DLM-1/ZBP1) and other DNA-sensing molecules. *Proceedings of the National Academy of Sciences*. **105**, 5477–5482 (2008).
45. K. Takahasi *et al.*, Nonself RNA-sensing mechanism of RIG-I helicase and activation of antiviral immune responses. *Molecular Cell*. **29**, 428–440 (2008).
46. J. Xing, S. Wang, R. Lin, K. L. Mossman, C. Zheng, Herpes simplex virus 1 tegument protein US11 downmodulates the RLR signaling pathway via direct interaction with RIG-I and MDA-5. *J. Virol.* **86**, 3528–3540 (2012).
47. C. Su, G. Zhan, C. Zheng, Evasion of host antiviral innate immunity by HSV-1, an update. *Virol. J.* **13**, 38 (2016).

48. M. K. Choi *et al.*, A selective contribution of the RIG-I-like receptor pathway to type I interferon responses activated by cytosolic DNA. *Proceedings of the National Academy of Sciences*. **106**, 17870–17875 (2009).

49. Y. Liu *et al.*, RIG-I-Mediated STING Upregulation Restricts Herpes Simplex Virus 1 Infection. *J. Virol.* **90**, 9406–9419 (2016).

50. S. B. Rasmussen *et al.*, Herpes simplex virus infection is sensed by both Toll-like receptors and retinoic acid-inducible gene- like receptors, which synergize to induce type I interferon production. *J. Gen. Virol.* **90**, 74–78 (2009).

51. A. Krug *et al.*, Herpes simplex virus type 1 activates murine natural interferon-producing cells through toll-like receptor 9. *Blood*. **103**, 1433–1437 (2004).

52. J. Lund, A. Sato, S. Akira, R. Medzhitov, A. Iwasaki, Toll-like Receptor 9–mediated Recognition of Herpes Simplex Virus-2 by Plasmacytoid Dendritic Cells. *Journal of Experimental Medicine*. **198**, 513–520 (2003).

53. Y. Guo *et al.*, Herpes simplex virus encephalitis in a patient with complete TLR3 deficiency: TLR3 is otherwise redundant in protective immunity. *J. Exp. Med.* **208**, 2083–2098 (2011).

54. M. Herman *et al.*, Heterozygous TBK1 mutations impair TLR3 immunity and underlie herpes simplex encephalitis of childhood. *J. Exp. Med.* (2012), doi:10.1084/jem.20111316.

55. S. Y. Zhang *et al.*, TLR3 Deficiency in Patients with Herpes Simplex Encephalitis. *Science*. **317**, 1522–1527 (2007).

56. H. J. Pegram, D. M. Andrews, M. J. Smyth, P. K. Darcy, M. H. Kershaw, Activating and inhibitory receptors of natural killer cells. *Immunol. Cell Biol.* **89**, 216–224 (2011).

57. I. A. York *et al.*, A cytosolic herpes simplex virus protein inhibits antigen presentation to CD8+ T lymphocytes. *Cell*. **77**, 525–535 (1994).

58. G. A. Bishop, J. C. Glorioso, S. A. Schwartz, Relationship between expression of herpes simplex virus glycoproteins and susceptibility of target cells to human natural killer activity. *Journal of Experimental Medicine*. **157**, 1544–1561 (1983).

59. H. Ghiasi, S. Cai, G. C. Perng, A. B. Nesburn, S. L. Wechsler, The role of natural killer cells in protection of mice against death and corneal scarring following ocular HSV-1 infection. *Antiviral Res.* **45**, 33–45 (2000).

60. S. Habu, K. Akamatsu, N. Tamaoki, K. Okumura, In vivo significance of NK cell on resistance against virus (HSV-1) infections in mice. *J. Immunol.* **133**, 2743–2747 (1984).

61. S. Nandakumar, S. N. Woolard, D. Yuan, B. T. Rouse, U. Kumaraguru, Natural killer cells as novel helpers in anti-herpes simplex virus immune response. *J. Virol.* **82**, 10820–10831 (2008).

62. H. F. Staats, J. E. Oakes, R. N. Lausch, Anti-glycoprotein D monoclonal antibody protects against herpes simplex virus type 1-induced diseases in mice functionally depleted of selected T-cell subsets or asialo GM1+ cells. *J. Virol.* **65**, 6008–6014 (1991).

63. J. F. Bukowski, R. M. Welsh, The role of natural killer cells and interferon in resistance to acute infection of mice with herpes simplex virus type 1. *J. Immunol.* **136**, 3481–3485 (1986).

64. W. Chmielarczyk, H. Engler, R. Ernst, U. Opitz, H. Kirchner, Injection of anti-thy-1.2 serum breaks genetic resistance of mice against herpes simplex virus. *J. Gen. Virol.* **66 (Pt 5)**, 1087–1094 (1985).

65. S. H. Kassim *et al.*, Dendritic cells are required for optimal activation of natural killer functions following primary infection with herpes simplex virus type 1. *J. Virol.* **83**, 3175–3186 (2009).

66. G. Caignard *et al.*, Genome-wide mouse mutagenesis reveals CD45-mediated T cell function as critical in protective immunity to HSV-1. *PLoS Pathog*. **9**, e1003637 (2013).

67. F. P. Siegal *et al.*, The nature of the principal type 1 interferon-producing cells in human blood. *Science*. **284**, 1835–1837 (1999).

68. J. M. Lund, M. M. Linehan, N. Iijima, A. Iwasaki, Cutting Edge: Plasmacytoid dendritic cells provide innate immune protection against mucosal viral infection in situ. *J. Immunol.* **177**, 7510–7514 (2006).

69. H. Hochrein *et al.*, Herpes simplex virus type-1 induces IFN-alpha production via Toll-like receptor 9-dependent and -independent pathways. *Proc. Natl. Acad. Sci. U.S.A.* **101**, 11416–11421 (2004).

70. A. Wollenberg *et al.*, Plasmacytoid Dendritic Cells: A New Cutaneous Dendritic Cell Subset with Distinct Role in Inflammatory Skin Diseases. *J. Invest. Dermatol.* **119**, 1096–1102 (2002).

71. B. M. Mitchell, J. G. Stevens, Neuroinvasive properties of herpes simplex virus type 1 glycoprotein variants are controlled by the immune response. *J. Immunol.* **156**, 246–255 (1996).

72. S. P. Deshpande, M. Zheng, M. Daheshia, B. T. Rouse, Pathogenesis of herpes simplex virus-induced ocular immunoinflammatory lesions in B-cell-deficient mice. *J. Virol.* **74**, 3517–3524 (2000).

73. S. N. Mueller, C. M. Jones, C. M. Smith, W. R. Heath, F. R. Carbone, Rapid cytotoxic T lymphocyte activation occurs in the draining lymph nodes after cutaneous herpes simplex virus infection as a result of early antigen presentation and not the presence of virus. *Journal of Experimental Medicine*. **195**, 651–656 (2002).

74. J. E. Knickelbein *et al.*, Noncytotoxic lytic granule-mediated CD8+ T cell inhibition of HSV-1 reactivation from neuronal latency. *Science*. **322**, 268–271 (2008).

75. R. A. Pereira, M. M. Simon, A. Simmons, Granzyme A, a noncytolytic component of CD8(+) cell granules, restricts the spread of herpes simplex virus in the peripheral nervous systems of experimentally infected mice. *J. Virol.* **74**, 1029–1032 (2000).

76. R. J. Whitley, D. W. Kimberlin, Herpes simplex encephalitis: children and

adolescents. *Semin Pediatr Infect Dis*. **16**, 17–23 (2005).

77. M. G. Smith, E. H. Lennette, H. R. Reames, Isolation of the virus of herpes simplex and the demonstration of intranuclear inclusions in a case of acute encephalitis. *The American Journal of Pathology*. **17**, 55–68.1 (1941).
78. S.-Y. Zhang, L. Abel, J.-L. Casanova, Mendelian predisposition to herpes simplex encephalitis. *Handbook of clinical neurology*. **112**, 1091–1097 (2013).
79. J. P. Stahl, A. Mailles, T. De Broucker, Steering Committee and Investigators Group, Herpes simplex encephalitis and management of acyclovir in encephalitis patients in France. *Epidemiol. Infect.* **140**, 372–381 (2012).
80. S. Dupuis *et al.*, Impaired response to interferon-alpha/beta and lethal viral disease in human STAT1 deficiency. *Nat. Genet.* **33**, 388–391 (2003).
81. A. Puel *et al.*, The NEMO mutation creating the most-upstream premature stop codon is hypomorphic because of a reinitiation of translation. *Am. J. Hum. Genet.* **78**, 691–701 (2006).
82. A. Casrouge *et al.*, Herpes Simplex Virus Encephalitis in Human UNC-93B Deficiency. *Science*. **314**, 308–312 (2006).
83. V. Sancho-Shimizu *et al.*, Herpes simplex encephalitis in children with autosomal recessive and dominant TRIF deficiency. *J. Clin. Invest.* **121**, 4889–4902 (2011).
84. R. Pérez de Diego *et al.*, Human TRAF3 Adaptor Molecule Deficiency Leads to Impaired Toll-like Receptor 3 Response and Susceptibility to Herpes Simplex Encephalitis. *Immunity*. **33**, 400–411 (2010).
85. F. G. Lafaille *et al.*, Impaired intrinsic immunity to HSV-1 in human iPSC-derived TLR3-deficient CNS cells. *Nature*. **491**, 769–773 (2012).
86. J.-L. Casanova, Severe infectious diseases of childhood as monogenic inborn errors of immunity. *Proceedings of the National Academy of Sciences*. **112**, E7128–37 (2015).
87. L. L. Andersen *et al.*, Functional IRF3 deficiency in a patient with herpes simplex encephalitis. *J. Exp. Med.* **212**, 1371–1379 (2015).
88. C. Lopez, Genetics of natural resistance to herpesvirus infections in mice. *Nature*. **258**, 152–153 (1975).
89. P. Lundberg *et al.*, A locus on mouse chromosome 6 that determines resistance to herpes simplex virus also influences reactivation, while an unlinked locus augments resistance of female mice. *J. Virol.* **77**, 11661–11673 (2003).
90. V. Sancho-Shimizu *et al.*, Genetic susceptibility to herpes simplex virus 1 encephalitis in mice and humans. *Curr Opin Allergy Clin Immunol*. **7**, 495–505 (2007).
91. U. Kumaraguru, I. A. Davis, S. Deshpande, S. S. Tevethia, B. T. Rouse, Lymphotoxin alpha-/- mice develop functionally impaired CD8+ T cell responses and fail to contain virus infection of the central nervous system. *J. Immunol.* **166**, 1066–1074 (2001).

92. D. B. Henken, M. E. Goldstein, J. R. Martin, Herpes simplex virus type-2 infection by a footpad route results in neuronal death in mouse spinal ganglia. *J. Neurol. Sci.* **115**, 177–183 (1993).

93. J. M. Webre *et al.*, Rabbit and mouse models of HSV-1 latency, reactivation, and recurrent eye diseases. *J. Biomed. Biotechnol.* **2012**, 612316 (2012).

94. J. R. Anderson, H. J. Field, An animal model of ocular herpes. Keratitis, retinitis and cataract in the mouse. *Br J Exp Pathol*. **65**, 283–297 (1984).

95. S. J. Kopp *et al.*, Infection of neurons and encephalitis after intracranial inoculation of herpes simplex virus requires the entry receptor nectin-1. *Proceedings of the National Academy of Sciences*. **106**, 17916–17920 (2009).

96. D. S. Mansur *et al.*, Lethal encephalitis in myeloid differentiation factor 88-deficient mice infected with herpes simplex virus 1. *The American Journal of Pathology*. **166**, 1419–1426 (2005).

97. T. J. Pasieka *et al.*, Host responses to wild-type and attenuated herpes simplex virus infection in the absence of Stat1. *J. Virol.* **83**, 2075–2087 (2009).

98. J. P. Wang *et al.*, Role of Specific Innate Immune Responses in Herpes Simplex Virus Infection of the Central Nervous System. *J. Virol.* **86**, 2273–2281 (2012).

99. L. S. Reinert *et al.*, Sensing of HSV-1 by the cGAS-STING pathway in microglia orchestrates antiviral defence in the CNS. *Nat Commun*. **7**, 13348 (2016).

100. J. Zimmermann *et al.*, Enhanced viral clearance and reduced leukocyte infiltration in experimental herpes encephalitis after intranasal infection of CXCR3-deficient mice. *J. Neurovirol.* **23**, 394–403 (2017).

101. T. R. Wuest, D. J. J. Carr, Dysregulation of CXCR3 Signaling due to CXCL10 Deficiency Impairs the Antiviral Response to Herpes Simplex Virus 1 Infection. *J. Immunol.* **181**, 7985–7993 (2008).

102. P. Griffiths, I. Baraniak, M. Reeves, The pathogenesis of human cytomegalovirus. *The Journal of Pathology*. **235**, 288–297 (2015).

103. R. M. McAllister, Cytomegalic inclusion disease. *Ergeb Mikrobiol Immunitatsforsch Exp Ther*. **39**, 1–13 (1966).

104. F. Mattes, J. McLaughlin, V. Emery, D. Clark, P. Griffiths, Histopathological detection of owl's eye inclusions is still specific for cytomegalovirus in the era of human herpesviruses 6 and 7. *Journal of Clinical Pathology*. **53**, 612–614 (2000).

105. D. S. Owers, A. C. Webster, G. F. M. Strippoli, K. Kable, E. M. Hodson, Pre-emptive treatment for cytomegalovirus viraemia to prevent cytomegalovirus disease in solid organ transplant recipients. *Cochrane Database Syst Rev*, CD005133 (2013).

106. J. R. Deayton *et al.*, Importance of cytomegalovirus viraemia in risk of disease progression and death in HIV-infected patients receiving highly active antiretroviral therapy. *Lancet*. **363**, 2116–2121 (2004).

107. M. G. Revello *et al.*, Role of prenatal diagnosis and counseling in the

management of 735 pregnancies complicated by primary human cytomegalovirus infection: a 20-year experience. *J. Clin. Virol.* **50**, 303–307 (2011).

108. J. G. Sissons, A. J. Carmichael, Clinical aspects and management of cytomegalovirus infection. *The Journal of infection*. **44**, 78–83 (2002).

109. G. Pawelec, J. E. McElhaney, A. E. Aiello, E. Derhovanessian, The impact of CMV infection on survival in older humans. *Curr. Opin. Immunol.* **24**, 507–511 (2012).

110. G. Pawelec, E. Derhovanessian, Role of CMV in immune senescence. *Virus Res.* **157**, 175–179 (2011).

111. A. Pera *et al.*, Immunosenescence: Implications for response to infection and vaccination in older people. *Maturitas*. **82**, 50–55 (2015).

112. L. Kananen *et al.*, Cytomegalovirus infection accelerates epigenetic aging. *Exp. Gerontol.* **72**, 227–229 (2015).

113. E. Paintsil, Y.-C. Cheng, in *Encyclopedia of Microbiology* (Elsevier, 2009), pp. 223–257.

114. P. Griffiths, S. Lumley, Cytomegalovirus. *Curr. Opin. Infect. Dis.* **27**, 554–559 (2014).

115. A. B. Campos, J. Ribeiro, D. Boutolleau, H. Sousa, Human cytomegalovirus antiviral drug resistance in hematopoietic stem cell transplantation: current state of the art. *Rev. Med. Virol.* **26**, 161–182 (2016).

116. K. K. Biron, Antiviral drugs for cytomegalovirus diseases. *Antiviral Res.* **71**, 154–163 (2006).

117. E. Poole, M. Wills, J. Sinclair, Human Cytomegalovirus Latency: Targeting Differences in the Latently Infected Cell with a View to Clearing Latent Infection. *New Journal of Science*. **2014**, 1–10 (2014).

118. L. Dupont, M. B. Reeves, Cytomegalovirus latency and reactivation: recent insights into an age old problem. *Rev. Med. Virol.* **26**, 75–89 (2016).

119. K. N. Fish, C. Soderberg-Naucler, L. K. Mills, S. Stenglein, J. A. Nelson, Human cytomegalovirus persistently infects aortic endothelial cells. *J. Virol.* **72**, 5661–5668 (1998).

120. J. L. Pollock, R. M. Presti, S. Paetzold, H. W. Virgin, Latent murine cytomegalovirus infection in macrophages. *Virology*. **227**, 168–179 (1997).

121. L. D'Aiuto *et al.*, Human induced pluripotent stem cell-derived models to investigate human cytomegalovirus infection in neural cells. *PLoS ONE*. **7**, e49700 (2012).

122. J.-P. Belzile, T. J. Stark, G. W. Yeo, D. H. Spector, Human cytomegalovirus infection of human embryonic stem cell-derived primitive neural stem cells is restricted at several steps but leads to the persistence of viral DNA. *J. Virol.* **88**, 4021–4039 (2014).

123. M. H. Luo, P. H. Schwartz, E. A. Fortunato, Neonatal neural progenitor cells and

their neuronal and glial cell derivatives are fully permissive for human cytomegalovirus infection. *J. Virol.* **82**, 9994–10007 (2008).

124. C. C. Rossetto, M. Tarrant-Elorza, G. S. Pari, Cis and trans acting factors involved in human cytomegalovirus experimental and natural latent infection of CD14 (+) monocytes and CD34 (+) cells. *PLoS Pathog*. **9**, e1003366 (2013).

125. V. G. Kew, J. Yuan, J. Meier, M. B. Reeves, Mitogen and stress activated kinases act co-operatively with CREB during the induction of human cytomegalovirus immediate-early gene expression from latency. *PLoS Pathog*. **10**, e1004195 (2014).

126. M. B. Reeves, T. Compton, Inhibition of inflammatory interleukin-6 activity via extracellular signal-regulated kinase-mitogen-activated protein kinase signaling antagonizes human cytomegalovirus reactivation from dendritic cells. *J. Virol.* **85**, 12750–12758 (2011).

127. M. J. Keller *et al.*, Reversal of human cytomegalovirus major immediate-early enhancer/promoter silencing in quiescently infected cells via the cyclic AMP signaling pathway. *J. Virol.* **81**, 6669–6681 (2007).

128. A. Krmpotić, I. Bubic, B. Polic, P. Lucin, S. Jonjić, Pathogenesis of murine cytomegalovirus infection. *Microbes Infect.* **5**, 1263–1277 (2003).

129. C. Sweet, The pathogenicity of cytomegalovirus. *FEMS Microbiol. Rev.* **23**, 457–482 (1999).

130. M. J. Reddehase, J. Podlech, N. K. A. Grzimek, Mouse models of cytomegalovirus latency: overview. *Journal of Clinical Virology*. **25**, 23–36 (2002).

131. P. Klenerman, A. Oxenius, T cell responses to cytomegalovirus. *Nat. Rev. Immunol.* **16**, 367–377 (2016).

132. S. M. Walton, N. Torti, S. Mandaric, A. Oxenius, T-cell help permits memory CD8+ T-cell inflation during cytomegalovirus latency. *Eur J Immunol*. **41**, 2248–2259 (2011).

133. M. F. Bachmann, P. Wolint, S. Walton, K. Schwarz, A. Oxenius, Differential role of IL-2R signaling for CD8+ T cell responses in acute and chronic viral infections. *Eur J Immunol*. **37**, 1502–1512 (2007).

134. A. W. Sylwester *et al.*, Broadly targeted human cytomegalovirus-specific CD4+ and CD8+ T cells dominate the memory compartments of exposed subjects. *Journal of Experimental Medicine*. **202**, 673–685 (2005).

135. H. Komatsu *et al.*, Large scale analysis of pediatric antiviral CD8+ T cell populations reveals sustained, functional and mature responses. *Immun Ageing*. **3**, 11 (2006).

136. H. Komatsu, S. Sierro, A. V Cuero, P. Klenerman, Population analysis of antiviral T cell responses using MHC class I-peptide tetramers. *Clin. Exp. Immunol.* **134**, 9–12 (2003).

137. M. Eggers, K. Radsak, G. Enders, M. Reschke, Use of recombinant glycoprotein antigens gB and gH for diagnosis of primary human cytomegalovirus infection

during pregnancy. *J. Med. Virol.* **63**, 135–142 (2001).

138. K. Schoppel, C. Schmidt, H. Einsele, H. Hebart, M. Mach, Kinetics of the Antibody Response against Human Cytomegalovirus-Specific Proteins in Allogeneic Bone Marrow Transplant Recipients. *J. Infect. Dis.* **178**, 1233–1243 (1998).
139. D. F. Bratcher *et al.*, Effect of Passive Antibody on Congenital Cytomegalovirus Infection in Guinea Pigs. *J. Infect. Dis.* **172**, 944–950 (1995).
140. Y. O. Alexandre, C. D. Cocita, S. Ghilas, M. Dalod, Deciphering the role of DC subsets in MCMV infection to better understand immune protection against viral infections. *Front Microbiol*. **5**, 378 (2014).
141. L. L. Lanier, Evolutionary struggles between NK cells and viruses. *Nat. Rev. Immunol.* **8**, 259–268 (2008).
142. A. Krug *et al.*, TLR9-dependent recognition of MCMV by IPC and DC generates coordinated cytokine responses that activate antiviral NK cell function. *Immunity*. **21**, 107–119 (2004).
143. K. Tabeta *et al.*, Toll-like receptors 9 and 3 as essential components of innate immune defense against mouse cytomegalovirus infection. *Proc. Natl. Acad. Sci. U.S.A.* **101**, 3516–3521 (2004).
144. E. Szomolanyi-Tsuda, X. Liang, R. M. Welsh, E. A. Kurt-Jones, R. W. Finberg, Role for TLR2 in NK cell-mediated control of murine cytomegalovirus in vivo. *J. Virol.* **80**, 4286–4291 (2006).
145. K. W. Boehme, M. Guerrero, T. Compton, Human Cytomegalovirus Envelope Glycoproteins B and H Are Necessary for TLR2 Activation in Permissive Cells. *J. Immunol.* **177**, 7094–7102 (2006).
146. M. Dalod *et al.*, Dendritic cell responses to early murine cytomegalovirus infection: subset functional specialization and differential regulation by interferon alpha/beta. *J. Exp. Med.* **197**, 885–898 (2003).
147. M. Lucas, W. Schachterle, K. Oberle, P. Aichele, A. Diefenbach, Dendritic cells prime natural killer cells by trans-presenting interleukin 15. *Immunity*. **26**, 503–517 (2007).
148. D. M. Andrews, A. A. Scalzo, W. M. Yokoyama, M. J. Smyth, M. A. Degli-Esposti, Functional interactions between dendritic cells and NK cells during viral infection. *Nat. Immunol.* **4**, 175–181 (2003).
149. C. Cocita *et al.*, Natural Killer Cell Sensing of Infected Cells Compensates for MyD88 Deficiency but Not IFN-I Activity in Resistance to Mouse Cytomegalovirus. *PLoS Pathog*. **11**, e1004897 (2015).
150. M. Swiecki, S. Gilfillan, W. Vermi, Y. Wang, M. Colonna, Plasmacytoid dendritic cell ablation impacts early interferon responses and antiviral NK and CD8(+) T cell accrual. *Immunity*. **33**, 955–966 (2010).
151. J. S. Orange, Natural killer cell deficiency. *J. Allergy Clin. Immunol.* **132**, 515–25; quiz 526 (2013).

152. M. Wagner, A. Gutermann, J. Podlech, M. J. Reddehase, U. H. Koszinowski, Major Histocompatibility Complex Class I Allele-specific Cooperative and Competitive Interactions between Immune Evasion Proteins of Cytomegalovirus. *Journal of Experimental Medicine*. **196**, 805–816 (2002).

153. N. Shifrin, D. H. Raulet, M. Ardolino, NK cell self tolerance, responsiveness and missing self recognition. *Semin. Immunol.* **26**, 138–144 (2014).

154. E. Tomasello, M. Bléry, F. Vély, E. Vivier, Signaling pathways engaged by NK cell receptors: double concerto for activating receptors, inhibitory receptors and NK cells. *Semin. Immunol.* **12**, 139–147 (2000).

155. V. M. Braud *et al.*, HLA-E binds to natural killer cell receptors CD94/NKG2A, B and C. *Nature*. **391**, 795–799 (1998).

156. R. E. Vance, J. R. Kraft, J. D. Altman, P. E. Jensen, D. H. Raulet, Mouse CD94/NKG2A is a natural killer cell receptor for the nonclassical major histocompatibility complex (MHC) class I molecule Qa-1(b). *Journal of Experimental Medicine*. **188**, 1841–1848 (1998).

157. C. A. O'Callaghan, A. Cerwenka, B. E. Willcox, L. L. Lanier, P. J. Bjorkman, Molecular competition for NKG2D: H60 and RAE1 compete unequally for NKG2D with dominance of H60. *Immunity*. **15**, 201–211 (2001).

158. A. Cerwenka, New twist on the regulation of NKG2D ligand expression. *J. Exp. Med.* **206**, 265–268 (2009).

159. H. Arase, E. S. Mocarski, A. E. Campbell, A. B. Hill, L. L. Lanier, Direct recognition of cytomegalovirus by activating and inhibitory NK cell receptors. *Science*. **296**, 1323–1326 (2002).

160. K. S. Campbell, J. Hasegawa, Natural killer cell biology: an update and future directions. *J. Allergy Clin. Immunol.* **132**, 536–544 (2013).

161. A. A. Scalzo, N. A. Fitzgerald, A. Simmons, A. B. La Vista, G. R. Shellam, Cmv-1, a genetic locus that controls murine cytomegalovirus replication in the spleen. *J. Exp. Med.* **171**, 1469–1483 (1990).

162. S. H. Lee *et al.*, Susceptibility to mouse cytomegalovirus is associated with deletion of an activating natural killer cell receptor of the C-type lectin superfamily. *Nat. Genet.* **28**, 42–45 (2001).

163. M. G. Brown *et al.*, Vital involvement of a natural killer cell activation receptor in resistance to viral infection. *Science*. **292**, 934–937 (2001).

164. H. Sjolin *et al.*, Pivotal role of KARAP/DAP12 adaptor molecule in the natural killer cell-mediated resistance to murine cytomegalovirus infection. *J. Exp. Med.* **195**, 825–834 (2002).

165. A. R. French *et al.*, DAP12 signaling directly augments proproliferative cytokine stimulation of NK cells during viral infections. *J. Immunol.* **177**, 4981–4990 (2006).

166. H. R. Smith *et al.*, Recognition of a virus-encoded ligand by a natural killer cell activation receptor. *Proc. Natl. Acad. Sci. U.S.A.* **99**, 8826–8831 (2002).

167. I. Bubic *et al.*, Gain of virulence caused by loss of a gene in murine cytomegalovirus. *J. Virol.* **78**, 7536–7544 (2004).

168. E. J. Adams *et al.*, Structural elucidation of the m157 mouse cytomegalovirus ligand for Ly49 natural killer cell receptors. *Proceedings of the National Academy of Sciences*. **104**, 10128–10133 (2007).

169. A. J. Corbett, J. D. Coudert, C. A. Forbes, A. A. Scalzo, Functional consequences of natural sequence variation of murine cytomegalovirus m157 for Ly49 receptor specificity and NK cell activation. *J. Immunol.* **186**, 1713–1722 (2011).

170. C. A. Forbes, A. A. Scalzo, M. A. Degli-Esposti, J. D. Coudert, Ly49C-dependent control of MCMV Infection by NK cells is cis-regulated by MHC Class I molecules. *PLoS Pathog*. **10**, e1004161 (2014).

171. M. Pyzik *et al.*, Viral MHC class I-like molecule allows evasion of NK cell effector responses in vivo. *J. Immunol.* **193**, 6061–6069 (2014).

172. J. P. Di Santo, Natural killer cell developmental pathways: a question of balance. *Annu. Rev. Immunol.* **24**, 257–286 (2006).

173. H. Arase, T. Saito, J. H. Phillips, L. L. Lanier, Cutting Edge: The Mouse NK Cell-Associated Antigen Recognized by DX5 Moncoclonal Antibody is CD49b (α2-Integrin, Very Late Antigen-2). *J. Immunol.* **167**, 1141–1144 (2001).

174. R. Kiessling, G. Bataillon, E. W. Lamon, E. Klein, The lymphocyte response to primary Moloney sarcoma virus tumors: definition of a non-specific component of the in vitro cellular hyporeactivity of tumor-bearing hosts. *Int. J. Cancer*. **14**, 642–648 (1974).

175. R. Kiessling, E. Klein, H. Pross, H. Wigzell, “Natural” killer cells in the mouse. II. Cytotoxic cells with specificity for mouse Moloney leukemia cells. Characteristics of the killer cell. *Eur J Immunol*. **5**, 117–121 (1975).

176. R. B. Herberman, M. E. Nunn, H. T. Holden, D. H. Lavrin, Natural cytotoxic reactivity of mouse lymphoid cells against syngeneic and allogeneic tumors. II. Characterization of effector cells. *Int. J. Cancer*. **16**, 230–239 (1975).

177. V. Kumar, M. E. McNerney, A new self: MHC-class-I-independent natural-killer-cell self-tolerance. *Nat. Rev. Immunol.* **5**, 363–374 (2005).

178. W. Leung, Infusions of allogeneic natural killer cells as cancer therapy. *Clin. Cancer Res.* **20**, 3390–3400 (2014).

179. T.-K. Yu, E. G. Caudell, C. Smid, E. A. Grimm, IL-2 Activation of NK Cells: Involvement of MKK1/2/ERK But Not p38 Kinase Pathway. *J. Immunol.* **164**, 6244–6251 (2000).

180. J. Chaix *et al.*, Cutting edge: Priming of NK cells by IL-18. *J. Immunol.* **181**, 1627–1631 (2008).

181. K. S. Frederiksen *et al.*, IL-21 induces in vivo immune activation of NK cells and CD8(+) T cells in patients with metastatic melanoma and renal cell carcinoma. *Cancer Immunol. Immunother.* **57**, 1439–1449 (2008).

182. S. C. C. Chiang *et al.*, Comparison of primary human cytotoxic T-cell and natural killer cell responses reveal similar molecular requirements for lytic granule exocytosis but differences in cytokine production. *Blood*. **121**, 1345–1356 (2013).

183. A. S. Dighe, E. Richards, L. J. Old, R. D. Schreiber, Enhanced in vivo growth and resistance to rejection of tumor cells expressing dominant negative IFN gamma receptors. *Immunity*. **1**, 447–456 (1994).

184. A. Martín-Fontecha *et al.*, Induced recruitment of NK cells to lymph nodes provides IFN-gamma for T(H)1 priming. *Nat. Immunol.* **5**, 1260–1265 (2004).

185. N. Dalbeth, M. F. C. Callan, A subset of natural killer cells is greatly expanded within inflamed joints. *Arthritis Rheum.* **46**, 1763–1772 (2002).

186. J. Yeung, C. W. E. So, Identification and characterization of hematopoietic stem and progenitor cell populations in mouse bone marrow by flow cytometry. *Methods Mol. Biol.* **538**, 301–315 (2009).

187. S. Okada *et al.*, In vivo and in vitro stem cell function of c-kit- and Sca-1-positive murine hematopoietic cells. *Blood*. **80**, 3044–3050 (1992).

188. M. Osawa *et al.*, In vivo self-renewal of c-Kit+ Sca-1+ Lin(low/-) hemopoietic stem cells. *J. Immunol.* **156**, 3207–3214 (1996).

189. G. Challen, N. Boles, K. Lin, M. Goodell, Mouse hematopoietic stem cell identification and analysis - Challen - 2008 - Cytometry Part A - Wiley Online Library. *Cytometry* (2008).

190. J. Seita, I. L. Weissman, Hematopoietic stem cell: self-renewal versus differentiation. *Wiley Interdiscip Rev Syst Biol Med*. **2**, 640–653 (2010).

191. S. H. Orkin, L. I. Zon, Hematopoiesis: An Evolving Paradigm for Stem Cell Biology. *Cell*. **132**, 631–644 (2008).

192. M. Kondo, I. L. Weissman, K. Akashi, Identification of clonogenic common lymphoid progenitors in mouse bone marrow. *Cell*. **91**, 661–672 (1997).

193. C. Seillet *et al.*, Deciphering the Innate Lymphoid Cell Transcriptional Program. *Cell Rep*. **17**, 436–447 (2016).

194. V. Male *et al.*, The transcription factor E4bp4/Nfil3 controls commitment to the NK lineage and directly regulates Eomes and Id2 expression. *J. Exp. Med.* **211**, 635–642 (2014).

195. W. Goh, N. D. Huntington, Regulation of Murine Natural Killer Cell Development. *Front Immunol*. **8**, 130 (2017).

196. J. W. Fathman *et al.*, Identification of the earliest natural killer cell-committed progenitor in murine bone marrow. *Blood*. **118**, 5439–5447 (2011).

197. S. Carotta, S. H. M. Pang, S. L. Nutt, G. T. Belz, Identification of the earliest NK-cell precursor in the mouse BM. *Blood*. **117**, 5449–5452 (2011).

198. Y. Yokota *et al.*, Development of peripheral lymphoid organs and natural killer cells depends on the helix-loop-helix inhibitor Id2. *Nature*. **397**, 702–706 (1999).

199. R. B. Delconte *et al.*, The Helix-Loop-Helix Protein ID2 Governs NK Cell Fate by

Tuning Their Sensitivity to Interleukin-15. *Immunity*. **44**, 103–115 (2016).

200. M. D. Boos, Y. Yokota, G. Eberl, B. L. Kee, Mature natural killer cell and lymphoid tissue–inducing cell development requires Id2-mediated suppression of E protein activity. *Journal of Experimental Medicine*. **204**, 1119–1130 (2007).

201. A. Diefenbach, M. Colonna, S. Koyasu, Development, differentiation, and diversity of innate lymphoid cells. *Immunity*. **41**, 354–365 (2014).

202. S. M. Gordon *et al.*, The transcription factors T-bet and Eomes control key checkpoints of natural killer cell maturation. *Immunity*. **36**, 55–67 (2012).

203. C. Banh, S. M. S. Miah, W. G. Kerr, L. Brossay, Mouse natural killer cell development and maturation are differentially regulated by SHIP-1. *Blood*. **120**, 4583–4590 (2012).

204. L. Chiossone *et al.*, Maturation of mouse NK cells is a 4-stage developmental program. *Blood*. **113**, 5488–5496 (2009).

205. S. Kim *et al.*, In vivo developmental stages in murine natural killer cell maturation. *Nat. Immunol.* **3**, 523–528 (2002).

206. Y. Hayakawa, M. J. Smyth, CD27 dissects mature NK cells into two subsets with distinct responsiveness and migratory capacity. *J. Immunol.* **176**, 1517–1524 (2006).

207. T. Choi, S. T. Ferris, N. Matsumoto, J. Poursine-Laurent, W. M. Yokoyama, Ly49-dependent NK cell licensing and effector inhibition involve the same interaction site on MHC ligands. *J. Immunol.* **186**, 3911–3917 (2011).

208. S. Kim *et al.*, Licensing of natural killer cells by host major histocompatibility complex class I molecules. *Nature*. **436**, 709–713 (2005).

209. N. C. Fernandez *et al.*, A subset of natural killer cells achieves self-tolerance without expressing inhibitory receptors specific for self-MHC molecules. *Blood*. **105**, 4416–4423 (2005).

210. Y. He, Z. Tian, NK cell education via nonclassical MHC and non-MHC ligands. *Cell. Mol. Immunol.* **14**, 321–330 (2017).

211. M. A. Ivarsson *et al.*, Differentiation and functional regulation of human fetal NK cells. *Journal of Clinical Investigation*. **123**, 3889–3901 (2013).

212. M. Yawata *et al.*, MHC class I–specific inhibitory receptors and their ligands structure diverse human NK-cell repertoires toward a balance of missing self-response. *Blood*. **112**, 2369–2380 (2008).

213. K.-M. Lee *et al.*, Requirement of homotypic NK-cell interactions through 2B4(CD244)/CD48 in the generation of NK effector functions. *Blood*. **107**, 3181–3188 (2006).

214. B. Tesi, H. Schlums, F. Cichocki, Y. T. Bryceson, Epigenetic Regulation of Adaptive NK Cell Diversification. *Trends Immunol.* **37**, 451–461 (2016).

215. D. K. Sojka *et al.*, Tissue-resident natural killer (NK) cells are cell lineages distinct from thymic and conventional splenic NK cells. *Elife*. **3**, e01659 (2014).

216. J. Ciriza, H. Thompson, R. Petrosian, J. O. Manilay, M. E. García-Ojeda, The

migration of hematopoietic progenitors from the fetal liver to the fetal bone marrow: Lessons learned and possible clinical applications. *Experimental Hematology*. **41**, 411–423 (2013).

217. L. Zamai *et al.*, Natural killer (NK) cell-mediated cytotoxicity: differential use of TRAIL and Fas ligand by immature and mature primary human NK cells. *Journal of Experimental Medicine*. **188**, 2375–2380 (1998).
218. H. Peng, E. Wisse, Z. Tian, Liver natural killer cells: subsets and roles in liver immunity. *Cell. Mol. Immunol.* **13**, 328–336 (2016).
219. C. Vosshenrich, M. García-Ojeda, A thymic pathway of mouse natural killer cell development characterized by expression of GATA-3 and CD127. *Nature* (2006).
220. H. Spits *et al.*, Innate lymphoid cells--a proposal for uniform nomenclature. *Nat. Rev. Immunol.* **13**, 145–149 (2013).
221. H. Spits, T. Cupedo, Innate lymphoid cells: emerging insights in development, lineage relationships, and function. *Annu. Rev. Immunol.* **30**, 647–675 (2012).
222. Y. Tanriver, A. Diefenbach, Transcription factors controlling development and function of innate lymphoid cells. *Int. Immunol.* **26**, 119–128 (2014).
223. H. Spits, J. H. Bernink, L. Lanier, NK cells and type 1 innate lymphoid cells: partners in host defense. *Nat. Immunol.* **17**, 758–764 (2016).
224. A. Marçais *et al.*, Regulation of mouse NK cell development and function by cytokines. *Front Immunol*. **4**, 450 (2013).
225. S. Dubois, J. Mariner, T. A. Waldmann, Y. Tagaya, IL-15Ralpha recycles and presents IL-15 In trans to neighboring cells. *Immunity*. **17**, 537–547 (2002).
226. E. Mortier, T. Woo, R. Advincula, S. Gozalo, A. Ma, IL-15Ralpha chaperones IL-15 to stable dendritic cell membrane complexes that activate NK cells via trans presentation. *J. Exp. Med.* **205**, 1213–1225 (2008).
227. W. Liao, J.-X. Lin, W. J. Leonard, Interleukin-2 at the crossroads of effector responses, tolerance, and immunotherapy. *Immunity*. **38**, 13–25 (2013).
228. N. Arenas-Ramirez, J. Woytschak, O. Boyman, Interleukin-2: Biology, Design and Application. *Trends Immunol.* **36**, 763–777 (2015).
229. S. E. Adunyah, B. J. Wheeler, R. S. Cooper, Evidence for the involvement of LCK and MAP kinase (ERK-1) in the signal transduction mechanism of interleukin-15. *Biochem. Biophys. Res. Commun.* **232**, 754–758 (1997).
230. X. Xu, Y. L. Sun, T. Hoey, Cooperative DNA binding and sequence-selective recognition conferred by the STAT amino-terminal domain. *Science*. **273**, 794–797 (1996).
231. J.-X. Lin *et al.*, Critical Role of STAT5 transcription factor tetramerization for cytokine responses and normal immune function. *Immunity*. **36**, 586–599 (2012).
232. S. M. Russell *et al.*, Interaction of IL-2R beta and gamma c chains with Jak1 and Jak3: implications for XSCID and XCID. *Science*. **266**, 1042–1045 (1994).
233. V. A. Boussiotis *et al.*, Prevention of T cell anergy by signaling through the

gamma c chain of the IL-2 receptor. *Science*. **266**, 1039–1042 (1994).

234. M. Laplante, D. M. Sabatini, mTOR signaling in growth control and disease. *Cell*. **149**, 274–293 (2012).

235. J. D. Powell, K. N. Pollizzi, E. B. Heikamp, M. R. Horton, Regulation of immune responses by mTOR. *Annu. Rev. Immunol.* **30**, 39–68 (2012).

236. X. Xu, L. Ye, K. Araki, R. Ahmed, mTOR, linking metabolism and immunity. *Semin. Immunol.* **24**, 429–435 (2012).

237. A.-H. Pillet, F. Bugault, J. Thèze, L. A. Chakrabarti, T. Rose, A programmed switch from IL-15- to IL-2-dependent activation in human NK cells. *J. Immunol.* **182**, 6267–6277 (2009).

238. J. A. Toomey, F. Gays, D. Foster, C. G. Brooks, Cytokine requirements for the growth and development of mouse NK cells in vitro. *J. Leukoc. Biol.* **74**, 233–242 (2003).

239. C. C. Liu, B. Perussia, J. D. Young, The emerging role of IL-15 in NK-cell development. *Immunol. Today*. **21**, 113–116 (2000).

240. A. Marçais *et al.*, The metabolic checkpoint kinase mTOR is essential for IL-15 signaling during the development and activation of NK cells. *Nat. Immunol.* **15**, 749–757 (2014).

241. A. M. Ring *et al.*, Mechanistic and structural insight into the functional dichotomy between IL-2 and IL-15. *Nat. Immunol.* **13**, 1187–1195 (2012).

242. L. Chiossone *et al.*, Molecular analysis of the methylprednisolone-mediated inhibition of NK-cell function: evidence for different susceptibility of IL-2– versus IL-15–activated NK cells. *Blood*. **109**, 3767–3775 (2007).

243. R. Sun, J. Fan, H. Wei, C. Zhang, Z. Tian, Use of interleukin-15 for preparation of adherent NK cells from human peripheral blood: comparison with interleukin-2. *J. Immunol. Methods*. **279**, 79–90 (2003).

244. F. Tamzalit *et al.*, IL-15.IL-15Rα complex shedding following trans-presentation is essential for the survival of IL-15 responding NK and T cells. *Proceedings of the National Academy of Sciences*. **111**, 8565–8570 (2014).

245. R. Moriggl *et al.*, Stat5 is required for IL-2-induced cell cycle progression of peripheral T cells. *Immunity*. **10**, 249–259 (1999).

246. K. Imada *et al.*, Stat5b is essential for natural killer cell-mediated proliferation and cytolytic activity. *Journal of Experimental Medicine*. **188**, 2067–2074 (1998).

247. P. Sathe *et al.*, Innate immunodeficiency following genetic ablation of Mcl1 in natural killer cells. *Nat Commun*. **5**, 4539 (2014).

248. N. D. Huntington *et al.*, Interleukin 15-mediated survival of natural killer cells is determined by interactions among Bim, Noxa and Mcl-1. *Nat. Immunol.* **8**, 856–863 (2007).

249. D. Gotthardt *et al.*, STAT5 Is a Key Regulator in NK Cells and Acts as a Molecular Switch from Tumor Surveillance to Tumor Promotion. *Cancer Discov*. **6**, 414–429 (2016).

250. M. Yang *et al.*, PDK1 orchestrates early NK cell development through induction of E4BP4 expression and maintenance of IL-15 responsiveness. *J. Exp. Med.* **212**, 253–265 (2015).

251. M. Yang *et al.*, NK cell development requires Tsc1-dependent negative regulation of IL-15-triggered mTORC1 activation. *Nat Commun*. **7**, 12730 (2016).

252. X. M. Ma, J. Blenis, Molecular mechanisms of mTOR-mediated translational control. *Nature Reviews Molecular Cell Biology*. **10**, 307–318 (2009).

253. T. R. Fenton, I. T. Gout, Functions and regulation of the 70kDa ribosomal S6 kinases. *Int. J. Biochem. Cell Biol.* **43**, 47–59 (2011).

254. B. Magnuson, B. Ekim, D. C. Fingar, Regulation and function of ribosomal protein S6 kinase (S6K) within mTOR signalling networks. *Biochem. J.* **441**, 1–21 (2012).

255. R. J. O. Dowling, M. Zakikhani, I. G. Fantus, M. Pollak, N. Sonenberg, Metformin inhibits mammalian target of rapamycin-dependent translation initiation in breast cancer cells. *Cancer Research*. **67**, 10804–10812 (2007).

256. N. Hay, N. Sonenberg, Upstream and downstream of mTOR. *Genes & Development*. **18**, 1926–1945 (2004).

257. M. Shimobayashi, M. N. Hall, Making new contacts: the mTOR network in metabolism and signalling crosstalk. *Nature Reviews Molecular Cell Biology*. **15**, 155–162 (2014).

258. M. O. Li, Y. Y. Wan, S. Sanjabi, A.-K. L. Robertson, R. A. Flavell, Transforming growth factor-β regulation of immune responses. *Annu. Rev. Immunol.* **24**, 99–146 (2006).

259. S. Viel *et al.*, TGF-β inhibits the activation and functions of NK cells by repressing the mTOR pathway. *Science Signaling*. **9**, ra19–ra19 (2016).

260. J. P. Marcoe *et al.*, TGF-β is responsible for NK cell immaturity during ontogeny and increased susceptibility to infection during mouse infancy. *Nat. Immunol.* **13**, 843–850 (2012).

261. C. Li *et al.*, JNK MAP kinase activation is required for MTOC and granule polarization in NKG2D-mediated NK cell cytotoxicity. *Proceedings of the National Academy of Sciences*. **105**, 3017–3022 (2008).

262. X. Chen, P. P. Trivedi, B. Ge, K. Krzewski, J. L. Strominger, Many NK cell receptors activate ERK2 and JNK1 to trigger microtubule organizing center and granule polarization and cytotoxicity. *Proc. Natl. Acad. Sci. U.S.A.* **104**, 6329–6334 (2007).

263. D. Urlaub, R. Bhat, B. Messmer, C. Watzl, Co-Activation of Cultured Human Natural Killer Cells: Enhanced Function and Decreased Inhibition. *J. Toxicol. Environ. Health Part A*. **79**, 1078–1084 (2016).

264. R. P. Donnelly *et al.*, mTORC1-dependent metabolic reprogramming is a prerequisite for NK cell effector function. *J. Immunol.* **193**, 4477–4484 (2014).

265. M. P. Keppel, N. Saucier, A. Y. Mah, T. P. Vogel, M. A. Cooper, Activation-specific metabolic requirements for NK Cell IFN-γ production. *J. Immunol.* **194**, 1954–1962 (2015).

266. N. Nandagopal, A. K. Ali, A. K. Komal, S.-H. Lee, The Critical Role of IL-15-PI3K-mTOR Pathway in Natural Killer Cell Effector Functions. *Front Immunol*. **5**, 187 (2014).

267. A. M. Jamieson *et al.*, The Role of the NKG2D Immunoreceptor in Immune Cell Activation and Natural Killing. *Immunity*. **17**, 19–29 (2002).

268. P. Spear, M.-R. Wu, M.-L. Sentman, C. L. Sentman, NKG2D ligands as therapeutic targets. *Cancer Immun.* **13**, 8 (2013).

269. S. Butcher, K. L. Arney, G. P. Cook, MAFA-L, an ITIM-containing receptor encoded by the human NK cell gene complex and expressed by basophils and NK cells. *Eur J Immunol*. **28**, 3755–3762 (1998).

270. M. Ito *et al.*, Killer cell lectin-like receptor G1 binds three members of the classical cadherin family to inhibit NK cell cytotoxicity. *Journal of Experimental Medicine*. **203**, 289–295 (2006).

271. S. H. Robbins *et al.*, Cutting edge: inhibitory functions of the killer cell lectin-like receptor G1 molecule during the activation of mouse NK cells. *J. Immunol.* **168**, 2585–2589 (2002).

272. M. E. McNerney, K.-M. Lee, V. Kumar, 2B4 (CD244) is a non-MHC binding receptor with multiple functions on natural killer cells and CD8+ T cells. *Mol. Immunol.* **42**, 489–494 (2005).

273. S. G. Tangye, H. Cherwinski, L. L. Lanier, J. H. Phillips, 2B4-mediated activation of human natural killer cells. *Mol. Immunol.* **37**, 493–501 (2000).

274. S. Parolini *et al.*, X-linked lymphoproliferative disease. 2B4 molecules displaying inhibitory rather than activating function are responsible for the inability of natural killer cells to kill Epstein-Barr virus-infected cells. *Journal of Experimental Medicine*. **192**, 337–346 (2000).

275. H. Nakajima *et al.*, Patients with X-linked lymphoproliferative disease have a defect in 2B4 receptor-mediated NK cell cytotoxicity. *Eur J Immunol*. **30**, 3309–3318 (2000).

276. U. J. E. Seidel, P. Schlegel, P. Lang, Natural Killer Cell Mediated Antibody-Dependent Cellular Cytotoxicity in Tumor Immunotherapy with Therapeutic Antibodies. *Front Immunol*. **4** (2013), doi:10.3389/fimmu.2013.00076.

277. I. Anegón, M. C. Cuturi, G. Trinchieri, B. Perussia, Interaction of Fc receptor (CD16) ligands induces transcription of interleukin 2 receptor (CD25) and lymphokine genes and expression of their products in human natural killer cells. *Journal of Experimental Medicine*. **167**, 452–472 (1988).

278. T. E. O'Sullivan, J. C. Sun, L. L. Lanier, Natural Killer Cell Memory. *Immunity*. **43**, 634–645 (2015).

279. S. Paust, U. H. von Andrian, Natural killer cell memory. *Nat. Immunol.* **12**, 500–508 (2011).

280. A. Cerwenka, L. L. Lanier, Natural killer cell memory in infection, inflammation and cancer. *Nat. Rev. Immunol.* **16**, 112–123 (2016).

281. M. G. Netea *et al.*, Trained immunity: A program of innate immune memory in health and disease. *Science*. **352**, aaf1098 (2016).

282. J. G. O'Leary, M. Goodarzi, D. L. Drayton, U. H. von Andrian, T cell- and B cell-independent adaptive immunity mediated by natural killer cells. *Nat. Immunol.* **7**, 507–516 (2006).

283. J. G. van den Boorn *et al.*, Inflammasome-Dependent Induction of Adaptive NK Cell Memory. *Immunity*. **44**, 1406–1421 (2016).

284. J. C. Sun, J. N. Beilke, L. L. Lanier, Adaptive immune features of natural killer cells. *Nature*. **457**, 557–561 (2009).

285. R. K. Reeves *et al.*, Antigen-specific NK cell memory in rhesus macaques. *Nat. Immunol.* **16**, 927–932 (2015).

286. S. Lopez-Vergès *et al.*, Expansion of a unique CD57^{+}NKG2Chi natural killer cell subset during acute human cytomegalovirus infection. *Proceedings of the National Academy of Sciences*. **108**, 14725–14732 (2011).

287. M. Della Chiesa *et al.*, Phenotypic and functional heterogeneity of human NK cells developing after umbilical cord blood transplantation: a role for human cytomegalovirus? *Blood*. **119**, 399–410 (2012).

288. B. Foley *et al.*, Human cytomegalovirus (CMV)-induced memory-like NKG2C(+) NK cells are transplantable and expand in vivo in response to recipient CMV antigen. *J. Immunol.* **189**, 5082–5088 (2012).

289. B. Foley *et al.*, Cytomegalovirus reactivation after allogeneic transplantation promotes a lasting increase in educated NKG2C+ natural killer cells with potent function. *Blood*. **119**, 2665–2674 (2012).

290. M. Gumá *et al.*, Human cytomegalovirus infection is associated with increased proportions of NK cells that express the CD94/NKG2C receptor in aviremic HIV-1-positive patients. *J. Infect. Dis.* **194**, 38–41 (2006).

291. L. L. Lanier, Up on the tightrope: natural killer cell activation and inhibition. *Nat. Immunol.* **9**, 495–502 (2008).

292. I. Hwang *et al.*, Identification of human NK cells that are deficient for signaling adaptor FcRγ and specialized for antibody-dependent immune functions. *Int. Immunol.* **24**, 793–802 (2012).

293. J. Lee *et al.*, Epigenetic modification and antibody-dependent expansion of memory-like NK cells in human cytomegalovirus-infected individuals. *Immunity*. **42**, 431–442 (2015).

294. H. Schlums *et al.*, Cytomegalovirus infection drives adaptive epigenetic diversification of NK cells with altered signaling and effector function. *Immunity*. **42**, 443–456 (2015).

295. Z. Wu *et al.*, Human cytomegalovirus-induced NKG2C(hi) CD57(hi) natural killer cells are effectors dependent on humoral antiviral immunity. *J. Virol.* **87**, 7717–

7725 (2013).

296. R. Romee *et al.*, Cytokine activation induces human memory-like NK cells. *Blood*. **120**, 4751–4760 (2012).

297. M. A. Cooper *et al.*, Cytokine-induced memory-like natural killer cells. *Proceedings of the National Academy of Sciences*. **106**, 1915–1919 (2009).

298. J. W. Leong *et al.*, Preactivation with IL-12, IL-15, and IL-18 induces CD25 and a functional high-affinity IL-2 receptor on human cytokine-induced memory-like natural killer cells. *Biol. Blood Marrow Transplant.* **20**, 463–473 (2014).

299. R. Alnabhan, A. Madrigal, A. Saudemont, Differential activation of cord blood and peripheral blood natural killer cells by cytokines. *Cytotherapy*. **17**, 73–85 (2015).

300. J. Ni, M. Miller, A. Stojanovic, N. Garbi, A. Cerwenka, Sustained effector function of IL-12/15/18-preactivated NK cells against established tumors. *J. Exp. Med.* **209**, 2351–2365 (2012).

301. M. P. Keppel, L. Yang, M. A. Cooper, Murine NK cell intrinsic cytokine-induced memory-like responses are maintained following homeostatic proliferation. *J. Immunol.* **190**, 4754–4762 (2013).

302. M. Luetke-Eversloh *et al.*, Human cytomegalovirus drives epigenetic imprinting of the IFNG locus in NKG2Chi natural killer cells. *PLoS Pathog*. **10**, e1004441 (2014).

303. A. Balasubramani, R. Mukasa, R. D. Hatton, C. T. Weaver, Regulation of the Ifng locus in the context of T-lineage specification and plasticity. *Immunol. Rev.* **238**, 216–232 (2010).

304. F. A. Ran *et al.*, Genome engineering using the CRISPR-Cas9 system. *Nat Protoc*. **8**, 2281–2308 (2013).

305. D. Ge *et al.*, Genetic variation in IL28B predicts hepatitis C treatment-induced viral clearance. *Nature*. **461**, 399–401 (2009).

306. V. Suppiah *et al.*, IL28B is associated with response to chronic hepatitis C interferon-alpha and ribavirin therapy. *Nat. Genet.* **41**, 1100–1104 (2009).

307. Y. Tanaka *et al.*, Genome-wide association of IL28B with response to pegylated interferon-alpha and ribavirin therapy for chronic hepatitis C. *Nat. Genet.* **41**, 1105–1109 (2009).

308. M. J. Ciancanelli *et al.*, Infectious disease. Life-threatening influenza and impaired interferon amplification in human IRF7 deficiency. *Science*. **348**, 448–453 (2015).

309. S. Hardy, V. Legagneux, Y. Audic, L. Paillard, Reverse genetics in eukaryotes. *Biol. Cell*. **102**, 561–580 (2010).

310. G. Caignard *et al.*, Mouse ENU Mutagenesis to Understand Immunity to Infection: Methods, Selected Examples, and Perspectives. *Genes (Basel)*. **5**, 887–925 (2014).

311. T. Gaj, C. A. Gersbach, C. F. Barbas, ZFN, TALEN, and CRISPR/Cas-based

methods for genome engineering. *Trends Biotechnol.* **31**, 397–405 (2013).

312. I. Barbaric, G. Miller, T. N. Dear, Appearances can be deceiving: phenotypes of knockout mice. *Briefings in functional genomics & proteomics*. **6**, 91–103 (2007).

313. E. M. Y. Moresco, X. Li, B. Beutler, Going forward with genetics: recent technological advances and forward genetics in mice. *The American Journal of Pathology*. **182**, 1462–1473 (2013).

314. S. M. Vidal, D. Malo, J. F. Marquis, P. Gros, Forward genetic dissection of immunity to infection in the mouse. *Annu. Rev. Immunol.* **26**, 81–132 (2008).

315. P. Moussa, J. Marton, S. M. Vidal, N. Fodil-Cornu, Genetic dissection of NK cell responses. *Front Immunol*. **3**, 425 (2012).

316. M.-P. Desrosiers *et al.*, Epistasis between mouse Klra and major histocompatibility complex class I loci is associated with a new mechanism of natural killer cell-mediated innate resistance to cytomegalovirus infection. *Nat. Genet.* **37**, 593–599 (2005).

317. M. D. Stadnisky, A. Manichaikul, A. G. Lundgren, M. G. Brown, NK gene complex and chromosome 19 loci enhance MHC resistance to murine cytomegalovirus infection. *Immunogenetics*. **61**, 755–764 (2009).

318. G. Burgio *et al.*, Interspecific recombinant congenic strains between C57BL/6 and mice of the Mus spretus species: a powerful tool to dissect genetic control of complex traits. *Genetics*. **177**, 2321–2333 (2007).

319. G. A. Boivin *et al.*, Mapping of clinical and expression quantitative trait loci in a sex-dependent effect of host susceptibility to mouse-adapted influenza H3N2/HK/1/68. *J. Immunol.* **188**, 3949–3960 (2012).

320. S. A. Wiltshire, J. Marton, G. A. Leiva-Torres, S. M. Vidal, Mapping of a quantitative trait locus controlling susceptibility to Coxsackievirus B3-induced viral hepatitis. *Genes Immun*. **16**, 261–267 (2015).

321. W. L. Russell *et al.*, Specific-locus test shows ethylnitrosourea to be the most potent mutagen in the mouse. *Proc. Natl. Acad. Sci. U.S.A.* **76**, 5818–5819 (1979).

322. J. K. Noveroske, J. S. Weber, M. J. Justice, The mutagenic action of N-ethyl-N-nitrosourea in the mouse. *Mamm. Genome*. **11**, 478–483 (2000).

323. S. P. Cordes, N-ethyl-N-nitrosourea mutagenesis: boarding the mouse mutant express. *Microbiol. Mol. Biol. Rev.* **69**, 426–439 (2005).

324. R. Balling, ENU mutagenesis: analyzing gene function in mice. *Annu Rev Genomics Hum Genet*. **2**, 463–492 (2001).

325. M. J. Justice, Capitalizing on large-scale mouse mutagenesis screens. *Nat. Rev. Genet.* **1**, 109–115 (2000).

326. J. S. Weber, A. Salinger, M. J. Justice, Optimal N-ethyl-N-nitrosourea (ENU) doses for inbred mouse strains. *Genesis*. **26**, 230–233 (2000).

327. B. Beutler, X. Du, Y. Xia, Precis on forward genetics in mice. *Nat. Immunol.* **8**, 659–664 (2007).

328. B. Beutler, Innate immunity and the new forward genetics. *Best Pract Res Clin Haematol*. **29**, 379–387 (2016).

329. M. J. Justice, J. K. Noveroske, J. S. Weber, B. Zheng, A. Bradley, Mouse ENU mutagenesis. *Human Molecular Genetics*. **8**, 1955–1963 (1999).

330. B. Beutler, Mutagenetix (TM). *https://mutagenetix.utsouthwestern.edu*.

331. T. Wang *et al.*, Real-time resolution of point mutations that cause phenovariance in mice. *Proceedings of the National Academy of Sciences*. **112**, E440–9 (2015).

332. S. E. Bongfen *et al.*, An N-ethyl-N-nitrosourea (ENU)-induced dominant negative mutation in the JAK3 kinase protects against cerebral malaria. *PLoS ONE*. **7**, e31012 (2012).

333. J. M. Kennedy *et al.*, CCDC88B is a novel regulator of maturation and effector functions of T cells during pathological inflammation. *J. Exp. Med.* **211**, 2519–2535 (2014).

334. S. Torre *et al.*, THEMIS is required for pathogenesis of cerebral malaria and protection against pulmonary tuberculosis. *Infect. Immun.* **83**, 759–768 (2015).

335. S. Torre *et al.*, USP15 regulates type I interferon response and is required for pathogenesis of neuroinflammation. *Nat. Immunol.* **18**, 54–63 (2017).

336. K. E. Yuki *et al.*, Suppression of hepcidin expression and iron overload mediate Salmonella susceptibility in ankyrin 1 ENU-induced mutant. *PLoS ONE*. **8**, e55331 (2013).

337. M. M. Eva *et al.*, Altered IFN-γ-mediated immunity and transcriptional expression patterns in N-Ethyl-N-nitrosourea-induced STAT4 mutants confer susceptibility to acute typhoid-like disease. *J. Immunol.* **192**, 259–270 (2014).

338. M. Mancini *et al.*, (Quebec City, 2017).

339. A. McGregor, K. Y. Choi, Cytomegalovirus antivirals and development of improved animal models. *Expert opinion on drug metabolism & toxicology*. **7**, 1245–1265 (2011).

340. O. Kortekangas-Savolainen, E. Orhanen, T. Puodinketo, T. Vuorinen, Epidemiology of genital herpes simplex virus type 1 and 2 infections in southwestern Finland during a 10-year period (2003-2012). *Sexually transmitted diseases*. **41**, 268–271 (2014).

341. A. J. Frodsham, Genetics of infectious diseases. *Human Molecular Genetics*. **13**, R187–R194 (2004).

342. W. P. Halford, J. L. Maender, B. M. Gebhardt, Re-evaluating the role of natural killer cells in innate resistance to herpes simplex virus type 1. *Virol. J.* **2**, 56 (2005).

343. K. Honda *et al.*, IRF-7 is the master regulator of type-I interferon-dependent immune responses. *Nature*. **434**, 772–777 (2005).

344. G. K. Lima *et al.*, Toll-like receptor (TLR) 2 and TLR9 expressed in trigeminal ganglia are critical to viral control during herpes simplex virus 1 infection. *The American Journal of Pathology*. **177**, 2433–2445 (2010).

345. L. F. Kastrukoff, A. S. Lau, F. Takei, F. R. Carbone, A. A. Scalzo, A NK complex-linked locus restricts the spread of herpes simplex virus type 1 in the brains of C57BL/6 mice. *Immunol. Cell Biol.* **93**, 877–884 (2015).

346. K. Norose, A. Yano, X.-M. Zhang, E. Blankenhorn, E. Heber-Katz, Mapping of genes involved in murine herpes simplex virus keratitis: identification of genes and their modifiers. *J. Virol.* **76**, 3502–3510 (2002).

347. R. A. Pereira, A. Scalzo, A. Simmons, Cutting edge: a NK complex-linked locus governs acute versus latent herpes simplex virus infection of neurons. *J. Immunol.* **166**, 5869–5873 (2001).

348. E. M. Mace *et al.*, Mutations in GATA2 cause human NK cell deficiency with specific loss of the CD56(bright) subset. *Blood*. **121**, 2669–2677 (2013).

349. D. Vinh, S. Patel, G. Uzel, V. Anderson, A. Freeman, Autosomal dominant and sporadic monocytopenia with susceptibility to mycobacteria, fungi, papillomaviruses, and myelodysplasia. *Blood* (2010).

350. K. A. Ganapathi *et al.*, GATA2 deficiency-associated bone marrow disorder differs from idiopathic aplastic anemia. *Blood* (2014), doi:10.1182/blood-2014-06-580340.

351. L. Gineau, C. Cognet, N. Kara, F. Lach, Partial MCM4 deficiency in patients with growth retardation, adrenal insufficiency, and natural killer cell deficiency. *The Journal of …* (2012).

352. K. A. Risma, R. W. Frayer, A. H. Filipovich, J. Sumegi, Aberrant maturation of mutant perforin underlies the clinical diversity of hemophagocytic lymphohistiocytosis. *Journal of Clinical Investigation*. **116**, 182–192 (2006).

353. A. Kielczewska *et al.*, Ly49P recognition of cytomegalovirus-infected cells expressing H2-Dk and CMV-encoded m04 correlates with the NK cell antiviral response. *J. Exp. Med.* **206**, 515–523 (2009).

354. X. Xie, M. D. Stadnisky, M. G. Brown, MHC class I Dk locus and Ly49G2+ NK cells confer H-2k resistance to murine cytomegalovirus. *J. Immunol.* **182**, 7163–7171 (2009).

355. M. Pyzik *et al.*, Distinct MHC class I-dependent NK cell-activating receptors control cytomegalovirus infection in different mouse strains. *J. Exp. Med.* **208**, 1105–1117 (2011).

356. A. P. Davis, M. J. Justice, Mouse alleles: if you“ve seen one, you haven”t seen them all. *Trends in Genetics*. **14**, 438–441 (1998).

357. E. M. Y. Moresco, B. Beutler, Resisting viral infection: the gene by gene approach. *Curr Opin Virol*. **1**, 513–518 (2011).

358. E. Richer *et al.*, N-ethyl-N-nitrosourea-induced mutation in ubiquitin-specific peptidase 18 causes hyperactivation of IFN-αß signaling and suppresses STAT4-induced IFN-γ production, resulting in increased susceptibility to Salmonella typhimurium. *J. Immunol.* **185**, 3593–3601 (2010).

359. H. Yang *et al.*, A customized and versatile high-density genotyping array for the mouse. *Nat. Methods*. **6**, 663–666 (2009).

360. Y. Xia *et al.*, Bulk segregation mapping of mutations in closely related strains of mice. *Genetics*. **186**, 1139–1146 (2010).

361. M. Visser, M. Kayser, F. Grosveld, R.-J. Palstra, Genetic variation in regulatory DNA elements: the case of OCA2 transcriptional regulation. *Pigment Cell Melanoma Res*. **27**, 169–177 (2014).

362. E. M. Rinchik *et al.*, A gene for the mouse pink-eyed dilution locus and for human type II oculocutaneous albinism. *Nature*. **361**, 72–76 (1993).

363. S. Jordan *et al.*, Natural Killer Cells Are Required for Extramedullary Hematopoiesis following Murine Cytomegalovirus Infection. *Cell Host & Microbe*. **13**, 535–545 (2013).

364. J. A. Beck *et al.*, Genealogies of mouse inbred strains. *Nat. Genet.* **24**, 23–25 (2000).

365. S. Torre *et al.*, Susceptibility to lethal cerebral malaria is regulated by epistatic interaction between chromosome 4 (Berr6) and chromosome 1 (Berr7) loci in mice. *Genes Immun*. **14**, 249–257 (2013).

366. R. M. J. Deacon, C. L. Thomas, J. N. P. Rawlins, B. J. Morley, A comparison of the behavior of C57BL/6 and C57BL/10 mice. *Behav. Brain Res.* **179**, 239–247 (2007).

367. D. M. Lipoff *et al.*, Neocortical molecular layer heterotopia in substrains of C57BL/6 and C57BL/10 mice. *Brain Res.* **1391**, 36–43 (2011).

368. S. J. Rozzo, T. J. Vyse, K. Menze, S. Izui, B. L. Kotzin, Enhanced susceptibility to lupus contributed from the nonautoimmune C57BL/10, but not C57BL/6, genome. *J. Immunol.* **164**, 5515–5521 (2000).

369. K. R. Takahasi, Y. Sakuraba, Y. Gondo, Mutational pattern and frequency of induced nucleotide changes in mouse ENU mutagenesis. *BMC Mol. Biol.* **8**, 52 (2007).

370. N. Nguyen *et al.*, Random mutagenesis of the mouse genome: a strategy for discovering gene function and the molecular basis of disease. *Am. J. Physiol. Gastrointest. Liver Physiol.* **300**, G1–11 (2011).

371. C. N. Arnold *et al.*, ENU-induced phenovariance in mice: inferences from 587 mutations. *BMC Res Notes*. **5**, 577 (2012).

372. M. F. Lyon *et al.*, Genetic and molecular analysis of recessive alleles at the pink-eyed dilution (p) locus of the mouse. *Proc. Natl. Acad. Sci. U.S.A.* **89**, 6968–6972 (1992).

373. T. Hirobe, How are proliferation and differentiation of melanocytes regulated? *Pigment Cell Melanoma Res*. **24**, 462–478 (2011).

374. S. Rosemblat *et al.*, Identification of a melanosomal membrane protein encoded by the pink-eyed dilution (type II oculocutaneous albinism) gene. *Proc. Natl. Acad. Sci. U.S.A.* **91**, 12071–12075 (1994).

375. N. Puri, J. M. Gardner, M. H. Brilliant, Aberrant pH of melanosomes in pink-eyed dilution (p) mutant melanocytes. *J. Invest. Dermatol.* **115**, 607–613 (2000).

376. R. A. King, V. J. Hearing, D. J. Creel, W. S. Oetting, in *The Online Metabolic and Molecular Bases of Inherited Disease*, A. L. Beaudet et al., Eds. (The McGraw-Hill Companies, Inc., New York, NY, 2014).

377. A. R. French *et al.*, Escape of mutant double-stranded DNA virus from innate immune control. *Immunity*. **20**, 747–756 (2004).

378. B. Beutler *et al.*, Genetic analysis of innate resistance to mouse cytomegalovirus (MCMV). *Briefings in functional genomics & proteomics*. **4**, 203–213 (2005).

379. K. Crozat *et al.*, Analysis of the MCMV resistome by ENU mutagenesis. *Mamm. Genome*. **17**, 398–406 (2006).

380. G. A. Leiva-Torres, P.-A. Rochette, A. Pearson, Differential importance of highly conserved residues in UL24 for herpes simplex virus 1 replication in vivo and reactivation. *J. Gen. Virol.* **91**, 1109–1116 (2010).

381. A. Fortin *et al.*, Recombinant congenic strains derived from A/J and C57BL/6J: a tool for genetic dissection of complex traits. *Genomics*. **74**, 21–35 (2001).

382. M. Audry *et al.*, NEMO is a key component of NF-κB- and IRF-3-dependent TLR3-mediated immunity to herpes simplex virus. *J. Allergy Clin. Immunol.* **128**, 610–7.e1–4 (2011).

383. P. C. Reading, P. G. Whitney, D. P. Barr, M. J. Smyth, A. G. Brooks, NK cells contribute to the early clearance of HSV-1 from the lung but cannot control replication in the central nervous system following intranasal infection. *Eur J Immunol*. **36**, 897–905 (2006).

384. K. D. Geiger *et al.*, Interferon-gamma protects against herpes simplex virus type 1-mediated neuronal death. *Virology*. **238**, 189–197 (1997).

385. C. A. Biron, K. S. Byron, J. L. Sullivan, Severe herpesvirus infections in an adolescent without natural killer cells. *N. Engl. J. Med.* **320**, 1731–1735 (1989).

386. V. C. Lam, L. L. Lanier, NK cells in host responses to viral infections. *Curr. Opin. Immunol.* **44**, 43–51 (2017).

387. G. W. Herget *et al.*, Generalized herpes simplex virus infection in an immunocompromised patient--report of a case and review of the literature. *Pathol. Res. Pract.* **201**, 123–129 (2005).

388. G. G. Miller, J. S. Dummer, Herpes simplex and varicella zoster viruses: forgotten but not gone. *Am. J. Transplant.* **7**, 741–747 (2007).

389. M. Ramaswamy, A. M. Geretti, Interactions and management issues in HSV and HIV coinfection. *Expert Rev Anti Infect Ther*. **5**, 231–243 (2007).

390. A. J. St Leger, R. L. Hendricks, CD8+ T cells patrol HSV-1-infected trigeminal ganglia and prevent viral reactivation. *J. Neurovirol.* **17**, 528–534 (2011).

391. T. Gebhardt *et al.*, Different patterns of peripheral migration by memory CD4+ and CD8+ T cells. *Nature*. **477**, 216–219 (2011).

392. T. Hoey, U. Schindler, STAT structure and function in signaling. *Curr. Opin. Genet. Dev.* **8**, 582–587 (1998).

393. A. V. Villarino, Y. Kanno, J. J. O'Shea, Mechanisms and consequences of Jak-

STAT signaling in the immune system. *Nat. Immunol.* **18**, 374–384 (2017).

394. P. Tripathi *et al.*, STAT5 is critical to maintain effector CD8+ T cell responses. *J. Immunol.* **185**, 2116–2124 (2010).
395. X. Chen *et al.*, A reinterpretation of the dimerization interface of the N-terminal domains of STATs. *Protein Sci.* **12**, 361–365 (2003).
396. X. Mao *et al.*, Structural bases of unphosphorylated STAT1 association and receptor binding. *Molecular Cell*. **17**, 761–771 (2005).
397. D. Neculai *et al.*, Structure of the unphosphorylated STAT5a dimer. *J. Biol. Chem.* **280**, 40782–40787 (2005).
398. X. Liu, G. Robinson, K. Wagner, L. Garrett, Stat5a is mandatory for adult mammary gland development and lactogenesis. *Genes & …* (1997).
399. G. B. Udy *et al.*, Requirement of STAT5b for sexual dimorphism of body growth rates and liver gene expression. *Proc. Natl. Acad. Sci. U.S.A.* **94**, 7239–7244 (1997).
400. Y. Cui *et al.*, Inactivation of Stat5 in mouse mammary epithelium during pregnancy reveals distinct functions in cell proliferation, survival, and differentiation. *Molecular and Cellular Biology*. **24**, 8037–8047 (2004).
401. S. Y. Park *et al.*, Developmental defects of lymphoid cells in Jak3 kinase-deficient mice. *Immunity*. **3**, 771–782 (1995).
402. Z. Yao *et al.*, Stat5a/b are essential for normal lymphoid development and differentiation. *Proc. Natl. Acad. Sci. U.S.A.* **103**, 1000–1005 (2006).
403. L. M. Heltemes-Harris, M. J. L. Willette, K. B. Vang, M. A. Farrar, The role of STAT5 in the development, function, and transformation of B and T lymphocytes. *Ann. N. Y. Acad. Sci.* **1217**, 18–31 (2011).
404. P. Kavsak *et al.*, Smad7 binds to Smurf2 to form an E3 ubiquitin ligase that targets the TGF beta receptor for degradation. *Molecular Cell*. **6**, 1365–1375 (2000).
405. S. Wiesner *et al.*, Autoinhibition of the HECT-Type Ubiquitin Ligase Smurf2 through Its C2 Domain. *Cell*. **130**, 651–662 (2007).
406. H. Nakajima *et al.*, An indirect effect of Stat5a in IL-2-induced proliferation: a critical role for Stat5a in IL-2-mediated IL-2 receptor alpha chain induction. *Immunity*. **7**, 691–701 (1997).
407. R. A. Kirken *et al.*, Activation of JAK3, but not JAK1, is critical for IL-2-induced proliferation and STAT5 recruitment by a COOH-terminal region of the IL-2 receptor beta-chain. *Cytokine*. **7**, 689–700 (1995).
408. L. Abel *et al.*, Age-Dependent Mendelian Predisposition to Herpes Simplex Virus Type 1 Encephalitis in Childhood. *The Journal of Pediatrics*. **157**, 623–629.e1 (2010).
409. M. M. Simon *et al.*, Current strategies for mutation detection in phenotype-driven screens utilising next generation sequencing. *Mamm. Genome*. **26**, 486–500 (2015).

410. P. Fortes, K. V. Morris, Long noncoding RNAs in viral infections. *Virus Res.* **212**, 1–11 (2016).

411. B. Hu *et al.*, Functional prediction of differentially expressed lncRNAs in HSV-1 infected human foreskin fibroblasts. *Virol. J.* **13**, 137 (2016).

412. E. Yang, M. A. Henriksen, O. Schaefer, N. Zakharova, J. E. Darnell, Dissociation time from DNA determines transcriptional function in a STAT1 linker mutant. *J. Biol. Chem.* **277**, 13455–13462 (2002).

413. S.-H. Tan, M. T. Nevalainen, Signal transducer and activator of transcription 5A/B in prostate and breast cancers. *Endocr. Relat. Cancer*. **15**, 367–390 (2008).

414. A. T. Namanja, J. Wang, R. Buettner, L. Colson, Y. Chen, Allosteric Communication across STAT3 Domains Associated with STAT3 Function and Disease-Causing Mutation. *J. Mol. Biol.* **428**, 579–589 (2016).

415. W. J. Leonard, J. J. O'Shea, Jaks and STATs: biological implications. *Annu. Rev. Immunol.* **16**, 293–322 (1998).

416. R. B. Delconte *et al.*, CIS is a potent checkpoint in NK cell-mediated tumor immunity. *Nat. Immunol.* **17**, 816–824 (2016).

417. B. J. Schmiedel *et al.*, Generation and preclinical characterization of a Fc-optimized GITR-Ig fusion protein for induction of NK cell reactivity against leukemia. *Mol. Ther.* **21**, 877–886 (2013).

418. B. Liu *et al.*, Glucocorticoid-induced tumor necrosis factor receptor negatively regulates activation of human primary natural killer (NK) cells by blocking proliferative signals and increasing NK cell apoptosis. *J. Biol. Chem.* **283**, 8202–8210 (2008).

419. C. Buechele *et al.*, Glucocorticoid-induced TNFR-related protein (GITR) ligand modulates cytokine release and NK cell reactivity in chronic lymphocytic leukemia (CLL). *Leukemia*. **26**, 991–1000 (2012).

420. P. B. Essers, T. C. Pereboom, Y. J. Goos, J. T. Paridaen, A. W. MacInnes, A comparative study of nucleostemin family members in zebrafish reveals specific roles in ribosome biogenesis. *Developmental Biology*. **385**, 304–315 (2014).

421. C. H. Tay, R. M. Welsh, Distinct organ-dependent mechanisms for the control of murine cytomegalovirus infection by natural killer cells. *J. Virol.* **71**, 267–275 (1997).

422. A. M. Bolger, M. Lohse, B. Usadel, Trimmomatic: a flexible trimmer for Illumina sequence data. *Bioinformatics*. **30**, 2114–2120 (2014).

423. H. Li, R. Durbin, Fast and accurate long-read alignment with Burrows-Wheeler transform. *Bioinformatics*. **26**, 589–595 (2010).

424. A. McKenna *et al.*, The Genome Analysis Toolkit: a MapReduce framework for analyzing next-generation DNA sequencing data. *Genome Res.* **20**, 1297–1303 (2010).

425. P. Cingolani *et al.*, A program for annotating and predicting the effects of single

nucleotide polymorphisms, SnpEff: SNPs in the genome of Drosophila melanogaster strain w1118; iso-2; iso-3. *Fly (Austin)*. **6**, 80–92 (2012).

426. T. Nabekura, J.-P. Girard, L. L. Lanier, IL-33 receptor ST2 amplifies the expansion of NK cells and enhances host defense during mouse cytomegalovirus infection. *J. Immunol.* **194**, 5948–5952 (2015).

427. T. D. Holmes *et al.*, Licensed human natural killer cells aid dendritic cell maturation via TNFSF14/LIGHT. *Proceedings of the National Academy of Sciences*. **111**, E5688–96 (2014).

428. S. H. Lee, K. S. Kim, N. Fodil-Cornu, S. M. Vidal, C. A. Biron, Activating receptors promote NK cell expansion for maintenance, IL-10 production, and CD8 T cell regulation during viral infection. *J. Exp. Med.* **206**, 2235–2251 (2009).

429. K. Pallmer, A. Oxenius, Recognition and Regulation of T Cells by NK Cells. *Front Immunol*. **7**, 251 (2016).

430. J. G. Giri *et al.*, Utilization of the beta and gamma chains of the IL-2 receptor by the novel cytokine IL-15. *EMBO J*. **13**, 2822–2830 (1994).

431. C. Henney, K. Kuribayashi, D. Kern, S. Gillis, Interleukin-2 augments natural killer cell activity. *Nature* (1981).

432. E. Mrozek, P. Anderson, M. A. Caligiuri, Role of interleukin-15 in the development of human CD56+ natural killer cells from CD34+ hematopoietic progenitor cells. *Blood*. **87**, 2632–2640 (1996).

433. X. Cao *et al.*, Defective lymphoid development in mice lacking expression of the common cytokine receptor gamma chain. *Immunity*. **2**, 223–238 (1995).

434. R. E. Dickinson *et al.*, Exome sequencing identifies GATA-2 mutation as the cause of dendritic cell, monocyte, B and NK lymphoid deficiency. *Blood*. **118**, 2656–2658 (2011).

435. J. Cottineau *et al.*, Inherited GINS1 deficiency underlies growth retardation along with neutropenia and NK cell deficiency. *J. Clin. Invest.* **127**, 1991–2006 (2017).

436. C. R. Hughes *et al.*, MCM4 mutation causes adrenal failure, short stature, and natural killer cell deficiency in humans. *J. Clin. Invest.* **122**, 814–820 (2012).

437. K. Crozat *et al.*, Impact of β2 integrin deficiency on mouse natural killer cell development and function. *Blood*. **117**, 2874–2882 (2011).

438. K. Crozat *et al.*, Jinx, an MCMV susceptibility phenotype caused by disruption of Unc13d: a mouse model of type 3 familial hemophagocytic lymphohistiocytosis. *Journal of Experimental Medicine*. **204**, 853–863 (2007).

439. E. G. Reynaud *et al.*, Human Lsg1 defines a family of essential GTPases that correlates with the evolution of compartmentalization. *BMC Biol.* **3**, 21 (2005).

440. R. Y. L. Tsai, A nucleolar mechanism controlling cell proliferation in stem cells and cancer cells. *Genes & Development*. **16**, 2991–3003 (2002).

441. J. T. M. L. Paridaen *et al.*, The nucleolar GTP-binding proteins Gnl2 and nucleostemin are required for retinal neurogenesis in developing zebrafish. *Developmental Biology*. **355**, 286–301 (2011).

442. J. Qu, J. M. Bishop, Nucleostemin maintains self-renewal of embryonic stem cells and promotes reprogramming of somatic cells to pluripotency. *J. Cell Biol.* **197**, 731–745 (2012).

443. D. Achila, M. Gulati, N. Jain, R. A. Britton, Biochemical characterization of ribosome assembly GTPase RbgA in Bacillus subtilis. *J. Biol. Chem.* **287**, 8417–8423 (2012).

444. C. Saveanu *et al.*, Nog2p, a putative GTPase associated with pre-60S subunits and required for late 60S maturation steps. *EMBO J.* **20**, 6475–6484 (2001).

445. L. Meng, J. K. Hsu, R. Y. L. Tsai, GNL3L depletion destabilizes MDM2 and induces p53-dependent G2/M arrest. *Oncogene*. **30**, 1716–1726 (2011).

446. N. Boddapati, K. Anbarasu, R. Suryaraja, A. V. Tendulkar, S. Mahalingam, Subcellular distribution of the human putative nucleolar GTPase GNL1 is regulated by a novel arginine/lysine-rich domain and a GTP binding domain in a cell cycle-dependent manner. *J. Mol. Biol.* **416**, 346–366 (2012).

447. C. Beekman *et al.*, Evolutionarily Conserved Role of Nucleostemin: Controlling Proliferation of Stem/Progenitor Cells during Early Vertebrate Development. *Molecular and Cellular Biology*. **26**, 9291–9301 (2006).

448. D. Lara-Astiaso *et al.*, Immunogenetics. Chromatin state dynamics during blood formation. *Science*. **345**, 943–949 (2014).

449. H. Peng, Z. Tian, Re-examining the origin and function of liver-resident NK cells. *Trends Immunol.* **36**, 293–299 (2015).

450. B. Becknell, M. Caligiuri, Interleukin-2, interleukin-15, and their roles in human natural killer cells. *Advances in immunology* (2005).

451. J.-X. Lin, W. J. Leonard, The role of Stat5a and Stat5b in signaling by IL-2 family cytokines. *Oncogene*. **19**, 2566–2576 (2000).

452. L. M. Bradley, L. Haynes, S. L. Swain, IL-7: maintaining T-cell memory and achieving homeostasis. *Trends Immunol.* **26**, 172–176 (2005).

453. M.-S. Dai, X.-X. Sun, H. Lu, Aberrant expression of nucleostemin activates p53 and induces cell cycle arrest via inhibition of MDM2. *Molecular and Cellular Biology*. **28**, 4365–4376 (2008).

454. L. Golomb, S. Volarevic, M. Oren, p53 and ribosome biogenesis stress: the essentials. *FEBS Letters*. **588**, 2571–2579 (2014).

455. R. Rosby *et al.*, Knockdown of the Drosophila GTPase nucleostemin 1 impairs large ribosomal subunit biogenesis, cell growth, and midgut precursor cell maintenance. *Mol. Biol. Cell*. **20**, 4424–4434 (2009).

456. M. M. Kudron, V. Reinke, C. elegans nucleostemin is required for larval growth and germline stem cell division. *PLOS Genetics*. **4**, e1000181 (2008).

457. D. Gotthardt *et al.*, NK cell development in bone marrow and liver: site matters. *Genes Immun*. **15**, 584–587 (2014).

458. D. Simsek *et al.*, The Mammalian Ribo-interactome Reveals Ribosome Functional Diversity and Heterogeneity. *Cell*. **169**, 1051–1065.e18 (2017).

459. Z. Shi *et al.*, Heterogeneous Ribosomes Preferentially Translate Distinct Subpools of mRNAs Genome-wide. *Molecular Cell*. **67**, 71–83.e7 (2017).

460. S. J. Anderson *et al.*, Ablation of ribosomal protein L22 selectively impairs alphabeta T cell development by activation of a p53-dependent checkpoint. *Immunity*. **26**, 759–772 (2007).

461. I. Jurak, U. Schumacher, H. Šimić, S. Voigt, W. Brune, Murine cytomegalovirus m38.5 protein inhibits Bax-mediated cell death. *J. Virol.* **82**, 4812–4822 (2008).

462. H. A. Himburg *et al.*, Pleiotrophin mediates hematopoietic regeneration via activation of RAS. *J. Clin. Invest.* **124**, 4753–4758 (2014).

463. A. Wilson *et al.*, c-Myc controls the balance between hematopoietic stem cell self-renewal and differentiation. *Genes & Development*. **18**, 2747–2763 (2004).

464. M. Babić *et al.*, Cytomegalovirus immunoevasin reveals the physiological role of "missing self" recognition in natural killer cell dependent virus control in vivo. *J. Exp. Med.* **207**, 2663–2673 (2010).

465. Z. Dong *et al.*, Essential function for SAP family adaptors in the surveillance of hematopoietic cells by natural killer cells. *Nat. Immunol.* **10**, 973–980 (2009).

466. J. C. Sun, J. N. Beilke, N. A. Bezman, L. L. Lanier, Homeostatic proliferation generates long-lived natural killer cells that respond against viral infection. *J. Exp. Med.* **208**, 357–368 (2011).

467. M. H. Vitaterna *et al.*, Mutagenesis and mapping of a mouse gene, Clock, essential for circadian behavior. *Science*. **264**, 719–725 (1994).

468. S. Sabrautzki *et al.*, New mouse models for metabolic bone diseases generated by genome-wide ENU mutagenesis. *Mamm. Genome*. **23**, 416–430 (2012).

469. P. K. Potter *et al.*, Novel gene function revealed by mouse mutagenesis screens for models of age-related disease. *Nat Commun*. **7**, 12444 (2016).

470. M. J. Barnes *et al.*, Loss of T cell and B cell quiescence precedes the onset of microbial flora-dependent wasting disease and intestinal inflammation in Gimap5-deficient mice. *J. Immunol.* **184**, 3743–3754 (2010).

471. J. E. Jun *et al.*, Identifying the MAGUK protein Carma-1 as a central regulator of humoral immune responses and atopy by genome-wide mouse mutagenesis. *Immunity*. **18**, 751–762 (2003).

472. C. Dieterich *et al.*, Annotating regulatory DNA based on man-mouse genomic comparison. *Bioinformatics*. **18 Suppl 2**, S84–90 (2002).

473. A. Stachurska, M. M. Zorro, M. R. van der Sijde, S. Withoff, Small and Long Regulatory RNAs in the Immune System and Immune Diseases. *Front Immunol*. **5**, 513 (2014).

474. C. Y.-Y. Szeto *et al.*, Integrated mRNA and microRNA transcriptome sequencing characterizes sequence variants and mRNA-microRNA regulatory network in nasopharyngeal carcinoma model systems. *FEBS Open Bio*. **4**, 128–140 (2014).

475. I. Meyts *et al.*, Exome and genome sequencing for inborn errors of immunity. *J. Allergy Clin. Immunol.* **138**, 957–969 (2016).

476. M. Peplow, The 100,000 Genomes Project. *BMJ*. **353**, i1757 (2016).

477. B. E. Housden *et al.*, Loss-of-function genetic tools for animal models: cross-species and cross-platform differences. *Nat. Rev. Genet.* **18**, 24–40 (2017).

478. R. J. Platt *et al.*, CRISPR-Cas9 knockin mice for genome editing and cancer modeling. *Cell*. **159**, 440–455 (2014).

479. E. Metzakopian *et al.*, Enhancing the genome editing toolbox: genome wide CRISPR arrayed libraries. *Scientific Reports*. **7**, 2244 (2017).

480. S.-Y. Zhang, J.-L. Casanova, Inborn errors underlying herpes simplex encephalitis: From TLR3 to IRF3. *J. Exp. Med.* **212**, 1342–1343 (2015).

481. R. Whitley, A. D. Lakeman, A. Nahmias, B. Roizman, DNA restriction-enzyme analysis of herpes simplex virus isolates obtained from patients with encephalitis. *N. Engl. J. Med.* **307**, 1060–1062 (1982).

482. S.-Y. Zhang *et al.*, TLR3 immunity to infection in mice and humans. *Curr. Opin. Immunol.* **25**, 19–33 (2013).

483. G. M. Davey *et al.*, Cutting edge: priming of CD8 T cell immunity to herpes simplex virus type 1 requires cognate TLR3 expression in vivo. *J. Immunol.* **184**, 2243–2246 (2010).

484. R. Perales-Linares, S. Navas-Martin, Toll-like receptor 3 in viral pathogenesis: friend or foe? *Immunology*. **140**, 153–167 (2013).

485. F. A. Bonilla *et al.*, Practice parameter for the diagnosis and management of primary immunodeficiency. *J. Allergy Clin. Immunol.* **136** (2015), pp. 1186–205.e1–78.

486. M. Ott *et al.*, T-cell Responses to HSV-1 in Persons Who Have Survived Childhood Herpes Simplex Encephalitis. *Pediatr. Infect. Dis. J.* **36**, 741–744 (2017).

487. N. Koyanagi *et al.*, Herpes simplex virus-1 evasion of CD8+ T cell accumulation contributes to viral encephalitis. *J. Clin. Invest.* (2017), doi:10.1172/JCI92931.

488. A. C. Solomos, G. F. Rall, Get It through Your Thick Head: Emerging Principles in Neuroimmunology and Neurovirology Redefine Central Nervous System "Immune Privilege". *ACS Chem Neurosci*. **7**, 435–441 (2016).

489. Y. Mao *et al.*, IL-15 activates mTOR and primes stress-activated gene expression leading to prolonged antitumor capacity of NK cells. *Blood*. **128**, 1475–1489 (2016).

490. M. Pyzik, E.-M. Gendron-Pontbriand, N. Fodil-Cornu, S. M. Vidal, Self or nonself? That is the question: sensing of cytomegalovirus infection by innate immune receptors. *Mamm. Genome*. **22**, 6–18 (2011).

491. M. Mitrović *et al.*, The NK cell response to mouse cytomegalovirus infection affects the level and kinetics of the early CD8(+) T-cell response. *J. Virol.* **86**, 2165–2175 (2012).

492. M. Del Val *et al.*, Protection against lethal cytomegalovirus infection by a recombinant vaccine containing a single nonameric T-cell epitope. *J. Virol.* **65**,

3641–3646 (1991).

493. M. A. Spinner *et al.*, GATA2 deficiency: a protean disorder of hematopoiesis, lymphatics, and immunity. *Blood*. **123**, 809–821 (2014).

494. N. Schleinitz, F. Vély, J. R. Harlé, E. Vivier, Natural killer cells in human autoimmune diseases. *Immunology*. **131**, 451–458 (2010).

495. R. M. Plenge *et al.*, TRAF1-C5 as a risk locus for rheumatoid arthritis--a genomewide study. *N. Engl. J. Med.* **357**, 1199–1209 (2007).

496. P. K. Gregersen *et al.*, REL, encoding a member of the NF-kappaB family of transcription factors, is a newly defined risk locus for rheumatoid arthritis. *Nat. Genet.* **41**, 820–823 (2009).

497. F. Romagné, E. Vivier, Natural killer cell-based therapies. *F1000 Med Rep*. **3**, 9 (2011).

498. F. Romagné *et al.*, Preclinical characterization of 1-7F9, a novel human anti-KIR receptor therapeutic antibody that augments natural killer-mediated killing of tumor cells. *Blood*. **114**, 2667–2677 (2009).

499. S. Gasser, S. Orsulic, E. J. Brown, D. H. Raulet, The DNA damage pathway regulates innate immune system ligands of the NKG2D receptor. *Nature*. **436**, 1186–1190 (2005).